Delft University of Technology

Energy and Industry, Faculty of Technology, Policy and Management,
& Faculty of Electrical Engineering, Mathematics and Computer Science

to obtain the degree of Master of Science in Sustainable Energy Technology at Delft University of Technology

Modelling and sizing of an offshore hydrogen production value chain connected to the Port of Rotterdam

Author:
David Breedijk

Student number:
4452283

Thesis Commitee:
Prof. Dr. Ad van Wijk
Prof. Dr. Ir. Zofia Lukszo
Prof. Dr. Ir. Wiebren de Jong
Dr. Ir. Michiel Zaayer
Ir. Laurens Frowijn

Company supervisor:
Ir. Erik van der Heijden

An electronic version of this thesis is available at `http://repository.tudelft.nl/`

December 13, 2023

Preface

This thesis is written to conclude the MSc in Sustainable Energy Technology at Delft University of Technology. It is written in collaboration with the TU Delft and the Port of Rotterdam.

I would like to express my gratitude to everyone who helped me with this project. First of all, I would like to thank Ad van Wijk, my first supervisor from the start, for helping me come to my interesting research topic and guiding me along the way with the countless insights he gave me. I would also like to thank Zofia Lukszo for stepping in and taking over the role of first supervisor when it was needed and guiding me through the final stages of my project. I am grateful to have had both as a first supervisor to elevate my thesis to a higher level. Also, a very special thanks to Laurens Frowijn, who was my day-to-day supervisor from the TU Delft and was always ready to discuss my questions, concerns, and ideas, helping me improve my research so much. Furthermore, I would like to thank Michiel Zaayer and Wiebren de Jong for their constructive feedback and evaluation of my work as my thesis committee members.

I am also very grateful to the Port of Rotterdam for giving me the opportunity to work on this topic. I learned a lot from from the experiences at the Port of Rotterdam, broader than my research topic. A special thanks to Erik van der Heijden, who has been my company supervisor and supported me along the way. During my time at the Port of Rotterdam, I was able to look at my research from a market perspective, as I was brought in contact with many companies that operate in the hydrogen production value chain. I would also like to thank the members of the Rotterdam Wind Power Hub team, whose project team I joined during my internship. Many insights and experiences have been taken up through this project team.

Finally, I would like to thank my family and friends for their constant support throughout the process of writing this thesis.

Amsterdam, December 13, 2023

David Breedijk

Summary

In this thesis, the techno-economical feasibility of an offshore hydrogen production value chain connected to the Port of Rotterdam is investigated. An elaborate literature review has been done on the possible value chain technologies and configurations. A decision framework is constructed based on a multi-criteria decision analysis. The multi-criteria decision analysis provides a comprehensive decision-making tool to come to designs for offshore hydrogen production. Factors such as costs and technical factors have been taken into account, as well as safety and maintenance considerations and environmental impact.

Using the decision framework, three designs for hydrogen production using offshore wind turbines have been constructed. One design is the combination of best-performing technologies by the decision framework. This design makes use of the offshore decentral configuration, having a small electrolyser at the foot of each wind turbine. The electrolyser used is a PEM electrolyser, and feed water is supplied by a small reverse osmosis system. The hydrogen is transported to shore by pipelines, and offshore salt caverns are used to supply the hydrogen to shore by a baseload. The second design makes use of the offshore central configuration, where electrolysers are placed on an artificial island. PEM electrolysers are used, and reverse osmosis provides the water feed. The electricity from the wind farms is transported to the island by an HVAC infrastructure. Hydrogen is transported to shore through a pipeline. Salt caverns are used to supply the hydrogen by a baseload. The third design makes use of an onshore central configuration. Electricity is collected from the wind turbines and transported to shore by an HVDC infrastructure, where alkaline electrolysers produce hydrogen. A reverse osmosis plant supplies the water feed. Hydrogen is either directly supplied to the demand side or exchanged with salt caverns.

The three designs are simulated in a MATLAB model that is built from the ground up. The model is split up into two parts: a technical and a financial part. The technical part simulated the hydrogen production by using wind speed data from a KNMI station and predetermined wind farms as input. The working of the electrolysers, electricity cables, pipelines, compressors and storage facility are simulated to calculate the maximum baseload and efficiency that can be achieved per design. The value chain is then sized based on the maximum baseload. The financial part of the model uses the sizes of the value chain components to come to the total system costs and the levelised cost of hydrogen.

The offshore decentral design is able to supply the largest baseload to shore, followed by the offshore central and onshore central configurations, with baseloads of $7.93e^4$, $7.52e^4$ and $7.37e^4$ kgH_2/h respectively. The offshore decentral configuration also achieves the highest system efficiency with a value of 69.4%. The offshore central and onshore central configurations reached lower system efficiencies of 65.8% and 65.1%, respectively.

The offshore decentral configuration also achieves the lowest total system costs and system levelised cost of hydrogen. The system levelised cost of hydrogen is 5.14 $€_{2023}/kgH_2$ for this configuration when supplying the hydrogen with a baseload to the demand side on shore at a pressure of 50 bar in 2050, with a wind turbine capacity factor of 0.45. The largest shares of the system levelised cost of hydrogen are the levelised cost of hydrogen of the wind turbines and electrolysers components with 64% and 25%, respectively. The transport, storage, compressor and water feed components have a low share of the system LCOH with 5%, 4%, 1% and <1%, respectively. The offshore central configuration was found to achieve a system levelised cost of hydrogen of 5.69 $€_{2023}/kgH_2$, and the onshore central configuration had the highest system levelised cost of hydrogen of 6.14 $€_{2023}/kgH_2$ when supplying a baseload to the demand on shore at a pressure of 50 bar in 2050, with a wind turbine capacity factor of 0.45.

The offshore decentral configuration is found to be the best-performing design based on assessments through a multi-criteria decision analysis, a technical model and a financial model. It is, therefore, the most promising design.

List of Figures

List of Tables

List of Symbols

Abbreviations

AC	Alternating Current
AWE	Alkaline Water Electrolysis
BoP	Balance of Plant
CAPEX	Capital expenditures
CRF	Capital recovery factor
DC	Direct Current
GW	Gigawatt
H_2	Hydrogen
HER	Hydrogen Evolution Reaction
HHV	Higher heating value
HVAC	High Voltage Alternating Current
HVDC	High Voltage Direct Current
kV	Kilovolt
kWh	Kilowatt hour
LCOH	Liquid Organic Hydrogen Carrier
LHV	Lower heating value
llr	Lower load range
LOHC	Levelised cost of hydrogen
MCDA	Multi-criteria decision analysis
MW	Megawatt
Mt	Megatonne
OER	Oxygen Evolution Reaction
OPEX	Operating expenditures
PEM	Proton Exchange Membrane
PtH_2	Power to Hydrogen
PtG	Power to Gas
PoR	Port of Rotterdam
Re	Reynolds number
SoC	State of charge
SOEC	Solid Oxide Electrolyser Cell
TOTEX	Total expenditures
TRL	Technology Readiness Level
TWh	Terawatt hour

Latin letters

A	Area	$[m^2]$
c_p	Power coefficient	[-]
d	Distance	$[m]$
D	Diameter	$[m]$
E	Energy	$[J]$
f	Cable loss factor	$[\frac{\%}{km}]$
h	Height	$[m]$
L	Length	$[m]$
M	Molecular mass	$[\frac{g}{mol}]$
N	Pumping power	$[W]$
p	Pressure	$[Pa]$
P	Power	$[W]$
Q	Energy flow	$[MW]$
T	Temperature	$[K]$
U	Wind speed	$[\frac{m}{s}]$
v	Flow velocity	$[\frac{m}{s}]$
V_0	Volumetric flow rate	$]\frac{m^3}{s}]$
z	Compressibility factor	[-]
z_o	Surface roughness length	$[m]$

Greek letters

α	power law coefficient	[-]
η	Efficiency	[%]
ρ	Density	$[\frac{kg}{m^3}]$
ν	Dynamic viscosity	$[\frac{kg}{(m \cdot s)}]$
ζ	Resistance coefficient	[-]

Subscripts

ref	Reference height

Constants

R	Ideal gas constant	8.314 $\frac{J}{K \cdot mol}$

Contents

1 Introduction

The world is currently on a path to overshoot the 1.5°Celcius above preindustrial levels global warming target set by the Paris Climate Agreement in 2015 (Nations (2015),Farge & Vinnell (2023)). Current average temperatures have already increased by 1.1 °Celsius in 2021 compared to preindustrial levels IPCC (2023). If the 1.5 °Celsius target is not met, it can have drastic environmental consequences, such as heat waves, droughts, floods and ocean changes (Maizland (2022)). To limit the temperature rise to 1.5 °Celcius, emissions have to be cut drastically.

To lower emissions in the energy sector, renewable energy technologies are now widely deployed to generate renewable electricity. Even though electrification will increase the global electricity demand from around 20% to around 50% by 2050, there are still hard-to-abate end-use sectors that need green chemicals or fuels to decarbonise, such as heavy industry, long-distance transport, shipping and aviation (I.R.E.N.A. (2020), IEA (2023)). Hydrogen, or its derivatives, can be used to meet this demand.

Currently, there are multiple pathways to produce hydrogen. Generally, when hydrogen is produced with fossil fuels and emits CO_2, it is called 'grey' hydrogen. This can be done with natural gas as a feedstock by steam methane reforming or coal as a feedstock by gasification (Kilner (2022)). If the emitted CO_2 is captured and stored, it is indicated by 'blue' hydrogen. When electrolysis produces hydrogen using electricity from renewable energy sources as a feedstock, no carbons are emitted, and the hydrogen is called 'green' (Hermesmann & Müller (2022)).

Multiple sources can generate green electricity, such as wind, solar, geothermal, hydropower, or biomass. In the Netherlands in 2022, 40% of the electricity produced was green, with the primary sources being wind energy (45%) and solar energy (37%) (CBS (2023)). With available space on land becoming more scarce for renewable energy sources, the Dutch government views offshore wind energy as one of the most important pillars of its climate policy and aims to have around 70 GW of offshore wind power installed in 2050 (RVO (2023)). To utilise offshore wind power for the production of green hydrogen, some projects are currently being built, such as the Holland Hydrogen 1 in the Port of Rotterdam, which will become the largest green hydrogen plant in Europe (Shell (2022)). These planned projects all produce hydrogen onshore and have electrical connections from the offshore wind farm to the onshore production plant. However, hydrogen production could also take place offshore, which may be an attractive option due to the lower costs of hydrogen transmission to shore compared to electricity transmission from a certain distance to shore.

The objective of this thesis is to investigate the techno-economical feasibility of an offshore hydrogen production value chain connected to the Port of Rotterdam. The value chain consists of the offshore production, storage and transport of hydrogen. The electricity is generated at offshore wind farms, and the hydrogen is transported to shore to the port of Rotterdam by a baseload since that is more favourable for the demand side and maintains a constant pipeline pressure. The technical analysis gives insights into the possible technologies that can be used for the offshore value chain. It also sizes the components of the value chain to come to a maximum baseload. It will also look at the technical feasibility of system integration in the North Sea's energy system. Finally, the efficiency of the system will be analysed.

The economic analysis gives insights into the economic feasibility of the offshore hydrogen production value chain. The total costs are of importance, as well as the levelised cost of hydrogen (LCOH), given in $€_{2023}/kgH_2$. The LCOH is used to compare the results with alternative hydrogen production or import projects in the Port of Rotterdam. A scenario analysis is performed to gain insights into the influences on the outcomes of future technological developments and cost reductions, as well as the changes in some design choices. A sensitivity analysis will determine the factors with the highest influence on the levelised cost of hydrogen.

The structure of this report is as follows. Chapter 2 describes the problem analysis, including the research questions and scope of this research. Chapter 3 gives the theoretical background on offshore hydrogen production. Chapter 4 describes the research approach of this thesis, after which Chapter 5 gives the decision framework to come to the designs. The results are presented in Chapter 6, after which the discussion and conclusion are given in Chapters 7 and 8 respectively.

2 Problem Analysis

In this chapter, the problem analysis is described. A short introduction is given in Section 2.1, whereafter the main research questions are given in Section 2.2. The scope of the thesis is given in Section 2.3.

2.1 Background

As part of the Dutch government's ambitions to realise significant offshore wind energy capacity (70 gigawatts (GW) by 2050), the Port of Rotterdam (PoR) is to become a hydrogen hub for North-Western Europe. To achieve this, it is expected that around 20 megatonnes (Mt) of hydrogen could be throughput in the Port of Rotterdam (PoR (2020)), out of which 2 Mt will be produced locally from offshore wind farms. Current offshore wind farms use high voltage electricity cables to transport energy to shore, but could, in the future, also transport energy in the form of hydrogen to shore via a transport infrastructure. This hydrogen could be generated either at the wind turbines, on an offshore platform, on a dedicated island or in any hybrid form. The value chain of offshore hydrogen production starts at the wind turbines, where electricity is generated and ends on shore, where hydrogen will be delivered by a baseload to meet demand. Everything in between, namely the hydrogen production by electrolysers, the transport of hydrogen and the storage of hydrogen, will be considered as the offshore hydrogen production value chain.

The world's first offshore hydrogen production pilot is currently deployed by Lhyfe in France (Lhyfe (2023)). The offshore production pilot is coupled to an offshore floating wind turbine and produced its first kilos of hydrogen in June 2023. The pilot uses desalinated seawater and a 1MW electrolyser to produce up to 400 kg of hydrogen daily. In the Netherlands, a pilot named PosHYdon is being set up to have the first offshore electrolyser on a working offshore platform. Seawater is desalinated and is converted to hydrogen by electrolysis. Electricity from wind energy is used (PosHYdon (2023)). The Dutch government also plans to set up two larger projects, a pilot project of 50-100MW in 2028 and a demonstration project of a maximum of 500 MW in 2031 (Topsector (2023)). Looking at other countries on the North Sea, Denmark plans to construct two energy islands, which serve as hubs, to collect the electricity from offshore wind farms. At these energy islands, hydrogen can be produced from the electricity (D.E.A. (2022)). As part of the H2Mare project, Siemens is developing a wind turbine with a small electrolyser at the foot of the wind turbine to directly use the electricity from the wind turbine to produce hydrogen (F.M.E.R. (2021)).

As these projects use different system configurations, the question arises what the optimal configuration will be.

The objective of this thesis is to create a framework of design parameters and to give an outlook on the design of an offshore hydrogen production value chain within the energy system of the North Sea. This value chain generates its energy from offshore wind farms. Hydrogen is produced, stored, and supplied to shore using electricity generated by wind turbines. A qualitative literature study maps the different possibilities per component of the value chain. A decision framework is then used to discuss the best possibility per component and to build three promising designs. These designs are then modelled in MATLAB to size their components. With the model's output, a cost analysis can be done to determine whether such a value chain would be feasible compared to other ongoing projects. A special focus will be put on the Port of Rotterdam, to which the value chain will be connected.

2.2 Research Questions

The main research question of this thesis is: **What is the most promising techno-economically feasible design of a large-scale offshore value chain for hydrogen production connected to the Port of Rotterdam in 2050?**

The main research questions is answered by answering the following subquestions:

1. Which technologies for the offshore value chain are expected to be available from 2030 to 2050?
2. What decision framework is recommended to come to three promising designs?
3. What are possible designs for the offshore hydrogen production value chain on the North Sea to be integrated into the Dutch energy system?
4. How should the components and the totals systems be sized?

5. What would be the levelised cost of hydrogen upon arrival at the PoR, and how does this compare to other projects?

2.3 Scope

The scope of this thesis is the offshore hydrogen production value chain. This value chain starts at offshore wind farms, where electricity is produced and ends on shore, where a baseload of hydrogen is used to meet demand in the port of Rotterdam. The value chain will include hydrogen production by electrolysis, as well as the system configuration of the electrolysers. Also, the different types of transportation and storage of hydrogen will be analysed. The decision framework also only applies to the hydrogen value chain. For the sizing and modelling of the design, fixed-sized wind parks will be used. The system costs will only include the value chain, not consisting of the processing inland. The landings of the hydrogen/electricity are considered from a physical feasibility point of view. The system boundary of the offshore hydrogen value chain will consist of the following elements. First of all, the electricity is gathered from the wind turbines. To do this, switchgear, inter-array cables and offshore substations may be needed. The second element is the electrolyser. The electrolyser(s) can be placed offshore decentrally at the wind turbines, offshore centrally at the wind farm or onshore. Another element is the transportation of energy. This can be done by sending hydrogen to shore by pipelines or transporting electricity via cables. Finally, the storage of hydrogen offshore enables the balancing of weather or seasonal fluctuations to ensure a baseload supply to shore.

3 Theoretical Background

This chapter gives an overview of the working principles of the technologies that can be used in an offshore hydrogen production value chain. This chapter will serve as a base on which the research method will be explained in the next chapter, Chapter 4. Firstly, in Section 3.1, the three electrolyser system configurations for producing hydrogen with the electricity of offshore wind farms are given. Secondly, in Section 3.2, the three main water electrolysis technologies are discussed. Section 3.3 discusses the water feed to the electrolyser, whereafter Section 3.4 describes the total balance of plant of the electrolyser system. Section 3.5 looks at the different storage possibilities. Section 3.6 and 3.7 look into the modes of energy transport and different types of hydrogen distribution hub configurations, respectively.

3.1 Electrolyser System Configuration

When producing hydrogen with electricity directly from wind turbines, the electrolysers can either be placed decentrally or centrally. With a decentral configuration, each wind turbine is coupled to its electrolyser. With a central configuration, the electricity from multiple wind turbines is collected and coupled to an electrolyser. Also, the electrolysers can be placed offshore or onshore. Since transporting the electricity from offshore wind turbines to shore per wind turbine is not realistic, only three different system configurations for electrolysis are taken into account. Firstly, electrolysis can take place in a central configuration, either onshore or offshore. With a central configuration, the electrolysers get their electricity input from multiple wind turbines. With a decentral configuration, each wind turbine is connected to its own small electrolyser. Section 3.1.1 discusses the central onshore configuration, whereafter Sections 3.1.2 and 3.1.3 describe the offshore central and decentral configurations, respectively.

3.1.1 Onshore Central Configuration

Onshore, only the central option is considered. Onshore central electrolysis is performed by laying electricity cables from the offshore wind park to shore. Several conversion steps are needed to make this possible. Inside the nacelle of the wind turbine, a generator converts the kinetic energy to electricity. This generator produces alternating current electricity. Nowadays, a wind turbine also has a converter, which converts the alternating current to direct current and back again to alternating current to match the frequency and phase of the power grid (Turbinesinfo (2021)). Wind turbines are then connected to each other and the offshore substation via inter-array cables to collect and transform the generated electricity. These cables typically have a 33 kilovolts (kV) voltage, although larger turbines with a higher power rating might require 66kV cables. With fixed-pole wind turbines, these cables go down the tower and under the seabed to the offshore substation. With floating offshore wind turbines, dynamic cables are used that have a dynamic section that moves with the floating substructure (Lerch et al. (2021)).

At the offshore substation, the voltage is heightened even further for long-distance transmission, typically to 380 or 520 kV. From the substation, either high-voltage alternating current (HVAC) or high-voltage direct current (HVDC) cables are used to bring the power to shore. Which cable is used depends on the power rating and distance to the shore of the wind farm. To land power cables from shore, minimal distances between the cables, if multiple are used, and safety contours are obliged. Onshore, the HVDC cables will be connected to a substation, where the voltage will be lowered to match the regional grid voltage of 66kV, as well as converting it back to AC. At the electrolyser plant, the 66kV AC is converted to 1200V DC, as input for the electrolysers (Program (2022)).

The onshore electrolyser needs a total balance of plant, as described in Section 3.4. However, the desalination unit is not needed if a connection to a water supplier is possible on land. A schematic overview of an example of the centralized onshore configuration is given in Fig. 3.1.

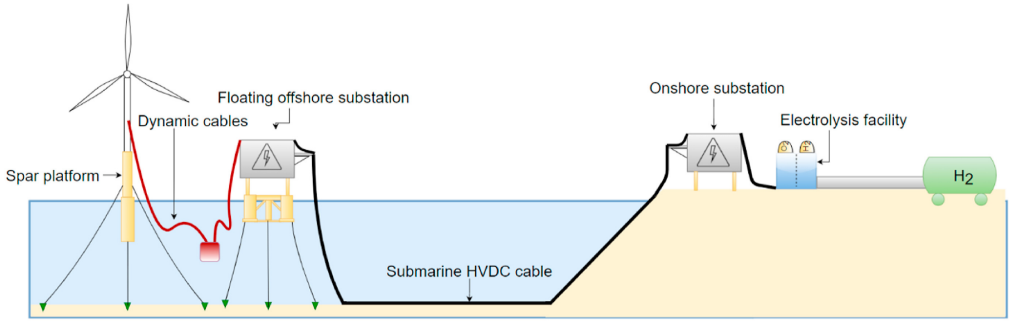

Figure 3.1: Schematic overview of the central onshore electrolysis configuration (Ibrahim et al. (2022)).

3.1.2 Offshore Central Confguration

The offshore central configuration has similarities to the onshore central configuration, especially in the first part of the system. Again, the generator inside the nacelle of the wind turbine produces alternating current electricity. The wind turbines are connected to each other and to an offshore substation via medium voltage inter-array cables to collect and transform the electricity. The offshore substation is needed to ensure the correct power feed, in terms of voltage and AC/DC, to the electrolyser. The use of static or dynamic inter-array cables depends on the choice of fixed-pole or floating wind turbines.

The offshore central electrolysis can have several configurations from here. The offshore substation can be placed on the same structure as the electrolyser. Another option is to have the offshore substation on a separate structure from the electrolyser. The structure(s) of the substation and electrolyser does also have several options. For both, a fixed structure can be used such as an (old) platform, as well as a semi-submersible platform, a floating vessel, or even an artificial island. For the electrolyser, the total balance of plant as described in Section 3.4 has to be present.

From the electrolyser, hydrogen can be transported by pipelines to shore. If a floating structure is used for the electrolyser, the first part of the pipeline is to be a flexible pipe because of the dynamic nature of the floating structure (Ibrahim et al. (2022)). This flexible pipeline then connects with a static pipeline offshore, with which the hydrogen is transported to shore. With a fixed structure, only static pipelines are sufficient. Other modes of transportation are discussed in Section 3.6. A schematic overview of an example of the centralised offshore configuration is given in Fig. 3.2. It should be noted that the shown configuration with a floating substation and a floating vessel with an electrolyser facility is not necessarily the only central offshore configuration but only an illustrative example.

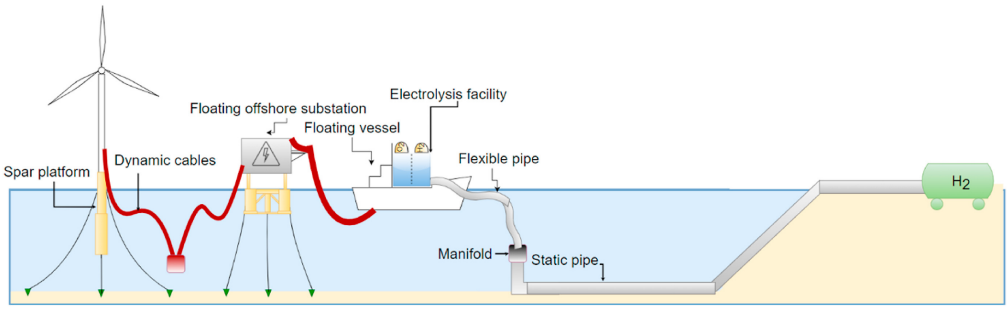

Figure 3.2: Schematic overview of the central offshore electrolysis configuration (Ibrahim et al. (2022)).

3.1.3 Offshore Decentral Configuration

With the offshore decentralised configuration, each wind turbine is connected to an electrolyser. The electrolyser can be located either in the turbine or at the foot of the turbine. Due to the electrolyser being at the turbine, no power transmission is needed to an offshore substation. As mentioned in Section 3.1.1, the alternating current outputted from the wind turbine generator is converted to direct current to flatten the frequency and then back to alternating current to match the frequency and phase of the array power grid. However, without power transmission, the alternating current output can be directly transformed into direct current with the right voltage for the electrolyser, saving on two conversion steps.

The electrolysis will take place at the foot of the turbine. For this configuration, a total balance of plant of the electrolyser is needed per electrolyser. Each electrolyser thus has its desalination unit. Both configurations can be used on either a fixed-pole wind turbine or a floating wind turbine. However, a floating wind turbine usually already has a platform at its foot, whereas for a fixed-pole wind turbine, this platform would have to be added for the decentralized electrolyser.

When hydrogen is produced, it will be transported by static pipelines from fixed-pole wind turbines or flexible pipelines from floating wind turbines to endure the dynamics of the floating wind turbine. These singular pipelines from each wind turbine then connect at a manifold, which is a device that connects many pipelines, allowing the further transport of the hydrogen from all pipelines through one pipeline. The output pipeline of the manifold is a static submarine pipeline connected to the shore. A schematic overview of an example of a decentralised offshore configuration is given in Fig. 3.3.

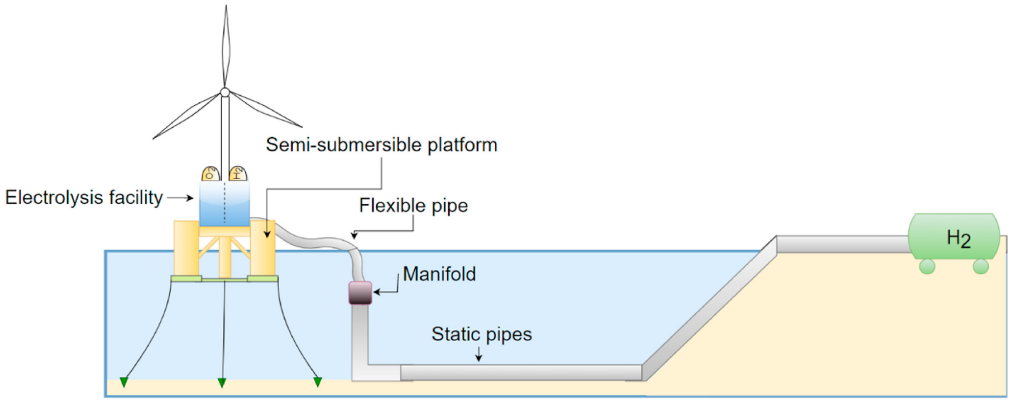

Figure 3.3: Schematic overview of the decentral offshore electrolysis configuration (Ibrahim et al. (2022)).

3.2 Water Electrolysis

Intermittent renewable electricity can be converted into a storable gas in a process called Power-to-gas (PtG). If hydrogen is produced by renewable electricity, it is called Power-to-hydrogen (PtH_2). Water electrolysis is performed to convert electricity to hydrogen.
The working principle of water electrolysis is based on a reduction-oxidation reaction. A simple electrolyser cell consists of two electrodes and an electrolyte. The electrodes need to be conducting and are often made of metal. The electrolyte is a media responsible for transporting the generated chemical charges from one electrode to the other. These chemical charges can be negatively charged, called anions, or positively charged, called cations. When an external DC voltage is applied over the electrodes, electrons flow from the anode to the cathode, enabling the reduction and oxidation reactions to take place in the solution. The oxidation reaction takes place at the anode, where oxygen gas is formed. The reduction reaction takes place at the cathode, where hydrogen gas is formed (I.R.E.N.A. (2020)).

The overall reaction of water electrolysis is divided into two half-reactions. As shown in Eq. 3.1, the oxygen evolution reaction (OER) occurs at the positive anode, and water is oxidised to produce O_2 (Yu et al. (2022)).

$$\text{Positive Anode:} \quad 2H_2O \rightarrow O_2 + 4H^+ + 4e^- \tag{3.1}$$

At the negative cathode, the hydrogen evolution reaction (HER) takes place, where hydrogen ions acquire electrons to produce H_2. This is shown in Eq. 3.2

$$\text{Negative Cathode:} \quad 2H^+ + 2e^- \rightarrow H_2 \tag{3.2}$$

Combining the two half-reactions results in the overall water electrolysis reaction, as shown in Eq. 3.3. Per two water molecules, two hydrogen gas molecules, and one oxygen gas molecule are formed.

$$\text{Overall:} \quad 2H_2O \rightarrow O_2 + 2H_2 \tag{3.3}$$

The half-reactions take place at the cell level of an electrolyser. Multiple cells can be stacked together to increase the amount of hydrogen produced. The cells are connected in series and have insulating material, seals and frames between each cell. End plates are fitted at both ends of the stack to avoid leaks and collect fluids (I.R.E.N.A. (2020)). The system level of an electrolyser is called the balance of plant and comprises all the subsystems necessary for the operation of the electrolyser. Examples are a water treatment subsystem and a power supply system. The balance of plant is further described in Section 3.4. Oxygen gas and waste heat are the two main by-products of the total electrolyser system.

There are three main water electrolysis technologies, namely Alkaline Water Electrolysis (AWE), Proton-Exchange Membrane water electrolysis (PEM) and Solid Oxide Electrolyser Cell (SOEC). AWE and PEM show a higher technology readiness level (TRL) than SOEC, which is still in the development stage (David et al. (2019),Schmidt et al. (2017)). The TRL was developed by NASA in the 1970s and indicates the development of a technology. The scale is from 1 to 9, whereby levels 1 to 3 indicate the technology is in the discovery phase, and levels 4 to 6 indicate the development phase. Levels 7 and 8 are the demonstration phase, and finally, level 9 is the deployment phase. Within each phase, the different levels indicate the differences within that phase (RVO (2022))

3.2.1 Alkaline

Alkaline electrolysis is the first commercialised electrolysis technology and currently has the highest installed capacity of all electrolyser technologies (Bermudez et al. (2022)). In 2023, 1459MW of alkaline electrolysers were installed, opposing 1125 megawatts (MW) of PEM electrolysers installed worldwide. (IEA (2022)). These electrolysers have a simple stack and system design. With alkaline water electrolysis, the electrodes are often made of Nickel. The separator in the electrolyte is a permeable polymer. This polymer solely allows the transport of hydroxide ions and water molecules. The liquid electrolyte usually consists of an aqueous solution of KOH or NaOH with a concentration of 25-30% (Chisholm et al. (2022)), (David et al. (2019)).

Water is split at the cathode to form H_2. In this process, hydroxide (OH^-) anions are released, which pass through the separator. These hydroxide anions recombine at the anode to form O_2. The half-reactions at the cathode and anode are respectively given by Eq. 3.4 and Eq. 3.5. A schematic diagram of alkaline water electrolysis is given in Fig. 3.4.

Alkaline electrolysers usually operate at a temperature between 70-90 $°C$ and a pressure of 1-30 bar (IEA (2022)).

$$2H_2O(l) + 2e^- \rightarrow H_2(g) + 2OH^-(aq) \tag{3.4}$$

$$2OH^-(aq) \rightarrow \frac{1}{2}O_2(g) + 2e^- + H_2O \tag{3.5}$$

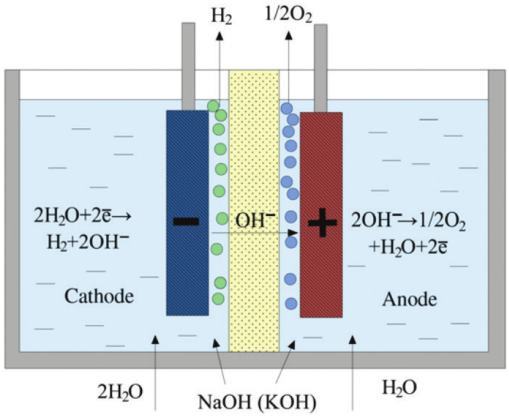

Figure 3.4: Schematic diagram of the alkaline electrolysis cell (Gandía et al. (2013)).

3.2.2 Proton Exchange Membrane

The development of PEM electrolysers started in the 1960s, and they are nowadays considered the most effective and safest electrolyser technology (Gandía et al. (2013)). With PEM electrolysis, the key component is the proton conducting membrane, which is made of polymer. These membranes are between several tens to several hundred micrometres thick, depending on the specific application. This membrane acts as a solid electrolyte, and therefore, no liquid electrolyte is present at a PEM electrolyser cell. Because there is no liquid electrolyte, the electrodes have to be held tightly to the membrane, this is called a zero-gap configuration. The PEM electrolysis process is highly acidic, and therefore, rare transition metals that are stable in acidic conditions are to be used as electrodes. At the Anode, Iridium is currently the most widely used in state-of-the-art PEM electrolysers, and at the Cathode, platinum is most used (Chisholm et al. (2022)). The water is fed in on the anodic side, and hydrogen gas leaves the anodic side.

At the anode, the water is split into oxygen and protons as per Eq. 3.6. These protons are then transferred through the membrane to the cathode. At the cathode, hydrogen is then generated, as per Eq. 3.7. A schematic diagram of the PEM electolysis cell is given in Fig. 3.5.

PEM electrolysers operate with a pressure of up to 70 bar and at a temperature range of 50-80 $°C$ (IEA (2022)).

$$H_2O(l) \rightarrow \frac{1}{2}O_2(g) + 2H^+(aq) + 2e^- \tag{3.6}$$

$$2H^+(aq) + 2e^- \rightarrow H_2(g) \tag{3.7}$$

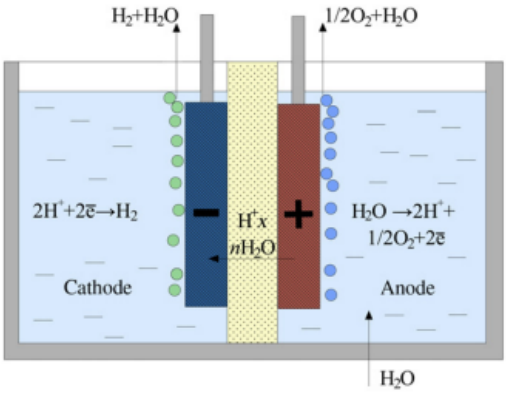

Figure 3.5: Schematic diagram of the PEM electrolysis cell (Gandía et al. (2013)).

3.2.3 Solid Oxide Electrolyser Cell

With Solid Oxide Electrolyser Cells, the membrane is made of oxide-ion conducting ceramics. This membrane also acts as an electrolyte, similar to the membrane of PEM cells. With current state-of-the-art SOECs, the membrane is made of yttria-stabilized zirconia, which only has sufficient ionic conductivity at very high temperatures. Thus, solid-oxide electrolysis operates at a much higher temperature than alkaline and PEM electrolysis, usually in the range of 800-1000°Celcius (Chisholm et al. (2022)), (Gandía et al. (2013)). Due to the high operating temperatures, water is not fed in as a liquid but as high-pressure steam, and the favourable kinetics at these temperatures allow for the use of simple nickel electrodes I.R.E.N.A. (2020).
The steam is fed in at the cathode, where it is reduced to hydrogen gas and oxide ions by Eq. 3.8. These oxide ions are transferred through the membrane to the anode, where they are oxidized to produce oxygen gas by Eq. 3.9. A schematic diagram of the Solix oxide electrolysis cell is given in Fig. 3.6.

$$H_2O(g) + 2e^- \rightarrow H_2(g) + O^{2-} \tag{3.8}$$

$$2O^{2-} - 2e^- \rightarrow O_2 \tag{3.9}$$

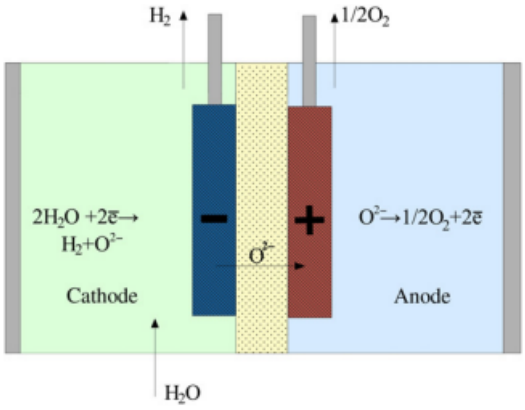

Figure 3.6: Schematic diagram of the solid oxide electrolysis cell (Gandía et al. (2013)).

3.3 Water Feed

Electrolysers use water as a feedstock to separate oxygen and hydrogen. It is desired to have this water as pure as possible. Minimal water purity levels depend on the electrolyser technology, electrode material and system design. Because of this, water treatment for electrolyser projects is often tailored to a specific project. When the water does not meet the purity requirements, degradation of the electrolyser cell can occur (I.R.E.N.A. (2020),Asghari et al. (2022)). Multiple impurities such as iron, chromium or copper can affect the membrane and catalysts of the electrolyser, shortening the lifetime. Instead of water purity, electrolyser manufacturers may set requirements in terms of water conductivity. The lower the conductivity of the water, the fewer ions and molecules will be present in the water (Madsen (2022)).

From a stoichiometric point of view, producing 1 kg of H_2, requires 9 kg of water as feed. Due to process inefficiencies, this usually rises to around 11 kg of water per kg H_2 Saulnier et al. (2020). A rule of thumb for water consumption of electrolysers is 200 L/h per MW, based on the assumption that most electrolysers require 45-55 kWh/kg H_2 (Madsen (2022)).

Seawater desalination plants can be divided into two categories. Namely, membrane solutions and thermal solutions. Over 70% of globally installed desalination plants use membrane technologies, and over 90% of the installed capacity since 2010 (Feria-Díaz et al. (2021)). Reverse osmosis is the most used technique in the membrane solutions category, having an installed capacity of 70% of total desalination units globally, and will be discussed in Section 3.3.1. Of the thermal solutions, Multi-stage flash is the most used technology, having a total share of 18% of total globally installed desalination units (Ayaz et al. (2022)). A new, promising thermal solution is membrane distillation, which requires much less energy input and operates at a lower temperature than multi-stage flash (Alsebaeai & Ahmad (2020)), and will be discussed in Section 3.3.2.

With water desalination comes brine. Brine is the by-product of water desalination and can have a large impact on the environment. The brine that is left after the desalination has a very high salt containment. When dumping large quantities of brine into the seawater, the marine ecosystems can be affected (Panagopoulos et al. (2019)).

3.3.1 Reverse Osmosis

Reverse osmosis is based on the principle of osmosis. With osmosis, water molecules move from a solution with a low solute concentration to a solution with a high solute concentration through a semi-permeable membrane. The semi-permeable membrane only allows the transfer of water molecules, blocking the solutes. Water molecules move from one solution to the other until an osmotic equilibrium is reached.

With reverse osmosis, an external pressure is applied to the high-solute solution. If the externally applied pressure is greater than the difference in osmotic pressure, water molecules will transfer through the membrane from the high-solute solution to the low-solute solution. Since this is the opposite flow direction of the naturally occurring osmosis, this process is called reverse osmosis (Qasim et al. (2019)).

Reverse osmosis requires between 2-4 kWh/m^3 purified water (Shemer & Semiat (2017)), and has a return rate of 40-45%, meaning that 40-45% of the feedwater outputs as purified water (Ayaz et al. (2022)).

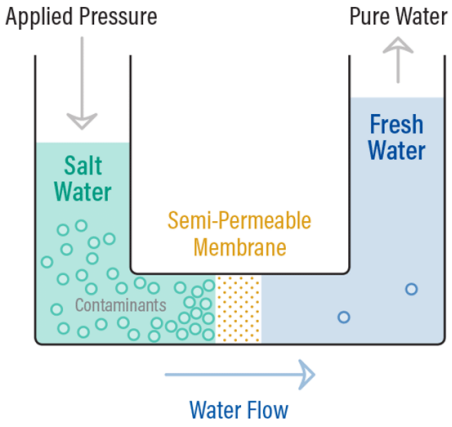

Figure 3.7: Schematic diagram of reverse osmosis (Kouli et al. (2018)).

3.3.2 Membrane Distillation

Membrane distillation is based on the use of a hydrophobic membrane. This membrane solely allows the transfer of water vapour molecules through its micropores and blocks the liquid. This process is driven by the partial vapour pressure difference through the membrane, created by the temperature gradient between

the two sides of the membrane. The solution does not have to reach its boiling point in order for membrane distillation to work. The vapour particles that are transferred through the membrane, condense on the permeate side of the membrane (Adewole et al. (2022a), Alkhudhiri et al. (2012)). Membrane distillation techniques are subcategorised into four different types, depending on how the membrane is configured. With direct contact membrane distillation, shown on the top-left of Fig. 3.8, the hot feed and the cold permeate are in direct contact with the membrane. With air gap membrane distillation, shown on the top-right of Fig. 3.8, the hot feed is in direct contact with the membrane, but an air gap is present between the membrane and the cold permeate. With sweep gas membrane distillation, shown on the bottom-left of Fig. 3.8, a gas sweeps the vapour at the condensing side of the membrane, and the vapour condenses outside the membrane. The last setup is called vacuum membrane distillation and is shown on the bottom-right of Figure 3.8, which has the same working principle as sweep gas membrane distillation, only it uses a vacuum created by a pump the make the condensation occur outside of the membrane (Adewole et al. (2022a), Alkhudhiri et al. (2012), Alsebaeai & Ahmad (2020)). The different configurations are given in Fig. 3.8

Membrane distillation techniques are still under development and have reported energy consumptions between 1 and 9000 kWh/m^3 Duong et al. (2017).

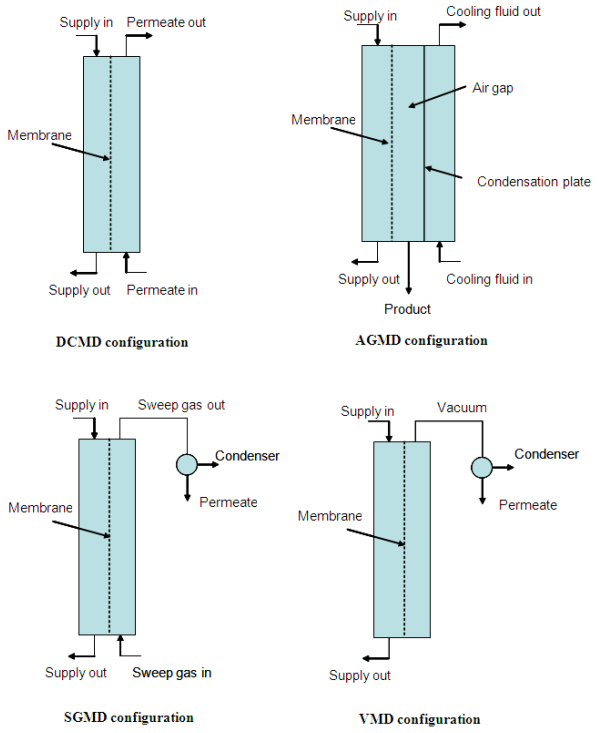

Figure 3.8: Schematic overview of the four different membrane distillation configurations (EMIS (2010)).

3.4 Electrolyser Balance of Plant

Balance of plant is a concept from process engineering that refers to all of the supporting systems that are needed for the operation of the main process. In this case, the main process is the electrolysis of the electrolysis cell, as discussed in Section 3.2. The balance of plant is thus the supporting systems that are needed for the electrolysis cell to function, consisting of at least a power supply system, a water management system, a hydrogen processing system and a cooling system, although exact configurations might vary depending on electrolyser technology (I.R.E.N.A. (2020)).

To ensure the operation of the electrolysis cell, a power supply is needed to provide the external current over the electrodes of the electrolysis cell. In this thesis, the power supply will come directly from the offshore wind farms with an alternating current output. Firstly, an AC/AC transformer is used to adjust the voltage level of the output of the wind turbines to the needed voltage level of the input of the electrolyser. Since the electrolyser needs a direct current feed, an AC/DC rectifier is needed. Also, sensors are used to monitor the power supply (Mancera et al. (2020), Sánchez et al. (2020)).

A water feed is needed to provide H_2O atoms to be split in the cell. As discussed in Section 3.3, this water needs to be purified. Since water feed from shore is unrealistic, seawater must be treated offshore by a desalination unit. This can either be a reverse osmosis or a thermal distillation system. Because the water is recirculated, a separator tank and control valve are needed to regulate the oxygen outflow. A PEM

electrolyser also needs a demister for water recirculation (Guo et al. (2019)). Other components of the water management system are pumps, valves, tubing and instrumentation.

The hydrogen processing system is connected to the output of the electrolyser. The generated hydrogen purity is ensured in a two-step process. Firstly, a gas-liquid separator separates the liquid from the dry hydrogen. This process is based on a high-pressure swing separator. The wet hydrogen is considered dirty and is processed further to retrieve wastewater. The dry hydrogen continues to the drying stage, where impurities are removed from the gas, this is based on pressure swing adsorption. A compression unit might also be part of the hydrogen processing system, depending on the actual electrolyser output pressure and desired output pressure for further processing. Throughout this system, sensors are in place to measure and control the pressure and temperature (Mancera et al. (2020)).

The cooling system comprises two heat exchangers and dedicated control valves. The heat exchangers are placed to heat the water management system and to cool the hydrogen processing system. An external air cooler is used to cool down the heated cooling water. This external air cooler also has its own pump (A. Kumar (2021)).

3.5 Storage

The hydrogen produced offshore will not have a constant production over time since the wind speed varies over time. Storage is needed to balance weather or seasonal production fluctuations to ensure a baseload supply to shore. This section discusses the working principles of different hydrogen storage technologies. The first two Sections look into the underground storage of hydrogen in depleted gas fields (3.5.1) and depleted salt caverns (3.5.2). Finally, Section 3.5.3 looks into several different technologies that can be used above-ground either onshore or at a hydrogen distribution hub. Aquifers are also considered an option for underground hydrogen storage, in locations where hydrocarbon reservoirs and salt caverns are not present. Since both hydrocarbon reservoirs and salt caverns are abundantly present in the Netherlands, aquifers are not considered.

3.5.1 Empty Hydrocarbon Reservoir

A hydrocarbon reservoir can be either an oil or gas reservoir. Once such a reservoir reaches the end of its production lifetime, it can be transformed into a storage facility. The reservoirs are geological traps, that are usually surrounded by a less permeable layer, called the cap rock, and an aquifer (Muhammed et al. (2023), Tarkowski (2019)). The pressurised gas is stored in the pores of the reservoir (Muhammed et al. (2022)). To keep the reservoir above the minimum pressure limit, cushion gas is injected. The cushion gas is never extracted from the reservoir. When an old natural gas field is used for hydrogen storage, some leftover natural gas will be present in the field, which can be used as a part of the cushion gas. The more storage cycles, the more the hydrogen will mix in the cushion gas. The working gas is the hydrogen that can be extracted until the lower pressure limit is reached (NAM (2022), Muhammed et al. (2022)). A schematic overview of hydrogen storage in an old hydrocarbon reservoir is given in Fig 3.9.

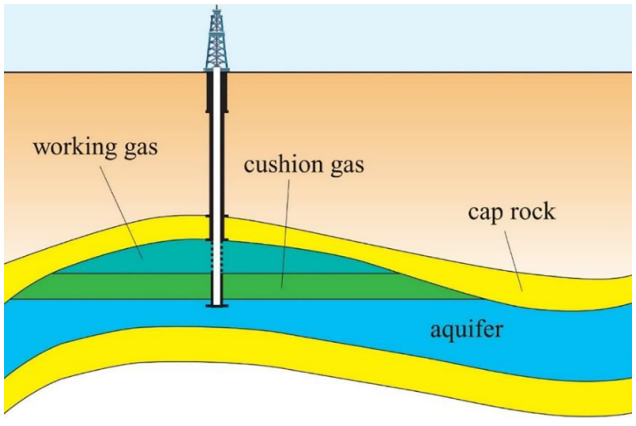

Figure 3.9: Schematic overview of underground hydrogen storage in an old hydrocarbon reservoir (Muhammed et al. (2023)).

The design of an empty hydrocarbon reservoir, re-used as underground hydrogen storage, needs several components. Firstly, injection facilities are needed. These consist of a compression unit, coolers and a suction knock-out drum. The production facility comprises a dehydration unit, a desulphurisation unit and a separation unit to separate the hydrogen gas from the other gases in the mixture. Over storage cycles, the mixture will become purer hydrogen gas since only pure hydrogen gas is injected into the reservoir (NAM

(2022)). Also, a pipeline from the hydrogen production facility to the storage facility and a hydrogen pipeline from the storage to the demand side is needed. The existing equipment, such as wells and compressors, can be used when re-using old hydrocarbon fields. The Netherlands has a large availability of old oil fields, and especially old gas fields. With these fields also come the equipment connected to them. Fig. 3.10 shows the locations of the oil and gas fields in the Netherlands that could, in the future, potentially be used as hydrogen storage.

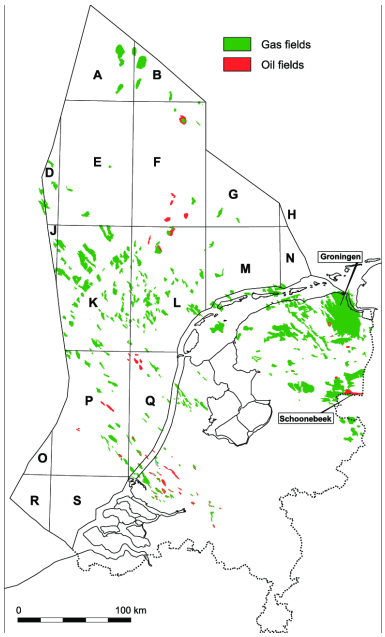

Figure 3.10: Locations of oil and gas fields in the Netherlands (Jager (2007)).

Several parameters can be designed depending on the storage facility's use. These include the pressure limits, the cycle's production capacity, and the ratio between the cushion gas and the working gas. The number of wells connected to the reservoir and the diameter of the tubings connected to the well are also parameters that can be designed to fit the use of the storage.

The total offshore hydrogen storage capacity is calculated to be 552 Terawatt hours (TWh). Of those 552 TWh, 78 gas fields were considered suitable for either short or long-cycle hydrogen storage, totalling 294 TWh. The other fields were either too small or too large, or no sufficient data was available to make calculations (EBN & TNO (2022)).

3.5.2 Salt Cavern

Salt caverns can be artificially made by drilling in a subterranean salt body. These salt bodies can be either salt domes or bedded salt formations. Salt domes are thick and homogeneous salt bodies. Because of this, strong and stable caverns can be made in the domes. Bedded salt formations are found at a shallower depth than salt domes, are thin, and usually consist of alternating salt and non-salt beds. Due to their thinness and heterogeneity, salt caverns constructed out of bedded salt formations are usually less stable (Thiyagarajan et al. (2022),Muhammed et al. (2022)). Because rock salt has a very low permeability, very little hydrogen is prone to leaking. Cushion gas is also used in salt cavern storage. The cushion gas needed is related to the cavern parameters such as depth, shape and permeability (Sambo et al. (2022)). Salt caverns have the injection and withdrawal of hydrogen take place from one single well. Underground, the salt cavern consists of the cavern itself, a hanging wall and a foot wall. The hanging wall and foot wall are safety measures and refer to the minimal thickness of the salt from the cavern to the upper and lower outer edges of the salt body. The hanging wall is suggested as 75% of the cavern diameter and the foot wall as 20% (Caglayan et al. (2020)). A schematic representation of an underground salt cavern is shown in Fig. 3.11

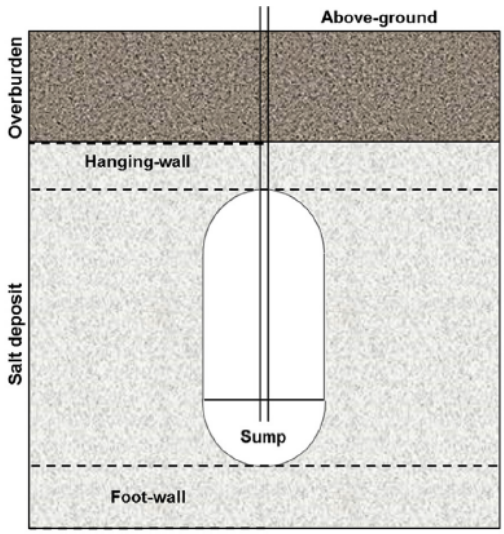

Figure 3.11: Schematic overview of an underground salt cavern for hydrogen storage (Caglayan et al. (2020)).

A hole is drilled into the salt body to construct a salt cavern. Freshwater or undersaturated brine is pumped into the salt body, which dissolves the salt. The salt is leached either directly or indirectly. With direct leaching, the water flows out at the bottom of the cavern, flowing upwards because of the lower density. The brine is then collected at the top of the cavern. With indirect leaching, the water is released at the top of the cavern and flows downwards, where it is collected. Once the cavern has the desired shape and volume, the leaching is stopped, and hydrogen gas is injected under high pressure, which pushes out the brine.

Fig. 3.12 shows the locations of salt structures in Europe. the Netherlands has a great potential for salt cavern storage in the northern parts.

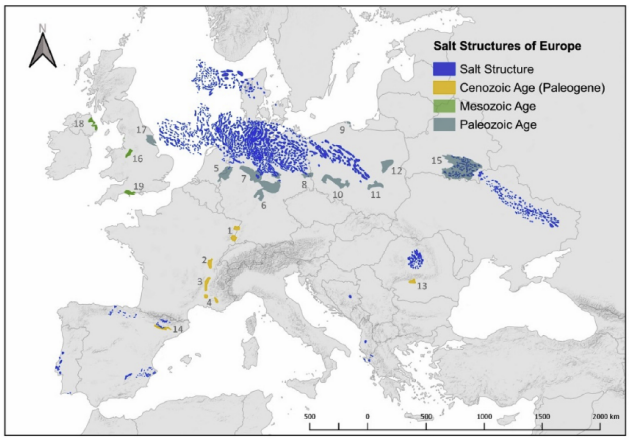

Figure 3.12: Overview of salt structures in Europe (Caglayan et al. (2020)).

No offshore salt caverns are yet constructed on the Dutch North Sea, but several salt structures show potential for constructing salt caverns. Five large salt structures are identified. These structures could contain over 50 salt caverns and have a combined theoretical storage capacity of 130 TWh. Seven more salt structures of medium size are identified. These structures could contain between 15 and 50 possible caverns and have a theoretical storage capacity of 41 TWh. Also, small salt structures are identified, possibly containing less than 15 caverns, but due to their small size and uncertainties in determining the structures, these are deemed unfavourable. The total theoretical storage capacity is thus 171 TWh (EBN & TNO (2022)).

3.5.3 Above-ground Storage

Apart from (offshore) underground storage, hydrogen can also be stored in various other forms on an energy island or onshore. Hydrogen can either be stored in a physical or material-based manner. Physical-based manners of hydrogen storage include compressed gas, cryo-compressed and liquid hydrogen. Material-based manners of hydrogen storage include adsorption methods, liquid organic hydrogen carriers, hydrides and chemical hydrogen storage. An overview of all different forms of hydrogen storage is given in Fig. 3.13

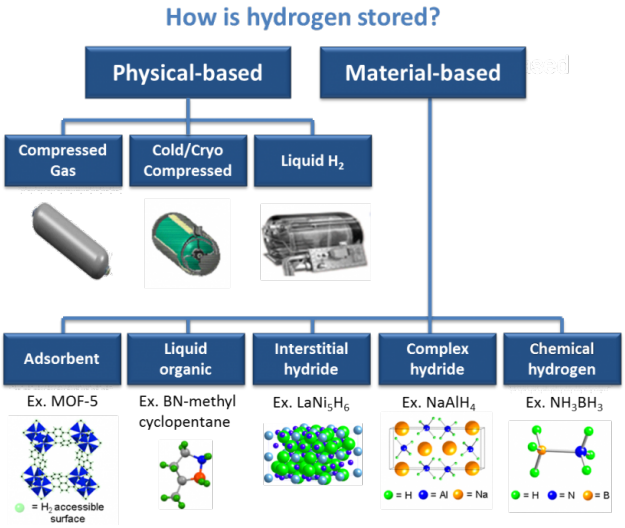

Figure 3.13: Overview of the different hydrogen storage techniques (of Energy (n.d.)).

With compressed hydrogen storage, hydrogen is compressed to very high pressures to increase its energy density. Pressurizing the hydrogen consumes around 15% of the lower heating value of hydrogen, although releasing the compressed hydrogen takes up no energy (Usman (2022). Compressed hydrogen is stored in cylindrical tanks, using materials that can withstand hydrogen embrittlement. Hydrogen embrittlement is the absorption of hydrogen atoms by a metal, causing the minimal stress level to create cracks to be lowered, which results in the embrittlement of the metal (Popov et al. (2018)).

Hydrogen can also be stored in liquid form (LH_2). In this form, hydrogen has a much higher energy density. The boiling point of hydrogen is -253 $°C$, to which the hydrogen has to be brought to liquefy. Liquified hydrogen has to be stored in such a manner that evaporation of the hydrogen is minimised. The evaporated hydrogen results in energy and hydrogen loss, as the evaporated hydrogen has to be released. If not released, the pressure becomes too high in the tank. This process is called the boil-off of hydrogen. Liquid hydrogen tanks are double-walled with a vacuum layer between the walls to minimise the heat exchange between the low-temperature hydrogen and the surroundings Andersson & Grönkvist (2019).

The cryo-compressed form of hydrogen storage is a combination between compressed hydrogen storage and liquified hydrogen storage. This is because the hydrogen is stored at cryogenic temperatures and put under a pressure of a minimum of 250 bar. This allows for even higher densities of the stored hydrogen while minimising the boil-off. The cryo-compressed form of hydrogen storage requires state-of-the-art storage tanks and large energy input (Usman (2022), Langmi et al. (2021).

Hydrogen storage through adsorption makes use of van der Waals bonds between the hydrogen and other materials, preferably with a high surface area (Andersson & Grönkvist (2019)). The van der Waals bond is a physical bond between atoms, which is relatively weak. Due to the weakness of this bond, with an enthalpy of 1-10 kJ/mol, low temperatures and pressures are sufficient to form these bonds, and it has fast kinetics, allowing high adsorption rates (Usman (2022)). To reach high storage capacities, however, cryogenic storage temperatures and high pressures are used since, at ambient conditions, the bonds easily break up. The storage of hydrogen through adsorption is a reversible process, and the offloading of hydrogen by breaking the bonds is called desorption. The desorption is fully reversible, and no byproducts are formed with it. Multiple materials have a high potential for hydrogen storage by adsorption, which includes porous materials such as zeolites, metal-organic frameworks, covalent organic frameworks and intrinsic microporosity (Langmi et al. (2021)).

Liquid organic hydrogen carriers (LOHC) are organic molecules that can have hydrogen chemically bonded to them and released from them. A LOHC can bond a hydrogen atom to it in a process called hydrogenation. This process takes place at a certain pressure and temperature, which can be different for different LOHCs, and bonds the hydrogen in the presence of a catalyst in an exothermic reaction. To offload the hydrogen atom, the molecule is brought to another temperature and lower pressure in the presence of a catalyst, in a process called dehydrogenation. The results of the dehydrogenation are the hydrogen atom and the original LOHC, which can be used again (Langmi et al. (2021), Usman (2022)). The working principle of hydrogen storage using LOHCs is schematically shown in Fig. 3.14

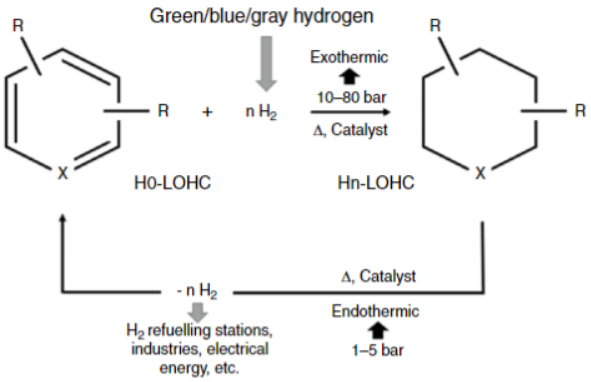

Figure 3.14: Schematic overview of the hydrogenation and dehydrogenation using a liquid organic hydrogen carrier (Langmi et al. (2021)).

Hydrogen can also be bonded to hydrides. These can be either metal hydrides or chemical hydrides. With metal hydrides, the hydrogen molecule splits into two hydrogen atoms. These hydrogen atoms diffuse into the metal structure as shown in Fig. 3.15. Because of these strong bonds, more energy is needed to store and release the hydrogen of the hydrides, but it also allows high storage capacities, even at ambient conditions (Usman (2022)). Metal hydrides can be classified into three groups, namely intermetallic hydrides, binary hydrides and complex metal hydrides, each with their specific attributes (Langmi et al. (2021)).

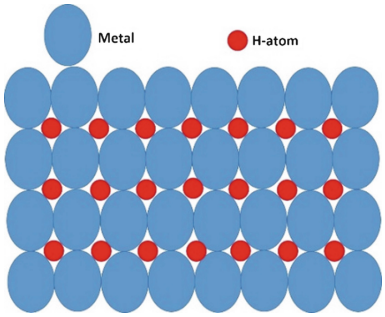

Figure 3.15: Hydrogen atoms diffused in the metal (S. & Demirocak (2017)).

The most important chemical hydrides are methanol, ammonia and formic acid. Methanol synthesis is a process whereby CO_x is combined with hydrogen molecules (Behrens (2016)) to form methanol and, depending on the number of hydrogen molecules, water. It allows a hydrogen volumetric storage capacity of 99 kg/m^3 (Andersson & Grönkvist (2019)). The dehydrogenation of methanol can have different pathways. It can be done via steam reforming, partial oxidation or methanol thermolysis. The hydrolysis of methyl formate produces formic acid. This is performed with a catalyst. Formic acid has a lower volumetric storage capacity than methanol, namely 53 kg/m^3, but has the advantage that the dehydrogenation step can be performed at ambient temperatures (Andersson & Grönkvist (2019)). The process of producing ammonia is called the Haber-Bosch process, which originates from the 1900s (Langmi et al. (2021)). Ammonia has a volumetric hydrogen storage capacity of 123 kg/m^3 (Andersson & Grönkvist (2019)). Since ammonia has been used for a long time already, the handling, storage and transport of ammonia are all mature technologies with a high TRL.

3.6 Transport

Offshore hydrogen transport is mainly possible in two different forms. Firstly, hydrogen can be compressed and transported via pipelines. These pipelines can either be new or repurposed from the existing gas network in the North Sea. These are described in Sections 3.6.1 and 3.6.2, respectively. Another option is to transport the hydrogen via ships. To do this, the hydrogen is either liquified, compressed, or bonded to a hydrogen carrier. This is discussed in Section 3.6.3. Finally, the transport of electrons to shore via high voltage cables is discussed in Section 3.6.4 for the onshore scenario.

3.6.1 Hydrogen Transportation via New Pipelines

The offshore-produced hydrogen can be transported to shore via new hydrogen pipelines. These pipelines must be made of a material that can withstand the diffusion of hydrogen atoms and hydrogen embrittlement.

Diffusion occurs when damage to the pipeline is done, and a (small) hole originates. The gas, in this case, hydrogen, leaks through the hole out of the pipeline. Due to the lightweight of hydrogen atoms, diffusion through the pipelines is 1.3 to 2.8 times larger than that of methane under the same conditions (labidine Messaoudani et al. (2016)). As described in Section 3.5.3, hydrogen embrittlement is the adsorption of hydrogen atoms by a metal, causing the minimal stress to create cracks to be lowered, which results in the embrittlement of the metal (Popov et al. (2018)). To extend the lifespan of the hydrogen pipelines, regular inspections should be carried out to detect possible hydrogen embrittlement.

Because hydrogen has a very low volumetric energy density of 10.79 MJ/m^3 at atmospheric temperature and pressure, the hydrogen is compressed when transported through a pipeline. This allows for far greater pipeline capacities. Therefore, compressors might be needed to compress the offshore-produced hydrogen to a higher pressure than it is outputted at the electrolyser. Because of pressure drops, multiple compressors might be necessary. A pressure drop over a pipeline is the difference in pressure from when a fluid is inputted in the pipeline and the pressure at the endpoint.

The pipeline energy flow is described by Equation 3.10 (Ibrahim et al. (2022)).

$$Q = V_0 \rho(HHV) = A\nu\rho(HHV) \tag{3.10}$$

In this equation, V_0 is the volumetric flow rate in m^3/s, ρ is the density in kg/m^3, HHV is the higher heating value, A is the cross-sectional area of the pipeline in m^2 and ν is the flow velocity in m/s.

The Reynolds number of the flow through a pipeline is given by Equation 3.11.

$$Re = \frac{\rho\nu D}{\eta} \tag{3.11}$$

Where ρ is the density in kg/m^3, ν is the flow velocity in m/s, D is the pipeline diameter in m and η is the dynamic viscosity in $kg/(m.s)$

If the Reynolds number exceeds 2000, which it almost always does with the sizes of offshore pipelines and the properties of hydrogen, the needed pumping power for turbulent flow is given by Equation 3.12 in W.

$$N = V_0 \delta p = A\nu\delta p = \frac{p}{4} D^2 \nu \delta p = \frac{\frac{p}{4} D^2 \nu \frac{L}{D}}{2} \rho \nu^2 \zeta \tag{3.12}$$

Where δp is the pressure drop in Pa, L is the pipeline length in m and ζ is the resistance coefficient.

As described in Section 3.1.2, hydrogen pipelines over long distances are static, but when connected to a floating structure, can also be dynamic. With both static and dynamic pipelines, a lot of experience has already been taken up by the oil and gas industry, and pipelines over long distances and deep depths already exist.

3.6.2 Hydrogen Transportation via Existing Pipelines

Because of a long history of oil and gas extraction on the Dutch North Sea, a lot of infrastructure is present in the North Sea. This infrastructure consists of platforms, oil and gas fields and pipelines. All of this infrastructure can be used for offshore hydrogen production. Since the extraction of oil and gas should become less every year (and eventually zero), it should be looked into converting this infrastructure for another use. To contribute to an offshore hydrogen value chain, the exhausted oil and gas fields could be used for offshore hydrogen storage as described in Section 3.5.1, old platforms could be used as offshore hydrogen production platforms, as mentioned in Section 3.1.2 and will be described in Section 3.7.2 in more detail, and the old oil and gas pipelines could be used to transport hydrogen.

Out of the many pipelines in the Dutch North Sea, two have been certified to be used for hydrogen transport. These are large-diameter pipelines from NGT and NOGAT. The NOGAT pipeline has a diameter of 24 inches and lands in Den Helder, and the NGT pipeline is 36 inches and lands in Eemshaven. These pipelines are already connected to empty gas fields, which can be used for large-scale hydrogen storage. They are also close to potential offshore salt cavern locations, which could be connected for hydrogen storage. When the storage facilities are used to create a baseload hydrogen supply to shore through the pipelines, it is estimated that the NGT pipeline could have a capacity of 17-24 GW, and the NOGAT pipeline a capacity of 17-20GW (NOGAT (2022)). Figure 3.16 shows the location of the pipelines, as well as the confirmed search areas for offshore wind farms.

Figure 3.16: NGT and NOGAT pipelines and the search areas of offshore wind farms (NOGAT (2022)).

Other pipelines of the Dutch North Sea infrastructure could later also be certified to allow hydrogen transport. Several factors must be considered to use a repurposed gas pipeline as a hydrogen pipeline. First of all, hydrogen embrittlement may occur. To avoid this, an inner coating can be applied to the pipeline, it can be intelligently monitored, the operating pressure can be managed, or degradation inhibitors could be mixed into the hydrogen (A.C.E.R. (2021),labidine Messaoudani et al. (2016)). Besides hydrogen embrittlement, hydrogen-enhanced fatigue can also occur by pressure variations and/or high pressures. This can be avoided by the same precautions as for hydrogen embrittlement, but the maximum operating pressure and the allowable pressure variations can be determined per pipeline to adjust the pipeline operation to them. The way inline inspections are carried out to find pipeline cracks might also have to be changed to be safe for hydrogen (HyWay27 (2021),ENTSOG et al. (2021)).

Secondly, some parts of the infrastructure might be more sensitive to the leakage of hydrogen atoms than methane atoms due to the smaller size of the hydrogen atoms. Examples of these parts are O-rings, membranes and valves. These parts will have to be checked for compatibility with hydrogen transport and replaced if necessary (HyWay27 (2021),ENTSOG et al. (2021)).

Thirdly, the gas pipelines might have to be extensively cleaned. Natural gas can have small traces of other atoms since a high purity of natural gas is usually unnecessary. An example is sulphur residues, which are added for the odorisation of natural gas. Hydrogen often does need high purities, and therefore, the pipelines would have to be extensively cleaned before using them for hydrogen transport (HyWay27 (2021)).

Fourthly, because of the lower energy density of hydrogen compared to methane, the flow speed of the transported hydrogen will be higher to reach the same pipeline capacities. The higher flow speed, in combination with the overall lower density of hydrogen compared to methane, has two consequences. Measurement devices along the pipelines might have to be replaced to be able to measure the hydrogen that travels faster than the methane and has a different gas composure. Also, the compressors might have to be replaced if the capacity of the pipeline is to be increased (HyWay27 (2021),Walters et al. (2020b),A.C.E.R. (2021),ENTSOG et al. (2021)).

Finally, due to the high flammability and colourless flame when hydrogen burns, extra precautions have to be taken compared to natural gas pipeline operations. The technicians working on the pipeline require different training, some methods when handling the pipelines have to be changed, and some machinery for working on the pipelines has different requirements and would have to be replaced (HyWay27 (2021),labidine Messaoudani et al. (2016)).

3.6.3 Hydrogen Transportation via Shipping

If an island is chosen as the layout of the hydrogen distribution hub, a port can be constructed from where hydrogen could be transported. Because of the low energy density of hydrogen, it is inefficient to transport the hydrogen without conversion. The gaseous hydrogen can be converted and shipped in any form described by Section 3.5.3. The conversion of hydrogen before it is loaded onto a ship is called the 'packing' of hydrogen and would have to be done at the hydrogen distribution hub island. The reconversion of the hydrogen derivative back to gaseous hydrogen is called 'unpacking' and is done onshore at the demand side of the hydrogen.

The hydrogen can be bonded to a liquid organic hydrogen carrier. This technology allows for easy ship transportation as the liquid is non-toxic, inexpensive, has a high energy density and has a lifetime of many cycles. Also, existing pumps and terminals can be used for the handling of LOHCs. The LOHC is relatively heavy, however, so more fuel is used by the ships than with other hydrogen carriers. The LOHC can be used again when the hydrogen is unpacked, which in principle is positive, but the ship has to ship back with a full load of LOHC, meaning it still weighs a lot and uses a lot of fuel, and it cannot take other cargo on its way back (Wang et al. (2021), ENTSOG et al. (2021)).

Hydrogen can also be liquified and transported by ship in its liquid form. To liquify the hydrogen, it is cooled down to -253°C and compressed. To keep it in that state, the ships must have well-insulated and pressurised tanks. Even with well-insulated and pressurised tanks, some hydrogen boils off. This boil-off can be used to power the ship, but usually, more hydrogen boils off and it needs to be released, as otherwise, pressures in the tank become too high. Liquid hydrogen ships are very similar to LNG tankers (Wang et al. (2021), ENTSOG et al. (2021)).

Hydrogen can also be converted to ammonia by having gaseous hydrogen react with gaseous nitrogen by the Haber-Bosch process. Ammonia liquifies at -33°C and has to be kept below that temperature by well-insulated tanks. Ammonia is already shipped in large quantities worldwide, and much experience has been gained. Also, infrastructure already exists and is proven. Ammonia can also be used to fuel the ship, and fuel demand is higher than the boil-off rate. The unpacking of ammonia is done via ammonia cracking. Ammonia cracking has very limited experience, however, and has yet to be proven at a large scale (Wang et al. (2021),ENTSOG et al. (2021)).

3.6.4 Electricity Transportation via Cables

Electricity is transported over large lengths at high voltages. This is done to minimise the dissipative losses in the cables. These losses depend on the type of conductor, cable length, cross-section and current type. A cable is considered high-voltage if it operates in the range of 35-800 kV (Ardelean et al. (2015)).

HVAC transformer stations have fewer losses and are cheaper than HVDC transformer stations. However, due to the skin effect and self-induced reactance, HVAC cables require a larger cross-sectional area than HVDC cables of the same amperage. The skin effect is the phenomenon that HVDC cables conduct over their entire cross-sectional area, but HVAC only conduct towards their surface, leaving a non-conducting zone in the centre of their cross-section (Ardelean et al. (2015)). The HVAC cables are thus more costly per unit length (Ibrahim et al. (2022)). A break-even point between HVDC cables and HVAC cables can be found, at which the extra costs per unit length of the HVAC cable break even with the lower transformer station costs. This distance was found to be between 50 - 60 km for submarine cables (Administration (2018), Sluis (2008)). Figure 3.17 shows the visualisation of the break-even point (The report of the figure found a break-even point of 50km for submarine cables). The initial costs for the HVDC substations are larger than those of the HVAC cables, but the costs per unit length are less.

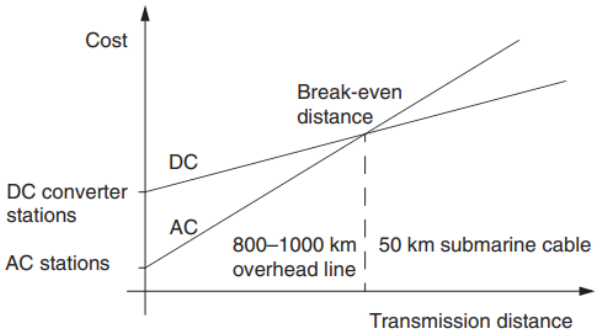

Figure 3.17: Visualisation of the break-even point between HVAC and HVDC cables. HVDC have higher substation investment costs but lower cost per unit length (Sluis (2008)).

Currently, the 525kV XLPE DC cables are considered the best available cables for the connection of offshore wind farms by the Dutch electricity transmission system operator TenneT. These cables can either be laid bundled or unbundled with a metallic return. The bundled layout is preferred because of its lower ecological footprint and installation costs (TenneT (2019)). For the landing of HVDC and HVAC cables, safety distances are in place between the cables and other structures. These safety distances apply to three different situations: The distance between cables offshore, the distance between cables near shore and the distance between cables onshore. For offshore 525 kV 2GW HVDC cables, 200 meters should be between each cable and a safety contour of 500m to both end sides is in place. For 220kV HVAC, those safety distances are the same, except for the distance to a hydrogen pipeline, which has to be 1000 meters instead of 500 meters. For the near-shore situation, 50 meters should be between each HVDC cable and a safety contour of 200 meters to each end side. For HVAC cables, the same spacing applies, but an outside contour of 400 meters is applied (HaskoningDHV (2021)).

3.7 Hydrogen Distribution Hub

When an offshore centralised configuration is used, the electricity is centralised and converted to hydrogen. From this centralised location, the hydrogen will be further transported to shore. The centralised location at which the hydrogen is produced and further transported is called a hydrogen distribution hub in this thesis. A hydrogen distribution hub can have several configurations, each of which is described in this Section. Section 3.7.1 describes the use of an offshore island made with sand, after which Section 3.7.2 describes the use of one or multiple offshore platforms. These can either be new or repurposed.

3.7.1 Island

The energy island can be used in the offshore centralised configuration. One wind farm can be connected, or the electricity of multiple wind farms can land on the island. Since the costs of making an island are significant, the most logical option is to have multiple wind farms connected. The electrolysers are placed on the island to convert the electricity into hydrogen.

Four main parts are needed to construct an offshore island. A revetment is needed to protect the island from waves and storms. Because conditions offshore on the North Sea can be much more harsh than at the coastline, stronger revetments are needed than for land expansion projects near shore. The bottom layer of the total island area comprises sand reclamation because this is cheaper than the layers coming on top of that. Under the revetment, a layer of rocks or concrete is used to strengthen the revetment and protect the island. Above the sand reclamation within the borders of the revetment, sandfill is used as a building material for the island. Finally, a port basin is also to be added to the island for access and possible shipping of products. The port basin is to be constructed on the lee side of the island regarding the wind and storms for protection. The size of the quays and protective breakwater that make up the port basin should be determined based on the use of the island and the consequent size of the ships. With these main building blocks, three types of islands can be constructed, namely a terp island, a polder island and a lagoon island. The polder island uses caissons filled with sand reclamation as part of the revetment (IJVERGAS (2020)). Figure 3.18 shows what an offshore energy island might look like.

Figure 3.18: Render of a possible layout of an offshore energy island (Vindo (2021)).

The island can have multiple uses besides hydrogen production to benefit the overall costs. It should at least include an HVDC power conversion station, cable landing facilities, hydrogen pipeline facilities and hydrogen production facilities, but could also include a maintenance basis from which maintenance to the offshore wind parks and offshore power facilities can be done, a data centre, hydrogen storage facilities or a coast guard basis to name a few.

3.7.2 (Old) Platform

Offshore platforms can also be used as an energy hub. The platforms can either be repurposed oil or gas platforms, which are abundantly present in the Dutch North Sea, or can be newly constructed. The offshore platforms can be used in the centralised offshore topology. For this topology, the electricity from a wind farm will be bundled and fed to an electrolyser on the platform. The entire balance of plant, as described in Section 3.4, will then be on the platform.

There are oil and gas platforms of different sizes. The larger platforms could host the hydrogen production facilities, whereas the smaller platforms could function as offshore electrical substations. When the platforms are at the end of their lifetime, they could be retrofitted for offshore hydrogen production instead of being decommissioned. There are multiple ongoing pieces of research and planned pilots regarding offshore hydrogen production on old platforms since the industry has yet gained little experience. Since some platforms differ regarding lifetime, equipment present, electrically interconnected and distance to the wind farm, a specific case study per project is to be done (Henry et al. (2022)). To repurpose an old platform, it is to be stripped

of all unnecessary equipment, leaving as much room as possible for the hydrogen production equipment. A platform usually consists of multiple floors and a foot structure and has a weight restriction that is to be accounted for.

When placing new platforms, they can be optimally designed for hydrogen production facilities. Also, their location regarding the wind farm(s) has a greater degree of freedom.

Although still uncertain and dependent on technological improvements, designs of 300-500 MW scale platforms have already been made (Buijs et al. (2022),Tractebel (2021)). Depending on the size of the wind farm, multiple platforms might be needed close to the wind farm. When building new platforms, they can be built next to each other and connected via a bridge for accessibility and maintenance. Figure 3.19 shows the possible layout of an offshore hydrogen production plant.

Figure 3.19: Render of a possible layout of an offshore hydrogen production platform(Tractebel (2021)).

When placing new platforms, floating platforms can also be considered. From the oil and gas industry, a lot of experience has already been taken up regarding the building of platforms. Conventional fixed structures are used up to depths of over 400 meters deep, and floating structures only are applied from those depths (Amaechi et al. (2022)). As can be seen in Figure 3.20, these depths are only reached around the shore of Norway and up north at the Norwegian Sea and the North Atlantic Ocean, which are all outside the search area of this thesis.

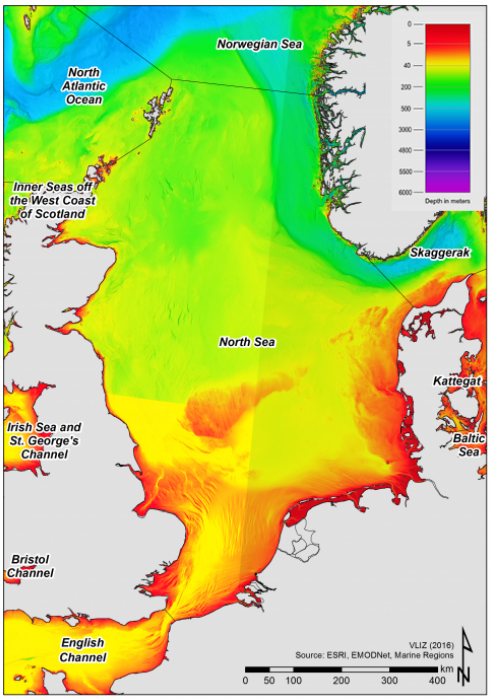

Figure 3.20: Map of the North Sea depth in meters depth (Marineregions.org (2016)).

4 Research Approach

In this Chapter, the research approach of this thesis is explained. Firstly, in Section 4.1, the overall framework of the thesis is given. After this, the more specific methodology of the building blocks of the overall framework is explained. This starts with the data gathering in Section 4.2, followed by the design selection in Section 4.3 and the modelling in Section 4.4. Finally, the outcome analysis is explained in Section 4.5.

4.1 Overall Framework

The goal of this thesis is to come up with a design to produce hydrogen offshore and see whether it is competitive with onshore hydrogen production from offshore wind farms. To do this, four phases have been identified and are indicated per colour in Fig. 4.1.

The first phase of this thesis is data gathering. This consists of the theoretical background, the literature review and interviews. In this phase, the knowledge from literature about the technologies for all components of the offshore hydrogen production value chain is gathered. Research on theoretical background yields literature on the value chain components. The components of the value chain have been identified in this step as the electrolyser, the water feed, the electrolyser system configuration, storage and transport. Apart from this, when a central electrolyser configuration is used, there is a design choice between platform(s) or an artificial island to house the electrolysers. The literature review then yields the working principles and parameters of these components, as well as the pros and cons of these technologies. This is used in the modelling, as well as in constructing the decision framework. Finally, interviews with several companies are conducted to gain their view on the different technologies. This is also an input to the decision framework. In the first phase, data gathering, the first subquestion of this thesis is answered.

The second phase, design selection, is indicated by the green blocks in Fig. 4.1. Using the inputs from the data gathering phase, a decision framework is constructed. The decision framework is made based on a multi-criteria decision analysis (MCDA). The MCDA is performed per component of the value chain, as described. The criteria that are used for the MCDA can differ per component, as different aspects can be of importance. The weight factors of the criteria used in the MCDA are based on the best-worst method, which offers a structured way to come to comparisons with a high consistency Rezaei (2015a) and will be described in more detail in Section 4.3. The decision framework yields the preferred technology per value chain component. Using this, a preferred design is constructed, as well as two other designs, for a total of three, that are used as input for the modelling phase. It is chosen to come to three designs, with a hard criterion set that every design should have a different electrolyser system configuration since this has the largest impact on the total design. This also shows the difference between the onshore configuration and offshore configurations. The first design combines the best scoring technologies of the MCDA. The second and third designs are made by starting with the other remaining electrolyser system configurations and constructing a design around it using the MCDA scores. With the second and third designs, the interactions between the components are also taken into account. Because of these interactions, it is possible that the best technologies per component do not perform as well as another set of technologies when looking at the performance of the total value chain. In the design selection phase, the second subquestion of this thesis is answered.

The third phase is indicated by the blue blocks and is the modleling. The design layouts and value chain component parameters from the first two phases are used as input to come to a simulation model of the designs. The model is made from the ground up in MATLAB. The first part of the model is electricity generation, in which the wind profiles and fixed wind farms are used to simulate electricity generation. Secondly, in the hydrogen generation part, the electricity is used to come to hydrogen production using the electrolyser parameters. The value chain components are sized in the third part using the components' parameters and the amount of hydrogen produced. The final part consists of the cost function and output of the system cost, component costs and LCOH. The model is described in more detail in Section 4.4. The third subquestion is answered in this phase.

In the fourth and final phase, the outcome analysis, the results are computed, analysed and compared. This phase is indicated by the red blocks in Fig. 4.1. Firstly, the technical and economical outcomes of the model are analysed and processed. This results in the LCOH, which is in turn used to present the results, and also to perform a scenario and sensitivity analysis. Apart from the model outputs, the decision framework outputs are used in this phase to present the preferred design, and analyse the system integration of all three designs. In this phase, the fourth and fifth subquestions are answered, as well as the main research question.

A total overview of the methodology of this thesis in building blocks is given in Fig. 4.1, with the colours indicating the phases.

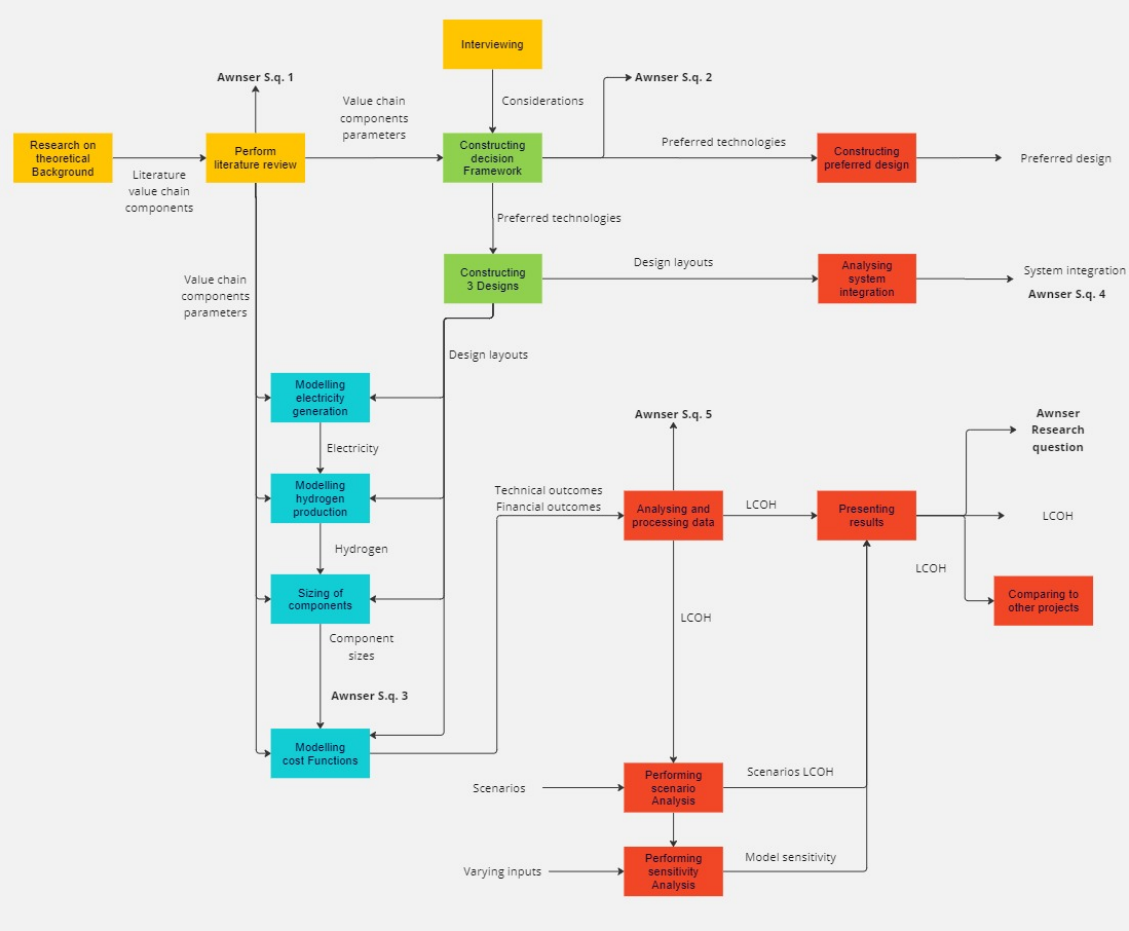

Figure 4.1: Schematic overview of the overall framework of this research. Yellow blocks correspond to the first phase: data gathering, the green blocks correspond to the second phase: design selection, and the blue blocks correspond to the third phase: modelling. Finally, the red blocks correspond to the fourth phase: outcome analysis.

4.2 Data Gathering

The theoretical background has been collected in the following order. Firstly, a wide search of ongoing or planned hydrogen production projects has been done to gain a first understanding of those kinds of projects. With this, a first understanding of possible components in the value chain has also been taken up. After this, specifically, offshore hydrogen production projects and papers have been looked up. This gave more insights into the specific offshore value chain components. Once all the components of the value chain were identified, the different technologies per component were looked into. This resulted in the description of the working principle per technology. They have been grouped per component of the value chain in Chapter 3. This list of technologies per component will be used as input to the decision framework, where all of the technologies will be rated per component.

4.2.1 Port of Rotterdam

This thesis was written during a graduation internship at the Port of Rotterdam. During the internship at the Port of Rotterdam, interviews with companies that are active in the Port of Rotterdam were held. Also, two conferences and a symposium were visited with the Port of Rotterdam. Finally, during the internship, the project team of the Rotterdam Wind Power Hub was joined.

Interviews and meetings were held at the start of the internship. An interview was held with Lhyfe, a company that deployed the first offshore hydrogen production pilot in France. Issues and considerations of offshore hydrogen production were discussed. The considerations were taken up and kept in mind when making the decision framework. Also, an interview with TNO was held. TNO is an independent research organisation conducting research into offshore hydrogen production. TNO is also part of the PosHYdon pilot. The PosHYdon pilot will have an electrolyser on an offshore platform off the Dutch coast. Issues and considerations were again discussed and taken into account when constructing the decision framework. The Port of Rotterdam is part of the North Sea Energy program. In this program, 40 international parties collaborate to investigate the potential of the North Sea for an integrated energy system. Internal documents

from the North Sea Energy program regarding offshore hydrogen production were consulted. Also, interviews were held with people from the Port of Rotterdam who contributed to the North Sea Energy program. Apart from the North Sea Energy program, a lot of specific knowledge was present at the Port of Rotterdam regarding multiple components of the offshore value chain, and these components have been discussed with internal experts at the Port of Rotterdam.

Two conferences were visited with the Port of Rotterdam. Firstly, the Offshore Energy Exhibition & Conference in Amsterdam was visited. This is a leading conference in Europe for the entire offshore energy industry. The visit to this conference was at the start of this thesis, and discussions with several companies and experts were held, gaining insights into offshore hydrogen production. Also, panel discussions were visited. The second conference visited was the World Hydrogen Summit in Rotterdam. This conference was later in the process of this thesis, and more specific considerations of offshore hydrogen production were discussed with companies and experts. Finally, a symposium in Rotterdam about hydrogen value chains was attended, as well as an online webinar about offshore wind energy from the Dutch Ministry of Economic Affairs and Climate Policy.

The project team of the Rotterdam Wind Power Hub was joined during the graduation internship. This project team investigates the possibility of constructing the Rotterdam Wind Power Hub, an extension of the Maasvlakte to house electrolysers coupled to offshore wind farms. The findings from this project team served as input for the decision framework and the onshore central configuration. With this project team, special focus was on programs from the Dutch government, such as the 'Programma Verkenning Aanlanding Wind op zee' (VAWOZ) and 'Programma Energiehoofdstructuur' (PEH). In the VAWOZ program, the Dutch government investigates the landing of offshore wind energy in both electricity and hydrogen. The PEH program establishes frameworks for the spatial integration of new energy infrastructure. In these programs, insights into the offshore hydrogen production value chain were gained. With the RWPH project team, two workshops were organised with industry players. The industry players were companies that are active in the hydrogen production value chain. The goal of these workshops was the opportunity framing of the RWPH. Issues and considerations of central onshore hydrogen production, as well as offshore hydrogen production, were discussed with the companies.

The activities during the internship at the Port of Rotterdam firstly helped to develop a clear perspective of offshore hydrogen production and the possible value chain components through internal documents, talks and interviews. Secondly, from talks and interviews with companies through the Port of Rotterdam, the conferences and workshops, a lot was learned about the considerations and issues that companies foresee for offshore hydrogen production. These considerations and issues were taken into account in the decision framework. Some of the considerations and issues were taken into account in the scenario analysis. Apart from the interviews with companies, a lot of considerations were also gathered while working with the Rotterdam Wind Power Hub team. These considerations regarded the onshore central configurations that were investigated by the project team, but also broader considerations about hydrogen production or space availabilities in the port area.

4.3 Design Selection

To come to the offshore designs, a multicriteria decision analysis is done. A multi-criteria decision analysis was chosen because it offers a well-structured process that can handle mixed sets of data and leads to rational and justifiable decisions (Blagojević et al. (2019),Gongora-Salazar et al. (2022)). The stakeholder perspective is taken from the perspective of the Port of Rotterdam. However, the Port of Rotterdam will not construct an offshore hydrogen production value chain itself, and the stakeholder perspective arises from the port's desire to align its infrastructure with the future demands of the industry. By adopting a stakeholder approach, the analysis reflects what is most likely to be undertaken by industry players and the Dutch government. Therefore, considerations from interviews with companies have also been taken into account. The MCDA is executed per component of the offshore hydrogen production value chain. Each component has a different contribution to the total value chain, and therefore, the criteria that are used per component might differ. For every component the MCDA is executed, a preferred technology is the output. Since the technologies of the components can also interact with each other, three designs are constructed from the output of the MCDAs since the combination of the preferred technologies does not have to be the best-performing total system per se. The criteria that are considered per component of the offshore value chain are given in Table 4.1.

	Electrolyser technology	Water feed	Electrolyser system configuration	Storage	Transprot	Hydrogen distribution hub
Cost	Yes	Yes	Yes	Yes	Yes	Yes
Technical	Yes	Yes	Yes	Yes	Yes	Yes
Flexibility	Yes	-	Yes	-	-	-
Safety	Yes	Yes	Yes	Yes	Yes	Yes
Maintenance	Yes	Yes	Yes	Yes	Yes	Yes
Environment	-	Yes	-	Yes	Yes	Yes
Durability	Yes	-	-	-	-	-

Table 4.1: Overview of the criteria per offshore value chain component that is used for the Multi-criteria-decision-analysis.

For each component of the value chain, criteria are chosen, which are further decomposed into sub-criteria. If two or more sub-criteria are present under a criterion, a weighted score is constructed for the criterion based on the scores of the sub-criteria. These scores are based on quantitative values per sub-criterion or qualitative descriptive text. The scores range from zero to one, with zero being the lowest, worst performing score, and one the best possible score. If three or more sub-criteria are present, the best-worst method is used to come to the weights per sub-criterion. This method offers a systematic and consistent approach to determining the weight factors and is further described in more detail below. If two sub-criteria are present, the weights are assigned manually. The sum of these weights equals 1, so the scores multiplied by the weights are between zero and one. If a criterion does not have sub-criteria, no weighted average is needed.

When the criteria scores are gathered, a matrix is constructed with the criteria and the technologies per component. In this matrix, the scores gathered in the last step are summarised, and weights are assigned per criterion. To come to these weights, the best-worst method is used. The weighted score per criterion is the criterion's weight times the technology's score for that criterion. When all the weighted scores per technology are summed, a preferred technology is the technology with the highest total score.

As previously stated, to come to the scores per (sub-)criteria, there are two options. If the (sub-)criterion is quantitative, the best-performing technology serves as a basis for normalising the scores. Using this method, every technology gets a value between one and zero, with one being the best and zero the worst possible score. This is shown by Eqs. 4.1 and 4.2. It should be noted that depending on whether it is preferable for the (sub-)criterion to have a maximal or minimal value, Eq. 4.1 or Eq. 4.2 should be used to come to a normalised score between one and zero. As an example, the cost is preferred to be as low as possible, and thus Eq. 4.1 is used. For efficiency, the preference is to be as high as possible, and Eq. 4.2 is used to come to normalised scores.

$$Score_j = \frac{N_{best}}{N_j} \tag{4.1}$$

$$Score_j = \frac{N_j}{N_{best}} \tag{4.2}$$

If the criterion is quantitative, it can be ranked within five categories very poor, poor, average, good, and very good. These categories are then qualified by giving 0, 0.25, 0.5, 0.75, and 1 points as a score, respectively, one being the best-performing technology and 0 for the worst-performing technology. An overview is given in Table 4.2.

Description	Score
Very poor	0
Poor	0.25
Average	0.50
Good	0.75
Very good	1

Table 4.2: Conversion table for qualifying quantitative criteria

The weight factors of the MCDA are determined by the best-worst method when there are more than two (sub-)criteria. The best-worst method can provide a systematic approach to determine the strength of the weight factors. Determining the strength can be one of the main sources of inconsistencies with multi-criteria decision-making (Rezaei (2015b)). To perform the best-worst method, firstly, the (sub-)criteria are determined. Then, the most important and the least important (sub-)criteria are identified. Thirdly, the

preference of the most important (sub-)criteria over all of the other (sub-)criteria is indicated by a number between 1 and 9, and the preference of all of the (sub-)criteria over the least important (sub-)criteria is also indicated by a number between 1 and 9. In this method, the most important criterion is indicated as best, and the least important criterion is indicated as worst. This results in a '*Best-to-Others*' vector, and a '*Others-to-Worst*' vector respectively. In the final step, the optimal weights are found. For each pair of w_B/w_j and w_j/w_W, the following should hold $w_B/w_j = a_{Bj}$ and $w_j/w_W = a_{jw}$, where w indicates the weights, and the subscripts B, W and j indicate the best, worst and any other criterion respectively. To satisfy the conditions for all j, the absolute difference between $\left|\frac{w_B}{w_j} - a_{Bj}\right|$ and $\left|\frac{w_j}{w_W} - a_{jW}\right|$ should be minimised. This results in the following problem that has to be solved for the optimal weights and ξ.

$$
\begin{aligned}
\min \quad & \xi \\
\text{s.t.} \quad & \left|\frac{w_B}{w_j} - a_{Bj}\right| \leq \xi, \text{ for all j}, \\
& \left|\frac{w_j}{w_W} - a_{jW}\right| \leq \xi, \text{ for all j}, \\
& \sum_j w_j = 1, \\
& w_j \geq 0, \text{ for all j}
\end{aligned}
\tag{4.3}
$$

Where ξ is the consistency index that should be minimised.

To solve this problem, an open-source tool of the best-worst method is used (Rezaei (2015a)). In this Excel tool, the (sub-)criteria can be entered manually. The relative scores between one and nine can also be entered manually. The tool then gives the consistency index and shows whether it is acceptable or not. This depends on the consistency threshold that applies to the amount of (sub-)criteria used and the highest and lowest relative score given. A solver add-in by Excel is then used to solve for the weights per (sub-)criterion.

Once the scores and weights of the decision framework are determined, the decision framework is used to come to the designs. The first design combines the technologies with the highest MCDA score. Per component of the value chain, the highest scoring technology is chosen, such that a design of the value chain is made by combining these technologies. For the second and third designs, the hard criterion is set that all three electrolyser system configurations are to be used in the model. This is done because the electrolyser system configuration is the most interesting component of the value chain to compare designs and has the most impact on the other components. The second and third designs take the electrolyser system configuration as a starting point, and combined with the decision framework, designs that also take the interactions of the value chain components into account are constructed.

4.3.1 Boundary Conditions

The three designs thus have different technologies used in their value chain. There are, however, also some conditions that apply to all three designs. These conditions are set to come to a fair comparison between the results of the model of each design. The first boundary conditions for all three designs are the size and location of the wind farms. In total, 10 GW rated power of wind turbines are placed. This is distributed over five wind farms so that each wind farm has a rated power of 2 GW. To set the location of the wind farms, the search areas for wind farms of the Dutch government after 2030 are used as an indication of the transportation lengths and wind profile but are not used directly. Since the offshore wind farm design is outside the scope of this thesis and because it is uncertain which search areas can be used, it is chosen that all wind farms have a distance of 20 km to a central point between the wind farms. For the offshore configurations, this central point is the starting point of the transportation pipeline to shore. Wind speed data, which is measured from a station close to the search areas, is looked up. Also, the wind farm layout is the same for each design. The spacing between each wind turbine is seven times the rotor diameter (Bussel (2006)). The distance between offshore wind turbines is set to minimise the impact of the wake effects. The wake effects themselves are not considered in this thesis for simplicity.

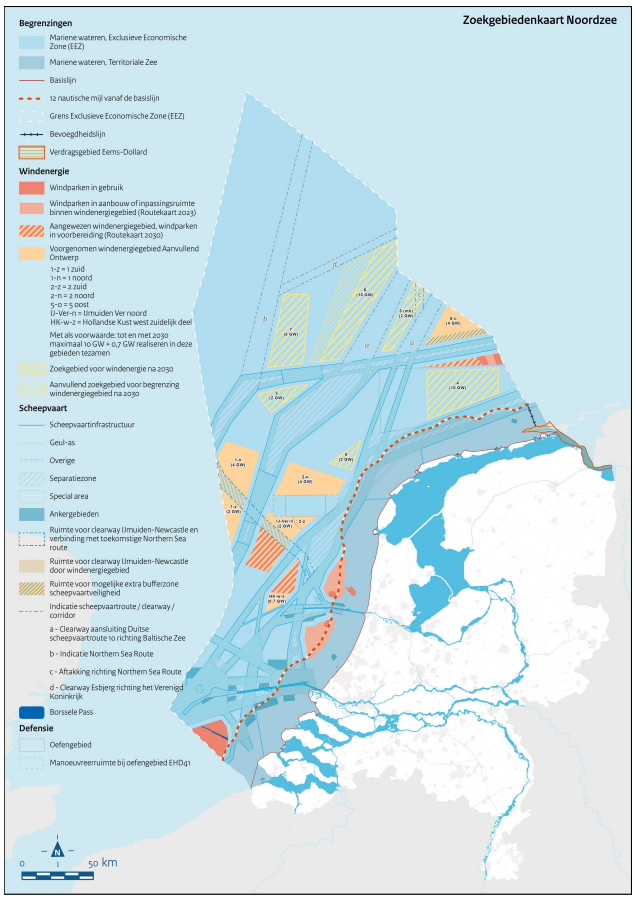

Figure 4.2: Search areas of wind farms on the Dutch North Sea after 2030. The yellow striped areas indicate the search areas for wind energy after 2030 (Rijksoverheid (2020)).

The second boundary condition is the wind turbine used within the wind farms. Over the years, wind turbines have grown in size and rated power. However, some limitations make it hard to grow beyond 15 MW for offshore wind turbines. Firstly, the blades cannot spin too fast because of erosion when they hit water droplets. So, as the blades get longer, the rotors would have to spin more slowly. Due to this, the blades have to be deflected more in order to produce the same amount of electricity. Due to this larger deflection, there are higher forces acting on the turbine, and the turbine would have to be strengthened by increasing the weight, thus increasing the cost. There is a point where the extra electricity produced does not weigh up to the extra costs, and the larger turbine becomes unprofitable. Secondly, because of the larger deflection, it is harder to design the turbine so that the blades do not hit the turbine under extreme weather conditions. Finally, to install larger turbines, larger port infrastructure and larger installation vessels that do not yet exist are needed. It is therefore chosen to use the 15MW NREL reference turbine as the turbine used in the model (Gaertner et al. (2020)). The important parameters from the turbine to be used are the rated power, to know the power produced by the turbine. The cut-in and cut-out wind speeds are used to construct the power curve of the turbine. The hub height is used to come to the corrected wind speed at hub height. The rotor swept area is used to come to the rated power of the turbine. The used parameters are given in Table 4.3. Since 15MW turbines are used, 133 wind turbines are used per wind farm to come to 1995 MW rated power per wind farm.

Wind turbine parameter	**Units**	**Value**
Rated power	MW	15
Cut-in wind speed	m/s	3
Cut-out wind speed	m/s	25
Rotor diameter	m	240
Hub height	m	150
Power coefficient	-	0.489

Table 4.3: Parameters of the NREL 15MW reference turbine that are used in the model (Gaertner et al. (2020)).

A third boundary condition of the designs is that the installed amount of electrolysers will be the same.

For the offshore decentral configuration, each wind turbine has its own small electrolyser. The summed installed capacity of the electrolysers is to be of the same size as the installed capacity of the electrolysers of the central configurations to be able to make a fair comparison.

A fourth boundary condition of the designs is that they supply the hydrogen to the landing location by a baseload. A baseload means that the flow of hydrogen is constant over a chosen time interval over the entire simulation time of the model. The baseload is constant over the time interval of an hour, which is also the time step of the model itself. This means that in every simulated time step of the model, the baseload of hydrogen supplied to the landing point is of the same size. The size of the baseload is an output of the model and is not a boundary condition. The industry that makes use of hydrogen in their processes would prefer to have a baseload supply if their processes are continuous. Also, it is assumed that the demand exceeds the baseload at every timestep. The entire baseload can be landed at the demand side at any time, and no part of the baseload has to be stored.

Furthermore, the location of the landing of the hydrogen onshore is kept constant over the designs. The hydrogen lands at the Port of Rotterdam. The hydrogen is brought to the Port of Rotterdam by a baseload. The distance of the Port of Rotterdam to the central point between the offshore wind farms is taken as 250km. As described in the first boundary condition, a central point between the wind farms is used for the offshore configurations, from which a large pipeline to the Port of Rotterdam starts. Apart from the location, the pressure with which the baseload lands onshore is kept constant over all the designs, and the compressors are sized on this. The landing pressure is chosen as 50 bar, as Gasunie has an intended pressure range of 35-50 bar for the Dutch hydrogen backbone onshore (HyWay27 (2021)).

Finally, the costs for the wind turbines are constant over every design. The CAPEX and OPEX are based on data from scenarios from the National Renewable Energy Laboratory (NREL (2022)), where the moderate scenario used 15 MW turbines.

4.4 Model

The model that is made in this thesis is a simulation model. The designs that are constructed are simulated by making a model in Matlab. With the parameters and equations of the selected components, a digital prototype is built. This digital prototype has been constructed entirely from the ground up without the use of pre-existing frameworks. The model uses wind speed data from a KNMI station as input and computes the production, transportation and storage of hydrogen and electricity. The hydrogen is to be supplied to shore via a baseload, which is used to meet an unlimited demand, meaning at every timestep, the baseload has off-take onshore. To supply the baseload, the technical part of the model determines the size of the baseload and the needed value chain component sizes. The financial part of the model calculates the costs associated with the sizings. The model simulates 30 years of operation of the value chain. Since some components have a shorter lifetime than 30 years, the lifetimes are considered in the model, and components are replaced when necessary.

This simulation model is deterministic, meaning that the behaviour of the components can be fully predicted. With the set of parameters and equations used in the model, the outcome will be the same over time, as no uncertainties or probabilities are involved. Furthermore, the model is dynamic, as the inputs and outputs are computed over time. The outputs of one instant serve as the inputs of other instances, and the system changes over time. Finally, the model is discrete since the wind profile is discrete in one-hour intervals; every calculation step is done with this interval.

The reason a simulation model was chosen is because these value chains on the North Sea have never been built before. First, a simulation model determines if these value chains on the North Sea are viable. If simulations show that there are very high costs for offshore-produced hydrogen, there is no need to optimise the system. But if the results from simulations show that offshore-produced hydrogen can compete with onshore projects price-wise, optimisation models can then be built to optimise the value chain in terms of location, size and components.

An overview of the model is shown in Fig. A.1 in Appendix A.

4.4.1 Generation

The first building block of the model is the generation. Hourly wind data is gathered from the KNMI weather station '201-D15-FA-1'. This weather station lies in the Dutch North Sea, around the search areas for future wind farms. The data from the KNMI station are given per hour. Since some data from 2022 was missing, the hourly average wind speeds from 2021 are used in the model. These hourly wind speeds are imported. The wind speeds are measured at a different height than the hub height of an offshore wind turbine. To estimate the wind speed at hub height, the wind speed at the measured height can be translated in two steps. Firstly, the logarithmic law is used to translate the windspeed at the measured height to the blending height. The blending height is a height until which the change in wind speed is affected by the local terrain roughness

Zaaijer et al. (2020). After this blending height, the wind speed is no longer affected by the local terrain roughness, and the power law is used in the second step instead of the logarithmic law. The logarithmic law is given in Eq. 4.4.

$$U(h) = U(h_{ref}) \cdot \frac{ln(\frac{h}{z_o})}{ln(\frac{h_{ref}}{z_o})} \tag{4.4}$$

Where U_h is the windspeed at the blending height of 60 meters, $U(h_{ref})$ is the windspeed at the height it was measured at the KNMI station in meters. h is the blending height of 60 meters, h_{ref} is the measurement height of the KNMI station, and z_o is the surface roughness, which is taken as 0.0002 meters for open sea (WebMet (n.d.)).

The power law is given in Eq. 4.5.

$$U(h) = U(h_{ref})(\frac{h}{h_{ref}})^{\alpha} \tag{4.5}$$

Where alpha is a coefficient and has a value of 0.11 for open sea (Zaaijer et al. (2020)). Here, $U(h_{ref})$ is the windspeed at a 60-meter height, and $U(h)$ is the windspeed at hub height.

Next, the power curve of a wind turbine is generated. Some parameters from the wind turbine are needed. Such as the rated power, which is the maximum power it can generate. The power coefficient of the turbine, which shows the efficiency of the wind turbine and usually lies between 0.4 and 0.5. The length of the turbine blades. The cut-in wind speed and the cut-out wind speed of the turbine. When the wind speed is too low, the rotors of the turbine do not move. The lowest wind speed with which the turbine will generate electricity is called the cut-in wind speed. When the wind speed becomes too high, the components within the turbine can be damaged and the turbine is turned off to prevent damage. This wind speed at which the turbine is turned off is called the cut-out wind speed. At the first part of the power curve, between the cut-in wind speed and the rated wind speed, the power of the turbine is maximized. Between the rated wind speed and cut-out wind speed, the generator is operating at full load, and therefore the power is constant. The power curve is shown in Fig. 4.3.

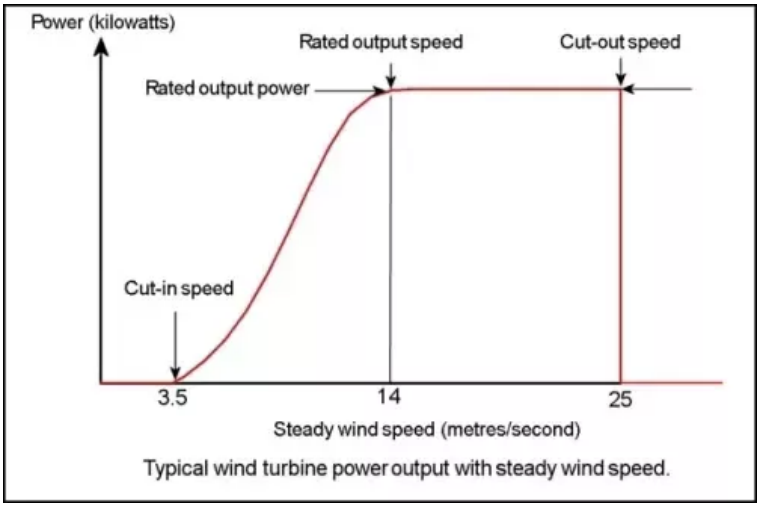

Figure 4.3: The power curve of a wind turbine (Cole (2022)).

To come to the power curve of the turbine that is used, first, the rated wind speed will be calculated using Eq. 4.4.1.

$$U_{rated} = (\frac{P_{rated}}{\frac{1}{2}\rho c_p A})^{\frac{1}{3}} \tag{4.6}$$

Where P_{rated} is the rated turbine power, ρ is the air density at hub height, c_p is the power coefficient of the turbine and A is the rotor swept area. With the rated wind speed, the wind turbine's power curve can be constructed. The described power curve is made in Matlab using the buckets between the named wind speeds: cut-in, rated and cut-out. The first bucket shows the wind speed (U) being below the cut-in wind speed (U_{in}), and thus the power (P) is zero. The second bucket shows the wind speed being between the cut-in wind speed and the rated wind speed (U_{rated}, and the power is given by Eq. 4.4.1.

$$P = \frac{1}{2}\rho c_p U^3 A \tag{4.7}$$

The third bucket is for the wind speed between the rated wind speed and the cut-out wind speed. Here, the turbine operates at rated power. Finally, above cut-out wind speed, the final bucket gives a power of zero.

With these buckets, the average wind speeds per hour from the KNMI data can be coupled to power using the formulas for the buckets. This yields the average power for that hour, which will be used to generate the electrical output. Since the data is in steps of hours, the electrical output is simply the power times one to come to Wh. Finally, the electrical output per turbine can be multiplied by the number of wind turbines in the wind farm by equation 4.8 to come to the total wind farm power. Using this method to sum the total wind farm power ignores the wake effect of the turbines in a wind farm for simplicity.

$$P_{farm} = \sum^{n_{turbines}} P_{turbine} \tag{4.8}$$

4.4.2 Power-to-Gas

To calculate the amount of hydrogen produced from the electricity that the wind farm generated, shown in Section 4.4.1, several steps are needed. Firstly, for the centralised offshore and onshore configuration, inter-array cables are used to collect the electricity per wind turbine at the farm. For the central offshore configuration, HVAC substation and cable losses are also present, while the onshore central configuration has HVDC substation and cable losses. The general formula for the cable losses is given in Eq. 4.9

$$Loss_{cable} = L_{cable} * f_{cablelosses} \tag{4.9}$$

Where L_{cable} is the cable length of which the losses are calculated expressed in km. $f_{cablelosses}$ is the cable loss factor for the cable over which the losses are calculated, expressed in %/km. The inter-array, HVAC and HVDC cables all have their specific cable loss factor and length depending on the configuration. The output of this formula is the % of the electricity lost by transportation through the inter-array cables.

As described in Section 3.1, the different electrolyser system configurations have a different number of electricity conversion steps. For the offshore decentral configuration, the AC output of the wind turbine is converted to 1000V DC power in one step. For the central offshore configuration, the power is either transported from the wind turbine by inter-array cables to the electrolyser on an offshore platform near the wind farm in three conversion steps or transported by both inter-array cables and HVAC cables to an island centrally located between multiple wind farms, in five conversion steps. Five conversion steps are also needed for the central onshore configuration, as inter-array cables and HVDC cables transport the electricity to shore. For each conversion step, an efficiency of 98.5% is used in Eq. 4.10 to come to total converter efficiency (Beik & Al-Adsani (2020)).

$$\eta_{converter,total} = \eta_{converter}^{n_{convertersteps}} \tag{4.10}$$

Where $\eta_{converter}$ is the efficiency per converter step in %, $n_{convertersteps}$ is the number of converter steps which differs for every configuration, and $Loss_{converter}$ is the % of electricity lost by the converters.

The electricity inputted into the electrolyser is calculated at every time step of the model by Eq. 4.11.

$$E_{e,in}(t) = E_{turbines,out}(t) \cdot (1 - (\frac{Loss_{Inter-array} + Loss_{HVAC} + Loss_{HVDC} + Loss_{converter}}{100}) \tag{4.11}$$

Where $E_{e,in}(t)$ is the electricity inputted into a single electrolyser per timestep. $E_{turbines,out}(t)$ is the electrical output of the turbines per timestep. Since the different electrolyser system configurations have different-sized electrolysers, the number of turbines connected per electrolyser differs. The offshore decentral configuration has one wind turbine connected to one small electrolyser, but, for the onshore central configuration, the electricity is brought to land per wind farm and thus $E_{turbines,out}$ is larger for the onshore central configuration compared to the offshore decentral configuration. The losses are all given in %.

With the electricity losses calculated, the electrolyser losses can be calculated. Firstly, the electrolyser degrades over time, which affects the efficiency of the electrolyser. The efficiency of the electrolyser is based on its power consumption. The initial efficiency of the electrolyser is given in Eq. 4.12, and the efficiency degradation is given in Eq. 4.13.

$$\eta_{electrolyser} = \frac{HHV_{H_2}}{Powerconsumption_{electrolyser}} \tag{4.12}$$

$$\eta_{electrolyser}(t+1) = \eta_{electrolyser}(t) - (\frac{f_{degradation}}{100 * 8760}) \tag{4.13}$$

Where $\eta_{electrolyser}$ is given in % and the higher heating value of hydrogen, as well as the power consumption of the electrolyser, are given in kWh/kgH_2. The degradation of the electrolyser is calculated for every time step in the model. This is denoted by $(t+1)$ and (t). $\eta_{electrolyser}$ is the efficiency of the electrolyser and $f_{degradation}$ is the degradation factor of the electrolyser given in %/year. As seen in Eq. 4.13, for every time step, the efficiency is the efficiency of the previous time step times the % loss per hour.

With the efficiency of the electrolyser, the hydrogen that is produced per time step can be calculated. The general formula used to calculate the amount of hydrogen produced by the electrolyser is given by Eq. 4.14

$$H_{2_{produced}}(t) = \frac{E_{e,in}(t) \cdot \eta_{electrolyser}(t)}{HHV_{H_2}} \tag{4.14}$$

Where E_{in} is the electrical energy that is inputted to the electrolyser in W and $\eta_{electrolyser}$ is the efficiency of the electrolyser in %. HHV_{H_2} is the higher heating value of hydrogen, which is 39.39 kWh/kg (Andersson & Grönkvist (2019)).

A battery system can store a surplus of electricity when the wind turbines are all operating on their rated power and discharge when the wind turbines can not supply enough power for the lower load range of the electrolyser. It should be noted that batteries are not used in the three constructed designs and are set to zero in the formulas. The scenario analysis will look into the use of batteries and use the formulas as well, not setting the batteries to zero. For the electrolyser system, consisting of the battery, electrolyser and balance of plant, there are four operating modes shown in Figure 4.4. Included in the balance of plant in the model is also the compressor power for the entire system. This includes the compressor power needed for hydrogen transport through pipelines, as well as the compressor power needed for underground hydrogen storage. The compressors will be sized on their maximum needed capacity. The operation of the compressors will, however, use the average hydrogen production of the system to calculate the compressors' electricity needs. The sizing will be done in Section 4.4.3. The electrolyser balance of plant power is taken as 3% of the installed electrolyser capacity. The total balance of plant power for the system is given by Eq. 4.15.

$$P_{BoP} = 0.03 \cdot P_{electrolyser} + P_{compressors} \tag{4.15}$$

For the first operating mode, shown in Fig. 4.4a, the battery and the turbines both have a power below the lower load range of the electrolyser. Also, their combined power is below the lower load range. The electrolyser can, therefore, not produce any hydrogen. However, the battery will be charged if the wind turbines produce power. The hydrogen produced and the state of the battery are given by Eq. 4.16.

$$H_{2_{prod}}(t) = 0 \tag{4.16a}$$

$$E_{battery}(t+1) = E_{battery}(t) + E_{e,in}(t) \tag{4.16b}$$

For the second operating mode, shown in Fig. 4.4b, the turbines do not produce enough power alone to reach the lower load range of the electrolyser and the balance of plant power. The battery, however, can deliver a power higher than the difference between the lower load range and balance of plant of the electrolyser and the power of the turbines, which needs to be overcome. The turbines' power can also be zero in this operating mode, in which case the battery will have to supply all of the power to come to the lower load range and balance of plant. Therefore, the battery can ensure that the electrolyser is on and producing hydrogen in its lower load range. The battery discharges by the difference between the lower load range and the turbine's power. The hydrogen produced and the state of the battery are given by Eq. 4.17

$$H_{2_{prod}}(t) = \frac{(((P_{electrolyser} \cdot llr - E_{e,in}(t)) \cdot \eta_{battery} + E_{e,in}(t)) \cdot \eta_{\text{electrolyser}}(t)}{HHV_{H_2}} \tag{4.17a}$$

$$E_{battery}(t+1) = E_{battery}(t) + (E_{e,in}(t) - (P_{electrolyser} \cdot llr + P_{BoP})) \cdot \eta_{battery} \tag{4.17b}$$

Fig. 4.4c shows the third operating mode of the system. In this case, the turbines are delivering power between the lower load range and the rated power of the electrolyser plus the power of the balance of plant. In this case, the electrolyser can operate solely on the power provided by the wind turbines, and the battery does neither charge nor discharge. The hydrogen produced and the state of the battery are given by Eq. 4.4c.

$$H_{2_{prod}} = \frac{(E_{e,in}(t) - P_{BoP}) \cdot \eta_{\text{electrolyser}}}{HHV_{H_2}} \tag{4.18a}$$

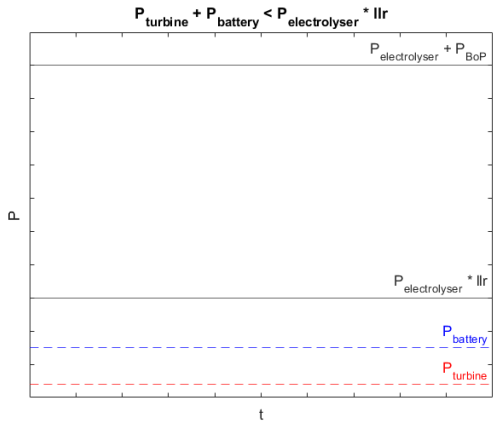

(a) Operating mode 1: The battery and wind farm together cannot overcome the lower load range of the electrolyser, the battery neither charges nor discharges.

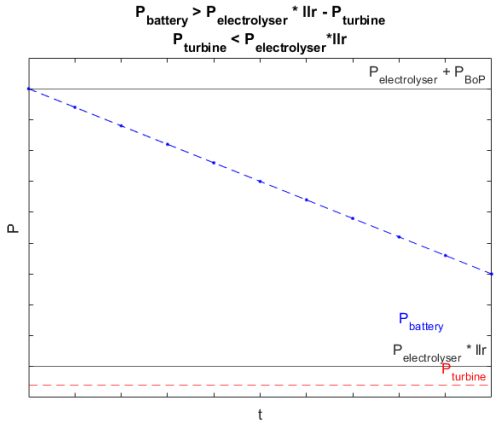

(b) Operating mode 2: The wind farm cannot overcome the lower load range of the electrolyser by itself, but with the help of the battery, it can. The battery discharges until empty.

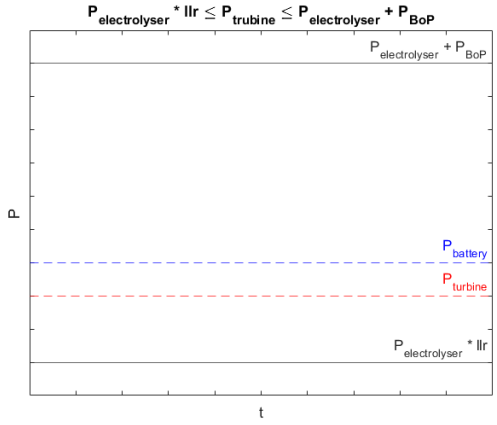

(c) Operating mode 3: The wind farm can overcome the lower load range of the electrolyser, the battery neither charges nor discharges.

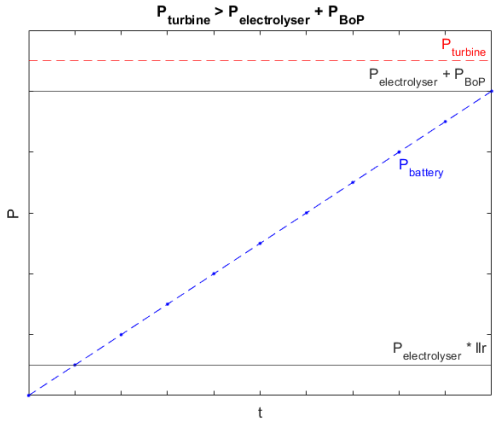

(d) Operating mode 4: The wind farm power is more than the rated capacity of the electrolyser and balance of plant, the battery charges until full.

Figure 4.4: The four operating modes of the electrolyser and battery system.

$$E_{battery}(t+1) = E_{battery}(t) \tag{4.18b}$$

The final operating mode is shown in Fig. 4.4d. In this case, the turbines produce more power than the rated power of the electrolyser plus the power of the balance of plant. Since more power is produced, this surplus can be stored in the battery, which charges by the difference between the turbine power and the rated electrolyser plus BoP power. The hydrogen produced and the state of the battery are given in Eq. 4.19

$$H_{2_{prod}} = \frac{P_{electrolyser} \cdot \eta_{\text{electrolyser}}}{HHV_{H_2}} \tag{4.19a}$$

$$E_{battery}(t+1) = E_{battery}(t) + (E_{e,in}(t) - (P_{electrolyser} + P_{BoP})) \cdot \eta_{battery} \tag{4.19b}$$

Also, some extra limitations are imposed on the battery to represent its physical operation. The battery can not store more energy than its full capacity. When fully discharging and charging a battery, called 'deep-cycling', the battery's lifetime can be shortened. When fully discharging, irreversible damage to the battery can be done. When a voltage is applied to an already-charged battery, capacity degradation can be accelerated (Renogy (2022)). Therefore, state of charge (SoC) limits of 20% and 80% are applied to the battery. The SoC is calculated using Eq. 4.20

$$SoC = \frac{E_{battery}(t)}{E_{battery,max}(t)} * 100\% \tag{4.20}$$

If the state of the battery at (t+1) becomes larger than the state of charge limit, the state of the battery at (t+1) will become the state of charge limit since it can not store more than that by the limitation. The surplus of energy will have to be curtailed. If the state of the battery at (t+1) is less than the capacity of

the battery, the extra energy can be stored within the battery. If the state of the battery becomes smaller than the lower state of charge limit, the state of the battery will remain at the lower limit since it cannot discharge further by the limitation. This is imposed in the model by Eq. 4.21.

$$E_{battery}(t+1) = \begin{cases} E_{battery,max} \cdot SoC_{limit,upper}, & \text{if } E_{battery}(t+1) \geq E_{battery,max} \cdot SoC_{limit,upper} \\ E_{battery}(t+1), & \text{if } E_{battery,max} \cdot SoC_{limit,lower} \leq E_{battery}(t+1) \leq P_{battery} \\ E_{battery,max} \cdot SoC_{limit,lower}, & \text{if } E_{battery}(t+1) < E_{battery,max} \cdot SoC_{limit,lower} \end{cases} \tag{4.21}$$

Another limitation of the battery is the maximum charging or discharging per timestep. The difference is SoC per timestep is calculated using Eq. 4.22.

$$\Delta SoC = \left| \frac{E_{battery}(t+1) - E_{battery}(t)}{P_{battery}} \right| \leq \Delta SoC_{max} \tag{4.22}$$

If ΔSoC is larger than the allowable threshold set, ΔSoC is capped to the threshold. This can either be during charging or discharging.

4.4.3 Sizing

If an offshore decentralised configuration is used, collection pipelines are laid throughout the wind farm to collect the hydrogen produced at the turbines. The spacing of offshore wind farms is taken into account to calculate the length of the collection pipelines. Each collection pipeline is connected to a string of wind turbines. The strings come together outside the wind farm at a meeting point to go on as one pipeline to a central point. The total distance of the collection pipelines per wind farm is thus the spacing between two turbines times the number of turbines minus one, plus the length to the meeting point of the strings for each string, plus the length to the central point between the wind farms. Figure C.1 in Appendix C shows the layout of the hydrogen collection pipeline. For the offshore wind farm in this thesis, a spacing of 7 times the rotor diameter is chosen (Bussel (2006)). Eq. 4.23 is used to calculate the length.

$$L_{pipeline} = n_{strings} \cdot (7 \cdot D_{rotor} \cdot (n_{turbines} - 1) + L_{meetingpoint}) + L_{centralpoint} \tag{4.23}$$

Where $L_{pipeline}$ is the collection pipeline length in km, D_{rotor} is the wind turbine rotor diameter in meters, and $n_{turbines}$ is the number of wind turbines in a wind farm. $n_{strings}$ is the number of hydrogen collection pipeline strings, and $L_{meetingpoint}$ is the length from each string to a meeting point where the collection pipelines come together. $L_{centralpoint}$ is the length of the pipeline that continues to the central point from where the hydrogen from all wind farms is collected.

To calculate the capacities of the pipelines used and choose a pipeline diameter that can transport the needed hydrogen capacity, Eq. 4.24 is used.

$$Capacity_{pipeline,max} = \frac{max(H_{2_{produced}}(t)) \cdot HHV_{H_2}}{t} \tag{4.24}$$

Where $Capacity_{pipeline,max}$ is the maximum needed capacity in kW. HHV_{H_2} is the higher heating value of hydrogen in kWh/kg and t is time in hours. The maximum produced hydrogen is taken as the maximum produced hydrogen from the electrolysers coupled to the pipeline. As an example, for the hydrogen collection pipeline, the maximum produced hydrogen will be that of all of the decentral electrolysers of one wind farm, as that is the maximum capacity it has to transport. The pipeline to shore will be the maximum hydrogen produced of all electrolysers, as the total hydrogen produced is collected and transported to shore.

For hydrogen transport over pipelines, the pressure drop is used to come to the necessary compressor capacity. The pressure drop is simplified by looking at a relationship between the pipeline diameter and pressure. A more detailed analysis would consider the changing hydrogen density, temperature and flow velocity by the pressure change. A formula for the pressure drop is derived from Fig. 4.5.

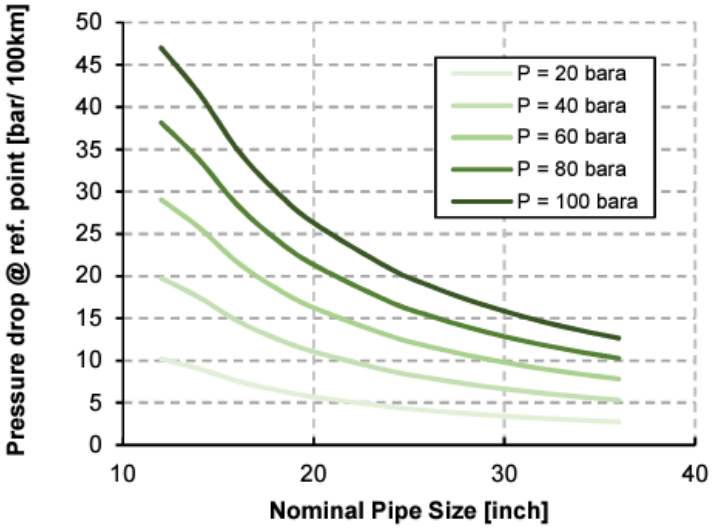

Figure 4.5: The pressure drop of hydrogen transport over different diameter pipelines under different pressures. (Walters et al. (2020a))

The pressure drop of a 12-inch pipeline, as well as a 36-inch pipeline, is formulated. The formula of the pressure drop of the 12-inch pipeline is given by Eq. 4.25.

$$dp_{12-inch} = 11 + (p_{12-inch} - 20) \cdot \frac{9}{20} \tag{4.25}$$

Where $p_{12-inch}$ is the pressure in the 12-inch pipeline. Since the pressure drop depends on the pipeline pressure, a different pipeline pressure results in a different pressure drop. To include this relationship in the model, the pipeline is split up into segments of 1 kilometre. For every kilometre, the pressure drop is calculated for that segment by Eq. 4.26, after which the pressure for the next segment is calculated by Eq. 4.27.

$$dp_{12-inch}(x) = 11 + (p_{12-inch}(x) - 20) \cdot \frac{9}{20} \tag{4.26}$$

$$p_{12_inch}(x+1) = p_{12-inch}(x) - (dp_{12-inch}(x)/100) * dL \tag{4.27}$$

Where (x) indicates the current kilometre section over which the formulas are calculated and dL is the length of the segment, thus one kilometre.

For the 36-inch pipeline, the pressure drop formula that is derived from Fig. 4.5 is given by Eq. 4.28.

$$dp_{36-inch} = 3 + (p_{36-inch} - 20) \cdot \frac{1}{8} \tag{4.28}$$

For every segment, the pressure drop and pipeline pressure are calculated by Eq. 4.29 and Eq. 4.30, respectively.

$$dp_{36-inch}(x) = 3 + (p_{36-inch}(x) - 20) \cdot \frac{1}{8} \tag{4.29}$$

$$p_{36_inch}(x+1) = p_{36-inch}(x) - (dp_{36-inch}(x)/100) * dL \tag{4.30}$$

Using these equations and the assumption that the hydrogen has to land on shore with a minimal pressure of 50 bar to be inputted in the onshore pipelines at the Port of Rotterdam, the minimal input pressure at the transportation pipelines offshore can be found by trial and error. The model will try an input pressure at the start of the pipeline and keep raising the input pressure until the output pressure matches the set pressure on the demand side on land. If a collection pipeline is also used, the input pressure of the pipeline to shore is set as the desired output pressure for the collection pipeline, and the same approach is followed. Once the input pressure is known, in combination with the output pressure of the electrolyser, the compression capacity can be found using Eq. 4.4.3.

$$P_{compressor,pipeline} = \frac{Q}{3600 \cdot 24 \cdot HHV_{H_2}} \cdot \frac{Z \cdot T \cdot R}{M_{H_2} \cdot \eta_{comp}} \cdot \frac{N_{g\gamma}}{\gamma - 1} \cdot [(\frac{p_{out}}{p_{in}})^{\frac{\gamma-1}{N_\gamma}} - 1] \tag{4.31}$$

Where P is the compression power in kW, Q is the hydrogen flow rate in kWh/d, based on the higher heating value (39.39 kWh/kg) of hydrogen. Z is the compressibility factor of hydrogen and is dimensionless. T is the compressor temperature in K, and R is the ideal gas constant in $\frac{J}{K \cdot mol}$. M_{H_2} is the molecular mass of hydrogen in grams/mol. η_{comp} is the isentropic efficiency of the compressor and is dimensionless. N_γ is the number of compression stages and is dimensionless, and γ is the dimensionless diatomic constant. Finally, p_{in} and p_{out} are the inlet and outlet pressure respectively. The needed compressor power is calculated multiple times, depending on the electrolyser system configuration of the design. Multiple pipelines can be present per design, and multiple compressors per pipeline could also be present.
To come to the flow rate in kWh/day, Eq. 4.32 is used to convert from the kg/h outputs of the model. The maximum flow in kg/h is used when sizing the pipelines, as they should be able to transport the maximum flow. The average flow in kg/h is used by Eq. 4.33 to come to an average flow in kWh/day, on which the electricity use of the compressors will be based in the model.

$$Q_{max} = max(H2_{prod}(t)) \cdot 24 \cdot HHV_{H2} \tag{4.32}$$

$$Q_{avg} = avg(H2_{prod}(t)) \cdot 24 \cdot HHV_{H2} \tag{4.33}$$

For the storage facility, the electricity consumption of the compressors is used. This is calculated by Eq 4.34.

$$P_{compressor,storage,max} = E_{compressor,storage} \cdot max(H_{2_{storage,in}}) \tag{4.34}$$

Where $P_{compressor,storage}$ is the maximum needed compressor power on which the compressors will be sized. $E_{compressor,storage}$ is the electrical power consumption of the compressors that are used in kWh/kgH_2. $max(H_{2_{storage,in}}$ is the maximum amount of hydrogen that is inputted into the storage facility in one time step in the model.

The total compressor power that will be installed and included in the balance of plant, as described by Eq. 4.15, will be given by Eq. 4.35

$$P_{compressors} = P_{compressor,storage,max} + \sum P_{compressor,pipeline} \tag{4.35}$$

To simulate the storage facility and the baseload of hydrogen to shore, two balancing equations are used. These balancing equations follow from the two possible operating modes for the storage facility and the baseload. To cover the baseload, either the hydrogen production is sufficient and will supply the baseload, after which the remaining hydrogen will be stored offshore (4.36). Or the produced hydrogen is not enough to supply the baseload, and the produced hydrogen will be complemented by hydrogen that is extracted from the storage facility (4.37).

$$H_{2_{produced}} = H_{2_{baseload}} + H_{2_{storage,in}} \tag{4.36}$$

Where $H_{2_{produced}}$ is the hydrogen that is produced offshore, $H_{2_{baseload}}$ is the baseload to shore and $H_{2_{storage,in}}$ is the excess of hydrogen that is stored offshore.

$$H_{2_{baseload}} = H_{2_{produced}} + H_{2_{storage,out}} \tag{4.37}$$

Where $H_{2_{storage,out}}$ is the hydrogen extracted from the storage facility to complement the hydrogen produced.

Using these balancing equations, the storage facility is either complemented with hydrogen or depleted of hydrogen. Similar to the battery system, this is done by three operating modes. The first operating mode is derived from the first balancing equations and is thus used when the produced hydrogen is larger than the baseload. Eqs. 4.38, 4.39 and 4.40 are then used to determine the storage levels.

$$H_{2_{storage,in}}(t) = H_{produced}(t) - Baseload \tag{4.38}$$

$$H_{2_{storage,out}}(t) = 0 \tag{4.39}$$

$$Storage(t+1) = Storage(t) + H_{2_{storage,in}}(t) \tag{4.40}$$

The second operating mode is derived from the second balancing equation and is thus used when the produced hydrogen is not enough to cover the baseload and hydrogen from the storage facility is taken to complement it. Eqs. 4.41, 4.42 and 4.43 are then used to determine the storage levels.

$$H_{2storage,in}(t) = 0 \tag{4.41}$$

$$H_{2_{storage,out}}(t) = Baseload - H_{2_{produced}}(t) \tag{4.42}$$

$$Storage(t+1) = Storage(t) - H_{2_{storage,out}}(t) \tag{4.43}$$

The final operating mode is used when the produced hydrogen is exactly the same as the baseload, and thus no hydrogen is stored or depleted. Since no storage is used in this operating mode, Eqs. 4.44, 4.45 and 4.46 are used to determine the storage levels.

$$H_{2storage,in}(t) = 0 \tag{4.44}$$

$$H_{2_{storage,out}}(t) = 0 \tag{4.45}$$

$$Storage(t+1) = Storage(t) \tag{4.46}$$

Finally, the baseload is sized by a loop in the model. The storage levels are simulated by Eqs. 4.40, 4.43 and 4.46. The storage levels are looped in the model with different sizes of baseloads. The baseload starts small and, with every loop, gets increasingly larger. At the end of every loop, it is then checked if the baseload can be met by looking at the storage levels. The storage level drops below zero if the baseload is too large for the simulated system. The maximum possible baseload is then determined to be the priorly looped baseload. Also, it was chosen to start the simulation with the storage facility partially filled. The amount of hydrogen in the storage facility at the start of the model equals around three weeks of hydrogen production from the system.

4.4.4 Cost Functions

To determine the costs of the total system, the capital expenditures and operating expenditures per component are calculated, where available. The capital and total expenditures are given in €$_{2023}$. The OPEX are divided into variable and fixed OPEX. The fixed OPEX is static and not dependent on production output and is given in €$_{2023}/year$. The variable OPEX depends on the production output and is given in €$_{2023}$. Fuel or electricity costs are examples of variable OPEX. Also, the replacement costs of components are included in the variable OPEX. Since the electricity is delivered by the wind turbines included in the system, the variable OPEX of electricity cost is included in the CAPEX and OPEX of the wind turbines. The total expenditures are calculated by Eq. 4.47.

$$TOTEX = CAPEX + OPEX_{variable} + OPEX_{fixed} \tag{4.47}$$

Where CAPEX is the initial investment in €$_{2023}$, OPEX$_{variable}$ is the present value of the replacement costs in €$_{2023}$ and OPEX$_{fixed}$ is the operating cost in €$_{2023}/year$.

To express the net present value of the variable OPEX, Eq. 4.48 is used.

$$OPEX_{variable} = \sum_{n=1}^{n_{replacements}} \frac{C_{t_n}}{(1+i)^{t_n}} \tag{4.48}$$

Where $n_{replacements}$ is the number of component replacements over the system's lifetime. C is the replacement cost, t is the year the replacement takes place, and i is the inflation rate.

To calculate the LCOH of the system, Eq. 4.49 is used.

$$LCOH_{system} = \frac{TOTEX_{annualised}}{H_{2,prod,annualised}} \tag{4.49}$$

Where $H_{2,prod,annualised}$ is the hydrogen produced by the system per year and $TOTEX_{annualised}$ are the total expenditures per year. The total expenditures per year are calculated for each component separately by Eq. 4.50.

$$TOTEX_{annualised} = CAPEX_{annualised} + OPEX_{variable,annualised} + OPEX_{fixed} \tag{4.50}$$

To translate the CAPEX and variable OPEX of the components to an annual cost over the component's lifetime, the costs are multiplied by the capital recovery factor (CRF). This results in an annualised CAPEX and variable OPEX that represents the annual expenditure needed for interest and depreciation. The capital recovery factor is found by Eq. 4.51.

$$CRF = \frac{r_i(1+r_i)^n}{(1+r_i)^n - 1} \tag{4.51}$$

Where r_i is the discount rate in %, and n is the component's lifetime. The same discount rate will be applied for all components. The lifetime of each component is different, and therefore, the CRF will be calculated for each component individually. It should be noted that if the lifetime of a component is higher than the system lifetime considered, the system lifetime will be used in Eq. 4.51.

When the CRF of the component is found, the CAPEX and variable OPEX are annualised by Eqs. 4.52 and 4.53 resepctivily.

$$CAPEX_{annualised} = CAPEX_{component} \cdot CRF \tag{4.52}$$

$$OPEX_{variable,annualised} = OPEX_{variable,component} \cdot CRF \tag{4.53}$$

Combining Eqs. 4.49, 4.47, 4.52 and 4.53 results in the final formula for the calculation of the system LCOH given by Eq. 4.54.

$$LCOH_{system} = \frac{(CAPEX + OPEX_{variable}) \cdot CRF + OPEX_{fixed}}{H_{2,prod,annualised}} \tag{4.54}$$

Wind turbines

For the costs of the wind turbines, Eq. 4.55 is used to come to the CAPEX of the wind turbines used.

$$CAPEX_{wind} = Capacity_{wind} \cdot Cost_{wind} \tag{4.55}$$

Where $CAPEX_{wind}$ is in €$_{2023}$, $Capacity_{wind}$ is given in kW and $Cost_{wind}$ is given in €$_{2023}/kW$.
To come to the OPEX of the wind turbines, Eq. 4.56 is used.

$$OPEX_{fixed,wind} = CAPEX_{electrolyser} \cdot \%_{wind} \tag{4.56}$$

Where $\%_{electrolyser}$ are the operating and maintenance costs expressed in % of CAPEX per year.
The LCOH of the wind turbines is given by Eq. 4.57.

$$LCOH_{wind} = \frac{CAPEX_{wind} \cdot CRF_{wind} + OPEX_{fixed,wind}}{H_{2,prod,annualised}} \tag{4.57}$$

Electrolyser technology

For the electrolyser technology, the CAPEX, fixed OPEX and variable OPEX are given by Eqs. 4.58, 4.59 and 4.60 respectively.

$$CAPEX_{electrolyser,stack} = (Capacity_{electrolyser,stack} \cdot Cost_{electrolyser,stack}) \tag{4.58}$$

$$OPEX_{fixed,electrolyser,stack} = CAPEX_{electrolyser,stack} \cdot \%_{electrolyser_{stack}} \tag{4.59}$$

$$OPEX_{variable,electrolyser} = \sum_{n=1}^{n_{replacements}} \frac{CAPEX_{electrolyser,stack_{t_n}}}{(1+i)^{t_n}} \tag{4.60}$$

Where $Capacity_{electrolsyer}$ is the total installed electrolyser capacity in kW and $Cost_{electrolyser}$ are the electrolyser costs in €$_{2023}/kW$. $\%_{electrolyser}$ are the operating and maintenance costs expressed in % of CAPEX per year.

To come to the LCOH for the electrolyser, Eq. 4.61 is used.

$$LCOH_{electrolyser,stack} = \frac{(CAPEX_{elec,stack} + OPEX_{variable,elec,stack}) \cdot CRF_{elec,stack} + OPEX_{fixed,elec,stack}}{H_{2,prod,annualised}} \tag{4.61}$$

It should be noted that the electrolyser comprises a stack and a balance of plant, which both have a different lifetime. The above formulas are given for the stack of the electrolyser. The same formulas are used for the balance of plant of the electrolyser. Because of the different lifetimes, the capital recovery factor will be different. The total levelised cost of the electrolyser is given by Eq. 4.62.

$$LCOH_{electrolyser} = LCOH_{electrolyser,stack} + LCOH_{electrolyser,BoP} \tag{4.62}$$

Water feed

For the water feed, very limited data was found in the literature regarding the CAPEX and OPEX of water desalination systems. Instead, data on the levelised costs of water from desalination systems was found. The total costs for the desalinated water used by the system are given by Eq. 4.63

$$TOTEX_{waterfeed} = V_{water,tot} \cdot LCoW \tag{4.63}$$

Where $V_{water,tot}$ is the total volume of feed water needed by the electrolyser in m^3 and LCoW is the levelised cost of water in $€_{2023}/m^3$.

Since no seperate CAPEX and OPEX data was available, an assumption was made to sum the total costs and annualise the total costs by multiplying with the capital recovery factor for the water feed. The LCOH of the water feed is calculated by Eq. 4.64.

$$LCOH_{waterfeed} = \frac{TOTEX_{waterfeed} \cdot CRF_{waterfeed}}{H_{2,prod,annualised}} \tag{4.64}$$

Storage

For the storage technology, the CAPEX, fixed OPEX and variable OPEX are given by Eqs. 4.65, 4.67 and 4.66 respectively.

$$CAPEX_{storage} = (Capacity_{storage} \cdot Cost_{storage}) \tag{4.65}$$

$$OPEX_{fixed,storage} = CAPEX_{storage} \cdot \%_{storage} \tag{4.66}$$

$$OPEX_{variable,storage} = \sum_{n=1}^{n_{replacements}} \frac{CAPEX_{storage_{t_n}}}{(1+i)^{t_n}} \tag{4.67}$$

Where $Capacity_{storage}$ is the capacity needed for the storage facility in Wh, and $Cost_{storage}$ is the cost of the storage facility in $€_{2023}/Wh$. $\%_{storage}$ are the operating and maintenance costs expressed in % of CAPEX per year.

To come to the LCOH for storage, Eq. 4.68 is used.

$$LCOH_{storage} = \frac{(CAPEX_{storage} + OPEX_{variable,storage}) \cdot CRF_{storage} + OPEX_{fixed,storage}}{H_{2,prod,annualised}} \tag{4.68}$$

Transport

For the transport technologies, the CAPEX, fixed OPEX and variable OPEX are given by Eqs. 4.69, **??** and 4.71 respectively.

$$\begin{aligned} CAPEX_{transport} = {} & Capacity_{H_2} \cdot (Cost_{pipeline} \cdot L_{pipeline} \cdot f_{pipeline}) \\ & + Capacity_{electricity} \cdot (Cost_{cable} \cdot L_{cable}) + Capacity_{substation} \cdot Cost_{substation} \end{aligned} \tag{4.69}$$

$$OPEX_{fixed,transport} = \sum CAPEX_{transport} \cdot \%_{transport} \tag{4.70}$$

$$OPEX_{variable,transport} = \sum_{n=1}^{n_{replacements}} \frac{CAPEX_{transport_{t_n}}}{(1+i)^{t_n}} \tag{4.71}$$

Where the $Cost_{pipeline}$ and $Cost_{cable}$ are the costs for cables and pipelines in $€_{2023}/km/GW$. Each different-sized pipeline (e.g. 12-inch and 36-inch) or type of cable (e.g. HVAC, HVDC or inter-array cables) has its own specific cost per km. Since only some of the capacity of the pipeline transportation has to be utilised by the system, only the percentage that the system will fill will be used in the cost calculations, indicated by a factor, $f_{pipeline}$. $Cost_{substation}$ is given in $€_{2023}/MW$. $L_{pipeline}$ and L_{cable} are given in km and $Capacity_{substation}$ is given in MW. $\%_{transport}$ are the operating and maintenance costs expressed in % of CAPEX per year, which can be different for each subcomponent of the storage component. For the

variable OPEX, the cables, pipelines and substations can have different lifetimes, and the variable OPEX will be calculated for each subcomponent individually. Also, the CRF will be different for each subcomponent of the transport component as the lifetimes differ. To come to the total transport component LCOH, all subcomponents will be summed.

To come to the LCOH for transport, Eq. 4.72 is used.

$$LCOH_{transport} = \frac{(CAPEX_{transport} + OPEX_{variable,transport}) \cdot CRF_{transport} + OPEX_{fixed,transport}}{H_{2,prod,annualised}} \tag{4.72}$$

Hydrogen distribution hub

The CAPEX, fixed OPEX and variable OPEX of the hydrogen distribution hub are given in Eq. 4.73, 4.74 and 4.75 respectively.

$$CAPEX_{hub} = Cost_{hub} \cdot \frac{Capacity_{electrolyser}}{500e3} \tag{4.73}$$

$$OPEX_{fixed,hub} = CAPEX_{hub} \cdot \%_{hub} \tag{4.74}$$

$$OPEX_{variable,hub} = \sum_{n=1}^{n_{replacements}} \frac{CAPEX_{hub_{t_n}}}{(1+i)^{t_n}} \tag{4.75}$$

Where $cost_{hub}$ is the cost of the hub in $€_{2023}/500MW$ installed electrolysers and $Capacity_{electrolyser}$ is the installed capacity of the electrolysers in kW. $\%_{hub}$ are the operating and maintenance costs expressed in % of CAPEX per year.

The LCOH calculation of the hydrogen distribution hub is given by Eq. 4.76.

$$LCOH_{hub} = \frac{(CAPEX_{hub} + OPEX_{variable,hub}) \cdot CRF_{hub} + OPEX_{fixed,hub}}{H_{2,prod,annualised}} \tag{4.76}$$

The values in the above-mentioned equations depend on whether platforms are used, or an island is used as the hydrogen distribution hub.

Compressors

Compressors are used for hydrogen transport through pipelines and underground hydrogen storage.

Eqs. 4.77, 4.78 and 4.79 give the CAPEX, fixed OPEX and variable OPEX of the compressor respectively.

$$CAPEX_{compressor} = (Capacity_{compressor} \cdot Cost_{compressor}) \tag{4.77}$$

$$OPEX_{fixed,compressor} = CAPEX_{compressor} \cdot \%_{compressor} \tag{4.78}$$

$$OPEX_{variable,compressor} = \sum_{n=1}^{n_{replacements}} \frac{CAPEX_{compressor_{t_n}}}{(1+i)^{t_n}} \tag{4.79}$$

Where $Capacity_{compressor}$ is the installed capacity of the compressors in W and $Cost_{compressor}$ is the cost of the compressors in $€_{2023}/W$. $\%_{compressors}$ are the operating and maintenance costs of the compressors expressed in % of CAPEX per year.

The LCOH for the compressors is calculated by Eq. 4.80.

$$LCOH_{compressor} = \frac{(CAPEX_{compressor} + OPEX_{variable,compressor}) \cdot CRF_{compressor} + OPEX_{fixed,compressor}}{H_{2,prod,annualised}} \tag{4.80}$$

Battery

A battery system can be used to store a part of the surplus of electricity, to power the electrolyser when there is no wind. A battery system will not be used in the original designs but will be included in the sensitivity analysis. The CAPEX, fixed OPEX and variable OPEX of the battery system are given in Eqs. 4.81, 4.82 and 4.83 respectively.

$$CAPEX_{battery} = (Capacity_{battery} \cdot Cost_{battery}) \tag{4.81}$$

$$OPEX_{battery} = CAPEX_{battery} \cdot \%_{battery} \tag{4.82}$$

$$OPEX_{variable,battery} = \sum_{n=1}^{n_{replacements}} \frac{CAPEX_{battery_{t_n}}}{(1+i)^{t_n}} \tag{4.83}$$

Where $Capacity_{battery}$ is the installed capacity of the battery in W and $Cost_{battery}$ is the cost of the battery in $€_{2023}/W$. $\%_{battery}$ are the operating and maintenance costs of the battery expressed in % of CAPEX per year.

To calculate the LCOH of the battery system, Eq. 4.84 is used.

$$LCOH_{battery} = \frac{(CAPEX_{battery} + OPEX_{variable,battery}) \cdot CRF_{battery} + OPEX_{fixed,battery}}{H_{2,prod,annualised}} \tag{4.84}$$

4.5 Outcome Analysis

The results from this thesis are divided into three sections. Firstly, the output of the decision framework is a result. The decision framework compares the different technologies on technical, economic, operational and environmental criteria. The design that is constructed based on the best-performing technologies based on the decision framework is an output of the decision framework. This is the best design, according to the MCDA, based on the chosen weights and scores. After constructing the first design, two more designs are constructed, with the hard criteria set that all three electrolyser system configurations are used. All three designs will be given. Also, the physical system integration on the Dutch North Sea is considered for all designs. This shows if the designs are feasible from a technical point of view.

Secondly, three designs are simulated in the model. The first part of the model yields the technical output. The three designs can be compared to each other based on these technical output parameters.

Finally, the second part of the model yields the financial results. Based on the financial output, the three designs can also be compared to each other.

4.5.1 Technical Outcomes

In this section, the technical results of the model are shown and analysed. The outputs from the model that are compared between designs are the maximum baseload that can be supplied to shore, the total hydrogen produced over the simulated time of the model and the maximum storage capacity needed. Finally, the system efficiency is calculated using Eq. 4.85.

$$\eta_{system} = \frac{\sum H_{2_{produced,total}} \cdot HHV_{H_2}}{sum(E_{turbines,total})} \tag{4.85}$$

4.5.2 Financial Outcomes

When computing the financial outcomes, important parameters of the technical outcomes are set as constant for all three designs. The parameters that are set as a constant are the baseload, maximum storage capacity and total hydrogen produced. This is done to allow for a fair comparison between the financial outcomes of the three designs.

To compare the financial parameters found in the literature, all values are converted to $€_{2023}$. This is done by, firstly, if necessary, adjusting the year of the costs by adjusting for inflation. To convert financial values from sources from other years before 2023 to 2023, Eq. 4.86 is used.

$$C_{2023} = C_Y \cdot (1 + i^{2023-Y}) \tag{4.86}$$

Where C_{2023} is the cost in 2023, C_Y is the cost in year Y, where Y is a year before 2023. i is the inflation rate, which is taken as 2% for every year. This is chosen because the target inflation rate of the European Central Bank is 2% (Bank (2023)), and the historical long-term inflation rate in the European Union is 2.22% from 1991 until 2023 (YCharts (2023), Economics (2023)). However, the inflation in 2022 and 2023 was extremely high, which contributed a lot to the historical inflation rate, and a smaller inflation rate of 2% is set in this thesis. Y is the year before 2023, so $2023 - Y$ is the number of years difference between the value that needs to be adjusted and 2023.

When adjusting the costs from a value further in time than 2023, it is calculated back to the current 2023 costs. This is done by rewriting Eq. 4.86 to Eq. 4.87

$$C_{2023} = \frac{C_Y}{1 + i^{Y-2023}} \tag{4.87}$$

Once the year has been adjusted, the valuta is converted, if necessary. The 2023 values for the conversion are taken into account and given in Appendix A.1. Furthermore, to convert financial values from sources from other years before 2023 to 2023, Eq. 4.86 is used.

For some sources, no clear year of costs was reported. For those sources, the year of publication was assumed as the year of cost, and the inflation correction from that year is considered.

The output parameter on which the financial outcomes will be compared is the levelised cost of hydrogen in $€_{2023}/kgH_2$.

4.5.3 Scenario Analysis

In the scenario analysis, several scenarios are simulated in the model to evaluate possible future outcomes. This is done to understand the potential impacts of various factors on the outcomes. Several input parameters are changed according to three scenarios. These scenarios are pessimistic, selected, and optimistic scenarios. Pessimistic and optimistic refer to the technological and financial developments of the technologies. With the pessimistic scenario, future developments are reduced, and cost reductions are lower than expected. In the optimistic scenario, on the other hand, extreme technological developments and cost reductions are made. The selected scenario makes use of the expected values from literature. With these scenarios, the parameters are set to their highest and lowest values found in literature.

Apart from changing the values of uncertain parameters, the design choices can also be altered to come to scenarios. For instance, the base scenario transports the hydrogen to shore by a baseload, but a scenario that does not use a baseload to transport the hydrogen to shore can be constructed.

The scenario analysis is performed in the following order. Firstly, the key parameters that will be adjusted are selected. Then, the scenarios are defined, after which the ranges for the parameters are set. Once the ranges are set, the model is run with the different values for the various parameters and the results are analysed to see what impact the different scenarios have on the outcomes. The outcome of the scenario analysis will be the most probable scenario on which a sensitivity analysis will be run.

The scenarios and the used parameter values are given in Chapter 7. The output that will be compared in the scenario analysis is the system LCOH. The system efficiency is not considered since, with renewable energy systems, the efficiency is of less importance than the system LCOH. The renewable energy input for the system considered in this thesis is wind power. Since wind power is abundantly available and always replenishes, it does not matter how efficiently the system operates. The decision on which of the designs considered in this thesis should be built depends on the system LCOH rather than on efficiency.

Unlike the financial results, the scenario analysis does not set the technical outputs at a constant value. This is done because technical parameters are also used for the scenario analysis. The technical parameters influence the hydrogen that can be produced, which, in turn, influences the LCOH. The parameters used in the scenario analysis are given in Chapter 7.

4.5.4 Sensitivity Analysis

Since there is a lot of uncertainty as to the extent the technological improvements and cost reductions will take place, it is essential to understand the impact of these uncertainties on the outcome of the simulations. The goal of the sensitivity analysis is to find out to what parameters the model is most sensitive to. Each parameter will be changed by -10% and +10% for their minimal and maximum value. The nominal values are taken from the most likely scenario from the scenario analysis.

The sensitivity analysis focuses on the financial output of the model, namely the LCOH. The technical outputs are of less importance, as described by Section 4.5.3. As with the scenario analysis, the LCOH calculations will not use the constant technical outcomes but rather the individual technical outcomes for each design, for the same reasons as described in Section 4.5.3.

The parameters used in the sensitivity analysis are given in Chapter 7.

5 Decision Framework

This chapter constructs a decision framework for all possible technologies per component of the value chain, as identified in Chapter 3. The decision framework is constructed by means of a multi-criteria decision analysis, as described by Section 4.3. The layout of this chapter is as follows. Firstly, the electrolyser technologies are discussed in Section 5.1, followed by the water feed in Section 5.2 and the electrolyser system configuration in Section 5.3. The storage technologies are discussed in Section 5.4, and the transport technologies in Section 5.5. Finally, in Section 5.6, the possible energy hub configurations are discussed.

5.1 Electrolyser Technology

Three electrolyser technologies are discussed in this section. These are the discussed electrolyser technologies of Section 3.2, namely Alkaline, PEM and SOEC. The multi-criteria decision analysis is performed over six criteria, which consist of multiple parameters and/or considerations. The six criteria chosen for the electrolyser technologies are cost (5.1.1), technical (5.1.2), flexibility (5.1.3), safety (5.1.4), maintenance (5.1.5) and durability (5.1.6). Finally, Section 5.1.7 gives the total weighted scores.

5.1.1 Cost

The first criterion on which the electrolyser technologies are rated is cost. This consists of both capital expenditures (CAPEX) and operating expenditures (OPEX).

Electrolyser technologies are expected to benefit from economies of scale. The cost reduction that is to be reached from scaling up is predicted to reach around 40% in the short term (2030) and 80% in the long term(2050)(I.R.E.N.A. (2020)). The manufacturers of electrolysers can have economies of scale when producing more electrolysers by investing in larger and automated production facilities. Since the technologies are at different maturity levels, different cost reductions are still possible. The CAPEX values found are based on the learning curve for electrolysers. The learning curve is defined as the reduction in costs per doubling of the installed capacity of a technology worldwide. The learning rate for electrolysers is found to be between 16% and 21%(I.R.E.N.A. (2020)). The CAPEX can have different scopes in literature. It always includes the production unit itself, but it can also include the balance of plant, system integration costs and cost of capital. The CAPEX given in Table 5.1 includes the production unit CAPEX, balance of plant and system integration costs. The future CAPEX of alkaline electrolysers is estimated to be between 400 and 900 EU_{2023}/kW_e in 2030 and between 200 and 700 EU_{2023}/kW_e in the long term in 2050. For PEM electrolysers, the CAPEX is estimated to be between 600 and 1500 EU_{2023}/kW_e in 2030 and between 200 and 900 EU_{2023}/kW_e in the long term in 2050, although less estimates are available for PEM electrolysers in the long term. Finally, for SOEC the CAPEX is estimated to be between 800 and 2800 EU_{2023}/kW_e in 2030 and between 500 and 1000 EU_{2023}/kW_e in 2050 (IEA (2019), Guidehouse (2020) Deloitte (2021), Program (2022)). Alkaline electrolysers can be realised at lower costs because of the absence of noble metals and its relatively mature stack components. PEM electrolysers use expensive platinum catalysts, and SOEC is not as technologically mature yet.

PEM electrolysers currently use the expensive metals platinum and iridium at the anode and cathode, making up a large share of the total cost. Potential for cost reduction lies in the reduction of membrane thickness, removing or re-designing the coatings and searching for other materials to function as electrocatalysts (I.R.E.N.A. (2020),Chisholm et al. (2022)). Alkaline electrolysers are expected to be and stay the cheapest because of the absence of expensive noble metals, and the maturity of the components (Schmidt et al. (2017)). For PEM electrolysers, a potential for cost reduction lies in the reduction of membrane thickness and removal or redesign of the coatings.

These projections are subject to uncertainty and depend on factors such as technology development, regulations, installed capacity, plant size and market demand. To come to the EU_{2023}/kW_e values, the conversion rates from USD to EU were used at the time of the reported value, after which an inflation rate of 2% per year was taken into account.

One source estimates the OPEX of electrolysers to be between 2 and 4 % of CAPEX/year for alkaline and PEM, while estimating between 5 and 7 % of CAPEX/year for SOEC. These percentages are given for current electrolysers and in 2030. No data for 2050 was available (Deloitte (2021)). Another source mentions an OPEX of 1-3 % CAPEX/year, without specifying which electrolyser technology was used (Christensen & Co (2020)).

	Alkaline	PEM	SOEC	Weight
CAPEX	1	0.82	0.6	0.7
OPEX	1	1	0.5	0.3

Table 5.1: Normalised cost MCDA scores table of the electrolyser technologies

For alkaline electrolysers, the 2050 estimates of 200-700 €/kW are used to come to an average value of 450 €/kW. The same was done for PEM and SOEC to come to the values of 550 €/kW and 750 €/kW respectively. Since alkaline has the lowest value, it was used to normalize by dividing it by the other values. Numbers are rounded to two decimals. For the OPEX, 3% of the CAPEX per year was used for alkaline and PEM, while 6% of the CAPEX per year was used for SOEC.
Due to the high investment costs of the electrolysers, it is decided to assign a weight of 0.7 to the CAPEX, and a value of 0.3 to the OPEX. The results of the cost parameters for the MCDA are given in Table 5.1.

5.1.2 Technical

The electrolyser technologies are also rated on their technical parameters. The technical parameters consist of efficiency, stack lifetime, hydrogen output pressure and hydrogen purity. Alkaline electrolysis is already a proven and mature technology, which is an advantage, but less technical development is expected to be made compared to PEM and SOEC since it is already mature. Anion exchange membrane (AEM) electrolysers are very similar to alkaline electrolysers and have several advantages, such as inexpensive materials and high stability. However, the TRL of AEM electrolysers is currently low (2-3), and AEM electrolysers are not considered in this thesis (I.R.E.N.A. (2020)).

The footprint of alkaline electrolysers was found to be almost twice that of PEM electrolysers. For alkaline electrolysers a value of 0.095 m^2/kW_e was given for 2030, whereas PEM electrolysers were expected to only need 0.048 m^2/kW_e in 2030 (Deloitte (2021)). For SOEC, a value of 0.084 m^2/kW_e was found (Topsoe (2021)). With offshore electrolysers, the footprint can be of large importance when using platforms or islands, where either limited area is available, or the area is costly. Since PEM has a high power density, compact designs are possible.

PEM electrolysers have the highest hydrogen output pressure. PEM can operate with an output pressure up to 80 bar, which is significantly higher than the output pressures alkaline and SOEC can reach, which are respectively 30 and 1 bar (IEA (2019), Guidehouse (2020), Deloitte (2021), I.R.E.N.A. (2020),S. S. Kumar & Lim (2022)). No data was found on future projections of output pressures of the electrolyser technologies, but research is being done to higher the output pressures. An advantage of having a high output pressure is that a smaller or even no compressor is needed when injecting the hydrogen into pipelines for transport, depending on the pipeline operating pressure. Compressors can be costly and use electricity, which otherwise could be used for extra electrolysis. To achieve this high output pressure, the disadvantages are that PEM electrolysers are relatively complex systems and the water feed needs to be of high purity.

PEM electrolysers can currently reach the highest purity of output gases (hydrogen and oxygen) of 99.999% of the three electrolyser technologies (S. S. Kumar & Himabindu (2019)). Alkaline reaches purities above 99.9 %, which can be brought up to 99.999 with by catalytic gas purification (S. S. Kumar & Lim (2022),Deloitte (2021),Guo et al. (2019),Buttler & Spliethoff (2018)). Furthermore, alkaline electrolysers use a liquid electrolyte, of which small traces can be present in the produced hydrogen, which requires removal before transport Ibrahim et al. (2022). SOEC electrolysers are reported to have a hydrogen output purity above 99 % (S. S. Kumar & Lim (2022),Deloitte (2021)). Future hydrogen purity levels are not available for the electrolyser technologies, although improvements are expected to be made because of research. The hydrogen purity levels are important because hydrogen applications may require a high level of hydrogen purity, for example, the manufacturing of advanced devices. When the hydrogen is not pure enough, a purification system will need to purify it further (Succi et al. (2020)).

The efficiency of electrolysers can be expressed in the power consumption needed to produce a kilogram of hydrogen. For alkaline electrolysers, currently 57-63 kWh/kgH_2 is needed but is expected to drop to 56-60 kWh/kgH_2 by 2030. For PEM electrolysers, the current power consumption is at 66-71 kWh/kgH_2 and is expected to drop to 58-63 kWh/kgH_2 by 2030. SOEC are the most efficient electrolysers, with a current power consumption of 47-53 kWh/kgH_2 and a future power consumption of 44-51 kWh/kgH_2 by 2030. It should be noted that this only holds for a combination with a fatal heat source. By 2050, It is expected that alkaline and PEM power consumption will drop below 53 kWh/kgH_2, and SOEC will even drop below 47 kWh/kgH_2 (Deloitte (2021), I.R.E.N.A. (2020)).

A possible advantage of SOEC electrolysers is that they are able to operate in reverse mode and act as a fuel cell. For offshore applications, especially when the electrolyser is off-grid connected to a wind farm, no use can be made of this ability however.

	Alkaline	PEM	SOEC	Weight
Footprint	0.51	1	0.57	0.3
Output pressure	0.38	1	0.01	0.10
Hydrogen purity	1	1	1	0.05
Efficiency	0.89	0.89	1	0.5

Table 5.2: Normalised technical MCDA scores table of the electrolyser technologies

For the footprint, a minimal value is preferred. This is achieved by PEM electrolysers with a value of $0.048 m^2/kW_e$. This value is used to normalise the other values, resulting in a normalised score of 0.57 for SOEC and 0.51 for alkaline. For the output pressures, a maximum value is preferred to reduce compressor costs. This is achieved by PEM, which can operate up to 80 bar, and has a normalised score of 1. For alkaline, the normalised score is 0.38 and for SOEC the normalised score is 0.01. For the hydrogen purity levels, the quantitative conversion Table 4.2 is used, since the purities are all very similar. Since a higher purity level is favourable, PEM scores the highest, followed by alkaline and then SOEC. Since the purity levels are all higher than industrial-grade hydrogen (99.95 %), all technologies have a 1 as a score. The electrolyser efficiency is expressed in power consumption. Because of this, a lower value would be preferred. The lowest value is found for SOEC electrolysers, meaning it gets a normalised score of 1. Alkaline and PEM have the same value and both get a normalised score of 0.89.

The weight factors are determined with the best-worst method. The best, or most important, criterion is the efficiency of the electrolyser. The worst criterion is hydrogen purity, as the purity of all electrolysers is high enough for the use case of this thesis. The best to others and others to worst tables, as well as the consistency factor, are given in Appendix A. The consistency factor associated with the chosen relative scores is acceptable according to the best-worst method. The total overview of technical aspect scores is given in Table 5.2.

5.1.3 Flexibility

The third category on which the electrolyser technologies are rated is flexibility. When coupled with a renewable energy source, the electrolysers must be able to respond quickly to electrical input changes, and it is beneficial to have a wide load range.

When coupling electrolysers to intermittent renewable energy sources, the start-up time and ramp-up/ramp-down time can be very important. The start-up time can be divided into the cold start-up time and hot start-up time. With a cold start-up, the electrolyser is shut off entirely and first has to heat up to operating temperatures, whereas the hot start-up time refers to when an electrolyser is shut off and not producing hydrogen but is kept on a stand-by modus at operating temperature (Lange et al. (2023)). The difference is thus whether the electrolyser has to heat up first or not. PEM offers great flexibility because of its quick hot and cold start-up time and fast ramp-up and ramp-down abilities. This flexibility allows PEM electrolysers to adapt to variable electrical input from intermittent offshore wind. The start-up time of PEM electrolysers is in the order of seconds, and the system can reach steady-state operations within a minute (Chandrasekar et al. (2021),Deloitte (2021)). PEM electrolysers can reach a load gradient up to 90%/s (Lange et al. (2023)). Apart from the long cold start-up time of over an hour for SOEC, it also has a very low load gradient compared to PEM of only 0.1-0.3 %/s and a relatively long hot start-up time of 15 minutes (Lange et al. (2023)). Alkaline electrolysis has a cold start-up time of 5-15 minutes, a slightly faster hot start-up time of 1-5 minutes, and a load gradient between 0.2 and 20 %/s (Lange et al. (2023), Deloitte (2021)). Alkaline has a slower response time than PEM electrolysers due to the use of a liquid electrolyte, which has a limited response to sudden fluctuations. PEM can thus have the fastest responses to fluctuations in electrical input, which frequently happens when coupled to intermittent renewable energy sources. Even though alkaline electrolysis might also be suitable to be coupled to renewable energy sources based on the flexibility parameters, frequent start and stop cycles should be avoided with alkaline electrolysers as they increase degradation. When using alkaline electrolysers, an electricity storage system is recommended to avoid start and stop cycles (Lange et al. (2023)). An issue of SOEC electrolysers currently is that the thermo-chemical cycling can lead to faster degradation of the electrolyser when the electrolyser is ramping up or down (I.R.E.N.A. (2020)).

Another important factor of the flexibility of the electrolyser technology is the load range. Because of the power curve of a wind turbine, a lower power may be generated than the rated power of the wind turbine when the wind speed is below the rated wind speed. The load variations for alkaline electrolysers lay between 10 and 100 %. For PEM the load range is between 0 and 160%, meaning the PEM electrolyser can operate above its nominal power, albeit not for long before degradation sets in. SOEC has a load range between 20 and 100 % Ibrahim et al. (2022),IEA (2019),Deloitte (2021)). Alkaline electrolysers are however more suitable for baseload operation, as the gas purity drops in a partial load operation (Lange et al. (2023)).

	Alkaline	PEM	SOEC	Weight
Start-up time	0.5	1	0	0.15
Load gradient	0.75	1	0.25	0.30
Load range	0.9	1	0.8	0.55

Table 5.3: Normalised flexibility MCDA scores table of the electrolyser technologies

Because PEM electrolysers have a start-up time in the order of seconds, PEM has the highest score. Since normalising the scores would result in extremely low scores for alkaline and SOEC, it was chosen to give alkaline an average score, and SOEC a very poor one. This is due to the large differences between alkaline and SOEC. Also for the load gradient, PEM offers the best solution, almost able to withstand 100 % load variation in a second. Alkaline has a large range of load gradients, ranging from very slow to reasonably fast. Looking at the upper range, a score of 0.75 is assigned to alkaline. For SOEC the load gradient is very low and a score of poor is given. For the load range, PEM scores best. Looking at the ranges, and keeping in mind that PEM can only shortly operate above 100 %, the following normalised scores are given. PEM scores best with a 100 % load range and thus a normalised score of 1. Alkaline has a range of 90 % on which it can operate and is given a normalised score of 0.9. SOEC has a load range of 80 % and a normalised score of 0.8.

Since there are three criteria, the weight factors are determined using the best-worst method. The best criterion is the load range since this has a large influence on the size of the battery system. The start-up time is of the least importance since the amount of times the electrolyser shuts off should be minimised. The total determination of the weight factors is given in Appendix A. An overview of all flexibility scores is given in Table 5.3.

5.1.4 Safety

The safety considerations are described in this section, and the electrolyser technologies are also rated on this criterion.

As mentioned in Section 3.2, alkaline electrolysers use a liquid electrolyte of potassium oxide (KOH). The electrolyte, which is a corrosive chemical and is present in an alkaline electrolyser at a concentration of 20-30%, increases the chance of leakage (Ibrahim et al. (2022),Chau et al. (2022)).

A safety consideration for PEM electrolysers is the high pressure under which they can operate. The largest hazard is the gas cross-permeation. Under high pressures, the mixing of oxygen and hydrogen can rise, and the mix can be an explosion hazard. The operation of PEM electrolysers is safe, if the correct safety precautions are taken (Grigoriev et al. (2011),Chau et al. (2022)).

SOEC can be less risky to operate because it uses less dangerous chemicals and has fewer parts than Alkaline and PEM. However, the high-temperature operation makes it less safe (Chau et al. (2022)).

	Alkaline	PEM	SOEC
Safety	0.75	0.75	0.5

Table 5.4: Normalised safety MCDA scores table of the electrolyser Technologies

In terms of safety, PEM and alkaline both score good, whereas SOEC scores poor due to the high temperatures and low experience. The converted scores are summarised in Table 5.4.

5.1.5 Maintenance

In this section, the maintenance considerations for the electrolyser technologies are given.

The use of an electrolyte with alkaline electrolysers comes with several disadvantages when placing the electrolyser offshore. Because of this electrolyte, the chance of leakage increases and maintenance has higher requirements. Also, the potassium oxide electrolyte has to be changed, which is costly and undesirable offshore because of the extra transport and optional storage necessities(Ibrahim et al. (2022)).

Since SOEC is yet to be commercialized, it is hard to give an exact indication of what the maintenance needs will be. But because of the high-temperature operation, SOEC requires specialized materials that have a short lifetime and thus need replacement more often (Chau et al. (2022)).

The maintenance of the electrolysers can be combined with the maintenance of the wind turbines when the offshore decentralised configuration is used.

	Alkaline	PEM	SOEC
Maintenance	0.25	0.75	0.25

Table 5.5: Normalised maintenance MCDA scores table of the electrolyser Technologies

Because of the electrolyte used in alkaline electrolysers, which has to be changed, it was chosen to score alkaline poor in terms of maintenance. For PEM electrolysers, no significant maintenance considerations are of interest, and it was scored a good. Since SOEC operates at very high temperatures, more maintenance is needed and it is also scored poor.

The converted scores are summarised in Table 5.4.

5.1.6 Durability

The conditions on the North Sea can be harsh, and the electrolyser technology should be durable to minimize downtime, maintenance and replacement.

For the stack lifetime, alkaline electrolysers are expected to reach between 90,000 and 100,000 hours in 2030 and between 100,000 and 150,000 hours in 2050. For PEM electrolysers this is estimated to be between 60,000 and 90,000 hours in 2030 and 100,000 and 150,000 hours in 2050. Finally, for SOEC, the stack lifetime is expected to be between 40,000 and 60,000 hours in 2030 and between 75,000 and 100,000 hours in the long term (IEA (2019), Deloitte (2021), I.R.E.N.A. (2020)). The efficiency degradation of alkaline electrolysers currently reaches up to 0.1 %/1000h of operation. Not many developments are expected to be made in this as it is expected to remain 0.1 %/1000h in 2030. For PEM electrolysers, a small development is expected from 0.2 %/1000h in 2020 to 0.1 %/1000h in 2030. SOEC currently stands at the highest efficiency degradation of 1.9 %/1000h and is only expected to improve to 0.5 %/1000h in 2030.

	Alkaline	PEM	SOEC	Weight
Lifetime	1	1	0.67	0.6
Efficiency degradation	1	1	0.2	0.4

Table 5.6: Normalised durability MCDA scores table of the electrolyser technologies.

For stack lifetime, a longer value is preferred. The highest value in 2050 is found for both Alkaline and PEM, which have the normalised score of 1. SOEC has a normalised score of 0.67. For efficiency degradation, both alkaline and PEM have the lowest, desirable, value. Both once again have a normalised score of 1. SOEC has a normalised score of 0.2 in this case.

Because of the high capital costs of electrolysers, the lifetime is given a higher weight than the efficiency degradation. The lifetime is given a weight of 0.6, whereas the efficiency degradation is given a weight of 0.4. An overview is given in Table 5.6.

5.1.7 Total Scores

The (weighted) scores of all criteria are summarized in Table 5.7. The best-worst method is used to come to the weights per criterion. The most important criterion is chosen to be the technical aspects since some of its sub-criteria are of large influence on an offshore value chain, such as the footprint, since space is limited, and the output pressure, which has a large influence on transportation. The least important criterion is chosen to be safety since this has a limited impact on the offshore value chain when precautions are taken. Maintenance also received a low weight, as the maintenance of the electrolysers can be combined with the maintenance of the wind turbines. The relative weights are given by the '*Best-to-Others*' and '*Others-to-Worst*' vectors, which are given in Appendix A. Also, the consistency index and threshold are given in Appendix A. The consistency index is below the consistency threshold according to the best-worst method and is thus acceptable.

	Alkaline	**PEM**	**SOEC**	Weight
Cost	1	0.85	0.55	0.25
Technical	0.75	0.95	0.8	0.35
Flexibility	0.8	1	0.55	0.1
Safety	0.75	0.75	0.25	0.05
Maintenance	0.25	0.5	0.25	0.1
Durability	1	1	0.5	0.15
Total score	**0.8**	**0.9**	**0.65**	

Table 5.7: Weighted scores table of electrolyser technologies.

The total scores are a summation of the technology score per criterion times the weight per criterion. The weighted scores are summed per technology and given in the bottom row of Table 5.7. As can be seen, PEM is the preferred technology, just over alkaline. SOEC is not preferred for offshore electrolysis.

5.2 Water Feed

In this section, the water feed technologies are discussed. The multi-criteria decision analysis is performed over five criteria, namely cost (5.2.1), technical considerations (5.2.2), safety(5.2.3) and maintenance considerations (5.2.4) and environmental considerations (5.2.5). The total weighted scores are given in Section 5.2.6.

5.2.1 Cost

The North Sea has a salinity of 34-35 g/L. At these salinity levels, the CAPEX of membrane distillation is slightly higher than the CAPEX for reverse osmosis. The CAPEX of reverse osmosis is dependent on membrane costs. With higher salinity levels, more stages, and thus membranes, are needed, and reverse osmosis comes to higher costs than membrane distillation (Zhang et al. (2022)). Also, the OPEX for membrane distillation is higher than the OPEX of reverse osmosis, being 2.5% of CAPEX per year for the membrane distillation plant, and 2% of the CAPEX per year for the reverse osmosis plant. However, the costs for the water treatment compared to the total costs of the offshore hydrogen value chain are limited. As mentioned in Section 3.3, one kg of hydrogen can be produced with 9 kg of water as feed. With a levelised cost of water between 0.5-1.25 € $/m^3$ for reverse osmosis, and 0.64 - 1.23 € $/m^3$ for membrane distillation, the added costs per kg hydrogen are in the range of 1 cent (Shemer & Semiat (2017), Al-Obaidani et al. (2008)). For membrane distillation, lower costs (0.64-0.66 € $/m^3$) are reached if a low-grade heat energy source can be used, such as the waste heat of an electrolyser. Without such a heat source, costs of 1.17-1.23 € $/m^3$ are reached.

	Reverse Osmosis	Membrane Distillation	Weight
CAPEX	0.74	1	0.5
OPEX	0.8	1	0.5

Table 5.8: Normalised cost MCDA scores table of the water desalination technologies

For the CAPEX, the average value of 0.88 € $/m^3$ is used for reverse osmosis. For membrane distillation, the average value of 0.65 € $/m^3$ of the lower costs with the availability of a low-grade heat energy source is used since the waste heat of an electrolyser can be used as this source. Since the costs are preferred to be as low as possible, membrane distillation has a normalised score of 1, and reverse osmosis has a normalised score of 0.74. Membrane distillation also scores best on OPEX, which is also preferred to be as low as possible, and thus has a score of 1. Reverse osmosis scores 0.8 on OPEX.

There is no clear significance of CAPEX or OPEX over the other, and thus both are given a weight factor of 0.5.

An overview of the scores is given in Table 5.8.

5.2.2 Technical

The water input for electrolysers needs to be free of salt and contaminations. When pure water is not used, the electrolyser loses performance and degrades faster (Ibrahim et al. (2022)). The purity of the water that is needed depends on several aspects, such as the type of electrolyser technology, materials used and system design. The purity of the water is often expressed in the conductivity of the water, since the lower the conductivity, the lower the concentration of ions and molecules that can be of harm to the electrolyser. For alkaline electrolysers, this maximum conductivity was found to be $5\mu S/cm$ (Ursúa et al. (2012)). For PEM electrolysers, the water needs to be purer and have a maximum conductivity of 1 $\mu S/cm$ (Ursúa et al. (2012)). No sources were found on the maximum allowed conductivity for SOEC, but since PEM electrolysers are described to be sensitive to water impurities, and SOEC is not, it is assumed that SOEC does not need the water to have a lower conductivity than PEM electrolysers.

Reverse osmosis is a very mature technology and has had a lot of technical developments. The deionized water that is outputted can have conductivity as low as 0.5 $\mu S/cm$ and could thus be used for every type of electrolyser technology. The energy consumption for reverse osmosis can be between 2 and 6 kWh/m^3 of treated water (Adewole et al. (2022b)).

Membrane distillation is a newer technology but has the lowest energy consumption and operating temperature of thermal desalination solutions. There is a wide range of membrane distillation projects, and their energy consumption ranges from 1 kWh/m^3 water produced, to as high as 9,000 kWh/m^3 water produced Adewole et al. (2022b), but several studies report an energy consumption of 140-300 kWh/m^3 when seawater

is used as a feed (Ullah et al. (2018)). The high salt rejection rate makes the output water usable for every type of electrolyser technology, as has already been proven on a pilot scale with a PEM electrolyser (van Medevoort et al. (2022)).

Membrane distillation needs significant thermal energy, but by using the waste heat from the electrolyser, costs could be reduced. Compared to reverse osmosis, membrane distillation uses much lower pressures, as it can be operated on near-atmospheric pressures, lowering the system's complexity (Adewole et al. (2022b)).

Both technologies are easy to scale for larger systems, but reverse osmosis has a lower space requirement, as the design can be more compact Adewole et al. (2022b). Since there is no phase change involved with reverse osmosis, the system is less complex. (Maawali et al. (2021)) shows that for a reverse osmosis plant and membrane distillation plant with the same water output, the reverse osmosis plant had a smaller footprint and weight. The reverse osmosis plant had an area of 15.33 m^2 and a weight of 15000 kg, while the membrane distillation plant had an area of 17.28 m^2 and a weight of 16200 kg.

	Reverse Osmosis	Membrane Distillation	Weight
Water conductivity	1	1	0.1
Energy consumption	1	0.02	0.15
Space requirements	1	0.89	0.5
Weight	1	0.93	0.2
System complexity	1	0.75	0.05

Table 5.9: Normalised technical MCDA scores table of the water desalination technologies

Since both reverse osmosis and membrane distillation output water with a water conductivity that is low enough to have the water used in every type of electrolyser, both technologies have a score of very good, and thus 1. The energy consumption is preferred to be as low as possible since more electrical energy is left for the electrolyser to produce hydrogen. Reverse osmosis scores best in this respect and has a normalised score of 1. The average values of the ranges reported above are used to come to a normalised score of 0.02 for membrane distillation. Since reverse osmosis typically requires less space and is more compact, it has a normalised score of 1. Membrane distillation has a normalised score of 0.89. The normalised scores of the weight are found to be 1 for reverse osmosis and 0.93 for membrane distillation. Finally, for system complexity, reverse osmosis scores better because it has fewer elements. Membrane distillation needs heating elements and has a phase change involved. Reverse osmosis scores a 1, and membrane distillation a 0.75.

Since the technical criterion consists of five sub-criteria, the best-worst method is used to come to the weight factors per sub-criterion. The most important criterion is the space requirement, as the space is expensive and limited offshore. The least important criterion is the system complexity, as the total offshore electrolyser systems are already complex, and the water feed system is relatively not as complex. The total overview of the best-worst method for the technical aspects of the water feed is given in Appendix A. The consistency index is acceptable according to the best-worst method.

The total scores and weight factors of the technical aspects are given in Table 5.9.

5.2.3 Safety

In terms of safety, reverse osmosis operates under high pressures, whereas membrane distillation operates under high temperatures. Both come with their own safety risks.

	Reverse Osmosis	Membrane Distillation
Safety	0.75	0.5

Table 5.10: Normalised safety MCDA scores table of the water desalination technologies

For safety, both high-temperature and high-pressure operations come with risks. However, since there is a lot more experience with reverse osmosis already, it was chosen to rate its safety aspects as good, whereas the newer, high-temperature operation of membrane distillation has a score of average.

5.2.4 Maintenance

Membrane fouling is the process in which particles accumulate in the membrane pores or on the membrane surface, reducing the number of pores that can be used for distillation. With reverse osmosis, the pre-treatment of the feed water is important to reduce membrane fouling. Since the fouling can only be reduced and not totally prevented, regular membrane cleaning is also necessary to keep the performance high. For membrane distillation, membrane fouling and pore wetting remain large challenges, and extensive cleaning

and regular membrane replacements are necessary. For reverse osmosis, the maintenance frequency is advised to be at least once a year (water inc. (2021)). For membrane distillation, however, a study found the optimal cleaning strategy to prevent membrane fouling to be to clean for 60 minutes every two days (Charfi et al. (2021)). It is expected to have more time between maintenance services in the future.

	Reverse Osmosis	Membrane Distillation
Maintenance	0.75	0.25

Table 5.11: Normalised maintenance MCDA scores table of the water desalination technologies

In terms of maintenance, reverse osmosis scores good, whereas membrane distillation scores poor, as many improvements are needed for offshore operations. The scores are summarized in Table 5.11.

5.2.5 Environment

The use of membrane distillation can have multiple advantages over reverse osmosis in terms of environmental impact. When using reverse osmosis with an offshore central configuration, the salty brine is disposed of at one location. Because of the high salt concentration, this can affect the local ecology. When a decentralized configuration is used, the brine is disposed of more sparsely, which limits the ecological impact. An environmental impact assessment can show the diffusion and impact of the brine at the disposal location through models (Ibrahim et al. (2022)). Apart from the brine, chemicals are used in the pre-treatment of the seawater, which also need to be disposed of. Reverse osmosis and membrane distillation both use chemicals for the pre-treatment of water (van Medevoort et al. (2022)). With membrane distillation, the brine has a lower salt concentration, reducing the ecological impact of the disposal. Also, membrane distillation has a higher water recovery, meaning less feed water is needed to produce one m^3 of pure water, and thus, less brine is produced.

	Reverse Osmosis	Membrane Distillation	Weight
Brine disposal	0.5	1	0.7
Chemicals	0.5	0.5	0.3

Table 5.12: Normalised environment MCDA scores table of the water desalination technologies

Membrane distillation scores a very good in terms of brine disposal, whereas reverse osmosis scores an average, since with a centralized configuration, the brine disposal can cause issues. Since membrane distillation and reverse osmosis both use chemicals, both receive a score of average.

Brine disposal was deemed to be more important than the use of chemicals when looking at environmental impact, as the brine is discharged into the sea. It is given a weight of 0.7, whereas the use of chemicals is given a weight of 0.3.

The scores and weights are summarized in Table 5.12.

5.2.6 Total Scores

The (weighted) scores of all criteria are summarized in Table 5.13. To come to the weights per criterion, the best-worst method is used. The most important criterion is chosen to be the technical aspects, as the water feed is only a small part of the total system and the technical aspects should be functioning well. The safety aspects are chosen to be the least important, as it has the lowest impact on the total value chain and costs.

The relative weights are given by the '*Best-to-Others*' and '*Others-to-Worst*' vectors, which are given in Appendix B.1. Also, the consistency index and threshold are given in Appendix B.1. The consistency index is below the consistency threshold according to the best-worst method and is thus acceptable.

	Reverse Osmosis	**Membrane Distillation**	Weight
Cost	0.75	1	0.15
Technical	1	0.8	0.45
Safety	0.75	0.5	0.05
Maintenance	0.75	0.25	0.2
Environment	0.5	0.85	0.15
Total score	**0.85**	**0.7**	

Table 5.13: Weighted scores table of the water feed.

As can be seen in Table 5.13, the preferred technology with the used criteria and weights is reverse osmosis. The preference for reverse osmosis over membrane distillation is not very high.

5.3 Electrolyser System Configuration

The electrolyser system configurations are discussed in this section. These are the decentral offshore configuration, the central offshore configuration and the central onshore configuration. The multi-criteria decision analysis is performed over five criteria, which are cost (5.3.1), technical (5.3.2), flexibility (5.3.3) and safety (5.3.4) and maintenance considerations (5.3.5).

5.3.1 Cost

The main difference in cost between the offshore and onshore configurations is the transport costs. For the onshore configuration, the electricity is first brought to shore via HVDC cables, and offshore and onshore substations are needed. The HVDC cable costs are considered in Section 5.5.1. An important factor and cost share of the central offshore configuration is the structure on which the hub will be built. This could be an energy island or (old) platforms. This is considered in Section 5.6.1.

The costs considered in this Section will be those of the needed infrastructure from the wind turbine to the central point from which either electricity or hydrogen transport to shore starts.

For the onshore central configuration, the costs consist of the inter-array cables within the wind farm, as well as the offshore substation(s), on which the voltage is heightened for the HVDC cables. Also, an onshore substation is needed for the landing of the HVDC cables on shore. For the inter-array cables, a CAPEX of 303.5 €/m was found(Martinez & Iglesias (2021)).

For the central offshore configuration, also inter-array cables are needed to collect the electricity from the wind turbines. The electricity is then used to run the electrolyser. The electrolyser can either be placed on a platform or an island. The costs for a platform or island are given more in-depth in Section 5.6.1.

Finally, for the decentral offshore configuration, the costs considered in this section are those of the pipelines from the wind turbines to a central manifold, at which the hydrogen produced at the different wind turbines is collected. Another cost consideration for this configuration is that each electrolyser needs its own balance of plant and water desalination unit. Also, fixed-pole wind turbines usually do not have a platform at its food on which the electrolyser could be placed. These platforms would have to be added.

	Onshore central	Offshore central	Offshore decentral
Cost	0.25	0.5	0.75

Table 5.14: Normalised cost MCDA scores table of the electrolyser system configurations

Since the costs of the components are given in other Sections in this Chapter, the costs for the electrolyser system configurations will be ranked quantitatively. The offshore decentralised configuration has the least amount of components. Even though it comes with extra costs per electrolyser, this configuration has the lowest CAPEX and receives a score of good. For the offshore centralised configuration, inter-array cables and possibly a platform are needed, similar to the onshore centralised configuration. However, the onshore centralised configuration also needs an onshore substation. Therefore the offshore central configuration scores a good, and the onshore centralised configuration scores a poor.

5.3.2 Technical

The total conversion steps needed for the centralised onshore configuration is the highest, with five conversion steps. The steps are described in Section 3.1. The centralised offshore configuration needs two conversion steps less, for a total of three steps when a platform is used. When an island is used, also five steps are needed. Finally, the decentralised offshore configuration only needs one conversion step.

The offshore decentral configuration has fewer conversion steps than the offshore and onshore central configurations but still has a more complex system. This is because every wind turbine has its own small electrolyser with its own small balance of plant and water feed. Not only does this add up to many system components, but it must also be fitted on a wind turbine, where limited space is available. The system complexity is less when a central configuration is used since the balance of plant of the electrolyser and the water feed are also central. However, when multiple GWs of wind power are used, multiple structures such as substations or electrolyser platforms are needed, adding to system complexity as well.

As described in Section 3.2, the main by-products of water electrolysis are oxygen gas and waste heat. Both the oxygen gas and the waste heat can be collected and used in other processes (Jonsson & Miljanovic (2022),van der Roest et al. (2023),Kato et al. (2005)). Since these processes are not directly related to the

hydrogen production value chain, the waste oxygen and heat can only be utilised onshore in the central onshore configuration. However, the waste heat could be used when membrane distillation is selected as the offshore water desalination technology.

	Onshore central	Offshore central	Offshore decentral	Weight
Conversion steps	0.2	0.33	1	0.6
Complexity	0.75	0.75	0.5	0.25
Conditions	0.75	0.75	0.5	0.05
By-products	0.75	0.5	0.5	0.1

Table 5.15: Normalised technical MCDA scores table of the electrolyser system configurations

The decentralised offshore configuration has a normalised score of 1 since it has the least amount of conversion steps. The centralised offshore configuration has a normalised score of 0.33, and the centralised onshore configuration has a normalised score of 0.2. In terms of system complexity, the decentralized offshore configuration scores the lowest. This is due to the high amount of system components that are needed when placing a separate electrolyser on each wind turbine. With every electrolyser also comes a separate water desalination system. A score of average was given to the decentralised offshore configuration. Both the centralised onshore and offshore configurations score a good. For the centralised offshore configuration, the system complexity lies mostly in the operation of the electrolyser, including the water desalination, offshore. It does, however, have fewer conversion steps than the onshore centralised configuration, as the centralised onshore configuration has five electrical conversion steps from the wind turbine to electrolyser, and the centralised offshore configuration only has three. Research is being done on the marinization of electrolysers. Due to the hostile and corrosive offshore conditions, the materials of electrolysers can be affected (Amores et al. (2021)). The offshore decentralised configuration is most vulnerable to harsh offshore conditions. When placing the electrolysers centralised on an offshore platform or island, more protection is possible. Offshore substations for transporting electricity to shore, are already deployed on similar platforms as the offshore electrolysers would be placed. Therefore, the centralised offshore and onshore configurations score a good, and the offshore decentralised configuration scores an average. The by-products of electrolysis, namely oxygen and heat, can both be utilised in the centralised onshore configuration, especially if the electrolysers are placed near an industrial cluster. For both of the offshore configurations, oxygen can not be utilised, since no offshore process in the value chain uses oxygen, and bringing the oxygen to land is too expensive compared to the value of the oxygen itself. The heat, however, could be utilised if membrane distillation is selected as the water desalination technology. The onshore central configuration scores a good, whereas both the offshore configurations score an average.

To come to the weight factors of the technical aspects, the best-worst method is used, since three sub-criteria are present. The most important sub-criterion is determined to be the amount of conversion steps, as this potentially saves energy and costs. The least important criterion is determined to be the offshore conditions, as all of the technologies are expected to be able to operate safely and reliably offshore in the future, as research is currently being done on the marinization of electrolysers. The consistency index is acceptable according to the best-worst method. The final scores are given in Table 5.15. The relative scores of the sub-criteria according to the best-worst method, and the following weights, as well as the consistency index, are given in Appendix A.

5.3.3 Flexibility

The decentralized offshore configuration shows the best flexibility. This has several reasons. First of all the system is flexible in terms of operation. When a single electrolyser or wind turbine fails, the production from the other wind turbines and electrolysers can easily continue. Since they are connected by hydrogen pipelines at a manifold, the failure of one electrolyser has no consequences for the others and can easily be replaced or fixed. With the central offshore configuration, the electricity of all the wind turbines is collected and bundled to be inputted in a central electrolyser. If the electrolyser or one of its subsystems fails, the hydrogen production from all wind turbines is affected and cannot continue until the problem is fixed. The same holds for the central onshore configuration.

The second reason why the offshore decentralized configuration shows more flexibility is because it is a modular system. Once a system is installed, it is easier to later add more capacity to the decentralized offshore configuration. More wind turbines can be built close to the existing ones, with their own small electrolysers, and the produced hydrogen can be added to the transportation pipeline. For the centralized offshore configuration, it might be more difficult to later add capacity. If the configuration with platforms is used, the only viable option is to add as many wind turbines to exactly fill the maximum capacity of the electrolysers that fit on a platform. If less is added, it might be too expensive to build/repurpose an entire

platform. This reduces the flexibility since only a certain amount of wind turbines can be added at a time. For the configuration with a dedicated offshore island, adding land once the island is finished is very expensive. This is because the revetments would have to be broken down and rebuilt. The only two viable options for adding capacity later are to add a lot of capacity to make it worth the costs or leave some extra space when building the island in the first place, for eventual later capacity addition. However, if no extra capacity will later be added, these are sunk costs. For the onshore central configuration, the expansion flexibility is also limited, since due to the high HVDC costs, it is only viable to build the number of extra wind turbines that exactly fill the 2GW HVDC cables.

	Onshore central	Offshore central	Offshore decentral	Weight
Failures	0.5	0.5	0.75	0.6
Modularity	0.5	0.75	1	0.4

Table 5.16: Normalised flexibility MCDA scores table of the electrolyser system configurations

The flexibility of the decentralised offshore configuration scores best because the operation can continue if one electrolyser fails. In the case of failure, most wind turbines can thus continue to, indirectly, produce hydrogen. For the centralised onshore and offshore configurations, a failure of the electrolyser causes a lot of wind turbines to not be able to contribute to hydrogen production. The amount of which, depends on the size of the electrolyser. The decentralised offshore configuration scores a good, and both of the centralised configurations have an average score. In terms of modularity, the offshore decentralised configuration scores best, as it is the easiest to add more capacity later on. For the offshore central configuration, it is worthwhile to add capacity in certain steps, as it is only viable to add the amount of capacity that can fill a platform. On an island, less capacity could also be added, but the distance from the wind farm to the island will determine the viable minimal capacity that can be added since expensive cables would have to be laid. For the onshore centralised configuration, 2GW of extra wind turbines would have to become available to later add electrolyser capacity, since TenneT is currently deploying a '2GW programme', to standardize the offshore substations and cables (TenneT (2022a)). The decentralised offshore configuration scores a very good, the centralised offshore configuration scores a good and the centralised onshore configuration scores an average.

It is chosen that the flexibility in terms of failures receives a slightly higher weight than the flexibility in terms of modularity. This is chosen because failures happen more often. Also, when constructing the system, a lot of thought already has gone into determining the size. However, the impact of adding capacity later on is much larger than the impact of a failure. therefore, a weight of 0.6 is given to failures, and 0.4 to modularity.

The scores and weights are given in Table 5.16.

5.3.4 Safety

In terms of safety considerations, the offshore decentralized configurations could have a high risk because of the system complexity and having two systems on one structure, as well as the offshore conditions. If something happens to one of the systems, the other could also be affected. Also in case of an accident, the response time by a crew might also be longer, especially if two or more accidents happen at once since the electrolysers are on separate structures. For the offshore centralized configuration, there is also a safety risk when platforms are used since the systems are densely built on limited space. Also, offshore conditions can impose a safety risk. The response time for the platforms might be lower than for the decentralized configuration since a helicopter can land on a platform. For the dedicated island, the offshore conditions might be of lesser importance, since it is the best-protected offshore configuration. Also, if there is always a crew present on the island, the response time might be the same as the onshore configuration. It does however have the largest asset risk, due to all of the electrolysers being in one place. A safety hazard for the onshore centralised configuration could be the presence of other industrial activities if the electrolysers are built near or in an industrial cluster. The offshore substations can have the same response time as the electrolyser platforms of the centralised offshore configuration.

	Onshore central	Offshore central	Offshore decentral
Safety	0.75	0.75	0.5

Table 5.17: Normalised safety MCDA scores table of the electrolyser system configurations

The decentralised offshore configuration scores an average on safety, as there are multiple systems on one structure. Also, the response time is lowest. For the centralised offshore and onshore configurations, platforms can be used, which have similar safety risks. The island configuration also has specific safety considerations.

Both centralised configurations were given a score of good. The safety scores of the electrolyser system configurations are given in Table 5.17.

5.3.5 Maintenance

For the maintenance of the configurations, there are parallels to the system complexity. With the offshore decentralized configuration, the O&M becomes challenging due to having two systems on one structure. The wind turbine has its own operating and maintenance needs, and the electrolyser system at the turbine adds to that. The maintenance also has to be done per electrolyser, whereas for the centralized configuration, the maintenance can be performed at the dedicated island, or at only a few offshore platforms. At the dedicated island, crew could permanently be present at the island, making the maintenance less expensive and easier, since otherwise, the crew would have to be moved per boat or helicopter offshore. The offshore configurations are also more dependent on weather conditions. When a storm or extreme weather conditions are present on the North Sea at the electrolyser location, it might not be possible to reach the location or get crew on the offshore structure. If a storm lasts for a few days, no maintenance or reparations can be done during that time, potentially costing a lot of money. The offshore maintenance, being centralized or decentralized, is thus much more difficult and expensive than the onshore configuration. The onshore electrolyser is easier to reach, and not dependent on weather.

	Onshore central	Offshore central	Offshore decentral
Maintenance	0.75	0.75	0.5

Table 5.18: Normalised maintenance MCDA scores table of the electrolyser system configurations

In terms of maintenance considerations, the centralised onshore configuration scores best, as it is not dependent on weather and is easy to reach because of the centralisation. The offshore substations, however, are harder to reach as there would be multiple needed, each located near a separate wind farm offshore. The centralised offshore configuration is harder to reach if platforms are used. In this case, a crew would have to be transported to multiple platforms, similar to the offshore substations of the centralised onshore configuration. On an island, the electrolysers would all be next to each other, making electrolyser maintenance easier. However, with this configuration offshore substations are also needed at the wind farms. An added advantage of an island could be to add facilities to house crew on the island, making it easier to deploy them for electrolyser and offshore substation maintenance. The offshore decentralised configuration scores lowest on maintenance since each wind turbine has its own small electrolyser. Thus to perform maintenance on all of the electrolysers, each separate offshore wind turbine would have to be stopped by. Both of the centralised configurations score a good, as their maintenance is similar, and the decentralised offshore configuration scores an average. The scores are given in Table 5.18.

5.3.6 Total Scores

The total weighted scores are summarised in Table 5.19. The best-worst method is used to come to the weights, whereby the technical aspects is chosen as the most important criterion, followed by the flexibility. The least important criterion was chosen to be the safety considerations. The consistency index is acceptable by the best-worst method. The consistency index as well as the relative weights and total weights of the best-worst method are given in Appendix B.1.

	Onshore central	**Offshore central**	**Offshore decentral**	Weight
Cost	0.25	0.50	0.75	0.15
Technical	0.41	0.48	0.81	0.45
Flexibility	0.5	0.6	0.85	0.25
Maintenance	0.75	0.75	0.5	0.1
Safety	0.75	0.75	0.5	0.05
Total score	0.45	0.55	0.75	

Table 5.19: Weighted scores table of the electrolyser system configurations.

As can be seen in Table 5.19, there is a preference for the offshore decentralised configuration, based on the scores and weights used. This is mainly because of the fewer conversion steps, which cuts down on costs and has a large impact on the technical score.

5.4 Storage

In this section, the storage options of Section 3.5 are discussed. The criteria that are discussed are the costs, technical specifications, safety and maintenance considerations and environmental considerations in Sections 5.4.1, 5.4.2, 5.4.4 and 5.4.5 respectively. Section 5.4.6 comes to the final weighted scores.

5.4.1 Cost

The costs of offshore underground hydrogen storage in depleted hydrocarbon reservoirs depend on whether components from the depleted fields can be reused. The total system design is described in Section 3.5.1. The CAPEX for a storage capacity of 4 TWh is estimated to be 3000 M€ for underground hydrogen storage in hydrocarbon fields (EBN & TNO (2022)). The 4 TWh of storage capacity consists of 24 wells, four platforms and ten 15MW compressors. The hydrogen is also purified when leaving the storage facility. The cushion gas is also taken into account for the CAPEX. For accurate CAPEX estimations of separate depleted fields, the characteristics of the field are of importance. These characteristics can determine the storage compression, and thus the amount and size of compressors. The purity level of the storage field and the needed purity of the hydrogen once extracted can determine the size and amount of the purification units. If components of the depleted hydrocarbon system can be reused for underground hydrogen storage, the CAPEX will be lower, since reusing components is less cost-intensive than building and installing new components. The OPEX is assumed to be 5% of the CAPEX per year (Gessel et al. (2023)).

For the salt caverns, it is estimated that 48 caverns of $750.000m^3$ have a total system investment cost of 5433 million € and a storage capacity of 8.65 TWh. These investment costs consist of the salt cavern costs, the pipeline costs and top side costs. The largest share of the salt cavern costs is the construction costs, as a field has to be constructed and the brine has to be carried off. The top side equipment among others consists of compressors, dehydration equipment, heating and cooling equipment and platforms. The operating costs are estimated to be 4% of the CAPEX per year (Eradus (2022), Gessel et al. (2023)).

(Cihlar et al. (2020)) estimates a range of 280 to 424 $€_{2019}$ per MWh H_2 stored in CAPEX for depleted hydrocarbon reservoirs. This includes the compressors and pipelines. However, the amount of compressors is highly dependent on the specific field and storage characteristics. The OPEX is estimated to be 4% of the CAPEX. The same source estimates 334 $€_{2019}$ per MWh H_2 stored in CAPEX for salt caverns. This is based on a design capable of storing 1160 tonnes of hydrogen, although it acknowledges that this is highly dependent on geography. This design includes compressors and pumps. The OPEX is also estimated to be 4% of CAPEX.

A significant part of the investment costs for underground hydrogen storage is the cushion gas. The cushion gas is used to keep the underground storage field under pressure when hydrogen is either injected or withdrawn. For salt caverns, the ratio of working gas to cushion gas is 1:1, whereas, for depleted hydrocarbon reservoirs, this ratio is 1:3. For large storage fields, these costs can become significant.

The cost estimations of the storage in salt caverns are deemed to be fairly accurate since there are already mature technologies for onshore underground storage in salt caverns. For the storage in depleted gas fields, the cost estimations are more unreliable since less experience has been taken up by the industry. It is unsure whether hydrogen will leak from these fields if it is lost or contaminated by the surrounding rocks, liquids and microorganisms, and if it will mix with the methane.

	Salt cavern	Hydrocarbon reservoir	Weight
CAPEX	1	0.95	0.7
OPEX	1	1	0.3

Table 5.20: Normalised cost MCDA scores table of the hydrogen storage technologies

For the CAPEX scores, a value of 352 $€_{2019}/MWhH_2$ is used for the depleted hydrocarbon reservoirs, as it is the average of the range given. For salt caverns, 334 $€_{2019}/MWhH_2$ is used. Since CAPEX is preferred to be as low as possible, the salt cavern has a normalised score of 1, and the depleted hydrocarbon reservoir has a normalised score of 0.95. For OPEX scores, both salt cavern and hydrocarbon reservoirs have an OPEX estimation of 4% of CAPEX, and thus both have a normalised score of 1.

Due to the high investment costs of the storage technologies, it is chosen to assign the CAPEX a weight of 0.7, and the OPEX a weight of 0.3.

The cost scores and weights are given in Table 5.20.

5.4.2 Technical

The TRL of underground hydrogen storage in gas fields is lower than that of salt caverns. The TRL of hydrogen storage in salt caverns for static feedstock is at 9, while the storage in salt caverns for a fast-cyclic

energy system currently has a lower TRL of 5-6. This is however still higher than the TRL of storage in gas fields, ranging from 3 to 4 for pure hydrogen storage, and having a TRL of 5 for blended hydrogen storage (Gessel et al. (2023)). The use of depleted hydrocarbon reservoirs for hydrogen storage has not yet been proven. Multiple researches are currently ongoing to investigate whether hydrocarbon reservoirs are feasible for hydrogen storage. One of the aspects that is under investigation is the storage integrity of the hydrocarbon reservoirs, since it is important that the hydrogen will not leak out of the caprock. Also, the flow properties of the reservoir are of importance, as well as the physical, chemical and microbiological characterisations of the reservoir. There are still some uncertainties about whether storage in depleted hydrocarbon reservoirs will be possible, whereas storage in salt caverns is already proven.

Depleted hydrocarbon reservoirs are usually significant in size and one or a few fields can cover the storage needs to supply a baseload to shore. TNO identifies 56 fields in the Dutch North Sea for the use of short cyclic storage. These short cyclic fields have a volume of 0.5-1.5 billion cubic metres. The total storage capacity of these 56 fields in total is 156,8 TWh (EBN & TNO (2022)). Salt caverns are constructed out of salt structures and a salt structure can consist of many salt caverns. These salt caverns are usually smaller than depleted hydrocarbon reservoirs in terms of storage capacity, and thus more separate caverns are needed. The total storage capacity of salt caverns is 171 TWh (EBN & TNO (2022)).

Since the salt caverns have to be newly constructed, there is no infrastructure yet present that can be reused. Only if a salt structure or cavern coincidentally lies very close to or beneath a platform, it may be reused. For the hydrocarbon reservoirs, many fields have infrastructure and equipment present from past production from the field. This infrastructure and equipment can be reused to reduce the complexity, costs and time of the construction.

The potential locations for salt caverns on the Dutch North Sea are mostly located far to the north of the North Sea, whereas the potential locations for hydrocarbon reservoirs are also located closer to the search area of future wind farms. If enough storage capacity can be realised close(r) to the wind farms, a cost reduction can be made in the reduction of pipeline length needed.

For salt caverns, in literature, a technical lifetime of 30 years is mentioned (TNO (2021), Reuß et al. (2017), Muhammed et al. (2023)). However, two projects in operation since 1972 and 1983, show that the underground storage of H_2 in salt caverns can have a longer lifetime if carefully operated. Therefore the lifetime will be set as 50 years (Aslannezhad et al. (2023)). For underground hydrogen storage in depleted hydrocarbon reservoirs, a lifetime of 30 years (Muhammed et al. (2023)), or 20-40 years (EBN & TNO (2022)) are mentioned in literature. Since no projects are operating longer than the mentioned lifetime, a lifetime of 30 years will be taken into account.

	Salt cavern	Hydrocarbon reservoir	Weight
TRL	1	0.64	0.15
Capacity	1	1	0.2
Reusing	0.25	0.75	0.1
Location	0.5	0.75	0.05
Lifetime	1	0.6	0.5

Table 5.21: Normalised technical MCDA scores table of the hydrogen storage technologies

Since hydrogen storage in depleted hydrocarbon reservoirs has not yet been proven, it scores low on TRL. However, the storage in salt caverns might be high for static feedstock storage, fast-cyclic storage is needed to ensure a baseload to shore, which has a lower TRL. The normalised scores are 1 for salt cavern and 0.64 for depleted hydrocarbon reservoir. The storage capacities of both salt caverns and depleted hydrocarbon reservoirs are very large on the Dutch North Sea. Since both available capacities can easily fulfil the system's need to supply a baseload, both are given a score of 1. Since there is a possibility of reusing infrastructure and/or equipment when storing hydrogen offshore in a depleted hydrocarbon reservoir, and salt caverns have to be newly constructed, hydrocarbon reservoir scores a good on reusing, whereas salt cavern scores a poor. The location of offshore depleted hydrocarbon reservoirs is also more favourable when compared to offshore salt caverns, as they are located closer to the search area of future wind farms. Because of this, depleted hydrocarbon reservoir scores a good, and salt cavern scores an average. In terms of lifetime, salt cavern has the longest lifetime, which is preferred, and has a normalised score of 1. The depleted hydrocarbon reservoir has a normalised score of 0.6.

The technical criterion for storage technologies has five sub-criteria, and therefore the best-worst method is used. The most important sub-criterion is chosen to be a lifetime, as it is costly and challenging to shut down the facility. Apart from decommissioning the facility after its lifetime, a new facility has to be found to replace it, if the rest of the total system is still producing hydrogen. The worst, or least important, criterion is chosen to be location, as the possible locations are relatively close to each other on the Dutch North Sea. The

consistency index is found to be acceptable according to the best-worst method. The total relative weights and final weights, as well as the consistency index, can be found in Appendix A.

The technical scores are summarized in Table 5.21.

5.4.3 Safety

One of the safety risks of underground hydrogen storage is the well integrity and stability. For both depleted hydrocarbon reservoirs as salt caverns, a geotechnical analysis would have to be performed per location to ensure integrity and stability. If the geotechnical analysis is positive and a location is deemed usable, no significant risks should be present. For salt caverns, more experience has already been gained, but it is expected that both should have available locations at the Dutch North Sea. Salt caverns are however considered to have higher structural integrity and a lower leakage potential than hydrocarbon reservoirs, thus requiring less monitoring and maintenance.

When infrastructure and equipment are reused, hydrogen can not only leak through the rock walls but can also leak through the reused equipment. Pipelines and closed wells have to be sealed properly for hydrogen.

Since the storage facility is used to ensure a baseload supply of hydrogen to shore, it will yield a lot of injection and withdrawal cycles. Due to injection or withdrawal, the temperature and pressure can change. This can lead to reservoir fatigue. For both salt caverns and depleted hydrocarbon reservoirs, research is ongoing.

	Salt cavern	Hydrocarbon reservoir
Safety	1	0.75

Table 5.22: Normalised safety MCDA scores table for the storage technologies

A detailed geotechnical analysis should give insights into the specific safety issues for a possible location of underground hydrogen storage in salt caverns or a depleted hydrocarbon field. However, the well integrity of hydrocarbon reservoirs is lower than that of salt caverns. Also, repurposing infrastructure and/or equipment for hydrogen can come with risks. Therefore salt cavern scores a very good, and the hydrocarbon reservoir scores a good. An overview of the scores is given in Table 5.22.

5.4.4 Maintenance

Due to the lower well integrity, the depleted hydrocarbon reservoir needs more monitoring and maintenance. However, since salt caverns have a lower capacity, multiple might be needed to fulfil the hydrogen storage needs, and thus more maintenance is needed.

	Salt cavern	Hydrocarbon reservoir
Maintenance	0.75	0.75

Table 5.23: Normalised maintenance MCDA scores table for the storage technologies

Both receive a score of good. The scores are given in Table 5.23.

5.4.5 Environment

In terms of the environment, the reuse of infrastructure and equipment at the depleted hydrocarbon reservoirs will have an advantage over installing new infrastructure and equipment. If no new platforms or pipelines are being built in the North Sea, it will have less impact on the marine life, whereas building new platforms and pipelines, will affect the seabed and marine life.

For the construction of salt caverns, brine has to be carried off. This can mainly be done in two manners. Firstly the brine can be transported to a processing facility on land to be processed into products or raw materials. However, since the promising salt structures are located far offshore, this can be a costly solution. Another solution is to treat the brine offshore and dispose of it in the North Sea. Due to strict regulations, the brine cannot be disposed of as is, but it has to be treated first.

The brine discharge from the construction of the salt caverns will have to be performed well to minimise environmental damage. With the first option to lay a pipeline to shore to a processing plant, the newly built pipeline will affect the seabed and marine life. The second option to dispose of the brine offshore will need brine treatment to ensure the brine complies with standards and regulations so that it does not harm the local ecosystem.

When CO_2 is used as a cushion gas for hydrogen storage in depleted hydrocarbon reservoirs, both the costs and environmental impact can be lowered. Since the cushion gas makes up a significant part of the

costs for an underground hydrogen storage facility, taking unwanted CO_2, that might be planned to be stored anyway as part of a carbon capture and storage project, might be cheaper than other cushion gasses. Also, capturing the CO_2 from another project or process and storing it underground as cushion gas, so that it does not reach the atmosphere, is a positive impact on the environment.

Some of the possible salt structures in the Dutch North Sea lay in Natura2000 areas. Natura2000 is a European network of nature reserves. These nature reserves are protected to defend certain animals and/or plants to maintain biodiversity. Because of this, extra regulations or costs could be involved when building an offshore hydrogen storage facility. It could also be blocked in total.

	Salt cavern	Gas field	Weight
Construction	0.25	0.75	0.8
Operation	0.75	0.75	0.2

Table 5.24: Normalised environmental MCDA scores table for the storage technologies

The construction of hydrogen storage in a depleted hydrocarbon reservoir has environmental advantages over the construction of a salt cavern. Namely, infrastructure and equipment can be reused, no brine has to be discharged and no Natura 2000 areas are affected. Therefore depleted hydrocarbon reservoir scores a good, against a score of poor for salt cavern. During the operation of both a depleted hydrocarbon reservoir and a salt cavern, CO_2 can be used as a cushion gas. Both score a good on operation.

It is chosen that construction receives a higher weight factor, as it has more impact on the environment. During operation, CO_2 could be used as a cushion gas, but will not necessarily be used. Construction receives a score of 0.8, whereas operation receives a 0.2 as a weight factor.

The scores and weights are summarised in Table 5.24.

5.4.6 Total Scores

The (weighted) scores of all criteria are summarized in Table 5.25. To come to the weights per criterion, the best-worst method is used. The most important criterion is chosen to be the technical aspects, as it has some important sub-criteria, such as the lifetime of the storage facility and the capacity. Cost is the second most important criterion. The environmental aspect is chosen to be the least important, as it has the lowest impact on the total value chain and costs. The relative weights are given by the 'Best-to-Others' and 'Others-to-Worst' vectors, which are given in Appendix B.1. Also, the consistency index and threshold are given in Appendix B.1. The consistency index is below the consistency threshold according to the best-worst method and is thus acceptable.

	Salt cavern	**Hydrocarbon reservoir**	Weight
Cost	1	0.97	0.25
Technical	0.9	0.71	0.45
Safety	1	0.75	0.05
Maintenance	0.75	0.75	0.15
Environment	0.35	0.75	0.1
Total score	**0.9**	**0.8**	

Table 5.25: Weighted scores table of the storage technologies.

As can be seen in Table 5.25, the salt cavern has a slight advantage over the hydrocarbon reservoir in the final score. This is mainly because of the higher technical score, which received the highest weight factor.

5.5 Transport

In this section, the transport options of Section 3.6 are discussed. The four criteria that are discussed are costs, technical specifications, safety considerations, maintenance considerations and environmental considerations in Sections 5.5.1, 5.5.2,5.5.3, 5.4.4 and 5.5.5 respectively. Section 5.5.6 comes to the final weighted scores.

5.5.1 Cost

When hydrogen is produced offshore, it can be sent to shore using pipelines. These pipelines can either be newly constructed or reused. For newly constructed offshore pipelines, estimations for medium and large pipelines are given. Medium pipelines are defined as 36 inches and large pipelines as 48 inches Backbone (2022). The new medium pipelines are expected to have a CAPEX of 3.7M€/km, with a minimum of 3.4

and a maximum of 4.6 M€/km (Backbone (2022)). Since there are no offshore hydrogen pipelines yet newly built, the CAPEX was estimated by multiplying the CAPEX of onshore pipelines of the same size by factor 1.7, since 1.7 is the factor that natural gas pipelines have a higher CAPEX offshore than onshore. For the new large offshore hydrogen pipelines a CAPEX of 4.8 M€/km was found, with a minimum of 4.3 and a maximum of 5.8 M€/km. For repurposed offshore hydrogen pipelines, the CAPEX is significantly lower. Small pipelines of 20 inches were found to have a CAPEX between 1.4 and 1.8 M€/km onshore, and a CAPEX between 2.4 and 3.1 M€/km for offshore pipeline. For the offshore reused offshore medium-sized pipelines, a CAPEX of 0.4 M€/km was found, with a minimum of 0.3 and a maximum of 0.5 M€/km. For the reused large-sized pipeline, the CAPEX was found to be 0.5 M€/km, with a minimum of 0.4 M€/km and a maximum of 0.6 M€/km (Backbone (2022)). The small offshore pipelines have a CAPEX of 0.3 M€/km, with a minimum of 0.2 M€/km and a maximum of 0.5M€/km. The OPEX of offshore pipelines is known to be very low from the offshore gas industry. An OPEX of 0.1% of the CAPEX is a typical, negligible, value. The pressure within the pipeline is higher than the output pressure of the electrolyser. Therefore, compression is needed. The compressor stations are found to have a CAPEX of 3.4M €/MW_e, with a minimum of 2.2 and a maximum of 6.7 M€/MW_e (Backbone (2022)).

The reference case of the Rotterdam Wind Power Hub will use the central onshore configuration, whereby electrons are sent to shore. The cost of landing electrons onshore depends on the technology used for the electricity cables. As described in Section 3.6.4, the break-even point between HVAC and HVDC cables is between 50 and 60 km for submarine cables. Since the search areas for wind farms are more than 60km from Rotterdam, only HVDC cables will be considered. The costs for HVDC cables are taken as 3.5 €/kW/km. The OPEX is estimated at 0.3 €/kW (Alvestad (2022)).

	New pipeline	Existing pipeline	Electricity cable	Weight
CAPEX	0.1	1	0.01	0.9
OPEX	1	1	1	0.1

Table 5.26: Normalised cost MCDA scores table of transportation technologies.

To come to a quantitative score to compare the CAPEX and OPEX of pipelines and electricity cables to each other, a reference of 10 GW and 200km is used. For this reference, medium-sized pipelines of 36 inches could be used. The CAPEX is taken as 3.7M €/km, and thus the total reference CAPEX would be 740M €. For the reused pipelines, the total reference CAPEX would be 80M €. For the HVDC cables, 3.5 €/kW/km is used in the case of 200km and 10 GW. This comes down to a CAPEX of 7 billion €. Since CAPEX is preferred to be as low as possible, existing pipelines receives a normalised score of 1. The normalised scores of new pipelines and electricity cables are 0.1 and 0.01 respectively. For the OPEX, both new and existing pipelines have a value of 0.1 % of CAPEX per year. For electricity cables, the OPEX is 0.3 €/kW. For the reference case, this would be an OPEX of 3M €, which is negligible when looking at the CAPEX. Since all OPEX is negligible, all OPEX score a very good. Because of this, CAPEX receives a weight of 0.9, and OPEX of 0.1.

5.5.2 Technical

The capacity of energy transport via hydrogen pipelines is much larger than the capacity via electricity cables. For the medium-sized pipelines of 26 inches, 4.7 GW capacity is estimated for new pipelines, while reused pipelines can reach 3.6 GW. This is based on a pressure of 50 bar and 75% capacity. For the large pipelines, 13 GW is estimated, both new and reused. This is based on a pressure of 80 bar and 75 % capacity (Backbone (2022)). Two pipelines have already been certified for the future repurposing and use of hydrogen production, as the technology to repurpose existing pipelines to hydrogen pipelines, already exists (A.C.E.R. (2021)). For these pipelines, described in Section 3.6.2, a capacity of 10-14GW is given for the 36-inch NGT pipeline, while a capacity of 10-12 GW is given for the 24-inch NOGAT pipeline. When a storage facility is used, and a baseload of hydrogen can be transported through the pipelines, the capacities can go up to 17-24GW for the NGT, and 17-20 GW for the NOGAT pipeline (Walters et al. (2020b), NGT & NOGAT (2022)). The calculations of the NGT and NOGAT pipeline are based on the higher heating value of hydrogen (39.39 kWh/kg), while the calculations of the European Hydrogen Backbone are based on the lower heating value of hydrogen (33.33 KWh/kg). Also, the capacity of hydrogen through a pipeline largely depends on the pipeline pressure, as can be seen in Fig. 5.1.

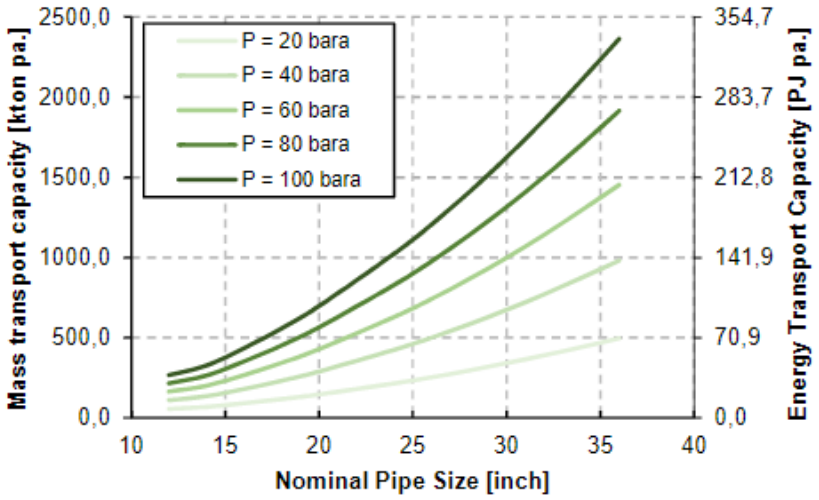

Figure 5.1: Pipeline diameter and pressures and corresponding capacities (Walters et al. (2020b)).

Since the output pressures of the electrolyser technologies are not as high as the transportation pressures, compressors are needed to further compress the hydrogen. The compression power is given by Equation 3.12.

The capacity of the electricity cables used in this thesis is considered to be 2GW. This is currently the largest capacity of cables that TenneT can install. For a pipeline with a capacity of 10GW, five electricity cables would have to be laid out. Also, upscaling through pipelines is easier, since if a new wind farm is built, and the pipeline has capacity left, it can be connected to the wind farm, instead of building an entire new HVDC connection to shore. (Ibrahim et al. (2022)).

For the pipelines, a pressure drop occurs over the length of the pipeline. To compensate for the pressure drop, either extra compressors can be placed along the pipeline, or the input pressure can be brought up to a certain pressure so that the pressure at the other end of the pipeline onshore still is the desired output pressure after the pressure drop. Typical values for pressure drops of hydrogen pipelines are the same as for natural gas pipelines and are estimated to be 3-10 bar/100km (Walters et al. (2020b)). The exact pressure drop depends on the input pressure and pipeline parameters such as diameter and distance. The amount of compressors, and thus electricity, depends on the needed output pressure.

For HVDC cables, the cable loss is estimated to be 0.3% /100km (Gordonnat & Hunt (2020)).

For the lifetime of offshore pipelines, 50 years was taken into account (Breunis (2021)). The same value for new as reused pipelines is used since when retrofitting pipelines, they are retrofitted to be operational for an entire new lifecycle. The needed compressors have a shorter lifetime of 25 years Breunis (2021)). The lifetime of HVDC cables was found to be 40 years (Chatzivasileiadis et al. (2012)). The other components needed for the use of HVDC cables, such as the converters and the offshore substations, have a shorter lifetime of 25 years (Breunis (2021)).

	New pipeline	Existing pipeline	Electricity cable	Weight
Capacity	1	1	0.1	0.65
Losses	0.75	0.75	0.75	0.1
Lifetime	1	1	0.8	0.25

Table 5.27: Normalised technical MCDA scores table of transportation technologies.

In terms of capacity, pipelines are able to transport much more energy per connection to shore. Electricity cables, on the other hand, are only able to connect 2 GW to shore per landing. Both new and existing pipelines have a normalised score of 1, and the electricity cable has a normalised score of 0.1. This is based on the lower capacity value given for the NGT and NOGAT pipelines.

The losses of HVDC cables are estimated to be 0.3%/100km. For the pipelines, the losses are expressed in pressure drop. The pressure drop depends on the input pressure and pipeline parameters. Since cable losses and pressure drops are hard to compare, they are scored quantitively. Both receive a score of good, as the electricity cable has a very low loss, and the pressure drop is easily compensated by compressors, also only requiring a relatively small amount of electricity Siachos (2022). The pressure drop over existing pipelines could be a fraction higher than over new pipelines, but because of the low electricity consumption of the compressors, and the marginal difference in pressure drop, both new and existing pipelines score a good.

The lifetime of the pipelines is taken as 50 years, whereas the lifetime of the electricity cables is taken as 40 years. However, the additional equipment, namely the compressors for the pipelines, and the substations for the electricity cables, have a shorter lifetime of 25 years. Since a longer lifetime is preferred, both of the pipeline technologies have a normalised score of 1, whereas the electricity cable has a normalised score of 0.8.

Three sub-criteria are present, and thus the best-worst method is used. The capacity is chosen as the most important criterion, because the amount of pipelines or cables that have to be laid, can have a large impact on the costs, environment and system integration. The least important sub-criterion is losses, as the transport losses are very small when looking at the total system losses. The consistency index is acceptable according to the best-worst method. In Appendix A, all of the relative weights, final weights and the consistency index are given.

The final scores are given in Table 5.21.

5.5.3 Safety

The largest safety risk for hydrogen pipelines is hydrogen leakage since hydrogen is a highly flammable gas (Khan et al. (2021)). Leakage can caused in multiple ways. Due to hydrogen embrittlement of the pipeline. This has a higher risk at the retrofitted pipelines, as they were not built for hydrogen transport but were later adjusted, and are already underway in their lifecycle. Another way the pipelines can degenerate is by corrosion. This is especially a risk in marine environments. Once again, the reused pipelines are at greater risk as they have been underwater for a longer time. Finally, other marine activity, such as a ship's anchor, can damage the pipelines. This has an equal risk for new and reused pipelines (N. S. Energy (2022)).

For the HVDC cables, the high voltage can be a risk during installation and maintenance. Safety precautions have to be taken into account by personnel working the cables. When the cables are in use, they heat up due to the electrical power flowing through them. Cooling and thermal monitoring equipment has to be used. Finally, other marine activity is also able to damage the HVDC cables, and leakage of cable fluids might occur.

	New pipeline	Existing pipeline	Electricity cable
Safety	0.75	0.5	0.75

Table 5.28: Normalised safety MCDA scores table of transportation technologies.

Both the new pipeline and the electricity cable have a score of good for safety considerations. This is because no significant safety risks are present. The safety risks that come with a marine environment are present for both. The new pipeline scores lower with a score of average. The safety scores are given in table 5.28.

5.5.4 Maintenance

The natural gas pipelines are monitored by computers to detect leaks, check for cracks, deformations or corrosion and make maintenance and/or repair schedules. This technique is called 'pigging', with which an instrument is sent through the pipeline. using this, the lifetime of pipelines is increased. The existing maintenance tools and equipment can easily be adjusted for use in hydrogen pipelines. This can be done in new hydrogen pipelines, as well as retrofitted pipelines (Khan et al. (2021), S. Energy (2020)). Due to the safety risks of hydrogen leakage, the valves from the pipelines would have to be inspected more often than natural gas pipeline valves (Khan et al. (2021)). HVDC cables are designed to have a low maintenance need. The HVDC cables are under maintenance once a year for oil tests, cooling system checks and isolation tests. Each maintenance service takes up to 48 hours (Unnewehr et al. (2020)).

	New pipeline	Existing pipeline	Electricity cable
Maintenance	0.75	0.75	0.75

Table 5.29: Normalised maintenance MCDA scores table of transportation technologies.

For both pipelines and electricity cables, no significant maintenance risks are identified. With both technologies, a lot of experience and optimisation has been done. Therefore both receive a score of good.

5.5.5 Environmental

The environmental impact of reusing existing pipelines is the lowest. This is because these pipelines are already there and only need to be adjusted slightly for hydrogen transport. Also, these networks are already available, and already socially accepted (A.C.E.R. (2021)). However, when cleaning the pipelines before the

hydrogen is transported through them, the brine has to be caught and disposed of correctly, and not to be dumped in the North Sea (Mahmoud & Dodds (2022)).

For the laying of new hydrogen pipelines, the environmental impact is higher due to the impact on the local marine life where the pipeline is to be laid. However, due to the high capacities of the pipelines, only one pipeline would have to be laid for multiple GW-scale wind farms.

Due to this, the environmental impact of the installation of HVDC cables is the largest. When looking at multiple GW-scale, multiple HVDC cables would have to be laid to shore, as well as multiple offshore substations. Also when landing onshore, the HVDC cables have the largest impact, as each needs its own landing on shore, consisting of large safety margins between each landing, as described in Section 3.6.4, consuming a large part of the land onshore. Apart from the cables, also a converter station on the land of 5.5 ha is needed per landing, and possibly a 380kV station of 15-20 ha (Rijksoverheid (2023)).

	New pipeline	Existing pipeline	Electricity cable
Environment	0.75	1	0.5

Table 5.30: Normalised environmental MCDA scores table of transportation technologies.

In terms of environmental impact, existing pipelines have the lowest impact. The existing pipeline scores a very good. A new pipeline has a relatively low impact, as it has a high capacity and one new pipeline can replace a lot of 2 GW electricity cables. Because of this it is chosen to score the new pipeline a score of good, and the electricity cable a score of average. The environmental scores of the transportation technologies are given in Table 5.30.

5.5.6 Total Scores

The (weighted) scores of all criteria are summarized in Table 5.31. To come to the weights per criterion, the best-worst method is used. The most important criterion is chosen to be the technical aspects, as the sub-criteria capacity and lifetime are deemed to be very important. Cost is the second most important criterion. The environmental aspect is chosen to be the least important, as it has the lowest impact on the total value chain and costs. The relative weights are given by the 'Best-to-Others' and 'Others-to-Worst' vectors, which are given in Appendix B.1. Also, the consistency index and threshold are given in Appendix B.1. The consistency index is below the consistency threshold according to the best-worst method and is thus acceptable.

	New pipeline	**Existing pipeline**	**Electricity cable**	Weight
Cost	0.19	1	0.11	0.25
Technical	0.98	0.98	0.33	0.45
Safety	0.75	0.5	0.75	0.15
Maintenance	0.75	0.75	0.75	0.01
Environment	0.75	1	0.5	0.05
Total score	**0.7**	**0.9**	**0.4**	

Table 5.31: Weighted scores table of the transport technologies.

As can be seen in Table 5.31, there is a clear preference of pipelines over electricity cables. The existing pipelines also have a preference over new pipelines. The existing pipeline mostly scores higher on cost and technical, which have high weights.

5.6 Hydrogen Distribution Hub

This Section discusses the hub configurations as discussed in Section 3.7. The multi-criteria decision analysis is performed over four criteria. Firstly, the costs are discussed in Section 5.6.1. thereafter the technical considerations are discussed in 5.6.2, the safety consideration in 5.6.3, the maintenance considerations in 5.6.4 and the environmental considerations in Section 5.6.5. Finally, the total weighted scores are given in Section 5.6.6

5.6.1 Cost

As described in Section 3.7.1, an energy island can have multiple uses, apart from the production and transport of hydrogen. To be able to make a comparison with other designs, these extra uses are not taken into account, and only the necessary infrastructure for hydrogen production and transport will be considered.

This includes the electrolysers, electricity transport from the wind farm to the island, including the necessary converter stations, hydrogen transport to shore, including the compressors and the desalination units. These components have been described in Sections 5.1,5.2 and 5.5, and will not be taken into account in this Section. The costs for the island that will be taken into account in this Section are the construction of the island itself, consisting of the revetment, breakwater, sand fill and the harbour with quay walls, as well as the necessary facilities to be able to operate the island, consisting of a helicopter platform, living areas and a lay-down area. The unit price of every component of the island is given in Table 5.32 (van der Veer et al. (2020)).

Description	**Unit price**
Revetment	200.000 €/m
Breakwater	225.000 €/m
Sand fill	7,50 €/m^3
Harbour (Quay walls)	125.000 €/m
Harbour (Slope and jetty)	25.000 €/m

Table 5.32: Components of the energy island with their corresponding unit costs van der Veer et al. (2020)

An island for 10GW electrolyser capacity can be estimated at around 1500 M€ (van der Veer et al. (2020)). This is done by taking the estimations of a 2GW, 5GW and 20GW island, and estimating a 10GW island based on those numbers. The estimations of the OPEX of the island are given as 3M€/year, independent of island size (van der Veer et al. (2020)). In this estimation, however, the OPEX of the cable landing facilities is included.

For the costs of a platform, either a new platform can be built, or an existing platform can be repurposed. When building a new platform, a foundation, jacket and topside structure would have to be constructed. However, when repurposing an existing platform, the foundation and jacket can be reused, and only a new topside structure would have to be made and installed. The topside structure houses all the process equipment, whose costs are discussed in Sections 5.1, 5.2 and 5.5. The cost of the topside structure in this section only applies to the steel for the structure and the installation costs. Table 5.33, gives an overview of the costs per tonne for the platform components. The price difference comes from the complexity of the assembly (DNV (2023)).

Structure element	**Steel cost factor**
Topside structure	6.000-9.000 €/tonne
Jacket	2.800-4.000 €/tonne
Foundation	1.000-2.000 €/tonne

Table 5.33: Components an offshore platform with their corresponding component cost factors DNV (2023)

As a rule of thumb, the mass of the topside structure is equal to the mass of the process equipment installed on the topside structure. Eq. 5.1 gives the jacket's mass.

$$m_{jacket} = d \cdot 1.7 \cdot m_{topside}^{0.4557} \tag{5.1}$$

Where d is the water depth in meters and $m_{topside}$ is the mass of the total topside (structure and equipment) in tonnes. The foundation of a platform is highly dependent on the soil conditions, water depth, currents and the mass it supports (DNV (2023)). A reference case shows a total platform cost of 65M€ for the cost and installation of the topside, jacket and foundation of a new platform that holds the equipment for a 500MW electrolyser, including the transformer and water treatment. The topside has a total cost of 42.75M€ and is the part that should be taken into account when repurposing an existing platform (DNV (2023)). The OPEX of an offshore platform mostly consists of annual inspections and potential repair costs. An offshore platform is designed for 30 years of operations, and the OPEX is estimated to be 4% of CAPEX per year (Eradus (2022)).

	Island	Existing platform	New platform	weight
CAPEX	0.57	1	0.66	0.7
OPEX	1	0.01	0.01	0.3

Table 5.34: Normalised cost MCDA scores table of hydrogen distribution hub configurations.

An island of 10GW electrolyser capacity is estimated at around 1500 M€. As an estimation for the platforms, 65M€ was taken as the cost for a new 500MW platform. An existing platform could be repurposed

for 42.75M€, based on estimations. To come to a comparable price, the island price is divided by 20 to come to a price per 500MW. The existing platform has the lowest price and has a normalised score of 1. The new platform has a normalised score of 0.66 and the island has a normalised score of 0.57. The OPEX of the island is given as 3M€/year, which comes down to 0.02% of CAPEX per year. The new and existing platforms both have an OPEX of 4% of CAPEX per year. The island thus has a normalised score of 1, whereas the platforms have a normalised score of 0.01. Because of the high CAPEX, it is decided to assign a weight of 0.7 to the CAPEX, and 0.3 to the OPEX.

The scores and weights are given in Table 5.34.

5.6.2 Technical

The lifetime of an artificial island is taken to be 80 years (DEA & EY (2022)). Offshore platforms are usually designed for a twenty, thirty or forty-year lifetime. A lifetime of thirty years is considered here for newly built platforms (Eradus (2022)). A lifetime extension analysis has to be performed when reusing existing platforms to determine the lifetime, but it is taken as 20 years in this thesis.

The water depth to which offshore fixed structures might be used for offshore platforms can be up to 400 meters (Amaechi et al. (2022)). Since the water depth at the Dutch North Sea does not exceed those depths, platforms can be used in every potential location. The building of an artificial island becomes much harder and especially more expensive when the water depth is increased. A realistic water depth to build an artificial island is up to 30 meters (van der Veer et al. (2020),International (2022). The potential locations in the North Sea are thus limited compared to platforms.

For the artificial islands, the footprint of the systems built on top of it is of importance to be able to make the island as small as possible for cost savings. For the platform, both the footprint and the weight of the systems are of importance, since the costs of the platform are mostly dependent on the weight (DNV (2023)). This makes PEM the most viable candidate for the platform configuration.

The island configuration can benefit from cost reductions by facilitating larger capacities than a platform could. Since the initial investment for an island is very high, if one is built, it can have a cost-benefit by making it large enough to facilitate multiple wind farms. Due to this, a technical issue arises. Inter-array 66kV AC cables are cost-effective up to a distance of 30km (van der Veer et al. (2020)). When multiple wind farms are connected, the island might lay within a 30 km radius of some of the wind farms, but outside of that radius for other wind farms. If the distance is larger than 30km, the electricity can be transported by HVAC cables. This requires more expensive cables, and expensive converter stations, increasing the investment costs. The platforms will most likely have a capacity of 500MW, and can thus always be built close to the wind farm, as all planned wind farms have a capacity larger than 500MW (Rijksoverheid (2019)).

	Island	Existing platform	New platform	weight
Lifetime	1	0.25	0.38	0.4
Water depth	0.5	1	1	0.2
Footprint limitations	0.75	0.5	0.5	0.25
Wind farm connection	0.5	0.75	0.75	0.16

Table 5.35: Normalised technical MCDA scores table of hydrogen distribution hub configurations.

A longer lifetime is preferred, and thus, the island has the largest normalised score of 1. The new platform has a normalised score of 0.38, and the existing platform has the lowest normalised score of 0.25. The depth of the Dutch North Sea is very suitable for fixed platforms. Both new and existing platforms score a very good on this aspect. Since the construction of an island is only suitable for limited locations on the North Sea, it has a score of average. Both the island and platform benefit from a small electrolyser footprint, since space is limited and expensive. For the platforms, the electrolyser weight is also of importance, since the platform's costs depend on the weight. The island scores a good, and the platforms score an average. For the wind farm connection, the platforms score a good, since the platforms can always be built close to a wind farm. For the island, the optimal spot between multiple wind farms can still be HVAC distance from the furthest wind farm, and thus the score of average is given.

For the technical considerations, four sub-criteria are present, and thus the best-worst method is used. The lifetime is the most important sub-criterion, as building a new distribution hub comes with high costs. The wind farm connection is of the least importance, as all connections are relatively close by. The consistency index is acceptable by the best-worst method and the relative weights and consistency index are given in Appendix A.

The scores are summarized in Table 5.35.

5.6.3 Safety

In terms of safety considerations, the artificial island will have a faster response time in case of accidents since the crew is permanently present on the island. There is also a helicopter pad present, as well as a harbour, that can be used in case of an evacuation. Finally, the control room, living areas and helicopter pad can be built closely together for easier access (van der Veer et al. (2020)). A negative safety consideration for the island is that all of the equipment is centralized in one location, and in the case of a storm or a large fire, all of the equipment might be damaged. The platforms come with a longer response time since no permanent crew is present. However, not all of the equipment is centralized in one location when using platforms, which might be a safety advantage.

	Island	Existing platform	New platform
Safety	0.75	0.75	0.75

Table 5.36: Normalised safety MCDA scores table of hydrogen distribution hub configurations.

Since neither the platforms nor the island has a very significant safety risk, all three are given a score of good, which is given in Table 5.36.

5.6.4 Maintenance

The maintenance of the assets on an artificial island will be quicker and easier than the maintenance on a platform since all of the assets are centralized. On an island, living areas will be present to always have personnel on-site for easy access to maintenance, and the harbour allows for easy transportation of spare parts. There might also be room for a lay-down area for spare parts so that maintenance can also be carried out more easily. In terms of maintenance for the island itself, regular inspections should take place since the harsh offshore conditions can cause corrosion and erosion.

Offshore platforms are influenced by wind above water, and by waves and currents on their subwater structure. It is therefore important to carry out regular inspections, and if needed, repairs (Sidiq et al. (2023)). Since no on-site personnel is present at the platforms, boats or helicopters are needed to reach them. This can make for harder access if a storm or bad weather is present near the platform, potentially delaying the inspections or repairs. Also since there are multiple platforms, the maintenance has to be performed at several locations, instead of one location, as with the island configuration.

	Island	Existing platform	New platform
Maintenance	1	0.5	0.5

Table 5.37: Normalised maintenance MCDA scores table of hydrogen distribution hub configurations.

The island scores a very good in terms of maintenance, as the equipment is centralised, with crew present, and even a lay-down area is optional. The platforms receive a score of average as they are dependent on weather and transportation. The maintenance scores are summarized in Table 5.37.

5.6.5 Environmental

During the construction of the artificial island, some negative effects on the local ecology. For example, the lights and noise during construction offshore can disorient migrating birds, thinking they have reached land. The underwater noise will cause fish and sea mammals to leave the area, albeit temporarily and without permanent hearing damage, and the seabed, with different species living on it, will be affected by dredging (van der Veer et al. (2020)). Once in operation, the island can also have positive effects. A part of the seabed is obviously lost due to the island, and on the side of the island where the waves come in, the island will be constructed of hard materials and a rough environment will arise for ecological development. However, on the lee side of the island, a calm environment arises, and the sandy slopes of the island are perfect for flora and fauna to settle. This will attract various underwater species. The local species it attracts can, in turn, be food for local fish, sea mammals and birds, so that a thriving ecology can arise (van der Veer et al. (2020)).

For the construction of an offshore platform, the largest environmental impact will be during the construction phase, the same as for the construction phase of an island. However, when constructing a platform, piles need to be driven into the seabed, causing much more underwater noise than the construction of an island. This can lead to communication problems between species, overall disturbance and even hearing problems (Abhinav et al. (2020)). A positive effect of a platform, however, is that when in operation after the construction phase, the underwater structures of the platforms can act as artificial reefs, creating a local habitat. Also, since fishing is almost always prohibited around offshore structures, they can act as

small marine protected areas (Abhinav et al. (2020)). For existing platforms, no drilling is needed since the underwater structures are reused. It has been found that reusing offshore platforms show a more positive environmental impact than current standard decommissioning procedures (Leporini et al. (2019)).

	Island	Existing platform	New platform
Environment	0.5	0.75	0.5

Table 5.38: Normalised environmental MCDA scores table of hydrogen distribution hub configurations.

Both the island and the new platform have a negative impact during the construction phase, but a positive impact when in operation, on the local marine ecology. They are both given a score of average. The existing platform does not have to be constructed, but only has a positive impact on the ecology and thus has a score of good. The final scores are given in Table 5.38.

5.6.6 Total Scores

The (weighted) scores of all criteria are summarized in Table 5.39. The best-worst method is used to come to the weights per criterion. The most important criteria are the technical aspects and the costs, which are given the same weight. The environmental aspect is chosen to be the least important, as it has the lowest impact on the total value chain and costs. The relative weights are given by the 'Best-to-Others' and 'Others-to-Worst' vectors, which are given in Appendix B.1. Also, the consistency index and threshold are given in Appendix B.1. The consistency index is below the consistency threshold according to the best-worst method and is thus acceptable.

	Island	**Existing platform**	**New platform**	Weight
Cost	0.7	0.7	0.47	0.35
Technical	0.75	0.56	0.61	0.35
Safety	0.75	0.75	0.75	0.1
Maintenance	1	0.5	0.5	0.15
Environment	0.5	0.75	0.5	0.05
Total score	**0.75**	**0.65**	**0.55**	

Table 5.39: Weighted scores table of the hub configurations.

The island configuration has a clear preference over both of the platform configurations. This is mostly because of the higher technical score, which is mostly built up of the higher lifetime score.

6 Results

In this Chapter, the results are given. Firstly, Section 6.1 gives the three simulated designs in the model, and their physical system integration is analysed. The results of the model are divided into the technical results in Section 6.2 and the financial results in Section 6.3.

6.1 Designs

This section of the results gives the three simulated designs in the model. The designs are given generally in terms of their value chain components, as well as in more detail with parameters such as pipeline diameters and compressor power. The offshore decentral design is discussed in Section 6.1.1, after which the offshore central and onshore central designs are discussed in Section 6.1.2 and 6.1.3

6.1.1 Design 1: Offshore Decentral Configuration

The first design is constructed by selecting the best-performing technology per value chain component against the decision framework. For the electrolyser technology, PEM electrolysis is used, as it outperformed alkaline and SOEC against the decision framework. For the water feed, reverse osmosis is used, and as the electrolyser system configuration, an offshore decentral configuration is used, with the electrolysers located at the foot of the wind turbines. Salt caverns are used as a storage technology. For transport technology, reusing existing pipelines is to be used where available. System integration shows where existing pipelines can be used, and where they are unavailable, new hydrogen pipelines are considered. Finally, for the offshore decentral configuration, there is no need for an offshore island or platform, so the hydrogen distribution hub is not taken into consideration for this design. An overview of the components is given in Table 6.3.

Value chain component	**Technology**
Electrolyser technology	PEM
Water feed	Reverse osmosis
Electrolyser system configuration	Decentralised offshore
Storage	Salt cavern
Transport	Existing pipeline
Hydrogen distribution hub	n.a.

Table 6.1: Value chain component technologies for design 1.

The start of the value chain is at the foot of the wind turbines, where the electrolysers and water desalination units are placed on a small platform on the foot of a wind turbine. For the NREL turbines used, the rotor diameter is 240 meters, and the number of turbines per 2GW wind farm is 133. Collection pipelines are laid through the wind farm, to which every turbine is connected. To reduce the pressure drop in the hydrogen collection pipelines, multiple pipelines are laid in the wind farm to reduce the length per pipeline. The wind turbines are placed in an 11 by 12 layout, with one extra turbine at the edge to come to 133 turbines per wind farm. The collection pipelines are laid in a line, collecting the hydrogen at 11 wind turbines each. This is shown in Fig. 6.1.

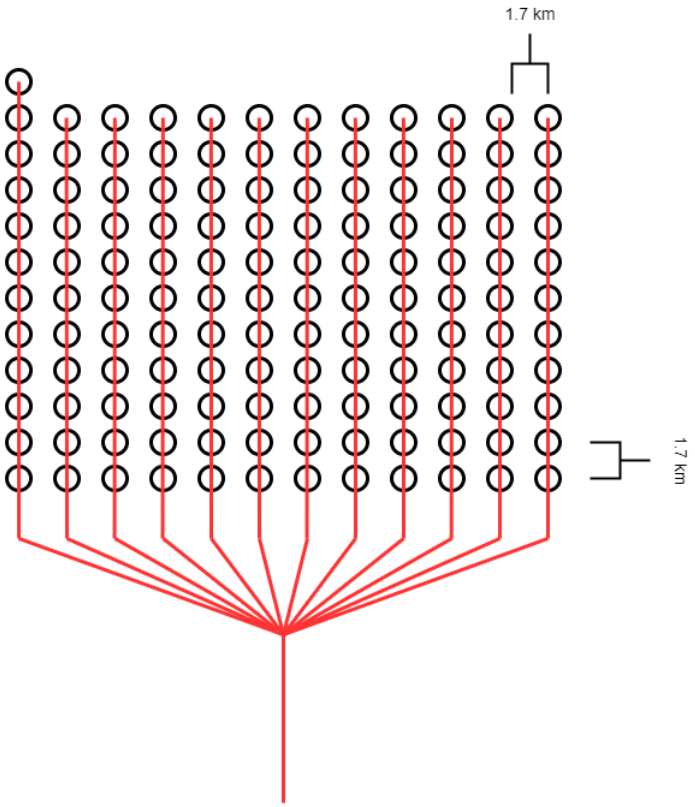

Figure 6.1: Hydrogen collection pipelines layout for one wind farm.

The spacing between the turbines is 1.7 km, by Eq. 4.23. The black circles indicate the wind turbines, whereas the red line indicates the hydrogen collection pipelines. Using the simplified pressure drop calculation for a 12-inch pipeline by Eq. 4.25 with an input pressure of 50 bar, which is the output pressure of the PEM electrolyser, and an average pipeline length of 21.5 km, the pressure drop is around 4 bar. The length per pipeline is 10 times the spacing between two turbines, plus an average of 4.5 km to come from the last turbine to the meeting point of all collection pipelines. Because of the low pressure drop and the high output pressure of the PEM electrolyser, no compressors are needed for the hydrogen collection pipeline. A manifold connects the hydrogen collection pipelines in the wind farm to continue to the start of the pipeline to shore as one pipeline. The layout of the five wind farms and the pipeline to shore is given in Appendix C. Only the pipelines from the farm to the starting point of the pipeline to shore are given for one wind farm but are present for all wind farms. The total hydrogen collection pipeline length over all wind farms is 1390km. The maximum produced hydrogen is 245 kg per electrolyser in an hour. Using Eq. 4.24, a pipeline capacity of 1.4 GW is needed. For the collection pipeline, a pipeline with a diameter of 12 inches is used. To come to the capacity for the pipeline to shore and to the storage facility, the maximum collection pipeline capacity is multiplied by the number of wind farms, which is five. The pipelines to shore and to the storage facility need to have a capacity of 7 GW, and it was chosen to use a 36-inch pipeline for these pipelines. Since the capacity of the 36-inch pipeline is larger than the needed capacity, only the percentage needed is used in the cost calculations.

Using the North Sea Energy Atlas, it was found that 75 km of the 36-inch pipeline to shore could make use of the 36-inch NGT pipeline by repurposing that pipeline. This makes the total pipeline to shore consist of 75 km repurposed pipeline and 175 km newly laid pipeline (N. S. Energy (2023)). Also, for simplicity, one pipeline is laid to the storage facility because, per timestep, hydrogen is only either inserted or withdrawn from the storage facility, and the flow is in one direction. A newly laid pipeline is used for this, as no existing infrastructure is present to be repurposed. Space is available at the PoR to land a 36-inch pipeline (PoR (2023)).

In the offshore decentral configuration, there are also multiple compressors present. As an assumption, the hydrogen is to be delivered onshore with a pressure of 50 bar. Based on pressure drop calculations done in Section 4.4, the input pressure of the 36-inch pipeline to shore is calculated. No compressors are needed for the hydrogen collection pipeline. As the input pressure for the pipeline to shore, the output pressure of the electrolysers and the pressure drop over the hydrogen collection pipelines are taken into account. Also, a compressor is present at the storage facility to pressurise the hydrogen for underground storage.

The electricity consumption of the compressors for the storage facility is 1.1kWh/kg H2 (Groenenberg et al. (2020)).

The location of the storage facility is close to the search areas of the wind farms. Comparing Fig. 3.12 with Fig. 4.2 shows that the salt structures on the Dutch North Sea are in the same area as the search areas for the offshore wind farms. Starting from the central point between the wind farms, a distance of 20 km is chosen as the length of the pipeline to the salt caverns.

Since the electrolyser is placed at the foot of the wind turbine, only one conversion step of the electricity is needed to come to the 1000V DC input power needed for the electrolyser. Also, no inter-array cables or HVDC/HVAC cables are needed.

A total overview of the system of the first design is shown in Fig. 6.2.

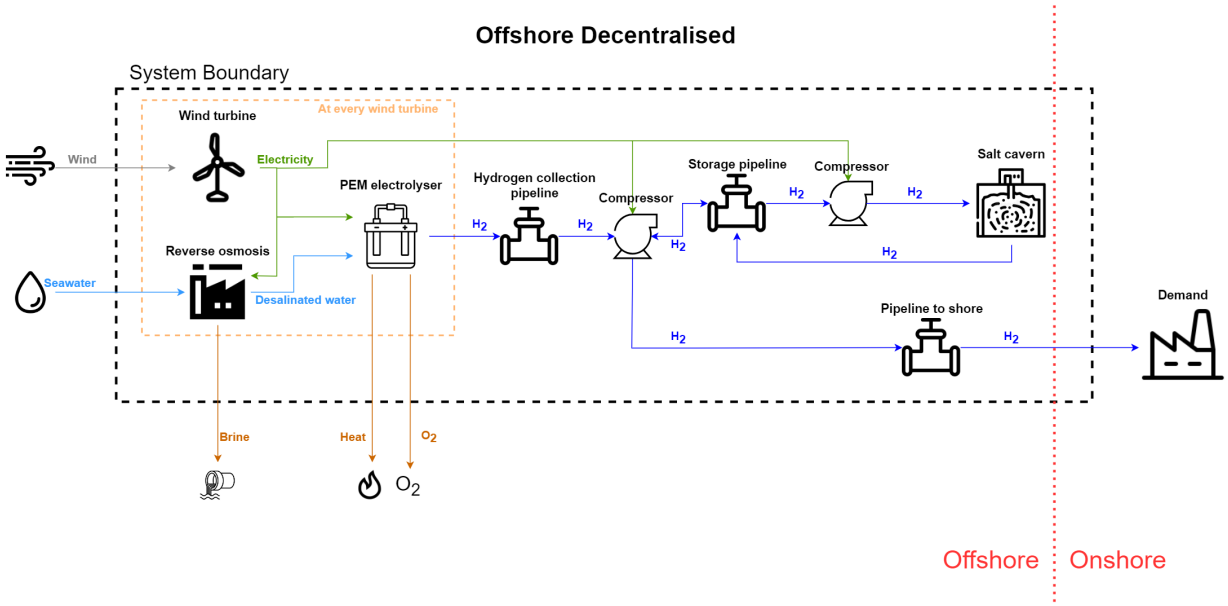

Figure 6.2: Schematic representation of the components of the offshore decentral design, including the system boundary.

The black dotted line shows the system boundaries. The wind and water are not included in the system boundaries, as well as the demand. Each flow has been identified with its colour. Light Blue is water, grey is wind, orange is by-products, green is electricity, and dark blue is hydrogen. The orange dotted line shows the subsystem per wind turbine, as the decentral configuration has a small electrolyser and reverse osmosis plant per wind turbine. The wind turbine converts wind power into electricity, which is used at the reverse osmosis plant and the electrolyser, but also at the compressors. The reverse osmosis plant uses seawater and electricity to produce desalinated water, which comes with brine as a by-product. Thirdly, the electrolyser uses desalinated water and electricity to produce hydrogen, which come with heat and oxygen as by-products. The hydrogen is then collected and transported to a central point by the hydrogen collection pipelines. Depending on the amount of hydrogen produced at the specific time, the hydrogen is either transported to storage or shore. When it is transported to storage, it is transported by a pipeline. Before entering the salt cavern, the hydrogen is compressed by a compressor. Once hydrogen is needed from the storage to complement a baseload, the hydrogen is transported through the same pipeline in the reverse direction. Since the hydrogen was stored under high pressure, no compressors are needed. Before transporting the hydrogen to shore, the compressors increase the pressure of the hydrogen to have it land onshore at 50 bar. The demand is outside the system boundaries. To supply electricity to the compressors at the start of the pipeline to shore and at the storage facility, 1 string of 11 turbines, as shown in Fig. 6.1, is used. An inter-array cable is laid to the compressors. The installed compressor capacity is 142 MW and can thus be supplied by 11 turbines. The red dotted line indicates the offshore and onshore components.

6.1.2 Design 2: Offshore central Configuration

For the second design, a different electrolyser system configuration is chosen than the electrolyser system configuration of the first design. The starting point for the second design is the offshore central configuration. Since the space is very valuable offshore, again, a PEM electrolyser is selected as the electrolyser technology. PEM electrolysers offer advantages in space requirements as well as flexibility, which are both beneficial

offshore. For the water desalination technology, reverse osmosis is selected because of its technical advantages over membrane distillation. Also, for the storage technology, the same technology, namely salt caverns, is selected. Salt caverns were selected mainly because of their advantageous technical aspects over hydrocarbon reservoirs, and are more suitable to short term fluctuations. For the transport technology, existing pipelines are to be used since hydrogen is produced offshore. If not available, new pipelines have to complement. However, electricity cables are also needed to transport the electricity from the wind turbines to centralised electrolysers. Finally, an island configuration is to be used, mainly because of its cost and technical advantages over the use of platforms.

Value chain component	**Technology**
Electrolyser technology	PEM
Water feed	Reverse osmosis
Electrolyser system configuration	Centralised offshore
Storage	Salt cavern
Transport	Existing pipeline & Electricity cable
Hydrogen distribution hub	Island

Table 6.2: Value chain component technologies for design 2.

For the second design, the central offshore configuration is used. The value chain starts at the wind turbine, where converters convert the electricity to 66 kV AC current, to be transported by inter-array cables from the wind turbines to the offshore substations. The length of the 66 kV inter-array cables per wind farm is taken as 350 km. This is based on two existing projects, namely a 2.1 GW wind farm at the coast of New York, which has a 66 kV inter-array cable length of 350 km, and Hollandse Kust Noord, a Dutch offshore wind farm of 759 MW with a 66 kV inter-array cable length of 140 km (Equinor & BP (2023),Eneco (2023)). The inter-array cables transport the electricity to offshore HVAC substations. For the HVAC substations, a capacity of 700 MW is used, as that is standard for HVAC substations used by TenneT on the Dutch North Sea (TenneT (2022b)). 3 HVAC substations are thus used per wind farm.

For the offshore central configuration, an island is used as the hydrogen distribution hub. The HVAC cables go from the HVAC substations at the wind farms to the central island, which is located in the middle of the wind farms, with a distance of 20 km to each substation. On the island, HVAC substations are placed to convert the electricity back to a lower DC voltage, which is the final and fifth electrical converter step, as well as the PEM electrolysers, a reverse osmosis water desalination plant and potentially batteries.

From the island, two pipelines are laid out. The first pipeline is a pipeline that transports the produced hydrogen to shore. For this pipeline, a 36-inch pipeline is used, with 75 km of it being the repurposed NGT pipeline and 175 km is newly being laid. This is the same as for the offshore decentral configuration, based on the same reasoning. Also, a 36-inch pipeline is newly laid to the storage facilities. Space is available at the Port of Rotterdam to land a 36-inch pipeline (PoR (2023)).

For the offshore central configuration, compressors are present at the start of the 36-inch pipelines, as well as at the storage facility. The size of the compressors at the pipelines is based on the pressure drop through the pipelines, whereas the compressors at the storage facilities are sized based on the amount of hydrogen that is put in the storage facility.

A total overview of the system of the second design is given in Fig. 6.3.

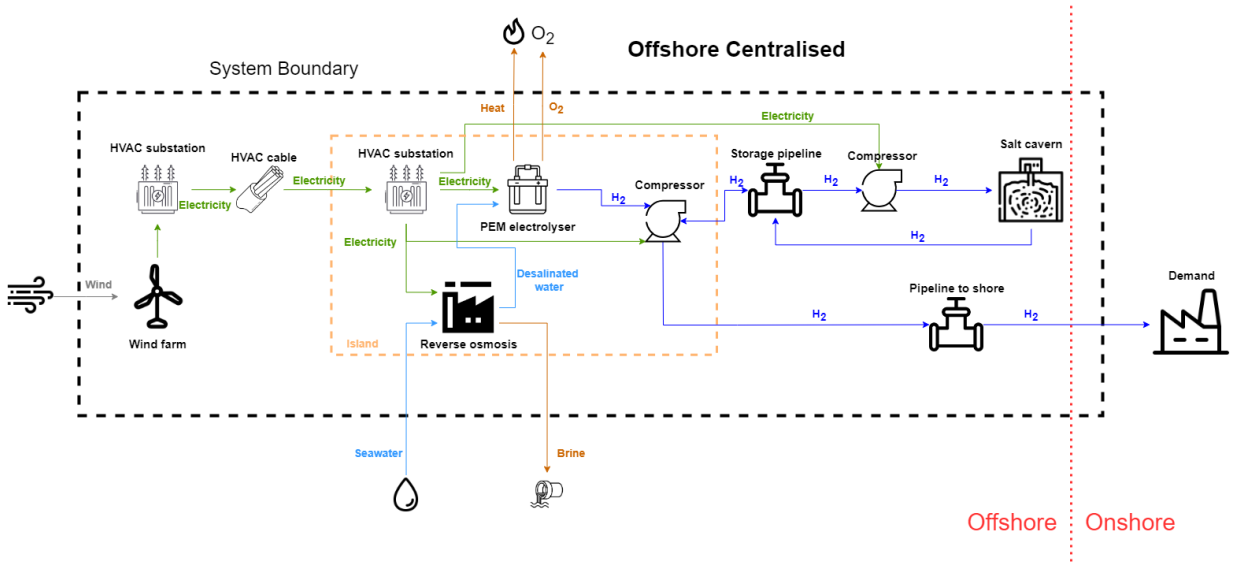

Figure 6.3: Schematic representation of the components of the offshore central design, including the system boundary.

Again, the black dotted line shows the system boundary, and the wind, seawater and demand are outside of it. Light blue indicates the water flow, green indicates electricity flow, dark blue indicates hydrogen flow, and brown indicates the flow of by-products. The red dotted line indicates which components are offshore and which are onshore, and the orange dotted line indicates which components are on the island. Electricity is generated at the wind farms. The electricity is transported to the island via an HVAC infrastructure, on which electrolysis, hydrogen compression, and water desalination take place. The same mechanics of the pipelines and salt cavern take place to supply a baseload to demand, as with the offshore central configuration.

6.1.3 Design 3: Onshore Central Configuration

The third design makes use of the onshore central configuration. For an onshore configuration, space requirements are of less importance, and the alkaline electrolyser is chosen for this configuration because of its lower costs. For water desalination, reverse osmosis is used again because of its simplicity. Salt caverns are to be used for the storage technology. The energy transport to shore has to be done with electricity cables in this configuration, but a pipeline is also needed to transport the hydrogen from and to the storage facility. Finally, since no hydrogen distribution hub is to be used in this configuration, none is selected.

Value chain component	**Technology**
Electrolyser technology	Alkaline
Water feed	Reverse osmosis
Electrolyser system configuration	Centralised onshore
Storage	Salt cavern
Transport	Electricity cable & Pipeline
Hydrogen distribution hub	n.a.

Table 6.3: Value chain component technologies for design 3.

The third design is the onshore central electrolyser configuration. At each wind turbine, the electricity is converted to 66 kV AC current for the inter-array cables. The same inter-array cable length per wind farm is taken as for the second design. However, for the onshore central configuration, the electricity is transported to shore over a long distance, and thus, HVDC cables and substations are used. TenneT is working on a standardised HVDC offshore substation that will be used from 2028 onwards TenneT (2022b). The capacity of this standardised HVDC substation will be 2 GW. The 2 GW HVDC substation will also be used in this design. Because of this, each wind farm only needs one HVDC offshore substation. From the offshore substation, HVDC cables will be laid to shore, each having a length of 250 km. Onshore, another substation is needed per 2 GW cables to convert the power back to 1000 V DC input power for the electrolyser, making for a total of five converter steps. Next to the onshore substations will be alkaline electrolysers and a reverse osmosis water desalination plant.

To make use of the storage facility, a new 250 km 36-inch pipeline is laid to the salt caverns. To transport the hydrogen through the pipeline, compressors are present at the beginning of the pipeline. Also, at the

storage facility, compressors will be present to pressurise the hydrogen for underground storage.

A total overview of the system of the third design is given in Fig. 6.4.

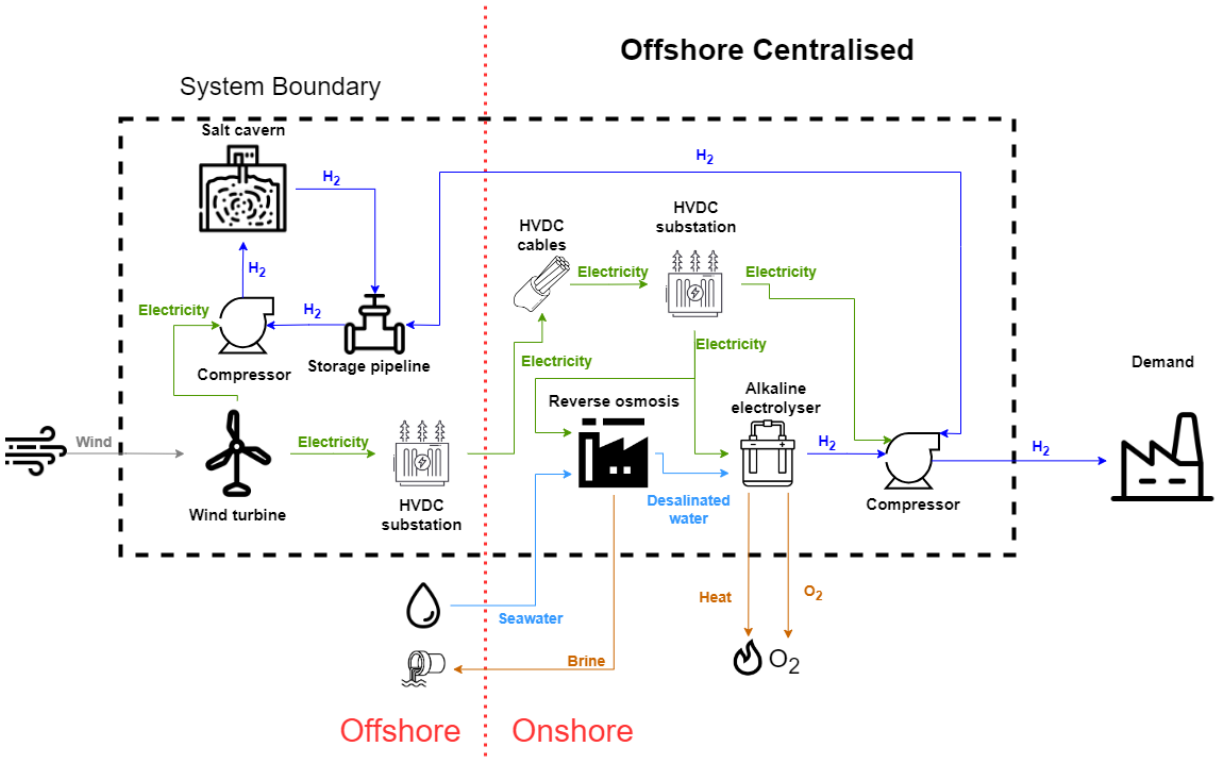

Figure 6.4: Schematic representation of the components of the onshore central design, including the system boundary

Again, the block dotted line indicates the system boundary, the green arrows indicate electricity flow, the light blue arrows indicate water flow, the brown arrows indicate by-product flow, and the dark blue arrows indicate hydrogen flow. The red dotted line indicates which components are offshore and which are onshore. This design makes use of an HVDC infrastructure to transport electricity to shore. The electrolysis, hydrogen compression, and water desalination occur onshore. As this design assumes to be at the demand, no pipeline between the compression and demand is considered. Also, as found in the RWPH project, it is likely that no space is available in the Port of Rotterdam to lay pipelines for a water feed or heating network connecting to the electrolysis location (PoR (2023)). Due to this, a reverse osmosis plant is used, and heat is dissipated into the atmosphere.

6.1.4 Input parameters

Table 6.4 gives an overview of the different technical parameters for each design that are changed in the model to run the simulations. Designs 1 and 2 use PEM electrolysers, and the electrolyser parameters are the parameters of PEM electrolysers, found in Section 5.1. For design 3, alkaline electrolysers are used. Designs 2 and 3 use 66 kV inter-array cables to bundle the electricity at the offshore substations. The losses of the 66 kV inter-array cables are taken as 0.6% (Gasnier et al. (2016)). The different electrolyser system configurations also come with different needs for pipelines and cables. Design 1 does not use cables, whereas designs 2 and 3 make use of HVAC and HVDC cables, respectively, accompanied by their substations. Design 1 is the only design that uses a hydrogen collection pipeline, as the hydrogen is produced per turbine, of which the length is given per wind farm. Both designs 1 and 2 have a length of 250 km for the 36-inch hydrogen pipeline to shore, and both are a distance of 20 km to the salt cavern storage facility. Design 3 sends electricity to land instead of hydrogen, thus not requiring a pipeline to shore. However, a hydrogen pipeline is needed to come to and from the storage facility. Finally, the model is run once to size the compressors. Once the compressors are sized, their rated power is an input to the model.

Parameter	Unit	Design 1	Design 2	Design 3
Electrolyser power consumption	kWh/kg H_2	53.2	53.2	53.2
Electrolyser Lifetime	h	125 000	125 000	125 000
Electrolyser efficiency degradation	% /1000 h	0.1	0.1	0.1
Electrolyser output pressure	bar	50	50	20
Electrolyser lower load range	%	0	0	10
Electrical converter steps	-	1	5	5
Hydrogen collection pipeline length	km	200	-	-
Hydrogen pipeline to shore length	km	250	250	-
Hydrogen pipeline to storage facility length	km	20	20	250
HVDC cable length	km	-	-	250
HVDC cable losses	%/100km	-	-	0.35
HVAC cable length	km	-	20	-
HVAC cable losses	%/100km	-	0.7	-
Inter-array cable losses	%	-	0.6	0.6
Installed compressor capacity	MW	141	135	219
Average compressor power consumption	MWh	49	42	76

Table 6.4: Technical input parameters for the different designs in the model

The financial parameters of the design are needed to calculate the component and system LCOH, as well as the total costs of the system. In Chapter 5, the financial parameters per technology are given and they are summarised in Table 6.5. The given values are all in $€_{2023}$. For the 36-inch pipeline, more capacity is available than needed for the designs. Since it is probable that multiple projects can be connected to a large pipeline to shore, similar to how pipelines in the oil and gas industry are laid on the Dutch North Sea, only the share of capacity used by the designs will be paid for. The values for the 36-inch pipeline are therefore given in $€_{2023}/km/GW$. The 12-inch pipeline is laid specifically for the first design, as it transports the hydrogen from the decentral electrolysers to the central point between the wind farms. These pipelines will not be shared with other projects, and the full price is paid. The costs are therefore given in $€_{2023}/km$. The storage facility could also be shared with other projects if the constructed salt caverns are large enough, and the cost is given in $€_{2023}/MWh$.

Parameter	Unit	Value	Source
PEM electrolyser CAPEX	€$_{2023}/kW$	550	IEA (2019), Guidehouse (2020) Deloitte (2021), Program (2022)
PEM electrolyser OPEX	% CAPEX/year	3	Deloitte (2021)
Alkaline electrolyser CAPEX	€$_{2023}/kW$	450	IEA (2019), Guidehouse (2020) Deloitte (2021), Program (2022)
Alkaline electrolyser OPEX	% CAPEX/year	3	Deloitte (2021)
Water feed	€$_{2023}/m^3H_2O$	1	Shemer & Semiat (2017) Al-Obaidani et al. (2008)
Salt cavern CAPEX	€$_{2023}/MWh$	362	Cihlar et al. (2020), Eradus (2022) Gessel et al. (2023)
Salt cavern OPEX	% CAPEX/year	4	Eradus (2022), Gessel et al. (2023)
New 12 inch pipeline CAPEX	M€$_{2023}/km$	1.5	Backbone (2022)
New 36 inch pipeline CAPEX	k€$_{2023}/km/GW$	185	Backbone (2022)
Reused 36 inch pipeline CAPEX	k€$_{2023}/km/GW$	20	Backbone (2022)
Pipeline OPEX	% CAPEX/year	0.1	Rioux et al. (2021)
HVDC cable CAPEX	M€$_{2023}/km$	1.6	Alvestad (2022)
HVAC cable CAPEX	M€$_{2023}/km$	2.6	Nieradzinska et al. (2016)
Inter-array cable CAPEX	k€$_{2023}/km$	433	Catapult (2021)
Cable OPEX	% CAPEX/year	2	DNV (2021)
HVDC offshore substation CAPEX	k€$_{2023}/MW$	600	Timmers et al. (2023) Catapult (2021)
HVDC onshore substation CAPEX	k€$_{2023}/MW$	150	Timmers et al. (2023) Catapult (2021)
HVAC offshore substation CAPEX	k€$_{2023}/MW$	150	Timmers et al. (2023),Catapult (2021)
Offshore substation OPEX	% CAPEX/year	2	Larsson (2021)
Onshore substation OPEX	% CAPEX/year	0.7	Larsson (2021)
Island CAPEX	M€$_{2023}/500MW_{electrolyser}$	75	van der Veer et al. (2020)
Island OPEX	M€$_{2023}$/year	3	van der Veer et al. (2020)
Compressor CAPEX	M€$_{2023}$/MW	2	van Schot & Jepma (2020)
Compressor OPEX	% CAPEX/year	2	van Schot & Jepma (2020)
Wind turbine CAPEX	€$_{2023}/kW$	2406	NREL (2022)
Wind turbine OPEX	% CAPEX/year	3	NREL (2022)
Inflation rate	%	2	DeNederlandscheBank (2022)
Discount rate	%	8	GrantThornton (2017)

Table 6.5: Financial parameters used in the model.

6.2 Technical Results

The electricity generation part of the model was constant over all three designs. Each wind turbine generated 59 GWh of electricity per year, for a total of 39 TWh over all wind turbines per year. In total, over the lifetime of the simulation, 1.2 PWh of electricity was generated by the wind turbines. It was found that the wind turbines had a capacity factor of 0.45.

Running the model with the parameters given in Table 6.4 yields the technical outputs of the model. These outputs are summarised in Table 6.6.

Output parameter	Unit	Design 1	Design 2	Design 3
Maximum baseload	kg/h	$7.93e^4$	$7.52e^4$	$7.37e^5$
Total hydrogen produced	Mt	20.85	19.75	19.54
Maximum storage capacity	TWh	3.72	3.70	3.69
System efficiency	%	69.4	65.8	65.1

Table 6.6: Technical output parameters of all three designs.

As seen in Table 6.6, the technical outputs of the three designs are very similar.

The maximum baseload of the offshore decentral design is slightly higher than the other two designs, with the onshore central configuration having the lowest baseload. The offshore central baseload is only 5% less than the offshore decentral baseload. The onshore central configuration has a maximum baseload of only 7% less than the offshore decentral configuration. The total amount of hydrogen produced follows the same pattern. The offshore decentral configuration produced the most hydrogen over the simulated time, followed by the offshore central and onshore central configurations. Again, the value for the offshore central

configuration is only 5% less than the offshore decentral configuration. The onshore central configuration has a value that is 6% lower than the offshore decentral configuration. Fig. 6.5 shows the produced hydrogen over the runtime of the model for the offshore decentral configuration. The efficiency degradation of the electrolyser can not be seen because the assumption is made that the electrolyser stacks are replaced in groups per year and not all together at once. Therefore, the average efficiency between the efficiency at the start of the electrolyser lifetime and at the end of the electrolyser lifetime is taken into account. Section 7.4 will explain this choice in further detail. The horizontal line indicated the maximum baseload.

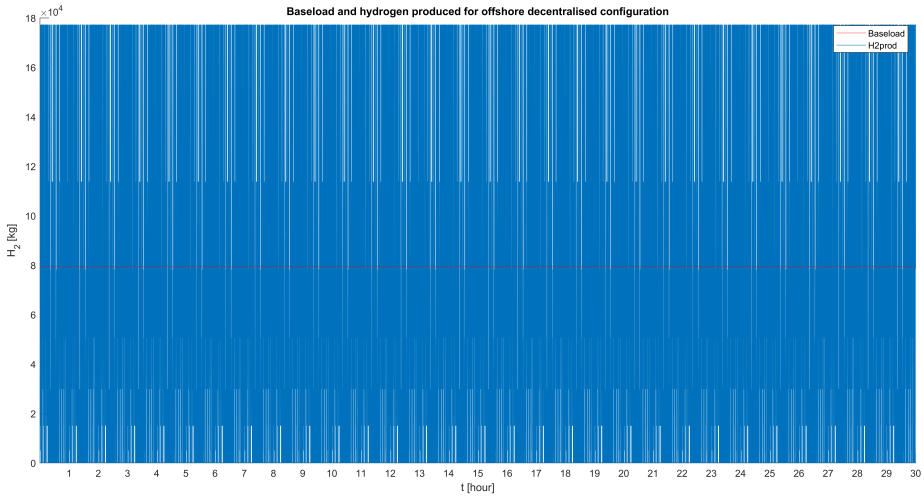

Figure 6.5: Produced hydrogen and maximum possible baseload in kg for the offshore decentralised configuration.

A plot of the baseload and produced hydrogen over a smaller timeframe shows the variations of the produced hydrogen, as shown in Fig. 6.6. If the amount of hydrogen produced is higher than the baseload, the baseload is directly supplied by the electrolysers and the additional hydrogen is transported to the storage facility. If the amount of hydrogen produced is below the baseload, the production at the electrolysers can not cover the total baseload, and hydrogen is extracted from the storage facility to supplement it.

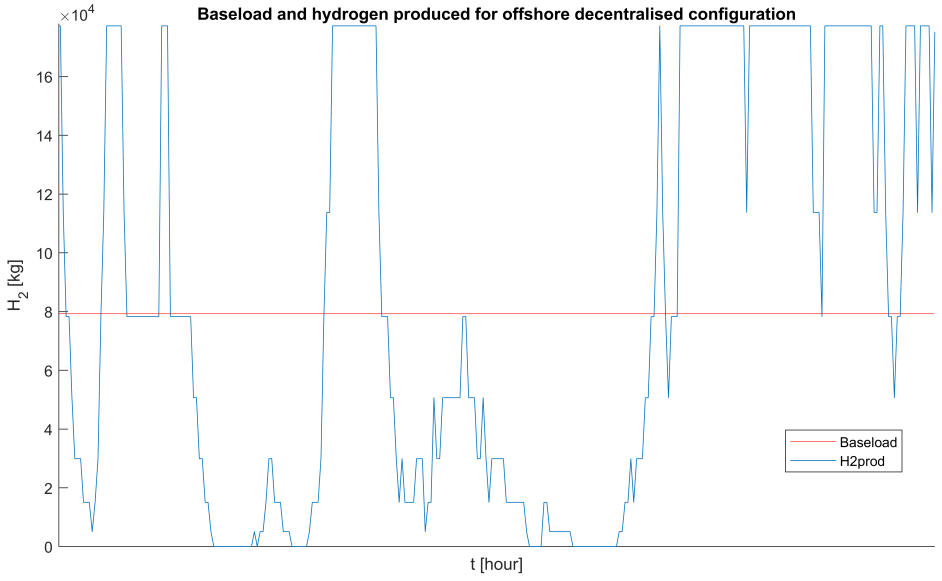

Figure 6.6: Produced hydrogen and maximum possible baseload in kg for the offshore decentralised configuration.

The offshore decentral configuration has the largest maximum storage capacity, followed by the offshore central and onshore central configurations. However, since both the offshore central and onshore central configurations need less than 1% less storage capacity than the offshore decentralised configuration, the storage capacity is considered equal for all configurations. Fig. 6.7 shows the content of the storage facility.

It can be seen that there is a seasonal behaviour in the amount of hydrogen produced and thus inputted in the storage. This is because of the seasonal behaviour of the wind velocity on the North Sea, which is higher in winter than in summer. This causes the yearly peaks and valleys. When there is less wind, more hydrogen is taken out of the storage facility to supply the baseload to shore. If more wind power is available during winter, more hydrogen is produced, often more than the baseload, and more hydrogen can be stored. With the baseload found by the model, the storage facility almost depletes every year and is filled up to its maximum value every year. At the highest point, more than 11 kton of hydrogen is stored in the storage facility. At the start of the simulation, the storage facilities are filled with three weeks' worth of hydrogen production, as otherwise, the valley of the first year makes the storage content drop below zero, already for very small baseloads.

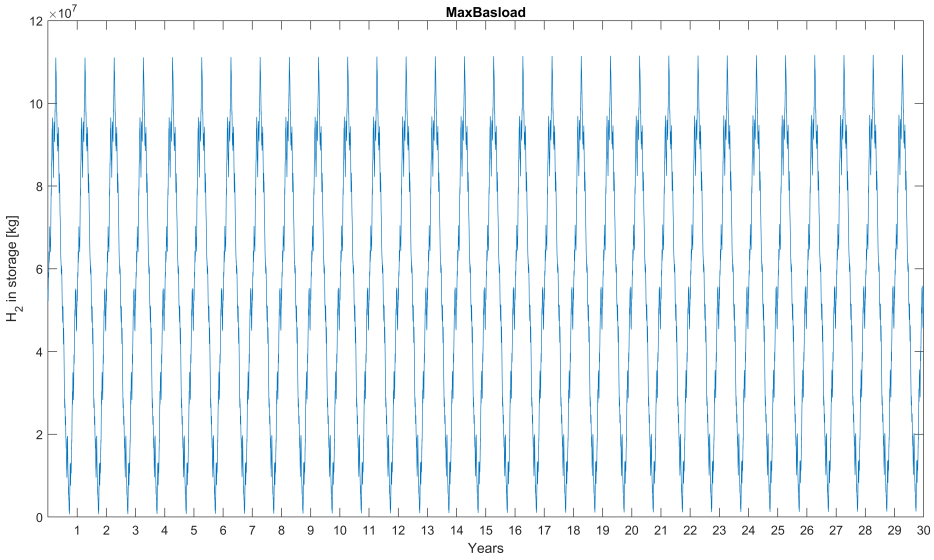

Figure 6.7: The hydrogen stored in the salt cavern in kg for the offshore decentral configuration.

Fig. 6.8 shows the amount of hydrogen in the storage facility over the first year. The seasonal variations can be seen, as well as the starting storage level.

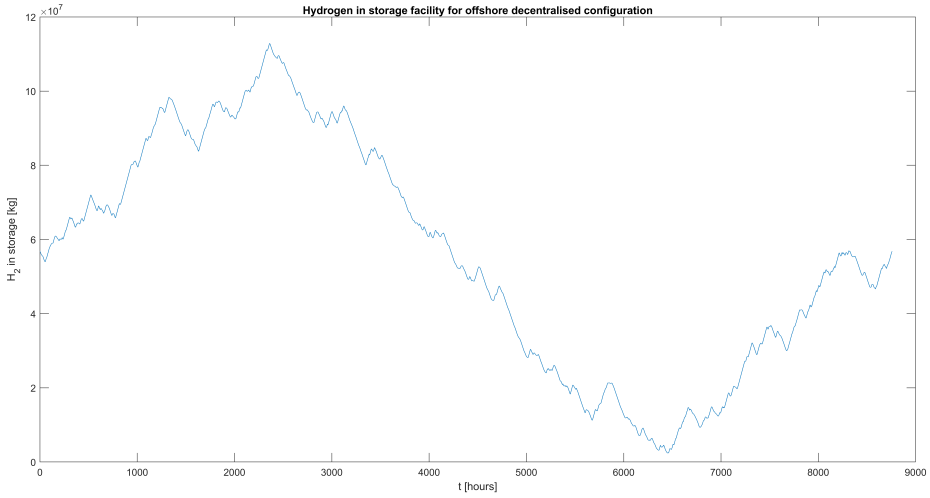

Figure 6.8: The hydrogen stored in the salt cavern in kg for the offshore decentralised configuration over one year.

The total system efficiencies are calculated using Eq. 4.85. The efficiency of the offshore decentral configuration is highest, followed by the offshore central configuration. The onshore central configuration system efficiency is the lowest. However, the efficiencies are very close to each other. This is because the highest losses come from the electrolyser. Designs 1 and 2 make use of a PEM electrolyser, whereas design 3 makes use of an alkaline electrolyser. Since the power consumption of PEM and alkaline electrolysers were

found to be the same in 2050, their efficiencies are the same. Another loss comes from the conversion steps, where design 1 has only one conversion step, and designs 2 and 3 have five conversion steps. The efficiencies of these conversion steps are, however, high. Another difference is the transportation efficiencies. Design one makes use of a collection pipeline, as well as a pipeline to shore. To transport hydrogen through these pipelines, compressors that use electricity are needed. For the offshore central design, only a pipeline to land is used, and thus, less compressor power is installed, but there is an extra loss from the electricity transport by HVAC cables. Finally, for the third design, a pipeline from the electrolysers to the storage facility requires a large installed compressor power because of the lower output pressure of the alkaline electrolyser. Also, a boundary condition was set that the hydrogen arrives at the demand side with a pressure of 50 bar, so the hydrogen produced onshore is elevated to 50 bar. Added to the loss of electricity to the compressors is the transportation loss of the HVDC cables. The average compressor power used is 49MW for the offshore decentral configuration and 42MW and 76MW for the offshore central and onshore central configuration, respectively.

6.3 Financial Results

Since the technical output parameters are all very close to each other for the three designs, the parameters are kept constant for every design. This is done to make a fair comparison between the costs and LCOHs of the systems. The baseload will be set to $7.5e^4$ kg/hr, and the maximum storage capacity to 3.7 TWh. The total hydrogen produced is set to 20 Mt.

Running the model with the abovementioned technical output parameters and the financial parameters in Table 6.5 yields the financial results. The cost functions, as described in Section 4.4.4, are used. A table of the CRFs of the components is given in Appendix D. If the lifetime of a component is longer than the simulated lifetime of the system, the system lifetime is used. Residual values of components after the simulated system lifetime are not considered. As described in Section 6.2, the electrolysers were not replaced all at once, but a share is replaced each year to negate the effect of the efficiency degradation. This has been taken into account when calculating the replacement costs of the electrolysers.

Firstly, the offshore decentral configuration results are shown. As can be seen in Fig. 6.9, the largest contribution of the levelised cost of hydrogen for this configuration comes from the wind turbines, being 3.30 $€_{2023}/kg$. Secondly, the PEM electrolysers make up for 1.30 $€_{2023}/kg$, which is divided into the electrolyser stacks (0.73 $€_{2023}/kg$) and the electrolyser balance of plant (0.57 $€_{2023}/kg$). The water feed costs are insignificant, accounting for 0.03 $€_{2023}/kg$. The component LCOH of the storage facility is 0.19 $€_{2023}/kg$. The collections pipelines, the pipeline to land and the pipeline to the storage facility are all included in the transport component LCOH, and the transport component LCOH is 0.26 $€_{2023}/kg$. Finally, the compressors have a component LCOH of 0.06 $€_{2023}/kg$. The total system LCOH for the offshore decentralised configuration is 5.14 $€_{2023}/kg$.

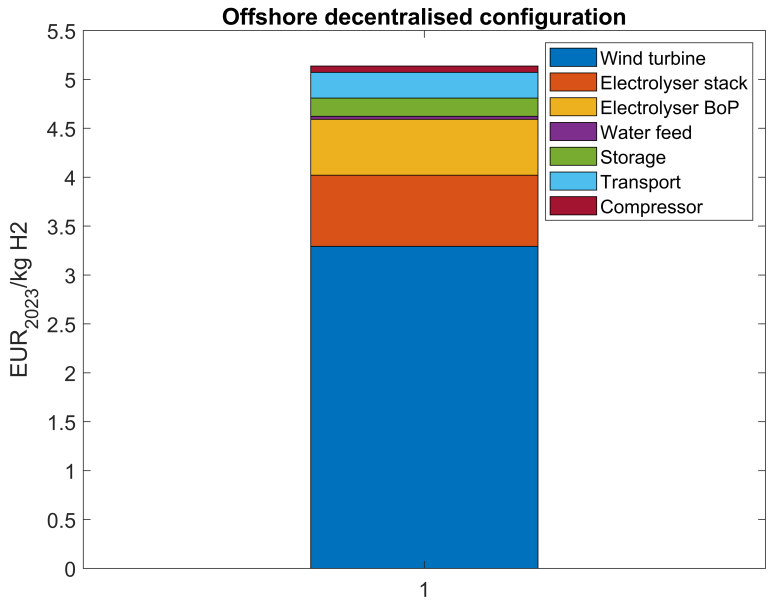

Figure 6.9: Total system LCOH of the offshore decentralised configuration, built up out of component LCOHs

The percentages of the component LCOHs to the system LCOH for the offshore decentralise configuration are given in Fig. 6.10. The largest share, with 64%, is from the wind turbine component. Second is the electrolyser component, accounting for 25% of the total system LCOH. The electrolyser is split up in the electrolyser stack (14%) and the electrolyser BoP (11%). The transport component is 5% of the system LCOH, and the storage component accounts for 4% of the system LCOH. Finally, the compressor and water feed component have a very small percentage of the system LCOH, with 1% and $< 1\%$, respectively.

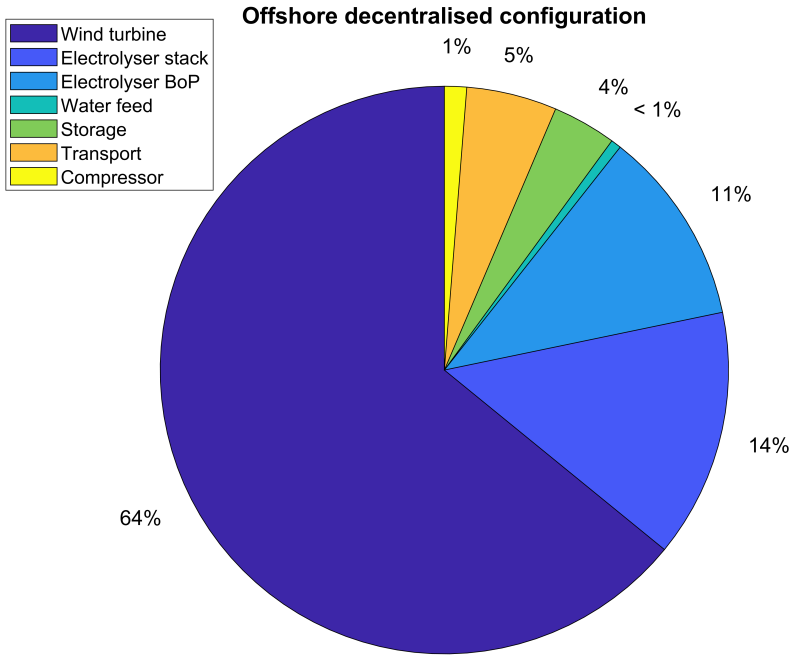

Figure 6.10: Pie chart breakdown of the offshore decentralised configuration component LCOH.

The total annualised cost breakdown of the offshore decentral configuration is given in Fig. 6.11. The wind turbine component has the highest annualised costs, mostly because of the CAPEX. Since no replacements are needed, the annualised OPEX is relatively low. For the electrolyser stack and balance of plant, replacements are needed. This can be seen in the relatively high OPEX compared to CAPEX. The electrolyser has the largest annualised total costs after the wind turbines. The compressors are also replaced. The hydrogen collection pipelines have a large total length, and therefore, the annualised CAPEX is relatively high. However, since no replacements are needed, the annualised OPEX is low. The same holds for the storage facility because no replacements are needed, so the OPEX is low compared to the CAPEX. The 36-inch pipelines and the water feed have the lowest annualised costs together with the inter-array cables used to supply electricity to the compressors.

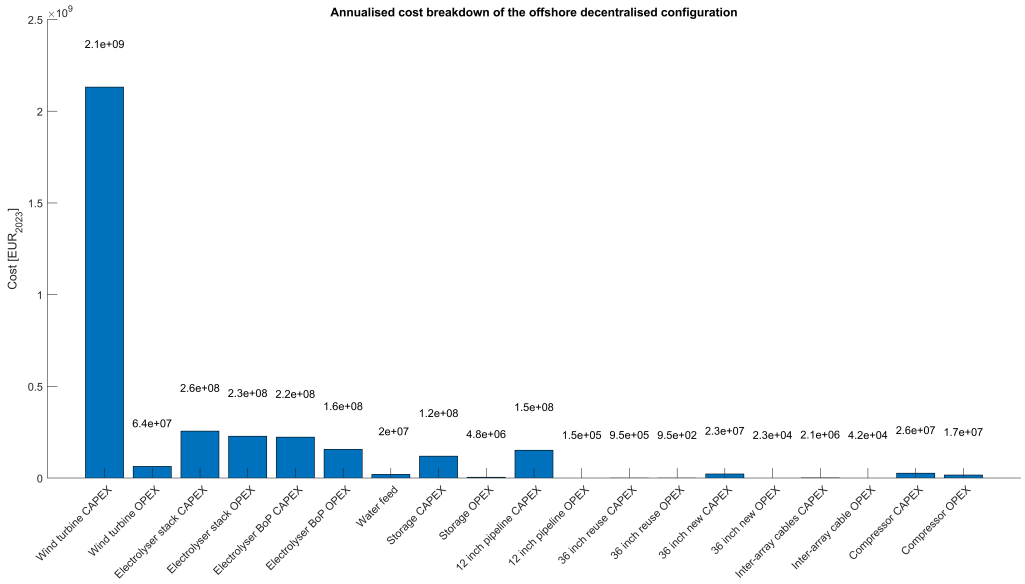

Figure 6.11: Annualised cost breakdown of the offshore decentralised configuration components.

Secondly, the offshore central configuration is run. The LCOHs of the components can be seen in Fig. 6.12. Again, the wind turbine component LCOH is the largest share of the system LCOH and is 3.30 $€_{2023}/kg$, since the same sized wind farms and hydrogen produced have been used. The installed electrolyser capacity is the same as for the offshore decentral design, and also PEM electrolysers are used. Therefore, the electrolyser component LCOH is the same, with 1.30 $€_{2023}/kg$, comprising of the electrolyser stack (0.73 $€_{2023}/kg$) and the electrolyser BoP (0.57 $€_{2023}/kg$). The water feed cost is again insignificant, being 0.03 $€_{2023}/kg$. The storage facility is set to a constant value for all designs, as well as the produced hydrogen, and therefore the component LCOH is equal for all designs, being again 0.19 $€_{2023}/kg$. An extra component for the offshore central configuration is the hydrogen distribution hub, which, in this design, is an island. The island component LCOH is 0.16 $€_{2023}/kg$. The transport component LCOH includes the pipelines to shore and to the storage facility, as well as the electrical infrastructure for bringing electricity to the electrolysers on the island. The component LCOH for the transport component is 0.67 $€_{2023}/kg$. Finally, the compressor component LCOH is 0.06 $€_{2023}/kg$. The total system LCOH for the offshore central configuration is 5.69 $€_{2023}/kg$.

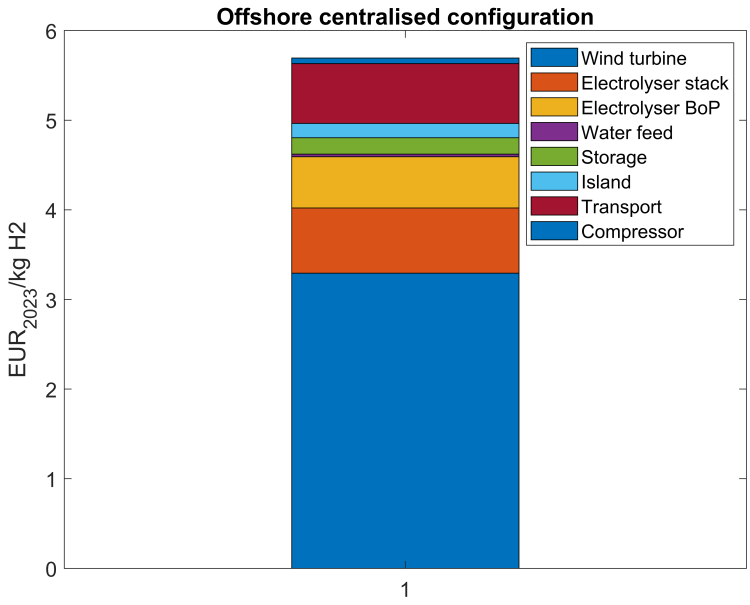

Figure 6.12: Total system LCOH of the offshore central configuration, built up out of component LCOHs

Fig. 6.13 shows the percentages of the component LCOHs to the total system LCOH. The wind turbine component has the largest share, with 58% of the total system LCOH. The second largest share is from the electrolyser component with 23%, with the electrolyser stack (13%) and the electrolyser BoP (10%). The next largest share is of the transport component, with 12% of the total system LCOH. The storage component and hydrogen distribution hub both have a share of 3% of the total system LCOH. Finally, the compressor and water feed components have a share of 1% and <1%, respectively.

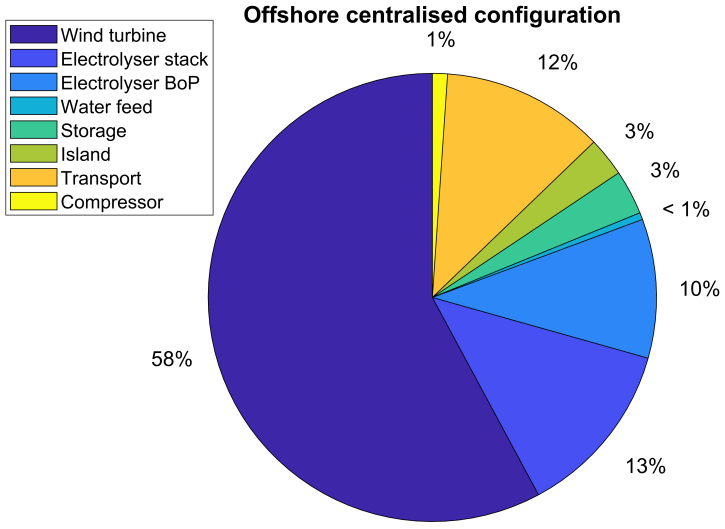

Figure 6.13: Total system LCOH of the offshore centralised configuration, built up out of component LCOHs

The total annualised cost breakdown of the offshore central configuration is given in Fig. 6.14. The highest annualised costs are from the wind turbine component, mainly because of the annualised CAPEX. The electrolyser stack and balance of plant have a relatively high annualised CAPEX, and because of the replacements, also have a relatively high annualised OPEX. The storage and hydrogen distribution hub components have a similar annualised CAPEX and OPEX. The annualised CAPEX of the HVAC substations contributes largely to the high transport component costs, as well as a significant share of the HVAC cables and inter-array cables. Finally, the compressor and water feed annualised costs are relatively low.

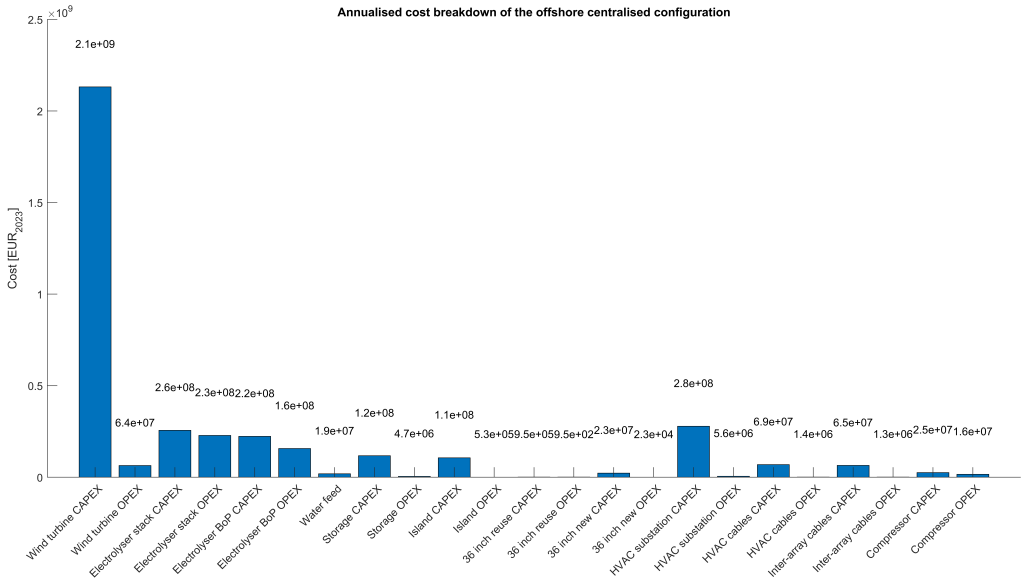

Figure 6.14: Annualised cost breakdown of the offshore central configuration components.

Finally, the onshore central configuration is run. The component LCOHs are given in Fig.6.15. The wind turbine component LCOH is again 3.30 €$_{2023}/kg$. The alkaline electrolysers cost less than the PEM electrolysers, and the electrolyser component LCOH is 1.07 €$_{2023}/kg$, consisting of the stacks (0.60 €$_{2023}/kg$) and the balance of plant (0.47 €$_{2023}/kg$). The water feed is again insignificant with a component LCOH of 0.03 €$_{2023}/kg$. The storage has a component LCOH of 0.19 €$_{2023}/kg$, similar to the storage component LCOH of the other designs. the transport component includes the electrical infrastructure to transport the electricity from the wind farms to shore by HVDC cables and has a component LCOH of 1.47 €$_{2023}/kg$. Finally, the compressor component LCOH is 0.10 €$_{2023}/kg$. The total system LCOH for the onshore central configuration is 6.14 €$_{2023}/kgH_2$.

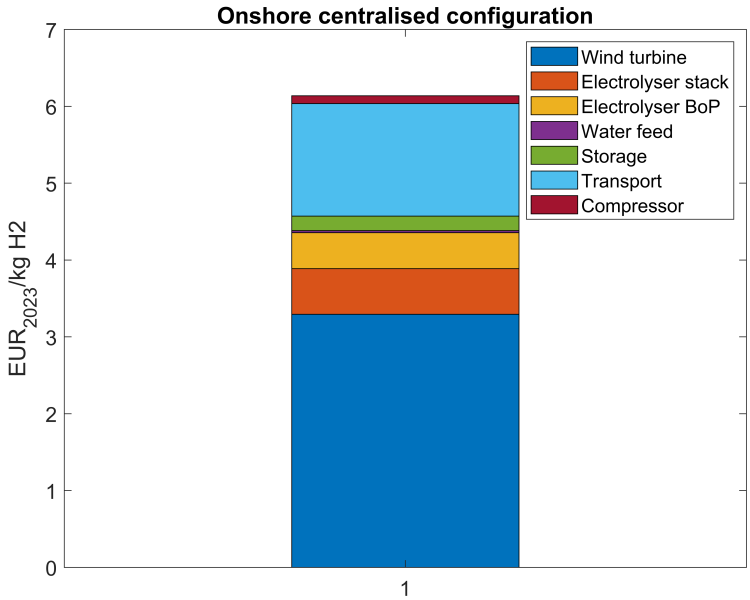

Figure 6.15: Total system LCOH of the onshore centralised configuration, built up out of component LCOHs

Fig. 6.16 shows the component LCOH percentages of the total system LCOH. The wind turbines have a share of 54%. The transport component has a large share with 24%. The electrolyser stack and balance of plant have a share of 10% and 8%, respectively, combing to 18% for the electrolyser component. The LCOH of the storage component is 3% of the total system LCOH, and the compressors and water feed have a share of the total LCOH of 2% and <1%, respectively.

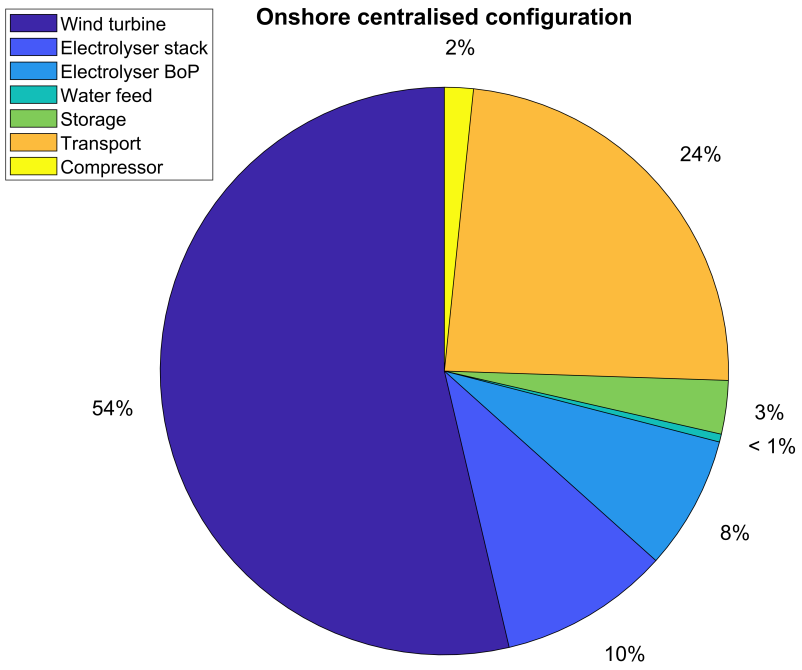

Figure 6.16: Pie chart breakdown of the onshore centralised configuration component LCOH.

The total cost breakdown of the onshore centralised configuration is given in Fig. 6.17.

The highest costs are from the wind turbines' annual costs. The electrolyser annualised CAPEX and OPEX are lower than the first two designs, as alkaline electrolysers are used onshore. The storage and HVDC offshore substations CAPEX and OPEX are similar, and after the wind turbines, the highest cost contributions. The HVDC onshore substations have significantly lower annualised costs than the offshore substations. The other contributions to the transport component include the inter-array cables, the 36-inch pipeline and the HVDC cables. The compressor has relatively low annualised costs, even with replacing the compressors. Finally, the water feed has a very low annualised cost.

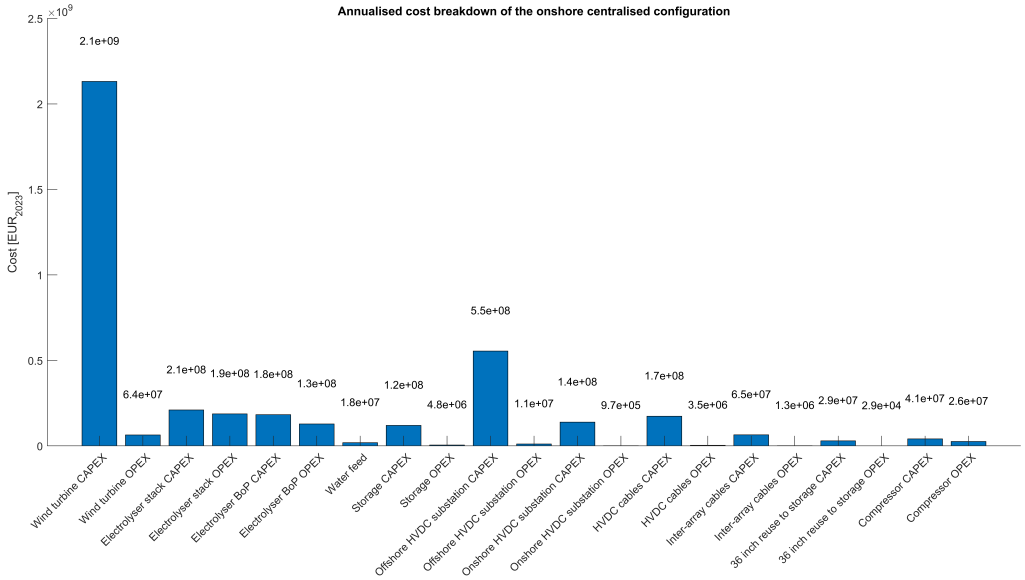

Figure 6.17: Component cost breakdown of the onshore centralised configuration.

The LCOHs of all the components of every design are given in Fig. 6.18. The wind turbine LCOH has the same size for every design. The offshore decentral and central configurations use PEM electrolysers, whereas the onshore central configuration uses alkaline electrolysers. Since the installed capacity of electrolysers is constant over the designs, the difference comes from the cost difference between PEM and alkaline. The hydrogen produced is kept constant for the financial analysis, and thus, the amount of water needed remains constant as well. Therefore, the water feed LCOH is constant over the designs. The storage is also kept constant, and the same LCOH is found for every design. The offshore central design is the only design that uses a hydrogen distribution hub, indicated by the light-blue LCOH block in Fig. 6.18. The largest differences are in the transport component LCOH. The offshore decentral configuration only uses pipelines and one inter-array cable to supply electricity to the compressors. Multiple collection pipelines are laid per wind farm and have a high cost contribution, but the OPEX is relatively low, and only one pipeline to shore is needed. The offshore central configuration also uses a single hydrogen pipeline to shore, but a lot of electrical infrastructure is needed to transport the electricity from the wind farms to the island. Inter-array cables, as well as HVAC substations and cables, are needed. This is more cost-intensive than the hydrogen collection pipelines. Also, six HVAC substations are needed per wind farm. The capacity of the HVAC substations is 700 MW, needing three per wind farm. Also, substations are needed at the wind farm, and more substations are needed where the electricity lands, in this case, on the island. The total of 30 HVAC substations contribute significantly to the transport component LCOH of this design. The onshore central design makes use of HVDC substations. The HVDC substations are more expensive than HVAC substations, but fewer are needed. With a capacity of 2 GW, only one substation is needed per wind farm offshore and one onshore. Still, the HVDC offshore substations have an annual cost twice as high as the offshore HVAC substations. The onshore substation is significantly less cost-intensive than the offshore substation. The onshore central configuration uses HVDC cables, whereas the offshore centralised configuration uses the more expensive HVAC cables, but the HVDC cable length is much longer than the HVAC cable length. This makes the onshore central transport component LCOH higher than the offshore central transport component LCOH. Finally, the difference in installed compressor capacity only makes for a small change in LCOH.

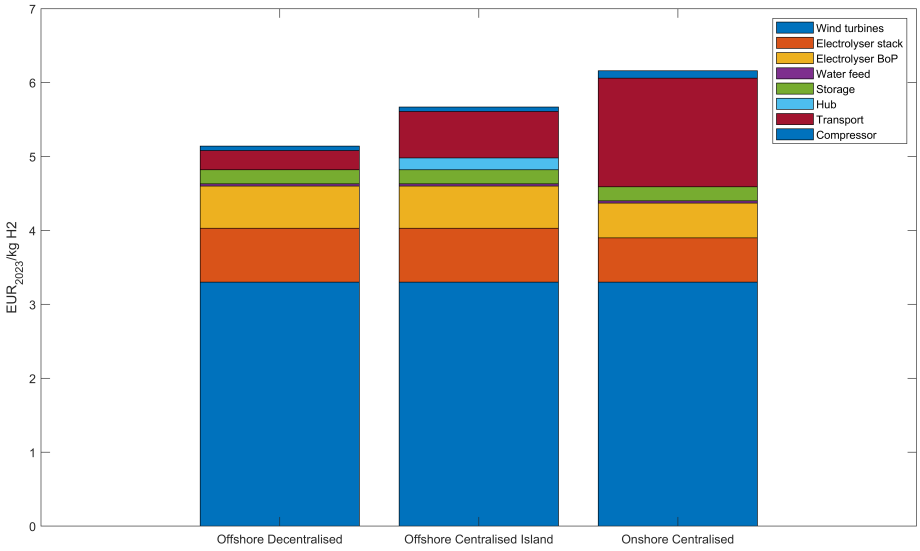

Figure 6.18: Total system LCOH of all configurations, built up out of component LCOHs

The total annualised costs per component for all designs are given in Table 6.7. Per component, the annualised CAPEX and OPEX of all technologies used are summed to calculate the total cost of the component. The annualised CAPEX and OPEX from Figures 6.11, 6.14, and 6.17 are used.

Component	Design 1	Design 2	Dsign 3
Wind turbine	2 196	2 196	2 196
Electrolyser	865	865	708
Water feed	19	19	19
Storage	123	123	123
Hub	-	107	-
Transport	178	423	977
Compressor	43	41	67
System	**3 424**	**3 774**	**4 090**

Table 6.7: All component annualised costs for the designs and the total annualised costs costs for all designs. All values are given in M€$_{2023}$

.

The offshore decentral configuration has the lowest total annualised system cost of 3424 M€$_{2023}$. The offshore central configuration has a total annualised system cost of 3774 M€$_{2023}$. Finally, the onshore central configuration has the highest annualised total system cost of 4090 M€$_{2023}$.

The LCOHs per component for all designs are summarised in Table 6.8.

Component	Design 1	Design 2	Dsign 3
Wind turbine	3.30	3.30	3.30
Electrolyser	1.30	1.30	1.07
Water feed	0.03	0.03	0.03
Storage	0.19	0.19	0.19
Hub	-	0.16	-
Transport	0.26	0.67	1.47
Compressor	0.06	0.06	0.06
System	**5.14**	**5.69**	**6.14**

Table 6.8: All component LCOHs for the designs, and the total system LCOH for all designs. All values are given in €$_{2023}/kgH_2$

.

The offshore decentral configuration has the lowest system LCOH with 5.14 €$_{2023}/kgH_2$. The offshore central configuration has a system LCOH of 5.69 €$_{2023}/kgH_2$. The onshore central configuration has the highest system LCOH of 6.14€$_{2023}/kgH_2$. Compared to the offshore decentral configuration, the offshore central configuration has a 11% higher LCOH. The onshore central configuration almost has a 20% higher system LCOH compared to the offshore decentral configuration and an 8% higher system LCOH compared to the offshore central configuration.

7 Discussion

In this chapter, the scenario analysis and sensitivity analysis are performed in section 7.1 and 7.2. Next, the subquestions of the research question are answered in Section 7.3, after which the limitations of this thesis are discussed in Section 7.4. Finally, recommendations from this thesis are given in Section 7.5.

7.1 Scenario analysis

The scenario analysis is done over a few scenarios. Firstly, parameters with uncertainty in their value used in the model are considered. Secondly, design choices are altered to come to scenarios. Since the three designs use different technologies, the scenario analysis will be performed per design. Firstly, in Section 7.1.1, the scenario analysis of the offshore decentral configuration will be performed, followed by the scenario analysis of the offshore central and onshore central configurations in Sections 7.1.2 and 7.1.3 respectively. Finally, Sections 7.1.4 discusses the insights that can be drawn from the scenario analysis.

7.1.1 Scenario Analysis Offshore Decentral Configuration

Firstly, the scenario analysis is performed over the offshore decentral configuration. The input parameters used for the scenario analysis are given in table 7.1. The pessimistic values represent the scenario with low technological developments or cost reductions, whereas the optimistic scenario represents the opposite.

Input parameter	Unit	Optimistic	Selected value	Pessimistic
Electrolyser power consumption	kWh/kgH_2	47	53.2	69
Electrolyser CAPEX	$€_{2023}/kW$	200	550	900
Electrolyser stack lifetime	h	150 000	125 000	75 000

Table 7.1: Input parameters for the scenario analysis, including their ranges, for the offshore decentral configuration.

The power consumption of PEM electrolysers is expected to decrease. In the pessimistic scenario, low technological developments are made, and the power consumption is set as the lower limit found in literature. For the optimistic value, the upper limit is used. The CAPEX is also expected to decrease. Again, the lower and upper limits found in literature are used. The lifetime of PEM electrolysers is expected to increase. As the pessimistic value, a low lifetime of 75,000 hours is taken. For the optimistic value, the highest value found in literature is used. From the interviews with companies, it became clear that the electrolyser performance and costs are an important uncertainty, especially the performance and costs of electrolysers when placing them offshore. Some companies refer to a possible marinisation factor as a factor of extra costs for offshore electrolysers. However, as this factor is lower than the pessimistic scenario of the electrolyser CAPEX, it is discussed in that scenario. Due to the harsh environment offshore, performance, such as lifetime, could be lower than onshore. Also, the costs of making electrolysers that withstand these conditions could be higher than those of electrolysers onshore. These considerations of companies are taken into account with the scenario analysis and are discussed in Section 7.1.4.

Also, some design choices are made that could be altered. The design choices were chosen as constants as boundary conditions for the simulations. An overview of the design choices used for the scenario analysis is given in Table 7.2.

Design choice	Unit	Min. value	Selected value	Max. value
Electrolyser capacity	GW	5	8	10
Distance to shore	km	75	250	350
Battery capacity	GW	2.7	-	6.7
Turbines per H_2 collection pipeline	-	33	11	165
Discount rate	%	6	8	10
Baseload	-	No	Yes	-

Table 7.2: Input parameters for the scenario analysis, including their ranges.

The electrolyser capacity was set as 8GW. This is based on a 12 MW electrolyser per 15 MW wind turbine. The ratio of electrolyser capacity per wind power capacity is a design choice and can be changed. As the minimum value, the electrolyser capacity is set as half of the wind turbine capacity. The wind power and electrolyser capacity are equal for the maximum value. The wind farms' location in the simulations is set to 250 km from the Port of Rotterdam. If the landing location is chosen as another location, or wind

farms are constructed closer to the Port of Rotterdam, the distance to shore can be lowered. 350 km is used as the maximum value. In the base case, no batteries are used. Batteries could, however, be used to store excess electricity from the wind turbines and supply electricity when there is no wind. As a minimum value, a 4MW battery is placed per 15MW wind turbine. A 10 MW battery is placed per 15 MW wind turbine for the maximum value. The hydrogen collection pipelines are laid per string of 11 wind turbines. As the minimum value, every hydrogen collection pipeline will collect the hydrogen from 33 wind turbines for four hydrogen collection pipelines per wind farm. As the maximum value, every wind farm has one hydrogen collection pipeline. The discount rate was set as 8% based on literature on offshore wind. A scenario with a lower and higher discount rate is set as the minimum and maximum value, namely 6% and 10%. Finally, the hydrogen is supplied to shore by a baseload. The final scenario does not use a baseload to supply the hydrogen to demand.

The results of the scenarios are given in table 7.3. The selected value shows a different LCOH than the system LCOH in Chapter 6, as the technical output parameters were no longer set constant over all designs. This is done because otherwise, changing the technical parameters in the scenario analysis would not yield a different result.

Parameter	$LCOH_{system}$ **(Optimistic)**	$LCOH_{system}$ **(Selected value)**	$LCOH_{system}$ **(Pessimistic)**
Electrolyser power consumption	4.42	4.93	6.27
Electrolyser CAPEX	4.14	4.93	5.73
Electrolyser stack lifetime	4.93	4.93	5.29

Table 7.3: Results of the scenario analysis of the input parameters of the offshore decentral configuration. All values are given in $€/kg$

For the electrolyser power consumption, the LCOH drops to 4.42 $€_{2023}/kg$ in the most optimistic scenario. When the power consumption barely has technological development, the system LCOH is 6.27 $€_{2023}/kg$. When the electrolyser CAPEX has the lowest value in the most optimistic scenario, the system LCOH is 4.14 $€_{2023}/kg$. In the pessimistic scenario, the LCOH is 5.73 $€_{2023}/kg$. Finally, in the optimistic scenario, the electrolyser stack lifetime is 150,000 hours. However, it still needs the same amount of replacements as the selected value, so no change in LCOH is observed. For the pessimistic scenario, three replacements are needed, and the system LCOH is 5.29 $€_{2023}/kg$.

The results of the scenarios of the design choices are given in Table 7.4.

Design choice	$LCOH_{system}$ **(Min. value)**	$LCOH_{system}$ **(Selected value)**	$LCOH_{system}$ **(Max. value)**
Electrolyser capacity	5.70	4.93	5.37
Distance to shore	4.91	4.93	4.96
Battery capacity	5.61	4.93	6.63
Turbines per H_2 collection pipeline	4.91	4.93	5.05
Discount rate	4.10	4.93	5.82
Baseload	4.70	4.93	-

Table 7.4: Results of the scenario analysis of the offshore decentral configuration. All values are given in $€/kg$

For the electrolyser capacity, both the minimum value and the maximum value used result in a higher system LCOH. There is an optimum ratio between wind turbines and electrolysers for this design, which is between the maximum and minimum values used. At the minimum value, less hydrogen can be produced due to the small electrolysers without dropping the costs enough to lower the LCOH. At the maximum value, the total costs rise while not much additional hydrogen is produced. Both increase the system LCOH.

The distance to shore does not have much influence on the system LCOH of the offshore decentral configuration. To transport energy to shore, pipelines are used with very low costs compared to other components.

When batteries are used, more hydrogen is produced as some of the electricity can be stored to be used later when there is no wind. However, since the batteries are very expensive, more costs are added than hydrogen produced, and thus, the LCOH increases for both scenarios where batteries are used.

A trade-off exists for the length of the hydrogen collection pipeline and, thus, the number of turbines connected to it. When increasing the length, the pressure drop happens over a larger length, and thus, the output pressure of the collection pipeline decreases. With a lower output pressure, more compressor power is needed to increase the pressure before transport to demand or storage. On the other hand, more separate

collection pipelines have a longer total length. The scenario with 33 turbines per collection pipeline shows the lowest system LCOH, while the scenario with one pipeline per wind farm has a very large pressure drop, and the LCOH increases because of the added compressor power needed. The scenario with 11 turbines per collection pipeline has a slightly higher system LCOH than the 33 turbines per collection pipeline scenario. For both, the pressure drop remains small, in the range of 4-8 bar, and the added compressor power needed for the 33 turbines per pipeline, compared to a string of 11 turbines per pipeline, has lower costs than the added pipeline length costs for the 11 turbines per string pipeline.

The discount rate was taken as 8%. When the discount rate is set at 6%, the LCOH decreases, while the LCOH increases when the discount rate is set to 10%. The discount rate is in the formula for calculating the LCOH, and increasing the discount rate increases the total costs without any additional hydrogen being produced.

Finally, when no baseload is used, no offshore storage is needed, and no pipeline to storage is needed. Also, the compression for both is no longer needed. The system LCOH decreases.

7.1.2 Scenario Analysis Offshore Central Configuration

Secondly, the scenario analysis is performed over the offshore central configuration. The input parameters used for the scenario analysis are given in Table E.1 in Appendix E. Table E.2 in Appendix E gives an overview of the design choices. Since no hydrogen collection pipelines are used in this configuration, the design choice is removed.

Since many of the values or results from the scenario analysis of the offshore central configuration follow the same trends as the offshore decentral configuration, only explanations will be given on the values that differ from the offshore decentral scenario analysis, and important differences are highlighted.

The results of the scenarios are given in table 7.3. The selected value shows a different LCOH than the system LCOH in Chapter 6, as the technical output parameters were no longer set constant over all designs.

Parameter	$LCOH_{system}$ **(Optimistic)**	$LCOH_{system}$ **(Selected value)**	$LCOH_{system}$ **(Pessimistic)**
Electrolyser power consumption	5.10	5.73	7.34
Electrolyser CAPEX	4.90	5.73	6.56
Electrolyser stack lifetime	5.73	5.73	6.11

Table 7.5: Results of the scenario analysis of the input parameters of the offshore central configuration. All values are given in €/kg

Since a PEM electrolyser is used for the offshore decentral and central configuration, the results from Table 7.5 are very similar to that of Table 7.3.

The system LCOHs, when changing the design choices of the offshore central configuration, are given in Table 7.6

Design choice	$LCOH_{system}$ **(Min. value)**	$LCOH_{system}$ **(Selected value)**	$LCOH_{system}$ **(Max. value)**
Electrolyser capacity	6.39	5.73	6.32
Distance to shore	5.70	5.73	5.75
Battery capacity	6.44	5.73	7.51
Discount rate	4.75	5.73	6.76
Baseload	5.51	5.73	-

Table 7.6: Results of the scenario analysis of the offshore central configuration. All values are given in €/kg

The scenarios for the design choices follow the same trends for the offshore central configuration as for the offshore decentral configuration. The explanation of the results thus follows the same reasoning as described in Section 7.1.1.

7.1.3 Scenario Analysis Onshore Central Configuration

Finally, the scenario analysis is performed over the onshore central configuration. The input parameters used for the scenario analysis are given in Table E.3 in Appendix E. Table E.4 in Appendix E gives an overview of the design choices. Since no hydrogen collection pipelines are used in this configuration, this design choice is removed. The onshore configuration uses alkaline electrolysers instead of PEM electrolysers, and different ranges are found.

Since many of the values or results from the onshore central configuration scenario analysis follow the same trends as the offshore decentral configuration, only explanations will be given on the values that differ from the offshore decentral scenario analysis, and important differences are highlighted.

The results of the scenarios are given in table 7.7. The selected value shows a different LCOH than the system LCOH in Chapter 6, as the technical output parameters were no longer set constant over all designs.

Parameter	$LCOH_{system}$ **(Optimistic)**	$LCOH_{system}$ **(Selected value)**	$LCOH_{system}$ **(Pessimistic)**
Electrolyser power consumption	5.70	6.40	7.06
Electrolyser CAPEX	5.78	6.40	7.01
Electrolyser stack lifetime	6.40	6.40	6.64

Table 7.7: Results of the scenario analysis of the input parameters of the onshore central configuration. All values are given in €/kg

The onshore central configuration makes use of an alkaline electrolyser. A noticeable difference is in the electrolyser stack lifetime pessimistic value. The optimistic value requires one replacement over the system's lifetime for alkaline and PEM electrolysers. However, the selected value also only requires one replacement, and therefore, the values are the same for the selected and optimistic values for every design. With the PEM electrolysers, a disappointing technological development in the stack lifetime leads to the electrolyser needing to be replaced an average of three times over the system's lifetime. For the alkaline electrolyser, however, the lifetime is already long enough that even with disappointing technological developments, the stacks only need to be replaced an average of two times, and thus, the LCOH increases less compared to the pessimistic scenario of the PEM electrolysers. It should be noted that replacements of the electrolyser stacks happen in shares per year instead of all electrolyser stacks at once. This is taken into account by calculating the average number of replacements and average year of replacement in the LCOH calculations. Due to the manner of taking the averages, the optimistic value does not show a lower LCOH. A more detailed explanation is given in Section 7.4.

The system LCOHs, when changing the design choices of the offshore central configuration, are given in Table 7.8

Design choice	$LCOH_{system}$ **(Min. value)**	$LCOH_{system}$ **(Selected value)**	$LCOH_{system}$ **(Max. value)**
Electrolyser capacity	8.18	6.40	6.97
Distance to shore	6.18	6.40	6.52
Battery capacity	6.94	6.40	8.00
Discount rate	5.29	6.40	7.58
Baseload	6.14	6.40	-

Table 7.8: Results of the scenario analysis of the onshore central configuration. All values are given in €/kg

For the electrolyser capacity, the minimum value results in a much higher system LCOH. This is because the onshore central configuration has the highest costs, and a lower hydrogen production makes the levelised costs much higher. Again, there is an optimal ratio as the minimum and maximum values have a higher LCOH than the selected value.

The distance to shore has more influence on the system LCOH of the onshore central configuration than for the offshore configurations. This is because the offshore configurations use pipelines to transport hydrogen to shore, which is relatively cheap. However, the onshore central configuration uses expensive HVDC cables. A change in the length of the cables has a large influence on the LCOH.

The use of a battery increases the system LCOH. However, with the onshore central configuration, alkaline electrolysers are used. The alkaline electrolysers have a lower load range of 10%, whereas the PEM electrolysers have a lower load range of 0%. The battery can thus be utilised more often by alkaline electrolysers than PEM electrolysers. For the PEM electrolysers, the batteries are used when there is now wind. For the alkaline electrolysers, the batteries are used when there is no wind or the wind power is not enough to overcome the lower load range. Because of this extra utilisation, more extra hydrogen was produced and the LCOH did not increase as much as with the offshore decentral and offshore central configurations. The same amount of excess wind power was available for all configurations, as the electrolyser and wind power capacities, as well as the electrolyser power consumption, are equal for all designs. However, when the battery is full, no additional electricity can be stored and has to be curtailed. Because of the extra utilisation of the batteries with the alkaline electrolysers to overcome the lower load range, the batteries can discharge more

often and are full less often. This is another reason that the batteries can produce more extra hydrogen in combination with alkaline electrolysers than with PEM electrolysers, and the LCOH increases less.

7.1.4 Insights

The scenario analysis shows that the future development of parameters can have a large influence on the system LCOH. Both the electrolyser power consumption and CAPEX have a large positive or negative influence, depending on whether the developments are optimistic or pessimistic. For the stack lifetime, optimistic technological developments have no influence as the number of replacements stays the same under the current assumptions. It is interesting to notice that even with pessimistic technological developments or cost reductions, the offshore decentral configuration still has a slightly lower LCOH than the selected value scenarios of the onshore central configuration. If a marinisation factor might apply, this shows that even with an increase of 60% for electrolyser CAPEX, the offshore decentral still has a lower system LCOH than the onshore central configuration. This also applies to the uncertainty of disappointing offshore performance of the electrolysers, as the pessimistic scenario of electrolyser power consumption and lifetime still reaches a lower system LCOH than the onshore central configuration. Also, the pessimistic scenario for electrolyser CAPEX and stack lifetime results in a lower system LCOH than the selected values scenario for the offshore central configuration. The pessimistic scenarios of the offshore central configuration all resulted in a higher system LCOH than the selected values scenarios of the onshore central configuration. When analysing the optimistic scenarios, it can be seen that the optimistic scenario of the electrolyser CAPEX is the only optimistic scenario of the offshore central configuration that resulted in a lower system LCOH than the selected values scenario of the offshore decentral configuration. No optimistic scenario of the onshore central configuration results in a lower system LCOH of the selected values scenarios of the offshore decentral configuration. However, equal system LCOHs of the selected values scenarios of the offshore central configuration were found at the optimistic scenarios of the electrolyser power consumption and electrolyser CAPEX of the onshore central configuration.

For the design choices, an optimal ratio between the electrolyser capacity and wind power capacity can be found. Increasing or decreasing the capacities by the values of the scenario analysis increases the system LCOH. When the electrolyser is decreased, less costs are made for the electrolyser component, but also, less hydrogen can be produced. When increasing the electrolyser capacity, more hydrogen can be produced, but the electrolyser component also has higher costs. Noticing this, the optimal ratio was found by running the model with different electrolyser capacity:wind turbine capacity ratios. For the offshore decentral configuration, this optimal ratio results in a 12.6 MW electrolyser per 15MW wind turbine, with a system LCOH of 4.86 $€_{2023}/kgH_2$. For the offshore central configuration, a 13.3 MW electrolyser per 15MW wind turbine results in the optimal ratio and a system LCOH of 5.63 $€_{2023}/kgH_2$. Finally, the optimal ratio of the onshore central configuration was found to be a 13.1 MW electrolyser per 15 MW wind turbine to come to a system LCOH of 6.25 $€_{2023}/kgH_2$. It should be noted that these optimal ratios are found using the boundary conditions and assumptions used in the model. One of these assumptions is that the partial load operation of the electrolyser operates at the same electrolyser power consumption as the full load operation. In reality, the partial load operation has a higher power consumption than the full load operation. When the electrolyser capacity is increased, the electrolyser operates more often in its partial load range and thus operates more often with a higher power consumption. This effect has not been taken into account when calculating the optimal ratios.

The distance to shore has very little influence on the offshore configurations that use pipelines. For the onshore central configuration, however, the length of the HVDC cables influences the system LCOH significantly more. However, even when the system is placed only 75km from shore, which is around the break-even distance for HVAC and HVDC electricity transport, as found in Section 3.6.4, the system LCOH is well above the system LCOH of the offshore configurations. A more in-depth analysis of the dynamics of changing the distance to shore is given in Section 7.2.4.

Using batteries percentually adds more costs than hydrogen produced for every design, and the system LCOH increases. The use of a battery might still be beneficial in operational terms instead of financial terms. For instance, an alkaline electrolyser can degrade faster when experiencing start and stop cycles. Also, avoiding start and stop cycles can avoid the start-up and ramping up/down times of the electrolysers, as described in Section 5.1.3. A detailed analysis of these mechanics is not made in this thesis, nor is it taken into account in the model.

For the number of turbines per hydrogen collection pipeline, the increase in number of turbines can decrease the LCOH. If too many turbines are added, however, the length and pressure drop become so high that the extra compressor costs increase the LCOH. It is found that using strings of 33 turbines results in a slightly lower LCOH than using strings of 11 turbines. However, when using one string for an entire wind farm, the total length and costs of the hydrogen collection pipeline may decrease, but the pressure drop

becomes so high that the extra compressor power negates the lower costs of the pipeline itself. It should be noted that the calculations are performed with the assumptions made in this thesis. For instance, the pressure drop over a 12-inch pipeline was approached by a linear relationship between pipeline diameter and pressure. This relationship does not consider the dynamics of having little hydrogen at the start of the collection pipeline and having hydrogen fed in per wind turbine at 50 bar.

The discount rate is set as 8%, but when choosing 6% or 10%, the LCOH is largely influenced. The discount rate is used to calculate the capital recovery factor. With a higher discount rate, the CRF increases. The CRF is, in turn, used to calculate the annualised costs of the components. With a higher CRF comes higher annualised costs. Finally, with higher annualised costs, a higher system LCOH is found. This explains that the system LCOH increases with an increased discount rate and vice-versa.

Finally, when no baseload is used, the LCOH decreases with the current assumptions because the storage facility and pipelines to the storage facility are removed. When no baseload is used, pressure swings in the pipeline to shore can complicate the transport, as large pressure swings can damage the pipelines. However, if a backbone is used, either offshore or onshore, the pressure does not have to be maintained solely by the system considered in this thesis. Removing the boundary condition of supplying a baseload to demand reduced the system LCOH the most for the onshore central configuration, as it has the largest transport length to the storage facility.

The selected values for all input parameter scenarios are chosen as the most likely scenarios, as these values are in the middle of the ranges of the values found in literature.

7.2 Sensitivity Analysis

The sensitivity analysis is performed over the selected values from the scenario analysis. The system LCOH is used as the dependent variable of the sensitivity analysis. The independent variables are given per configuration as different parameters depend on the configuration. Firstly, Section 7.2.1 performs the sensitivity analysis of the offshore decentral configuration, after which Sections 7.2.2 and 7.2.3 discuss the sensitivity analysis of the offshore central and onshore central configuration, respectively. Finally, insights from the sensitivity analysis are given in Section 7.2.4.

7.2.1 Sensitivity Analysis Offshore decentral configuration

The independent variables used in the sensitivity analysis for the offshore decentral configuration, including their ranges, are given in Table 7.9. All independent variables are varied by +/-10%. As with the scenario analysis, the technical output parameters are no longer set as constant, to be able to perform the sensitivity analysis over technical parameters.

Parameter	**Unit**	**Min. value** (-10%)	**Nominal value**	**Max. value** (+10%)
Electrolyser power consumption	kWh/kgH_2	47.9	53.2	58.5
Distance to shore	km	225	250	275
Discount rate	%	7.2	8	8.8
Electrolyser CAPEX	$€_{2023}/kW$	495	550	605
Salt cavern CAPEX	$€_{2023}/MWh$	326	362	398
New 36-inch pipeline CAPEX	$M€_{2023}/km/GW$	167	185	204
New 12-inch pipeline CAPEX	$M€_{2023}/km$	1.35	1.5	1.65
Compressor CAPEX	$M€_{2023}/MW$	1.8	2	2.2
Wind turbine CAPEX	$€_{2023}/kW$	2165	2406	2647

Table 7.9: Selected parameters for the sensitivity analysis for the offshore decentral configuration, including their ranges.

The results of the sensitivity analysis for the offshore decentral configuration are given in Table 7.10.

Parameter	$LCOH_{system}$ (Min. value)	$LCOH_{system}$ (Nominal value)	$LCOH_{system}$ (Max. value)
Electrolyser power consumption	4.48	4.93	5.39
Distance to shore	4.93	4.93	4.94
Discount rate	4.59	4.93	5.28
Electrolyser CAPEX	4.81	4.93	5.06
Salt cavern CAPEX	4.92	4.93	4.95
New 36-inch pipeline CAPEX	4.93	4.93	4.94
New 12-inch pipeline CAPEX	4.91	4.93	4.96
Compressor CAPEX	4.93	4.93	4.94
Wind turbine CAPEX	4.61	4.93	5.25

Table 7.10: Results of the financial sensitivity analysis of the offshore decentral configuration. All values are given in $€/kWh$

The results are expressed in percentage change from the nominal value in Fig. 7.1.

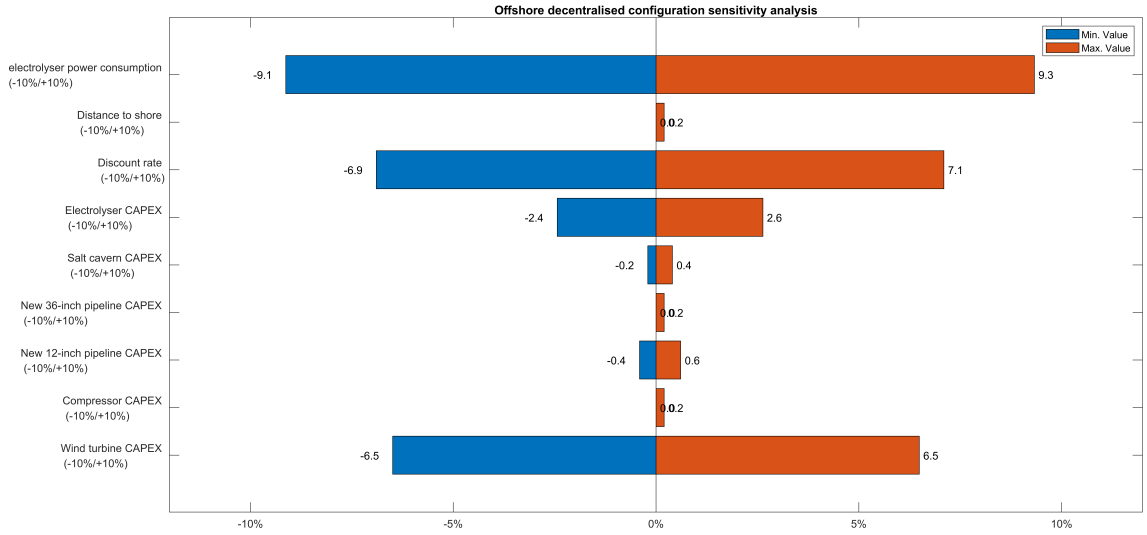

Figure 7.1: Percentual changes of the system LCOH when changing the independent variables of the sensitivity analysis for the decentral configuration.

As shown in Fig. 7.1, the model is most sensitive to changes in the electrolyser power consumption. When changing the electrolyser power consumption, the system LCOH almost scales with it. This is because the amount of hydrogen produced is directly influenced by the electrolyser power consumption, as the losses of the electrolyser are the highest losses of the system. The costs remain constant, so the LCOH scales with the hydrogen produced.

The model is the second most sensitive to changes in the discount rate. When changing the discount rate, the produced hydrogen is kept constant, but the costs change. The discount rate has a large influence on the calculations of the annualised costs, and changing the discount rate recurs in the LCOH calculations of every component.

Next, the model is most sensitive to the change in wind turbine CAPEX. The wind turbine costs make up the largest share of the system LCOH, as seen in Chapter 6, and thus, the wind turbine costs have a large influence on the system LCOH.

The model is also relatively sensitive to the electrolyser CAPEX, the second largest cost factor of the offshore decentral configuration.

The model is not sensitive to changes in distance to shore, salt cavern CAPEX, pipeline CAPEX or compressor CAPEX, as these components all have small cost contributions to the system LCOH, and a change in CAPEX does not influence the hydrogen production. If the distance to shore is decreased, costs, transport losses and needed compressor power are all decreased. However, the decreases are so small, that the LCOH only changed by 0.1%, which does not show in Fig. 7.1.

7.2.2 Sensitivity Analysis Offshore Central Configuration

The independent variables used in the sensitivity analysis for the offshore central configuration, including their ranges, are given in Table E.5 in Appendix E. Since no hydrogen collection pipeline is used, the new 12-inch pipeline CAPEX is replaced with the HVAC substation and cable CAPEX, inter-array cable CAPEX and the island CAPEX. All independent variables are varied by +/-10%.

The results of the sensitivity analysis for the offshore central configuration are given in Table 7.2.

Parameter	**Min. value** (-10%)	**Nominal value**	**Max. value** (+10%)
Electrolyser power consumption	5.19	5.73	6.27
Distance to shore	5.72	5.73	5.73
Discount rate	5.32	5.73	6.13
Electrolyser CAPEX	5.60	5.73	5.86
Salt cavern CAPEX	5.71	5.73	5.74
New 36-inch pipeline CAPEX	5.72	5.73	5.73
HVAC substation CAPEX	5.68	5.73	5.77
HVAC cable CAPEX	5.72	5.73	5.74
Inter-array cable CAPEX	5.72	5.73	5.74
Island CAPEX	5.71	5.73	5.74
Compressor CAPEX	5.72	5.73	5.73
Wind turbine CAPEX	5.40	5.73	6.06

Table 7.11: Selected parameters for the sensitivity analysis for the offshore central configuration, including their ranges.

The results are expressed in percentage change from the nominal value in Fig. 7.2.

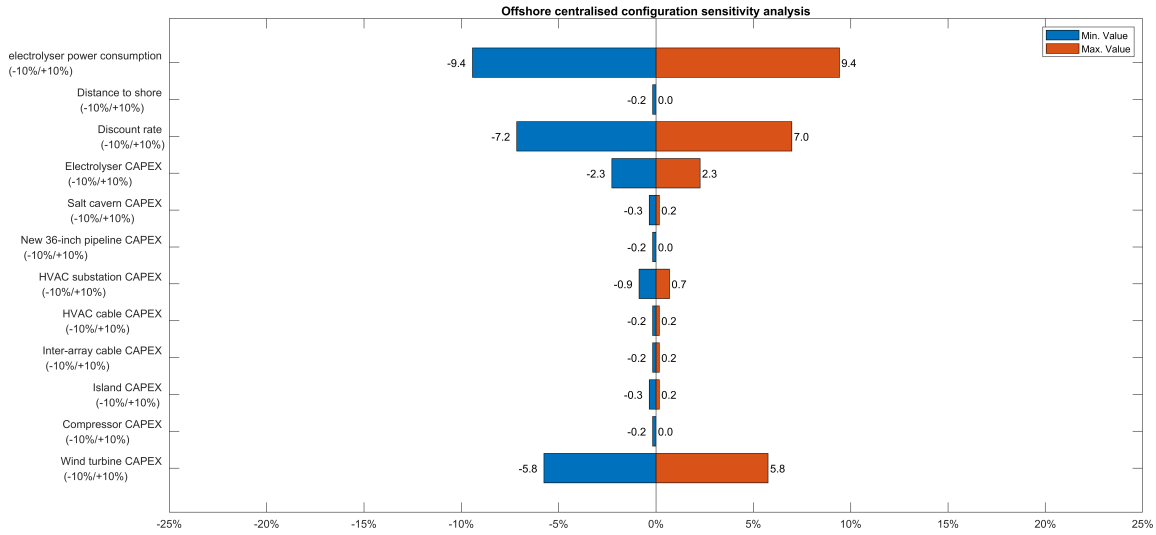

Figure 7.2: Percentual changes of the system LCOH when changing the independent variables of the sensitivity analysis for the offshore central configuration.

The sensitivity analysis of the offshore central configuration follows the same pattern as the offshore decentral configuration. The model is most sensitive to the electrolyser power consumption, discount rate and wind turbine CAPEX, respectively, for the same reasons as described in Section 7.2.1. The model for the offshore central configuration is a little less sensitive to wind turbine CAPEX and electrolyser CAPEX. As the total costs of the offshore central configuration are higher, the same change in CAPEX results in a smaller change in LCOH.

For the offshore central configuration also components were added that were not in the other configurations, such as the HVAC substation and cables and the island. The model is not sensitive to any of the three parameters.

7.2.3 Sensitivity Analysis Onshore Central Configuration

The independent variables used in the sensitivity analysis for the onshore central configuration, including their ranges, are given in Table E.6 in Appendix E. The CAPEX parameters over which the sensitivity analysis is performed are adjusted for the onshore central design. All independent variables are varied by +/-10%.

The results of the sensitivity analysis of the onshore central configuration are given in Table E.6.

Parameter	**Min. value** (-10%)	**Nominal value**	**Max. value** (+10%)
Electrolyser power consumption	5.80	6.40	7.00
Distance to shore	6.37	6.40	6.43
Discount rate	5.95	6.40	6.86
Electrolyser CAPEX	6.29	6.40	6.51
Salt cavern CAPEX	6.38	6.40	6.42
New 36-inch pipeline CAPEX	6.40	6.40	6.41
HVDC substation CAPEX	6.29	6.40	6.51
HVDC cable CAPEX	6.37	6.40	6.43
Inter-array cable CAPEX	6.39	6.40	6.41
Compressor CAPEX	6.39	6.40	6.41
Wind turbine CAPEX	6.06	6.40	6.74

Table 7.12: Selected parameters for the sensitivity analysis for the onshore central configuration, including their ranges.

The results are expressed in percentage change from the nominal value in Fig. 7.2.

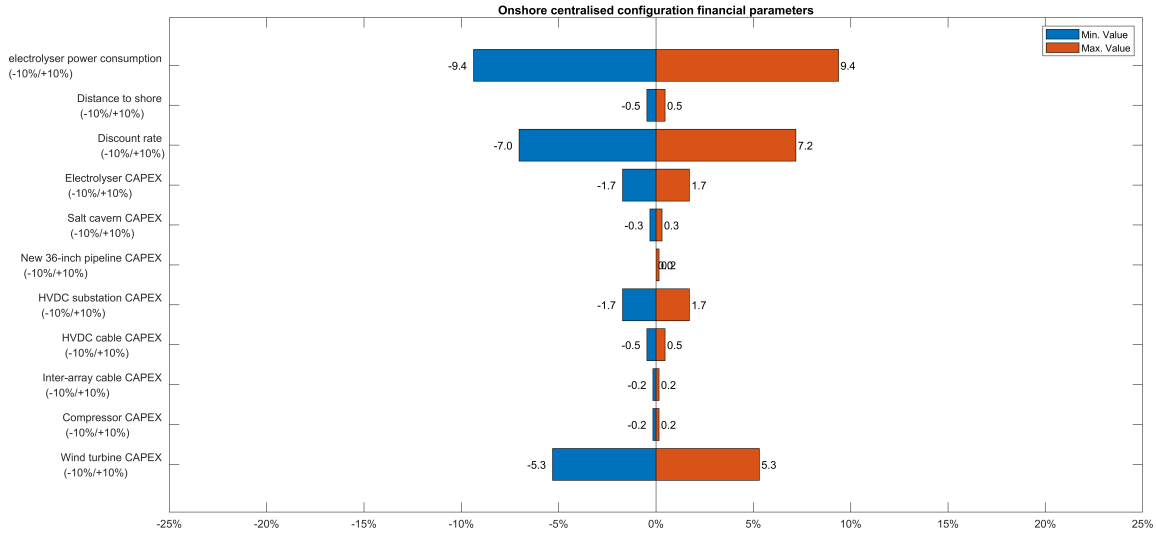

Figure 7.3: Percentual changes of the system LCOH when changing the independent variables of the sensitivity analysis for the onshore central configuration.

The sensitivity analysis of the onshore central configuration follows the same trends as the offshore decentral and central configuration. The electrolyser power consumption and discount rate have around the same percentual changes as for the other configurations, and the model is equally sensitive to these parameters for all configurations. However, since the total costs are higher for this configuration, the model is less sensitive to changes in individual component CAPEXs. As the HVDC substations have high CAPEX, the model is more sensitive to the HVDC substation CAPEX than to the HVAC substation CAPEX.

7.2.4 Insights

All three designs showed an equal sensitivity to the electrolyser power consumption. The electrolyser power consumption influences the amount of hydrogen produced directly. As other losses in the system, such as

the conversion losses and transport losses, are very low, the electrolyser power consumption has a very large influence on the hydrogen produced, and thus LCOH, which was shown in the sensitivity analysis. As the offshore decentral configuration has the lowest system losses, the largest sensitivity to the electrolyser power consumption was expected in this configuration. However, the offshore decentral configuration showed the lowest sensitivity to the electrolyser power consumption, albeit a very small difference. Also, as less hydrogen is produced, fewer compressors are needed, which would, very small, decrease the LCOH further. The onshore central configuration, where the lowest sensitivity of electrolyser power consumption was expected because of the highest losses of the other components, did, however, have the largest amount of compressors installed. The extra decrease in compressor capacity could have compensated for the smaller decrease in system losses compared to the offshore configurations, in combination with small variations due to the rounding of the system LCOH values.

The model has an equal sensitivity to the discount rate over all configurations. This is expected as the discount rate is in the LCOH calculations for every component, while the discount rate does not influence the produced hydrogen. Also, since the LCOH calculations are the same for every component, the discount rate has equal sensitivity for all component costs for all designs. Therefore, the system LCOH is equally sensitive to the discount rate for all designs. The small variations arise from the rounding of the LCOH values.

The model was not sensitive to the distance to shore for the offshore decentral and central configurations. For these configurations, pipelines are used to transport the hydrogen to shore. The contribution of these pipelines to the system LCOH is so small that almost no sensitivity is observed. Rounding the LCOH values explains the small variations in sensitivity for these configurations. For the onshore central configuration, HVDC cables are used to transport the electricity to shore. The HVDC cables themselves are less expensive than 36-inch pipelines per km. However, pipelines have multiple advantages. First of all, the pipelines have a much larger capacity. HVDC cables can transport 2GW of electricity to shore, which is enough for one wind farm. Thus, for the five wind farms used in this thesis, five HVDC cables have to be laid to shore. Only one pipeline is needed to transport the hydrogen produced from five wind farms to shore. This makes transport costs higher per km for electricity than that of (hydrogen) molecules, and thus, the system LCOH has a larger sensitivity to the distance of transport, albeit still small. Also, since the full capacity of the pipeline is not used, the pipeline can be shared with other projects. Larger pipelines can connect to multiple offshore projects by smaller pipelines, as with the offshore oil and gas industry. This results in the pipeline costs to shore being given in $€_{2023}/km/GW$ and that the transport costs per km decrease for the pipeline, and the system LCOH's sensitivity to the transport distance decreases. Finally, when converting electricity to hydrogen offshore, the largest system loss, which is the electrolyser loss, has already taken place before the transport to shore. This means that less energy has to be transported, and less transport losses are present. Due to the fact that the total annualised costs for the onshore central configuration were very high compared to the HVDC cable costs, a relatively low sensitivity was found.

The model showed a logical trend in sensitivity to the components' CAPEXs. When changing the CAPEX, only a cost change is caused, as the CAPEX does not influence the amount of hydrogen produced. Therefore, the model should have the largest sensitivity to the CAPEX of the components with the largest cost contributions to the system LCOH. Looking at the results from the sensitivity analysis, this is indeed the case. Also, as the total annualised costs are higher, changing one component's CAPEX should have less effect on the system LCOH. This can also be observed. When looking at the wind turbine CAPEX, for instance, the model becomes less sensitive to it if the configuration used has a higher system LCOH.

7.3 Key Findings

The subquestions of this research are answered and discussed individually in this section.

- **Which technologies for the offshore value chain are expected to be available from 2030 to 2050?**

  Firstly, the value chain components of an offshore hydrogen production value chain were identified. The value chain consists of an electrolyser, a water desalination plant, a hydrogen storage component and a transport component. Different electrolyser system configurations were also considered, and when an offshore centralised configuration is used, a value chain component of the hydrogen distribution hub is added.

  For the electrolyser technology, three technologies were taken into account. The technologies considered are alkaline electrolysis, proton exchange membrane electrolysis and solid oxide electrolyser cell electrolysis. Alkaline electrolysers have a simple stack design and currently have the highest installed capacity of all electrolyser technologies. PEM electrolysers use a proton-conducting membrane and have no liquid electrolyte present. Finally, SOEC electrolysers operate at high temperatures, using

steam as input instead of liquid water. Technological improvements and cost reductions are expected of these technologies to 2030 and 2050.

Seawater desalination plants can be divided into two categories. Namely membrane solutions and thermal solutions. The technologies considered for the water feed are reverse osmosis and membrane distillation. Reverse osmosis is a membrane solution that applies an external pressure to move water through a membrane and is currently the most used water desalination technique. Membrane distillation is a promising new thermal solution that is driven by a partial vapour pressure difference through a membrane.

The electrolyser system configuration has three possible technologies. Firstly, an offshore decentral configuration can be used. This configuration has a small electrolyser at the foot of each wind turbine to which it is coupled. The hydrogen is thus produced decentrally and is then collected to send to shore. Another offshore configuration is the offshore central configuration. In this configuration, the electricity from the wind turbines, or even multiple wind farms, is collected and transported to a central offshore location where electrolysis takes place. Finally, with the onshore central configuration, the electricity collected from the wind turbines can be transported to shore, to have the electrolysis take place at a central onshore location.

Two main underground storage technologies are considered. Firstly, hydrogen can be stored in empty hydrocarbon reservoirs by trapping the hydrogen between lowly permeable cap rocks. Another underground storage technology is trapping the hydrogen inside salt domes. Because of the low permeability, little hydrogen is prone to leaking. Salt caverns are constructed by injecting water into a salt body to dissolve the salt. Above-ground storage technologies are mentioned but not considered for the offshore hydrogen production value chain, as they take up a lot of space due to the high storage volumes.

Hydrogen can be transported by pipelines. These pipelines can be newly built, but also infrastructure from the oil and gas industry has the potential of being repurposed as hydrogen pipelines. When the onshore central configuration is used, electricity is sent to shore via electricity cables. Hydrogen transportation via shipping is mentioned but not taken into account for the value chain, as supplying a baseload via ships is not viable, and the transportation distance is more in favour of transport by pipeline.

Finally, with the offshore central configuration, the location of the central electrolysers is a value chain component. A man-made island can be constructed, and electricity from multiple wind farms can be collected to use for electrolysis on the island. The second technology has the electrolysers placed centrally per wind farm, where the electricity of multiple turbines is collected on a (repurposed) offshore platform.

- **What decision framework is recommended to come to three promising designs?**

  To evaluate the chosen technologies, and come to three promising designs, a decision framework is constructed. The technologies are to be evaluated on technical and financial parameters, but also on qualitative characteristics, such as the environmental impact and the safety and maintenance requirements.

  Because of the high amount and diversity of the decision criteria, it is chosen to perform a multi-criteria decision analysis. A multi-criteria decision analysis offers multiple advantages. Both qualitative and quantitative criteria can be taken into account, it can handle a large number of criteria, and it offers a structured and transparent manner of decision-making.

  For each value chain component, an MCDA was performed. Each MCDA resulted in a preferable technology per value chain component. The first design was constructed by combining these best-performing technologies according to the MCDA. A hard requirement was set that the other designs needed to make use of the other two remaining electrolyser system configurations. The decision framework was then used to construct these designs, as it offered a structured overview of the possible technologies with their advantages and disadvantages. Also, interactions between technologies from different value chain components are mentioned and can be taken into account.

  With the decision framework, more designs than the designs used in this thesis can be constructed.

- **What are possible designs for the offshore hydrogen production value chain on the North Sea to be integrated into the Dutch energy system?**

  Three designs are constructed with the decision framework and analysed on their physical system integration on the Dutch North Sea. The first design makes use of the offshore decentral configuration. The search areas for offshore wind farms after 2030 from the Dutch government were taken as an indication of the location of the offshore wind farms. The decentral offshore configuration makes use

of electrolysers and water desalination at the foot of the turbines. For the storage facility, many salt structures are available close to the search locations of the wind farms, and sufficient capacity is available in these salt structures to supply a baseload of hydrogen to shore. For hydrogen transportation, pipelines are used, and 75km of the pipeline to shore can be made out of reused pipelines. However, since only a part of this pipeline is used, it is probable that this pipeline will be reserved for other purposes. Still, a pipeline can be laid to shore, and sufficient space is available at the Port of Rotterdam to land a pipeline.

The second design makes use of an offshore central configuration. The same search areas are considered for the first design, as well as the same pipeline and storage facilities. This configuration, however, makes use of an island to house the electrolysers. A small part of the search areas is made available for the island if the island can not be located next to the search areas. The electrical infrastructure, consisting of the inter-array cables and offshore substations, is standard for offshore wind farms and thus can be placed in the available search areas. Again, the landing of a pipeline onshore at the Port of Rotterdam is possible.

Finally, the third design makes use of the onshore central configuration. This configuration makes use of HVDC cables and substations to transport electricity from the wind farms to shore. Space should be available to house the substations and inter-array cables since those lay within the search areas of the wind farms, but per wind farm, an HVDC cable needs to be laid to shore. This results in five HVDC cables, which have to be laid through the North Sea, as well as have a landing onshore. The landing requires space for the cables but also for the converters onshore. Not enough space is available at the Port of Rotterdam for these landings, and an additional exploitation of land to the Port of Rotterdam is needed for this configuration if it is to be connected to the Port of Rotterdam. The Rotterdam Wind Power Hub project is investigating the possibility of land reclamation. Finally, the salt caverns are all located on the northern part of the Dutch North Sea, and thus a pipeline to the salt caverns is needed from the electrolysers to the salt caverns.

- **How should the components and the totals systems be sized?**

  A boundary condition of this thesis is the use of five offshore wind farms, each consisting of 133 15MW wind turbines, for a combined total of just under 2GW per wind farm. Another boundary condition is that the hydrogen will be supplied to the demand side by means of a baseload. These boundary conditions are used for the sizing of the value chain.

  Firstly, the electrolyser capacity is a design choice, as electricity can be curtailed if additional electricity is present. It was chosen to have 12MW of electrolyser capacity per 15MW wind turbine for a total of 8GW. The scenario analysis showed that a slightly higher electrolyser capacity could result in a slightly lower system LCOH. For the offshore decentral configuration, hydrogen collection pipelines are laid in the wind farms to collect the hydrogen per wind turbine. The pipeline is sized to be able to collect the hydrogen produced when all wind turbines and electrolysers operate on rated capacity. This resulted in a 12-inch pipeline. Since the hydrogen is fed in at the output pressure of the PEM electrolysers, no additional compressors are needed at the hydrogen collection pipelines. The pipeline that transports the hydrogen from all wind farms to shore is also sized on maximum production and has a diameter of 36 inches. The total compressor power needed for this configuration is 142 MW. Finally, the size of the storage facility was determined by maximising the baseload and sizing the storage facility to the maximum level of hydrogen over the entire simulated time of the model, which is sized at 3.72TWh capacity.

  For the offshore central design, the inter-array cables, HVAC cables, and offshore substations are sized according to the future standards of TenneT. The size of the wind farms determines the amount of each needed. The hydrogen pipeline to shore and to the storage facility are sized on the maximum flow, as well as the compressor power. The pipeline to shore and to the storage facility is sized at 36 inches, and the total compressor power is 106 MW. The island is sized on the capacity of electrolysers, which is 8 GW. The storage is sized on the maximum baseload and has a 3.70 TWh capacity.

  For the onshore central design, the electrical infrastructure is sized on future TenneT standards. The pipelines and compressors are sized for maximum flow, resulting in a 36-inch pipeline and 220MW of compressor power. The storage facility is sized on the baseload and has a capacity of 3.69 TWh.

- **What would be the levelised cost of hydrogen upon arrival at the PoR, and how does this compare to other projects?**

  The lowest levelised cost of hydrogen was found for the offshore decentral configuration, using the assumptions and boundary conditions used in the model. The Levelised cost of hydrogen is found to be 5.14 $€_{2023}/kgH_2$. 64% of the total LCOH is from the component LCOH of the wind turbines. The

second largest share is the component LCOH of the electrolyser, accounting for 25%. The transport and storage components have a share of 5% and 4%, respectively. The compressor and water feed have very low component LCOHs with 1% and <1%.

The offshore central configuration has a system LCOH of 5.69 $€_{2023}/kgH_2$. The wind turbines account for 58% of it. The electrolyser and transport components have significant component LCOHs with 23% and 12%, respectively. The storage and hub components both account for 3% of the total system LCOH, while the compressors and water feed have a 1% and >1% share of the system LCOH.

Finally, the onshore central configuration has a system LCOH of 6.14 $€_{2023}/kgH_2$. The largest share is of the wind turbines with 54%, followed by the transport, electrolyser and storage components with 24%, 18% and 3%, respectively. The compressors account for 2% of the system LCOH, while the water feed stays below 1%.

The calculated LCOHs are outputted from the model when the technical outputs of the model are set as constants. These technical outputs include the maximum baseload, storage capacity and total hydrogen produced. These outputs were set as constants to allow for a fair comparison between the economic aspects of the designs. With all the designs having the same amount of hydrogen produced, the costs for the systems are calculated, and the LCOH is calculated. However, if the model does not set these technical outputs as constants, the designs use the actual technical outputs, and the LCOHs become different. For the offshore decentral configuration, this results in a slightly lower LCOH of 4.93 $€_{2023}/kgH_2$. For the offshore central configuration, the LCOH becomes slightly higher at 5.73 $€_{2023}/kgH_2$. Finally, for the onshore central configuration, the LCOH increases to 6.40 $€_{2023}/kgH_2$.

(Wingerden et al. (2023)) comes to a levelised cost of hydrogen in 2050 of 3.24 $€_{2023}/kgH_2$ when producing hydrogen offshore on the North Sea and transporting it to shore over a distance of 150km. Hydrogen storage was not considered. (Little et al. (2023)) reports a value of 2.5 $€_{2023}/kgH_2$ when using a 1320 MW offshore wind farm at 89km from shore on the North Sea in 2050 with an offshore central configuration. When using an onshore configuration, 3.2 $€_{2023}/kgH_2$ is found as the LCOH. (I.R.E.A (2022)) reports a value of around 1 $€_{2023}/kgH_2$ for hydrogen production in Europe in an optimistic scenario. This scenario assumes offshore wind power CAPEX of 1210-1656 $€_{2023}/kW$ and 126-297 $€_{2023}/kW$ electrolyser CAPEX. Both the wind power CAPEX and electrolyser CAPEX are lower than considered in this thesis. Using the optimistic value for electrolyser CAPEX in the scenario analysis also did not result in such a low system LCOH. It should be noted that storage is not considered in I.R.E.A (2022). The ERM-Dolphyn project expects a levelised cost of hydrogen of 2.24 $€_{2023}/kgH_2$, using decentral hydrogen production with floating wind turbines (Dolphyn (2021)). The discount rate was taken as 6%, which is lower than considered in this thesis, and no storage was used. Also, a higher wind capacity factor of 0.55 was considered. Finally, (D.B.E.I.S. (2021)) reports of around 1.75 $€_{2023}/kgH_2$ when producing hydrogen with PEM electrolysers with dedicated offshore wind.

Looking at the reported projected levelised costs of hydrogen, no total system LCOH is reported as in this thesis, as no offshore wind to baseload hydrogen projects are reported. The reported values are all significantly lower than the system LCOH found in this thesis, even if no baseload is applied. When comparing the levelised cost of hydrogen values from literature, it is important to know which components are included in the system LCOH, as well as the cost parameters, such as discount rate, that are used to calculate the system LCOH. Finally, the conditions that the hydrogen is supplied with, such as purity and pressure, are also important to note when comparing LCOH values.

7.4 Limitations

Some limitations to this thesis and the model are known. They are briefly mentioned and described below.

- **Model limitations**

  Some simplifications are made in the simulation model. Firstly, the model was programmed to run the system for 100% of the simulated time. For a more accurate representation of reality, maintenance or failures could also be simulated by making a component unavailable for a certain amount of time. Doing this, some other behaviours could be observed. An example of this is the flexibility of the decentral electrolysers, which can continue operating when one electrolyser fails.

  Secondly, the electrolyser power consumption is assumed to be constant over all load variations of the electrolyser. In reality, the partial load operation of an electrolyser is associated with a higher power consumption and, thus, a lower efficiency. This decreases the system efficiency and hydrogen produced and increases LCOH.

When modelling the batteries for the scenario analysis, the discharge capacity degradation of the batteries was not taken into account. In reality, the batteries lose discharge capacity over charging/discharging cycles.

For the efficiency of the storage facility, only the compressors were taken into account. A purification step of the hydrogen might also be needed, as well as auxiliary equipment. The costs of this are included in the OPEX, but the electricity consumption has only been taken into account by the compressors. The reaction speed of the storage facility was also not taken into account, and it is assumed that the flow direction of the storage facility and pipeline can change instantly.

The pressure drop over the pipelines was calculated by a simplified linear relation between pressure drop and pipeline diameter. In reality, the pressure drops behave slightly differently. However, as can be seen in the results, the compressor power makes up a very small share of the system LCOH.

- **Considered technologies**

  Not every possible technology is considered for all value chain components. Due to the fact that so many different technologies are available for some value chain components, choices are made regarding which technologies to consider and which not. For instance, for the electrolyser technologies, the most mature technologies were considered. Multiple other technologies are currently at a low TRL but could be available towards 2050. Examples of these include anion exchange membrane electrolysers, CO_2 electrolysers and direct seawater electrolysers.

- **Cost limitations**

  The costs of the used technologies have been taken into account using CAPEX and OPEX. The CAPEX includes the installation costs where they were specified. For some sources from literature, it was not specified whether installation costs were taken into account. Also, no decommissioning costs have been taken into account. Especially for offshore construction, the decommissioning costs can be of importance.

  Other project costs such as engineering costs, development costs, land costs and permits have not been considered. The offshore decentral configuration can benefit from these costs, as the wind turbine and electrolyser can be regarded and installed as one project. This can reduce the abovementioned costs. For the central configurations, the wind turbines and electrolysers are two separate projects, and the costs apply to both separate projects. Also, onshore, the cost of land is not considered. When connecting the onshore central configuration to the Port of Rotterdam, the cost of land is a significant cost factor, either as the cost of land in the current Port or as land reclamation, as investigated by the Rotterdam Wind Power Hub. Finally, the offshore decentral can have a cost reduction in the OPEX of the wind turbines and the electrolysers as they are placed together. Since placing the electrolysers decentral makes for more complex maintenance, it is beneficial to combine the maintenance with that of the wind turbines, as the maintenance for the wind turbines has to be performed for every configuration.

  The electrolyser stack replacement costs were approached by averages. The efficiency degradation of the electrolysers made the storage facility store a lot of hydrogen in the first years of the simulation when the electrolyser efficiencies were high and depleted a lot of hydrogen in the last years of the electrolyser stack lifetimes. This, however, surpassed the utility of the storage facility, as it was intended to compensate for the baseload, not store hydrogen over many years to complement the efficiency degradation. Therefore, it was chosen to have a share of the electrolysers replaced every year so that the efficiency remains constant over the simulated time, as the average efficiency between begin and end of the lifetime of the stacks. Doing this, the replacement costs of the electrolysers were approached by taking the lifetime of the electrolysers and calculating the average needed number of replacements. These replacements are then executed at the average replacement time, which is at half of the lifetime. If the total lifetime times two was lower than the simulated lifetime, another replacement cycle was added. The cost calculations, therefore, did consider the average costs of the replacements but did not consider the exact number of replacements as a simplification. Also, using this approach, electrolysers installed at the start are already to be replaced a year later, which, of course, would not happen in reality. A more realistic scenario is that the number of wind farms connected to either configuration is scaled up over time. This would also help to divide the replacements of the electrolysers better over time.

  Also, the residual values of the components were not taken into account. As some components have very long lifetimes, these residual values can be significant.

7.5 Recommendations

Some recommendations for policymakers and further research are mentioned and described below.

- Policymakers are encouraged to consider exploring offshore hydrogen production, as suggested by this thesis. When enough wind power is available for the offshore production of hydrogen, it can be a technical-feasible, cost-effective solution for local hydrogen production in the Netherlands. The local production of hydrogen can increase the security of supply for industry in the Netherlands in turbulent geopolitical times.

- A simulation model is constructed since little research has been done into the possible offshore hydrogen production value chain configurations. Also, from interviews with companies, it became clear that the electrolyser system configuration is an important topic for the designs of offshore hydrogen production, as not one configuration was clearly deemed more interesting. Some companies were investigating one configuration, while others were looking into other configurations. Also, the performance and costs of the electrolysers offshore were uncertain for market parties. With this simulation model, the first conclusions can be drawn when comparing the different configurations. Also, the uncertainties have been addressed in the scenario analysis. The model could be improved to not only simulate the possible configurations but also optimise the configurations for a chosen output. For instance, if all of the different technologies for the value chain components can be added to the model, an optimisation model can find the combination with the lowest LCOH, given a set of boundary conditions.

- Another point for future research is the interconnection between other energy hubs on the North Sea. A stand-alone system was designed in this thesis, but interconnection with other countries directly or via energy hubs is a possibility for the energy system on the North Sea. The interconnection of the designs made in this thesis could be further researched. The interconnection could be with hydrogen, but it can also be a hybrid system with hydrogen and electricity connections. Other dynamics, such as market dynamics, then come into play. As described in Chapter 2, Belgium and Denmark are looking into constructing energy islands to which this system or a possible Dutch energy island could be connected.

- The model made can serve as a strong basis for future model enhancements to simulate reality. First of all, system maintenance could be simulated closer to reality, as no downtime for maintenance has been considered. Secondly, the operation of certain components can be improved. For instance, the electrolyser partial load range operation has not been taken into account. Also, the ramp-up/down times and hot and cold start-up times of the electrolysers have not been taken into account. Since the electrolysers are directly coupled to wind turbines, these mechanics can be very important when simulating the system's behaviour. A more detailed representation of reality can give a better estimation of the system LCOH. Also, when dealing with the partial load ranges, start-up times and ramp-up/down times of electrolysers, a battery system could prove to be an effective solution for stand-alone systems, although it is shown that it is not necessarily a cost-effective solution under the current assumptions. It can be further investigated if batteries can improve the characteristics. Since the operations of the batteries are included in the MATLAB model, the model can serve as a basis for further research on this.

- The use of by-products can be investigated further. As no space was available at the Port of Rotterdam for a heating or water network to the electrolysis location of the onshore central configuration, the capture of by-products was not considered, and they were dissipated in the atmosphere. Future research could look into the use of these by-products. However, With the tenders of offshore wind farms, only one market party showed an interest in capturing the oxygen from the electrolysers. That market party also already had experience and assets for storing and transporting oxygen. All of the other market parties that submitted a tender saw no cost-effective use of oxygen as a by-product (PoR (2023)).

- In reality, a system such as the three designs simulated in this thesis will not be built and delivered all at the same time. A realistic scenario is that the total system will grow by connecting the wind farms when they are delivered. The scalability mechanics and costs of scaling the system per delivered component have not been taken into account for this thesis and can be looked into for a more accurate system LCOH estimate.

- The designs made in this thesis are site-specific for the Dutch North Sea. With minor adjustments, the model can be used to calculate the system LCOHs for other locations. When looking at the Netherlands and the Port of Rotterdam specifically, other configurations than the ones considered in this thesis can also be of interest. For instance, instead of landing the hydrogen directly at the Port of Rotterdam, a configuration can be made that lands the hydrogen in the Northern part of the Netherlands and transports the hydrogen to the Port of Rotterdam via the hydrogen backbone. The possibility of connecting the offshore designs to an offshore hydrogen backbone can also be considered.

8 Conclusion

This thesis aims to develop a techno-economically feasible design of a large-scale offshore hydrogen production value chain connected to the port of Rotterdam in 2050.

The answer to the main research question is tri-fold. A preferred design is given as an output of the decision framework, as well as an output of the technical and financial parts of the model.

A decision framework is constructed based on a multi-criteria decision analysis of the technologies of the value chain components. The decision framework takes technical and economic criteria into consideration, but also qualitative criteria such as the environmental impact and safety and maintenance requirements. It is found that the optimal design is an offshore decentral configuration. The design uses PEM electrolysers at the foot of every wind turbine. A reverse osmosis desalination plant is also present at the foot of each turbine to produce the water feed to the electrolyser. The hydrogen is collected from each wind turbine by 12-inch hydrogen collection pipelines. The collection pipelines per wind farm come together at a manifold on a central point between the wind farms. From there, the pipeline to shore starts. This pipeline is 36 inches and is partly made up of a repurposed existing pipeline, where available. The preferred storage technology is salt caverns, which are located near wind farms. The offshore decentral design, which is the preferred design, is also simulated in the model with two other designs. The model was made from the ground up and simulates the operation of the three constructed designs.

From the technical part of the model, mainly the system efficiencies were evaluated. From the three simulated designs, the offshore decentral configuration has the highest system efficiency of 69.4%. The offshore central design has a system efficiency of 65.8%, while the onshore central configuration has the lowest system efficiency at 65.1%. From the technical aspect, the offshore decentral configuration is also the preferred design. However, when evaluating renewable energy systems, efficiency is less important than the costs, as the energy source is unlimited.

Finally, the designs were compared to the economic outputs of the model. The system levelised cost of hydrogen from the offshore decentral configuration, when providing a baseload of hydrogen to shore at 50 bar in 2050, is 5.14 $€_{2023}/kgH_2$. The LCOHs of the offshore central and onshore central configurations are 5.69 $€_{2023}/kgH_2$ and 6.14 $€_{2023}/kgH_2$ respectively. these values are found when setting the technical outputs of the model constant to allow for a fair comparison between the cost parameters. However, if the technical outputs are not set constant, the offshore decentral configuration achieves a system levelised cost of 4.93 $€_{2023}/kgH_2$ when providing a baseload of hydrogen to shore at a pressure of 50 bar in 2050.

From an economic aspect, the offshore decentral configuration is thus the preferred design. This is because of multiple reasons. It is found that the largest differences in the LCOH for the three designs in this thesis come from the differences in the transport component LCOH. The first design uses only pipelines to transport energy to shore, whereas the offshore central and onshore central also require an electrical infrastructure. An advantage of the offshore decentral configuration is that the pipelines have a much higher capacity than the HVDC or HVAC cables. The hydrogen produced from all five wind farms was able to be transported to shore by one pipeline, whereas the HVDC cables needed to be laid for each wind farm, as they have a capacity of 2GW. This includes the costs of five HVDC cables, five offshore HVDC substations, and five HVDC onshore substations. Also, as the pipeline capacities are significantly larger than needed, the pipeline can be shared with other projects, thus also sharing the costs. Secondly, when hydrogen is produced offshore, the largest system losses are already undertaken before energy transport. This means that less energy has to be transported, and less transport losses occur.

When taking all results into consideration, the offshore decentral configuration is the preferred design of this thesis. Apart from scoring highest in the multi-criteria decision analysis, it yielded the best technical and the best economic results from the simulation model.

References

Abhinav, K. A., Collu, M., Benjamins, S., Cai, H., Hughes, A., Jiang, B., ... Zhou, B. Z. (2020, 9). *Offshore multi-purpose platforms for a blue growth: A technological, environmental and socio-economic review* (Vol. 734). Elsevier B.V. doi: 10.1016/j.scitotenv.2020.138256

A.C.E.R. (2021). *Transporting pure hydrogen by repurposing existing gas infrastructure: Overview of existing studies and reflections on the conditions for repurposing.*

Adewole, J. K., Maawali, H. M. A., Jafary, T., Firouzi, A., & Oladipo, H. (2022a, 12). A review of seawater desalination with membrane distillation: material development and energy requirements. *Water Supply*, *22*, 8500-8526. doi: 10.2166/ws.2022.337

Adewole, J. K., Maawali, H. M. A., Jafary, T., Firouzi, A., & Oladipo, H. (2022b, 12). *A review of seawater desalination with membrane distillation: material development and energy requirements* (Vol. 22). IWA Publishing. doi: 10.2166/ws.2022.337

Administration, U. E. I. (2018). *Assessing hvdc transmission for impacts of non-dispatchable generation.* Retrieved from `www.eia.gov`

Alkhudhiri, A., Darwish, N., & Hilal, N. (2012, 11). *Membrane distillation: A comprehensive review* (Vol. 287). doi: 10.1016/j.desal.2011.08.027

Al-Obaidani, S., Curcio, E., Macedonio, F., Profio, G. D., Al-Hinai, H., & Drioli, E. (2008, 10). Potential of membrane distillation in seawater desalination: Thermal efficiency, sensitivity study and cost estimation. *Journal of Membrane Science*, *323*, 85-98. doi: 10.1016/j.memsci.2008.06.006

Alsebaeai, M. K., & Ahmad, A. L. (2020, 6). *Membrane distillation: Progress in the improvement of dedicated membranes for enhanced hydrophobicity and desalination performance* (Vol. 86). Korean Society of Industrial Engineering Chemistry. doi: 10.1016/j.jiec.2020.03.006

Alvestad, K. (2022). *Combined hydrogen and offshore wind production design and market value.* Retrieved from `http://www.duo.uio.no/`

Amaechi, C. V., Reda, A., Butler, H. O., Ja'e, I. A., & An, C. (2022, 8). *Review on fixed and floating offshore structures. part i: Types of platforms with some applications* (Vol. 10). MDPI. doi: 10.3390/jmse10081074

Amores, E., Sánchez-Molina, M., & Sánchez, M. (2021, 6). Effects of the marine atmosphere on the components of an alkaline water electrolysis cell for hydrogen production. *Results in Engineering*, *10*. doi: 10.1016/j.rineng.2021.100235

Andersson, J., & Grönkvist, S. (2019, 5). *Large-scale storage of hydrogen* (Vol. 44). Elsevier Ltd. doi: 10.1016/j.ijhydene.2019.03.063

Ardelean, M., Minnebo, P., for Energy, E. C. J. R. C. I., & Transport. (2015). *Hvdc submarine power cables in the world : state-of-the-art knowledge.* Publications Office.

Asghari, E., Abdullah, M. I., Foroughi, F., Lamb, J. J., & Pollet, B. G. (2022, 2). *Advances, opportunities, and challenges of hydrogen and oxygen production from seawater electrolysis: An electrocatalysis perspective* (Vol. 31). Elsevier B.V. doi: 10.1016/j.coelec.2021.100879

Aslannezhad, M., Ali, M., Kalantariasl, A., Sayyafzadeh, M., You, Z., Iglauer, S., & Keshavarz, A. (2023, 3). *A review of hydrogen/rock/brine interaction: Implications for hydrogen geo-storage* (Vol. 95). Elsevier Ltd. doi: 10.1016/j.pecs.2022.101066

Ayaz, M., Namazi, M. A., ud Din, M. A., Ershath, M. I., Mansour, A., & el Hadi M. Aggoune. (2022, 10). *Sustainable seawater desalination: Current status, environmental implications and future expectations* (Vol. 540). Elsevier B.V. doi: 10.1016/j.desal.2022.116022

Backbone, E. H. (2022). *A european hydrogen infrastructure vision covering 28 countries.* Retrieved from `https://www.ehb.eu/maps`

Bank, E. C. (2023). Monetary policy. Retrieved from `https://www.ecb.europa.eu/ecb/tasks/monpol/html/index.en.html#:~:text=We%20keep%20prices%20stable%20by,2%25%20over%20the%20medium%20term.`

Behrens, M. (2016, 3). Chemical hydrogen storage by methanol: Challenges for the catalytic methanol synthesis from co2. *Recyclable Catalysis*, *2*. doi: 10.1515/recat-2015-0009

Beik, O., & Al-Adsani, A. S. (2020). *Dc wind generation systems: Design, analysis, and multiph. turbine technology.* Springer International Publishing. doi: 10.1007/978-3-030-39346-5

Bermudez, J. M., Evangelopoulou, S., & Pavan, F. (2022, 9). *Electrolysers tracking report.*

Blagojević, B., Jonsson, R., Björheden, R., Nordström, E.-M., & Lindroos, O. (2019). *Multi-criteria decision analysis (mcda) in forest operations-an introductional review* (Vol. 40).

Breunis, W. (2021). *Hydrogen gas production from offshore wind en-ergy.* Retrieved from `http://repository.tudelft.nl/.`

Buijs, L., Bulder, B., Koornneef, J., Peters, R., & Sponsor, M. W. (2022). *Offshore hydrogen for unlocking the full energy potential of the north sea.* Retrieved from `https://energy.ec.europa.eu/system/files/2022-09/220912_NSEC_Joint_Statement_Dublin_Ministerial.pdf`

Bussel, G. V. (2006). *Offshore wind farm aspects typical wind farm aspects electrical infrastructure 2 module 9: Wind farm aspects.* Retrieved from `www.hornsrev.dk`

Buttler, A., & Spliethoff, H. (2018, 2). *Current status of water electrolysis for energy storage, grid balancing and sector coupling via power-to-gas and power-to-liquids: A review* (Vol. 82). Elsevier Ltd. doi: 10.1016/j.rser.2017.09.003

Caglayan, D. G., Weber, N., Heinrichs, H. U., Linßen, J., Robinius, M., Kukla, P. A., & Stolten, D. (2020, 2). Technical potential of salt caverns for hydrogen storage in europe. *International Journal of Hydrogen Energy*, *45*, 6793-6805. doi: 10.1016/j.ijhydene.2019.12.161

Catapult. (2021). Wind farm costs.

CBS. (2023, 3). *Aandeel hernieuwbare electriciteit met 20 procent gestegen in 2022.* Retrieved from `https://www.cbs.nl/nl-nl/nieuws/2023/10/aandeel-hernieuwbare-elektriciteit-met-20-procent-gestegen-in-2022`

Chandrasekar, A., Flynn, D., & Syron, E. (2021, 8). Operational challenges for low and high temperature electrolyzers exploiting curtailed wind energy for hydrogen production. *International Journal of Hydrogen Energy*, *46*, 28900-28911. doi: 10.1016/j.ijhydene.2020.12.217

Charfi, A., Kim, S., Yoon, Y., & Cho, J. (2021, 9). Optimal cleaning strategy to alleviate fouling in membrane distillation process to treat anaerobic digestate. *Chemosphere*, *279*. doi: 10.1016/j.chemosphere.2021.130524

Chatzivasileiadis, S., Ernst, D., & Andersson, G. (2012, 7). The global grid. Retrieved from `http://arxiv.org/abs/1207.4096`

Chau, K., Djire, A., & Khan, F. (2022, 4). Review and analysis of the hydrogen production technologies from a safety perspective. *International Journal of Hydrogen Energy*, *47*, 13990-14007. doi: 10.1016/j.ijhydene.2022.02.127

Chisholm, G., Zhao, T., & Cronin, L. (2022, 1). Hydrogen from water electrolysis. In (p. 559-591). Elsevier. doi: 10.1016/B978-0-12-824510-1.00015-5

Christensen, A., & Co, A. (2020). *Assessment of hydrogen production costs from electrolysis: United states and europe.*

Cihlar, J., Lejarreta, A. V., Wang, A., Melgar, F., Jens, J., Rio, P., ... Impact., T. (2020). *Hydrogen generation in europe : overview of costs and key benefits.*

Cole, S. (2022). *Wind turbine power curve.* Retrieved from `https://theroundup.org/wind-turbine-power-curve/`

David, M., Ocampo-Martínez, C., & Sánchez-Peña, R. (2019, 6). *Advances in alkaline water electrolyzers: A review* (Vol. 23). Elsevier Ltd. doi: 10.1016/j.est.2019.03.001

D.B.E.I.S. (2021). *Hydrogen production costs 2021.*

D.E.A. (2022). *Denmark's energy islands.* Retrieved from `https://ens.dk/en/our-responsibilities/offshore-wind-power/denmarks-energy-islands`

DEA, & EY. (2022). *The energy island in the north sea teaser for potential investors.*

Deloitte, M. (2021). *Fueling the future of mobility: hydrogen electrolyzers.*

DeNederlandscheBank. (2022). The ecb's monetary policy. Retrieved from https://www.dnb.nl/en/the-euro-and-europe/the-ecb-s-monetary-policy/#:~:text=The%20price%20stability%20sought%20by,best%20when%20prices%20are%20stable.

DNV. (2021). *Study on an estimation method for the additional efficient operating expenditure of the dutch tso's offshore grid autoriteit consument markt (acm) openbaar.* Retrieved from www.dnvgl.com

DNV. (2023). *Cost and performance data for offshore hydrogen production report danish energy agency.*

Dolphyn. (2021). *The business of sustainability erm dolphyn hydrogen phase 2-final report comprising: Detailed design for 2mw scale prototype pre-feed for 10mw commercial scale demonstrator public report.* Retrieved from www.erm.com

Duong, H. C., Phan, N. D., Nguyen, T. V., Pham, T. M., & Nguyen, N. C. (2017, 12). Membrane distillation for seawater desalination applications in vietnam: Potential and challenges. *Vietnam Journal of Science and Technology*, *55*, 659. doi: 10.15625/2525-2518/55/6/10715

EBN, & TNO. (2022). *Haalbaarheidsstudie offshore ondergrondse waterstofopslag.* Retrieved from www.ebn.nl

Economics, T. (2023). Euro area inflation rate. Retrieved from https://tradingeconomics.com/euro-area/inflation-cpi#:~:text=Inflation%20Rate%20in%20Euro%20Area,percent%20in%20July%20of%202009.

EMIS. (2010). *Membrane distillation.*

Eneco. (2023). Hollandse kust (noord). Retrieved from https://www.eneco.com/wat-we-doen/duurzame-bronnen/windpark-hollandse-kust-noord/

Energy, N. S. (2022). *Safety integrity reliability of offshore hydrogen production installations 3.*

Energy, N. S. (2023). North sea energy atlas. Retrieved from https://north-sea-energy.eu/en/energy-atlas/

Energy, S. (2020). *Hydrogen infrastructure-the pillar of energy transition.*

ENTSOG, GIE, & Europe, H. (2021). How to transport and store hydrogen - facts and figures.

Equinor, & BP. (2023). Empire wind. Retrieved from https://www.empirewind.com/

Eradus, B. D. (2022). *The techno-economic feasibility of green hydrogen storage in salt caverns in the dutch north sea.*

Farge, E., & Vinnell, K. (2023). *World set to overshoot paris warming target, says un climate agency boss.* Retrieved from https://www.reuters.com/world/europe/ipcc-incoming-chair-world-set-overshoot-paris-warming-target-2023-07-27/#:~:text=GENEVA%2C%20July%2027%20(Reuters),had%20not%20been%20ambitious%20enough.

Feria-Díaz, J. J., Correa-Mahecha, F., López-Méndez, M. C., Rodríguez-Miranda, J. P., & Barrera-Rojas, J. (2021, 5). *Recent desalination technologies by hybridization and integration with reverse osmosis: A review* (Vol. 13). MDPI. doi: 10.3390/w13101369

F.M.E.R. (2021). *How partners in the h2mare flagship project intend to produce hydrogen on the high seas.* Retrieved from https://www.wasserstoff-leitprojekte.de/projects/h2mare

Gaertner, E., Rinker, J., Sethuraman, L., Zahle, F., Anderson, B., Barter, G., ... Viselli, A. (2020). *Definition of the iea wind 15-megawatt offshore reference wind turbine technical report.* Retrieved from www.nrel.gov/publications.

Gandía, L. M., Arzamendi, G., & Diéguez, P. M. (2013). Renewable hydrogen energy: An overview. In (p. 1-17). Elsevier B.V. doi: 10.1016/B978-0-444-56352-1.00001-5

Gasnier, S., Debusschere, V., Poullain, S., & François, B. (2016). *Technical and economic assessment tool for offshore wind generation connection scheme: Application to comparing 33 kv and 66 kv ac collector grids authors.*

Gessel, S. V., Fernández, C. Y., Fournier, C., & Geostock, . (2023). *Colofon hydrogen tcp-task 42 underground hydrogen storage contents.* Deltares.

Gongora-Salazar, P., Rocks, S., Fahr, P., Rivero-Arias, O., & Tsiachristas, A. (2022, 5). *The use of multicriteria decision analysis to support decision making in healthcare: An updated systematic literature review.* Elsevier Ltd. doi: 10.1016/j.jval.2022.11.007

Gordonnat, J., & Hunt, J. (2020, 12). Subsea cable key challenges of an intercontinental power link: case study of australia–singapore interconnector. *Energy Transitions*, *4*, 169-188. doi: 10.1007/s41825-020-00032-z

GrantThornton. (2017). *Renewable energy discount rate survey results-2017.*

Grigoriev, S. A., Porembskiy, V. I., Korobtsev, S. V., Fateev, V. N., Auprêtre, F., & Millet, P. (2011, 2). High-pressure pem water electrolysis and corresponding safety issues. *International Journal of Hydrogen Energy*, *36*, 2721-2728. doi: 10.1016/j.ijhydene.2010.03.058

Groenenberg, R., Juez-Larré, J., Goncalvez, C., Wasch, L., Dijkstra, H., Wassing, B., ... Kranenburg-Bruinsma, K. (2020). *Techno-economic modelling of large-scale energy storage systems.* Retrieved from `www.tno.nl`

Guidehouse. (2020). Hydrogen generation in europe. Retrieved from `http://www.europa.eu` doi: 10.2833/122757

Guo, Y., Li, G., Zhou, J., & Liu, Y. (2019, 12). Comparison between hydrogen production by alkaline water electrolysis and hydrogen production by pem electrolysis. In (Vol. 371). Institute of Physics Publishing. doi: 10.1088/1755-1315/371/4/042022

HaskoningDHV, R. (2021). *Rapportage onderzoek innovatie doorkruising waddengebied.*

Henry, A., McCallum, C., McStay, D., Rooney, D., Robertson, P., & Foley, A. (2022, 6). Analysis of wind to hydrogen production and carbon capture utilisation and storage systems for novel production of chemical energy carriers. *Journal of Cleaner Production*, *354*. doi: 10.1016/j.jclepro.2022.131695

Hermesmann, M., & Müller, T. E. (2022, 5). *Green, turquoise, blue, or grey? environmentally friendly hydrogen production in transforming energy systems* (Vol. 90). Elsevier Ltd. doi: 10.1016/j.pecs.2022.100996

HyWay27. (2021). *Waterstoftransport via het bestaande gasnetwerk? eindrapport voor het ministerie van economische zaken en klimaat.* Retrieved from `www.pwc.nl`

Ibrahim, O. S., Singlitico, A., Proskovics, R., McDonagh, S., Desmond, C., & Murphy, J. D. (2022, 5). *Dedicated large-scale floating offshore wind to hydrogen: Assessing design variables in proposed typologies* (Vol. 160). Elsevier Ltd. doi: 10.1016/j.rser.2022.112310

IEA. (2019). *The future of hydrogen.*

IEA. (2022). *Electrolysers.*

IEA. (2023). *Hydrogen.* Retrieved from `https://www.iea.org/energy-system/low-emission-fuels/hydrogen`

IJVERGAS. (2020). *Feasibility of hydrogen generation on a multifunctional island at ijmuiden ver.*

International, H. (2022). *Surveying the seabed for the danish energy island.*

IPCC. (2023, 7). Summary for policymakers. In (p. 3-32). Cambridge University Press. Retrieved from `https://www.cambridge.org/core/product/identifier/9781009157896%23pre2/type/book_part` doi: 10.1017/9781009157896.001

I.R.E.A. (2022). *Global hydrogen trade to meet the 1.5˚c climate goal.*

I.R.E.N.A. (2020). *Green hydrogen cost reduction scaling up electrolysers to meet the 1.5˚c climate goal h 2 o 2.* Retrieved from `www.irena.org/publications`

Jager, J. D. (2007). *Petroleum geology trap and seal assessment view project geology of the central european basin view project.* Retrieved from `https://www.researchgate.net/publication/312604683`

Jonsson, F., & Miljanovic, A. (2022). *Utilization of waste heat from hydrogen production a case study on the botnia link h2 project in luleå, sweden.*

Kato, T., Kubota, M., Kobayashi, N., & Suzuoki, Y. (2005). Effective utilization of by-product oxygen from electrolysis hydrogen production. In (Vol. 30, p. 2580-2595). Elsevier Ltd. doi: 10.1016/j.energy.2004.07.004

Khan, T. O. C. T. D., Young, M. A., & Layzell, C. B. (2021). *The techno-economics of hydrogen pipelines* (Vol. 1). Retrieved from www.transitionaccelerator.ca

Kilner, J. (2022). *Hydrogen production methods and its colours.* Retrieved from https://cicenergigune.com/en/blog/hydrogen-production-methods-colours

Kouli, M. E., Ferraro, A., Tselou, P., & Hristoforou, E. (2018). Desalination of brackish water/seawater via selective separation. In (Vol. 915, p. 196-201). Trans Tech Publications Ltd. doi: 10.4028/www.scientific.net/MSF.915.196

Kumar, A. (2021). Review of pem electrolyser and associated balance of plant system for green hydrogen generation. *International Journal of Current Advanced Research*, *10*, 24409-24412. Retrieved from http://dx.doi.org/10.24327/ijcar.2021 doi: 10.24327/ijcar.2021

Kumar, S. S., & Himabindu, V. (2019, 12). *Hydrogen production by pem water electrolysis – a review* (Vol. 2). KeAi Communications Co. doi: 10.1016/j.mset.2019.03.002

Kumar, S. S., & Lim, H. (2022, 11). *An overview of water electrolysis technologies for green hydrogen production* (Vol. 8). Elsevier Ltd. doi: 10.1016/j.egyr.2022.10.127

labidine Messaoudani, Z., Rigas, F., Hamid, M. D. B., & Hassan, C. R. C. (2016, 10). *Hazards, safety and knowledge gaps on hydrogen transmission via natural gas grid: A critical review* (Vol. 41). Elsevier Ltd. doi: 10.1016/j.ijhydene.2016.07.171

Lange, H., Klose, A., Lippmann, W., & Urbas, L. (2023, 5). *Technical evaluation of the flexibility of water electrolysis systems to increase energy flexibility: A review.* Elsevier Ltd. doi: 10.1016/j.ijhydene.2023.01.044

Langmi, H. W., Engelbrecht, N., Modisha, P. M., & Bessarabov, D. (2021, 1). Hydrogen storage. In (p. 455-486). Elsevier. doi: 10.1016/B978-0-12-819424-9.00006-9

Larsson, J. (2021). *Examensarbete 30 hp maj 2021 transmission systems for grid connection of offshore wind farms hvac vs hvdc breaking point.* Retrieved from http://www.teknat.uu.se/student

Leporini, M., Marchetti, B., Corvaro, F., & Polonara, F. (2019, 5). Reconversion of offshore oil and gas platforms into renewable energy sites production: Assessment of different scenarios. *Renewable Energy*, *135*, 1121-1132. doi: 10.1016/j.renene.2018.12.073

Lerch, M., De-Prada-Gil, M., & Molins, C. (2021, 10). A metaheuristic optimization model for the inter-array layout planning of floating offshore wind farms. *International Journal of Electrical Power and Energy Systems*, *131*. doi: 10.1016/j.ijepes.2021.107128

Lhyfe. (2023, 6). *Sealhyfe, the world's first offshore hydrogen production pilot, produces its first kilos of green hydrogen in the atlantic ocean.* Retrieved from https://www.lhyfe.com/press/lhyfe-announces-that-sealhyfe-the-worlds-first-offshore-hydrogen-production-pilot-produces-its-first-kilos-of-green-hydrogen-in-the-atlantic-ocean/

Little, A. D., Carlot, F., Klossa, A., Pluchet, J., Clauwaert, S., Viel, P., ... Houdt, Y. V. (2023). *O f f s h o r e w i n d h y d r o g e n i n t e g r a t i o n how sector coupling can support a resilient decarbonization of europe.*

Maawali, H. A., Adewole, D. J. K., Kharusi, A. A., Al-Qartoubi, J., Maamari, M. A., Balushi, R. A., & Mazrui, R. . A. (2021, 7). Comparative studies of membrane distillation and reverse osmosis for seawater desalination. *Journal of Student Research*, *10*. doi: 10.47611/jsr.v10i2.1208

Madsen, H. T. (2022, 10). *Water treatment for green hydrogen: What you need to know.*

Mahmoud, R. M. A., & Dodds, P. E. (2022, 12). A technical evaluation to analyse of potential repurposing of submarine pipelines for hydrogen and ccs using survival analysis. *Ocean Engineering*, *266*. doi: 10.1016/j.oceaneng.2022.112893

Maizland, L. (2022). *Global climate agreements: Successes and failures.* Retrieved from https://www.cfr.org/backgrounder/paris-global-climate-change-agreements

Mancera, J. J. C., Manzano, F. S., Andújar, J. M., Vivas, F. J., & Calderón, A. J. (2020, 5). An optimized balance of plant for a medium-size pem electrolyzer. design, control and physical implementation. *Electronics (Switzerland)*, *9*. doi: 10.3390/electronics9050871

Marineregions.org. (2016). North sea depth map.

Martinez, A., & Iglesias, G. (2021, 9). Multi-parameter analysis and mapping of the levelised cost of energy from floating offshore wind in the mediterranean sea. *Energy Conversion and Management*, *243*. doi: 10.1016/j.enconman.2021.114416

Muhammed, N. S., Haq, B., Shehri, D. A., Al-Ahmed, A., Rahman, M. M., & Zaman, E. (2022, 11). *A review on underground hydrogen storage: Insight into geological sites, influencing factors and future outlook* (Vol. 8). Elsevier Ltd. doi: 10.1016/j.egyr.2021.12.002

Muhammed, N. S., Haq, M. B., Shehri, D. A. A., Al-Ahmed, A., Rahman, M. M., Zaman, E., & Iglauer, S. (2023, 4). *Hydrogen storage in depleted gas reservoirs: A comprehensive review* (Vol. 337). Elsevier Ltd. doi: 10.1016/j.fuel.2022.127032

NAM. (2022). *Subsurface hydrogen storage in depleted gas fields.*

Nations, U. (2015). *Paris climate agreement.*

NGT, & NOGAT. (2022). *Offshore waterstof transport via hergebruik aardgasleidingen.*

Nieradzinska, K., MacIver, C., Gill, S., Agnew, G. A., Anaya-Lara, O., & Bell, K. R. (2016, 6). Optioneering analysis for connecting dogger bank offshore wind farms to the gb electricity network. *Renewable Energy*, *91*, 120-129. doi: 10.1016/j.renene.2016.01.043

NOGAT. (2022). *Offshore waterstof transport via hergebruik aardgasleidingen.*

NREL. (2022). Offshore wind annual technology baseline. Retrieved from `https://atb.nrel.gov/electricity/2022/offshore_wind`

of Energy, U. D. (n.d.). *Hydrogen storage.*

Panagopoulos, A., Haralambous, K. J., & Loizidou, M. (2019, 11). *Desalination brine disposal methods and treatment technologies - a review* (Vol. 693). Elsevier B.V. doi: 10.1016/j.scitotenv.2019.07.351

Popov, B. N., Lee, J. W., & Djukic, M. B. (2018, 6). Hydrogen permeation and hydrogen-induced cracking. In (p. 133-162). Elsevier Inc. doi: 10.1016/B978-0-323-52472-8.00007-1

PoR. (2020). *waterstofvisie-havenbedrijf-rotterdam.*

PoR. (2023). *Port of rotterdam internal.*

PosHYdon. (2023). *Poshydon proces.* Retrieved from `https://poshydon.com/nl/home/`

Program, H. I. (2022). *Hydrohub innovation program public report a one-gigawatt green-hydrogen plant advanced design and total installed-capital costs.*

Qasim, M., Badrelzaman, M., Darwish, N. N., Darwish, N. A., & Hilal, N. (2019, 6). *Reverse osmosis desalination: A state-of-the-art review* (Vol. 459). Elsevier B.V. doi: 10.1016/j.desal.2019.02.008

Renogy. (2022, 7). *Everything you need to know about lithium battery charging cycles.* Retrieved from `https://au.renogy.com/blog/everything-you-need-to-know-about-lithium-battery-charging-cycles/#:~:text=Lithium%2Dion%20battery%20packs%20should,to%201%20full%20discharge%20cycle.`

Reuß, M., Grube, T., Robinius, M., Preuster, P., Wasserscheid, P., & Stolten, D. (2017). Seasonal storage and alternative carriers: A flexible hydrogen supply chain model. *Applied Energy*, *200*, 290-302. doi: 10.1016/j.apenergy.2017.05.050

Rezaei, J. (2015a). *Best worst method.* Retrieved from `https://bestworstmethod.com/`

Rezaei, J. (2015b, 6). Best-worst multi-criteria decision-making method. *Omega (United Kingdom)*, *53*, 49-57. doi: 10.1016/j.omega.2014.11.009

Rijksoverheid. (2019). *Windenergie op zee.*

Rijksoverheid. (2020). Wind op zee na 2030. Retrieved from https://windopzee.nl/onderwerpen/wind-zee/wanneer-hoeveel/wind-zee-2030-0/

Rijksoverheid. (2023). *Ontwerp-programma energiehoofdstructuur ruimte voor een klimaatneutraal energiesysteem van nationaal belang.*

Rioux, B., Shabaneh, R., & Griffiths, S. (2021, 10). An economic analysis of gas pipeline trade cooperation in the gcc. *Energy Policy*, *157*. doi: 10.1016/j.enpol.2021.112449

RVO. (2022, 9). *Technology readiness level (trl).*

RVO. (2023). *Offshore wind energy plans 2030-2050.* Retrieved from https://english.rvo.nl/information/offshore-wind-energy/offshore-wind-energy-plans-2030-2050

S., D. E. S. S., & Demirocak. (2017). Metal hydrides used for hydrogen storage. In Sajid, L. J. L. C. Ying-Pin, & Bashir (Eds.), (p. 225-255). Springer Berlin Heidelberg. Retrieved from https://doi.org/10.1007/978-3-662-53514-1_8 doi: 10.1007/978-3-662-53514-1_8

Sambo, C., Dudun, A., Samuel, S. A., Esenenjor, P., Muhammed, N. S., & Haq, B. (2022, 6). *A review on worldwide underground hydrogen storage operating and potential fields* (Vol. 47). Elsevier Ltd. doi: 10.1016/j.ijhydene.2022.05.126

Saulnier, R., Minnich, K., & watersmartsolutionsca P Kim Sturgess. (2020). *Water for the hydrogen economy.*

Schmidt, O., Gambhir, A., Staffell, I., Hawkes, A., Nelson, J., & Few, S. (2017). Future cost and performance of water electrolysis: An expert elicitation study. *International Journal of Hydrogen Energy*, *42*. doi: 10.1016/j.ijhydene.2017.10.045

Shell. (2022). *Shell start bouw van europa's grootste groene waterstoffabriek in rotterdam.* Retrieved from https://www.shell.nl/media/nieuwsberichten/2022/holland-hydrogen-1.html

Shemer, H., & Semiat, R. (2017, 12). *Sustainable ro desalination – energy demand and environmental impact* (Vol. 424). Elsevier B.V. doi: 10.1016/j.desal.2017.09.021

Siachos, K. (2022). *Offshore green hydrogen production and transportation to shore via pipelines in the north sea with parallel natural gas transport.*

Sidiq, R. B., Utomo, C., & Silvianita. (2023, 1). Determining factors of fixed offshore platform inspections in indonesia. *Applied Sciences (Switzerland)*, *13*. doi: 10.3390/app13020737

Sluis, L. V. D. (2008). *Electrical power system essentials.* Retrieved from https://www.researchgate.net/publication/287814374

Succi, M., Macchi, G., & Riddle, S. (2020). *High-purity hydrogen: Guidelines to select the most suitable purification technology.*

Sánchez, M., Amores, E., Abad, D., Rodríguez, L., & Clemente-Jul, C. (2020, 2). Aspen plus model of an alkaline electrolysis system for hydrogen production. *International Journal of Hydrogen Energy*, *45*, 3916-3929. doi: 10.1016/j.ijhydene.2019.12.027

Tarkowski, R. (2019, 5). *Underground hydrogen storage: Characteristics and prospects* (Vol. 105). Elsevier Ltd. doi: 10.1016/j.rser.2019.01.051

TenneT. (2019). *Stakeholder consultation process offshore grid nl type: Position paper work stream: Technical topic: T01-2 gw hvdc grid design and reliability availability filename: Ttb-05415.*

TenneT. (2022a). *Offshore projects netherlands.* Retrieved from https://www.tennet.eu/projects/offshore-projects-netherlands#9605

TenneT. (2022b). Offshore projects netherlands. Retrieved from https://www.tennet.eu/projects/offshore-projects-netherlands

Thiyagarajan, S. R., Emadi, H., Hussain, A., Patange, P., & Watson, M. (2022, 7). *A comprehensive review of the mechanisms and efficiency of underground hydrogen storage* (Vol. 51). Elsevier Ltd. doi: 10.1016/j.est.2022.104490

Timmers, V., Egea-Àlvarez, A., Gkountaras, A., Li, R., & Xu, L. (2023, 7). All-dc offshore wind farms: When are they more cost-effective than ac designs? *IET Renewable Power Generation*, *17*, 2458-2470. doi: 10.1049/rpg2.12550

TNO. (2021). $h2_{l}arge - scale - underground - storage - salt - caverns_{2}021 - 12 - 16 - 093010_{l}nyn - 9$.

Topsector, E. (2023). *Wie versnelt innovatie in offshore waterstof?* Retrieved from `https://topsectorenergie.nl/nl/nieuws/open-innovation-call-voor-offshore-waterstof/`

Topsoe, H. (2021). *Soec high-temperature electrolysis.* Retrieved from `www.topsoe.com`

Tractebel. (2021). *offshore-hydrogen-production-platform.*

Turbinesinfo. (2021, 3). *How do wind turbines work?* Retrieved from `https://www.turbinesinfo.com/how-do-wind-turbines-work/`

Ullah, R., Khraisheh, M., Esteves, R. J., McLeskey, J. T., AlGhouti, M., el Hak, M. G., & Tafreshi, H. V. (2018, 5). *Energy efficiency of direct contact membrane distillation* (Vol. 433). Elsevier B.V. doi: 10.1016/j.desal.2018.01.025

Unnewehr, J. F., Waldl, H. P., Pahlke, T., Herráez, I., & Weidlich, A. (2020, 3). Reducing operational costs of offshore hvdc energy export systems through optimized maintenance. *Energies*, *13*. doi: 10.3390/en13051146

Ursúa, A., Gandía, L. M., & Sanchis, P. (2012). Hydrogen production from water electrolysis: Current status and future trends. In (Vol. 100, p. 410-426). Institute of Electrical and Electronics Engineers Inc. doi: 10.1109/JPROC.2011.2156750

Usman, M. R. (2022, 10). *Hydrogen storage methods: Review and current status* (Vol. 167). Elsevier Ltd. doi: 10.1016/j.rser.2022.112743

van der Roest, E., Bol, R., Fens, T., & van Wijk, A. (2023). Utilisation of waste heat from pem electrolysers – unlocking local optimisation. *International Journal of Hydrogen Energy*. doi: 10.1016/j.ijhydene.2023.03.374

van der Veer, E., Sweers, B., Kawale, D., van Unen, M., van Schot, M., Kee, J., ... van der Keere, L. (2020). *North sea energy offshore energy islands deliverable d3.8.*

van Medevoort, J., Kuipers, N., & ten Hoopen, P. (2022). *Sea2h2 hydrogen from seawater via membrane distillation and polymer electrolyte membrane water electrolysis.*

van Schot, M., & Jepma, C. (2020). *North sea energy a vision on hydrogen potential from the north sea d1.6 offshore hydrogen roadmap d. 1.7 analysis of current offshore market failures and the respective role of existing policy d. 1.8 recommendations on required policies to achieve a socially optimal state.*

Vindo. (2021). Vindo energy hub design.

Walters, C., Belfroid, S., & Koornneef, J. (2020a). *North sea energy technical assessment of hydrogen transport, compression, processing offshore as part of topsector energy: Tki offshore wind tki new gas.*

Walters, C., Belfroid, S., & Koornneef, J. (2020b). *North sea energy technical assessment of hydrogen transport, compression, processing offshore as part of topsector energy: Tki offshore wind tki new gas.*

Wang, A., Jens, J., Mavins, D., Moultak, M., Schimmel, M., Leun, K. V. D., ... Buseman, M. (2021). *Analysing future demand, supply, and transport of hydrogen european hydrogen backbone executive summary.* Retrieved from `https://transparency.entsog.eu/`

water inc., A. (2021). *How often should reverse osmosis system maintenance happen.* Retrieved from `https://angelwater.com/blog/reverse-osmosis-maintenance/#:~:text=Most%20of%20the%20filters%20on,system%20service%20at%20least%20annually.`

WebMet. (n.d.). *Surface roughness length.* Retrieved from `http://www.webmet.com/met_monitoring/663.html`

Wingerden, T. V., Geerdink, D., Taylor, C., & Hülsen, C. F. (2023). *Specification of a european offshore hydrogen backbone.*

YCharts. (2023). European union inflation rate. Retrieved from `https://ycharts.com/indicators/europe_inflation_rate#:~:text=European%20Union%20Inflation%20Rate%20(I%3AEUIR)&text=European%20Union%20Inflation%20Rate%20is,long%20term%20average%20of%202.22%25.`

Yu, M., Budiyanto, E., & Tüysüz, H. (2022, 1). *Principles of water electrolysis and recent progress in cobalt-, nickel-, and iron-based oxides for the oxygen evolution reaction* (Vol. 61). John Wiley and Sons Inc. doi: 10.1002/anie.202103824

Zaaijer, M., Viré, A., Dos, R. B., Pereira, S., & Daneshbodi, A. (2020). *Introduction to wind turbines: physics and technology editing (text and videos).*

Zhang, Z., Atia, A. A., Andrés-Mañas, J. A., Zaragoza, G., & Fthenakis, V. (2022, 6). Comparative techno-economic assessment of osmotically-assisted reverse osmosis and batch-operated vacuum-air-gap membrane distillation for high-salinity water desalination. *Desalination*, *532*. doi: 10.1016/j.desal.2022.115737

Appendices

A Appendix A

An overview of the model is given in Fig. A.1. The external inputs are shown on the left side. The blue blocks show the modelling steps. As the scenario and sensitivity analysis are also performed by the model, these blocks have the same colour in this figure. The outputs of intermediate steps that are used as inputs for the next steps are indicated with an arrow coming from that respective block. Lastly, the final outputs are indicated by the red blocks.

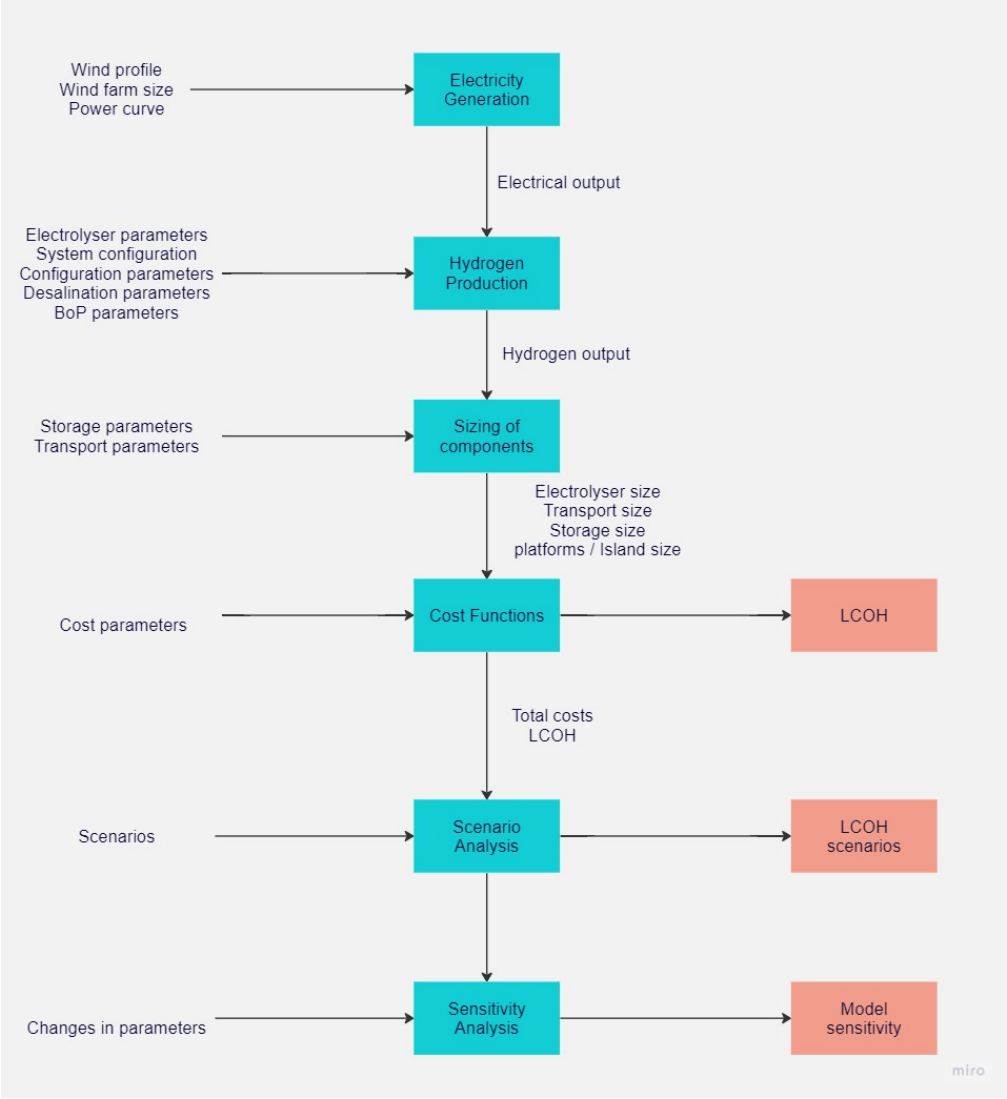

Figure A.1: Overview of the model with the four modelling steps. The model also performs the scenario analysis and sensitivity analysis.

Valuta	**Exchange rate to €$_{2023}$**
American dollar	0.95
British pound	1.15

Table A.1: Exchange rate from different valutas to €$_{2023}$

B Appendix B

Criteria Number = 4	Criterion 1	Criterion 2	Criterion 3	Criterion 4
Names of Criteria	Footprint	pressure	purity	efficiency

Select the Best	efficiency

Select the Worst	purity

Best to Others	Footprint	pressure	purity	efficiency
efficiency	2	6	9	1

Others to the Worst	purity
Footprint	8
pressure	4
purity	1
efficiency	9

Weights	Footprint	pressure	purity	efficiency
	0,31578947	0,10526316	0,05263158	0,52631579

Input-Based CR	0,20833333	The pairwise comparison consistency level is acceptable
Associated Threshold	0,2681	

Figure B.1: Best-Worst-Method of the technical aspects of the electrolyser technologies

Criteria Number = 4	Criterion 1	Criterion 2	Criterion 3	Criterion 4
Names of Criteria	Footprint	pressure	purity	efficiency

Select the Best	efficiency

Select the Worst	purity

Best to Others	Footprint	pressure	purity	efficiency
efficiency	2	6	9	1

Others to the Worst	purity
Footprint	8
pressure	4
purity	1
efficiency	9

Weights	Footprint	pressure	purity	efficiency
	0,31578947	0,10526316	0,05263158	0,52631579

Input-Based CR	0,20833333	The pairwise comparison consistency level is acceptable
Associated Threshold	0,2681	

Figure B.2: Best-Worst-Method of the flexibility aspects of the electrolyser technologies

Criteria Number = 5	Criterion 1	Criterion 2	Criterion 3	Criterion 4	Criterion 5
Names of Criteria	Water conductivity	Energy consumption	Space requirements	Weight	System complexity

Select the Best	Space requirements

Select the Worst	System complexity

Best to Others	Water conductivity	Energy consumption	Space requirements	Weight	System complexity
Space requirements	5	5	1	3	7

Others to the Worst	System complexity
Water conductivity	3
Energy consumption	3
Space requirements	7
Weight	5
System complexity	1

Weights	Water conductivity	Energy consumption	Space requirements	Weight	System complexity
	0,119437939	0,119437939	0,503512881	0,199063232	0,058548009

Input-Based CR	0,19047619	The pairwise comparison consistency level is acceptable
Associated Threshold	0,2819	

Figure B.3: Best-Worst-Method of the technical aspects of the water feed

Criteria Number = 5	Criterion 1	Criterion 2	Criterion 3	Criterion 4	Criterion 5
Names of Criteria	Water conductivity	Energy consumption	Space requirements	Weight	System complexity

Select the Best	Space requirements

Select the Worst	System complexity

Best to Others	Water conductivity	Energy consumption	Space requirements	Weight	System complexity
Space requirements	5	5	1	3	7

Others to the Worst	System complexity
Water conductivity	3
Energy consumption	3
Space requirements	7
Weight	5
System complexity	1

Weights	Water conductivity	Energy consumption	Space requirements	Weight	System complexity
	0,119437939	0,119437939	0,503512881	0,199063232	0,058548009

Input-Based CR	0,19047619	The pairwise comparison consistency level is acceptable
Associated Threshold	0,2819	

Figure B.4: Best-Worst-Method of the technical aspects of the electrolyser configuration

Criteria Number = 5	Criterion 1	Criterion 2	Criterion 3	Criterion 4	Criterion 5
Names of Criteria	TRL	Capacity	Reusing	Location	Lifetime

Select the Best	Lifetime

Select the Worst	Location

Best to Others	TRL	Capacity	Reusing	Location	Lifetime
Lifetime	4	3	6	8	1

Others to the Worst	Location
TRL	4
Capacity	6
Reusing	3
Location	1
Lifetime	8

Weights	TRL	Capacity	Reusing	Location	Lifetime
	0,15	0,2	0,1	0,05	0,5

Input-Based CR	0,178571429	The pairwise comparison consistency level is acceptable
Associated Threshold	0,2958	

Figure B.5: Best-Worst-Method of the technical aspects of the storage technologies

Criteria Number = 4	Criterion 1	Criterion 2	Criterion 3	Criterion 4
Names of Criteria	Lifetime	Water depth	Footprint limitations	Wind farm connection

Select the Best	Lifetime

Select the Worst	Wind farm

Best to Others	Lifetime	Water depth	Footprint limitations	Wind farm connection
Lifetime	1	2	2	3

Others to the Worst	Wind farm
Lifetime	2
Water depth	2
Footprint limitations	2
Wind farm connection	1

Weights	Lifetime	Water depth	Footprint limitations	Wind farm connection
	0,384615385	0,23076923	0,230769231	0,153846154

Input-Based CR	0,166666667	The pairwise comparison consistency level is acceptable
Associated Threshold	0,1667	

Figure B.6: Best-Worst-Method of the technical aspects of the hydrogen distribution hub

B.1 Total Scores Tables of Decision Framework

Criteria Number = 6	Criterion 1	Criterion 2	Criterion 3	Criterion 4	Criterion 5	Criterion 6
Names of Criteria	Cost	Technical	Flexibility	Safety	Maintenance	Durability

Select the Best	Technical

Select the Worst	Safety

Best to Others	Cost	Technical	Flexibility	Safety	Maintenance	Durability
Technical	2	1	5	8	5	3

Others to the Worst	Safety
Cost	7
Technical	8
Flexibility	3
Safety	1
Maintenance	3
Durability	6

Weights	Cost	Technical	Flexibility	Safety	Maintenance	Durability
	0,23255814	0,3875969	0,09302326	0,03875969	0,09302326	0,15503876

Input-Based CR	0,17857143	The pairwise comparison consistency level is acceptable
Associated Threshold	0,3154	

Figure B.7: Best-Worst-Method of the total scores of the electrolyser technologies

Criteria Number = 5	Criterion 1	Criterion 2	Criterion 3	Criterion 4	Criterion 5
Names of Criteria	Cost	Technical	Safety	Maintenance	Environment

Select the Best	Technical

Select the Worst	Safety

Best to Others	Cost	Technical	Safety	Maintenance	Environment
Technical	4	1	6	3	4

Others to the Worst	Safety
Cost	3
Technical	6
Safety	1
Maintenance	4
Environment	3

Weights	Cost	Technical	Safety	Maintenance	Environment
	0,138157895	0,473684211	0,065789474	0,184210526	0,138157895

Input-Based CR	0,2	The pairwise comparison consistency level is acceptable
Associated Threshold	0,2643	

Figure B.8: Best-Worst-Method of the total scores of the water feed

Criteria Number = 5	Criterion 1	Criterion 2	Criterion 3	Criterion 4	Criterion 5
Names of Criteria	Cost	Technical	Flexibility	Maintenance	Safety

Select the Best	Technical

Select the Worst	Safety

Best to Others	Cost	Technical	Flexibility	Maintenance	Safety
Technical	4	1	2	6	7

Others to the Worst	Safety
Cost	4
Technical	7
Flexibility	6
Maintenance	2
Safety	1

Weights	Cost	Technical	Flexibility	Maintenance	Safety
	0,133928571	0,455357143	0,267857143	0,089285714	0,053571429

Input-Based CR	0,214285714	The pairwise comparison consistency level is acceptable
Associated Threshold	0,2819	

Figure B.9: Best-Worst-Method of the total scores of the electrolyser system configurations

Criteria Number = 5	Criterion 1	Criterion 2	Criterion 3	Criterion 4	Criterion 5
Names of Criteria	Cost	Technical	Safety	Maintenance	Environment

Select the Best	Technical

Select the Worst	Safety

Best to Others	Cost	Technical	Safety	Maintenance	Environment
Technical	2	1	4	4	6

Others to the Worst	Safety
Cost	6
Technical	7
Safety	3
Maintenance	3
Environment	1

Weights	Cost	Technical	Safety	Maintenance	Environment
	0,257142857	0,428571429	0,128571429	0,128571429	0,057142857

Input-Based CR	0,2	The pairwise comparison consistency level is acceptable
Associated Threshold	0,2643	

Figure B.10: Best-Worst-Method of the total scores of the storage technologies

Criteria Number = 5	Criterion 1	Criterion 2	Criterion 3	Criterion 4	Criterion 5
Names of Criteria	Cost	Technical	Safety	Maintenance	Environment

Select the Best	Technical

Select the Worst	Safety

Best to Others	Cost	Technical	Safety	Maintenance	Environment
Technical	2	1	3	6	7

Others to the Worst	Safety
Cost	6
Technical	7
Safety	5
Maintenance	2
Environment	1

Weights	Cost	Technical	Safety	Maintenance	Environment
	0,257575758	0,434343434	0,171717172	0,085858586	0,050505051

Input-Based CR	0,19047619	The pairwise comparison consistency level is acceptable
Associated Threshold	0,2819	

Figure B.11: Best-Worst-Method of the total scores of the transport technologies

C Appendix C

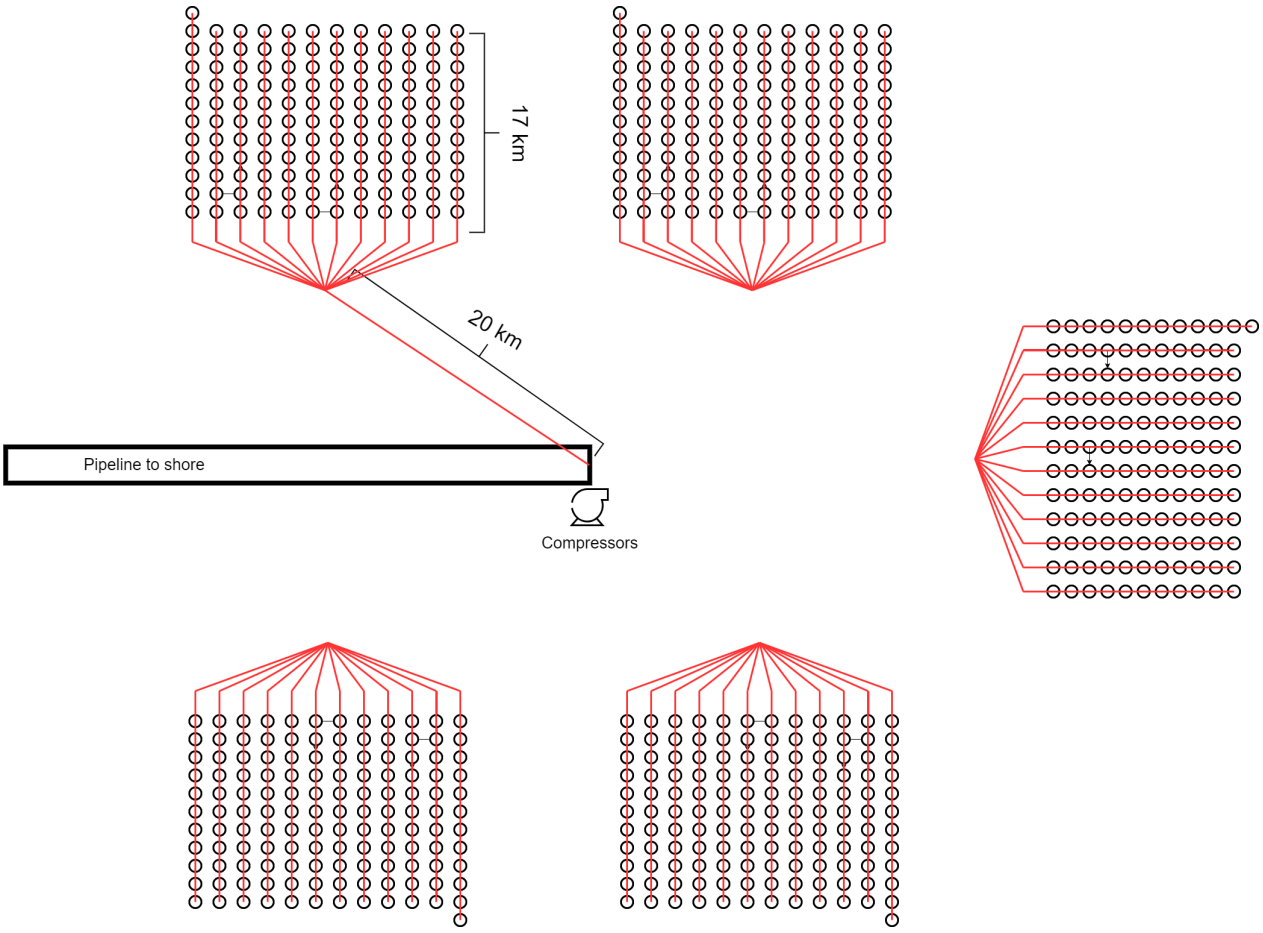

Figure C.1: Layout of the offshore decentralised configuration. Shown are the hydrogen collection pipelines and wind turbines, as well as the compressor and hydrogen pipeline to shore.

D Appendix D

Component	**n**	**CRF**
Wind turbines	30	0.089
Electrolyser stack	14.3	0.12
Electrolyser BoP	20	0.10
Water feed	30	0.089
Salt cavern	30	0.089
Substation	30	0.089
Pipeline	30	0.089
Electricity cables	30	0.089
Island	30	0.089
compressor	25	0.094

Table D.1: The lifetimes and CRFs of the components used.

E Appendix E

Input parameter	Unit	Optimistic	Selected value	Pessimistic
Electrolyser power consumption	kWh/kgH_2	47	53.2	69
Electrolyser CAPEX	$€_{2023}/kW$	200	550	900
Electrolyser stack lifetime	h	150 000	125 000	75 000

Table E.1: Input parameters for the scenario analysis, including their ranges, for the offshore central configuration.

Design choice	Unit	Min. value	Selected value	Max. value
Electrolyser capacity	GW	5	8	10
Distance to shore	km	75	250	350
Battery capacity	GW	2.7	-	6.7
Discount rate	%	6	8	10
Baseload	-	No	Yes	-

Table E.2: Design choices for the scenario analysis for the offshore central configuration, including their ranges.

Input parameter	Unit	Optimistic	Selected value	Pessimistic
Electrolyser power consumption	kWh/kgH_2	47	53.2	59
Electrolyser CAPEX	$€_{2023}/kW$	200	450	700
Electrolyser stack lifetime	h	150 000	125 000	95 000

Table E.3: Design choices for the scenario analysis, including their ranges, for the onshore central configuration.

Design choice	Unit	Min. value	Selected value	Max. value
Electrolyser capacity	GW	5	8	10
Distance to shore	km	75	250	350
Battery capacity	GW	2.7	-	6.7
Discount rate	%	6	8	10
Baseload	-	No	Yes	-

Table E.4: Input parameters for the scenario analysis for the onshore central configuration, including their ranges.

Parameter	Unit	Min. value (-10%)	Nominal value	Max. value (+10%)
Electrolyser power consumption	kWh/kgH_2	47.9	53.2	58.5
Distance to shore	km	225	250	275
Discount rate	%	7.2	8	8.8
Electrolyser CAPEX	$€_{2023}/kW$	495	550	605
Salt cavern CAPEX	$€_{2023}/MWh$	326	362	398
New 36-inch pipeline CAPEX	$€_{2023}/km/GW$	167	185	204
HVAC substation CAPEX	k$€_{2023}/MW$	135	150	165
HVAC cable CAPEX	M$€_{2023}/km$	2.3	2.6	2.9
Inter-array cable CAPEX	k$€_{2023}/km$	390	433	476
Island CAPEX	M$€_{2023}/500MW_{electrolyser}$	68	75	83
Compressor CAPEX	M$€_{2023}/MW$	1.8	2	2.2
Wind turbine CAPEX	$€_{2023}/kW$	2165	2406	2647

Table E.5: Selected parameters for the sensitivity analysis for the offshore centralised configuration, including their ranges.

Parameter	**Unit**	**Min. value** (-10%)	**Nominal value**	**Max. value** (+10%)
Electrolyser power consumption	kWh/kgH_2	47.9	53.2	58.5
Distance to shore	km	225	250	275
Discount rate	%	7.2	8	8.8
Electrolyser CAPEX	$€_{2023}/kW$	405	450	495
Salt cavern CAPEX	$€_{2023}/MWh$	326	362	398
New 36-inch pipeline CAPEX	$€_{2023}/km/GW$	167	185	204
HVDC substation CAPEX	k$€_{2023}/MW$	540	600	660
HVDC cable CAPEX	M$€_{2023}/km$	2.34	2.6	2.86
Inter-array cable CAPEX	k$€_{2023}/km$	390	433	476
Compressor CAPEX	M$€_{2023}/MW$	1.8	2	2.2
Wind turbine CAPEX	$€_{2023}/kW$	2165	2406	2647

Table E.6: Selected parameters for the sensitivity analysis for the onshore centralised configuration, including their ranges.